IPSO REACTION STUDIES OF AROMATIC SYSTEMS

A thesis

presented for the degree

of

Doctor of Philosophy in Chemistry

in the

University of Canterbury

by

Jane L. Calvert

University of Canterbury

Christchurch

New Zealand

1994

TABLE OF CONTENTS

Contents

Contents

LIST OF SCHEMES

LIST OF TABLES

LIST OF FIGURES

LIST OF FIGURES

ABSTRACT

The first section of this thesis is concerned with exploring the mechanism of reaction with nitrogen dioxide of a series of unsymmetrically substituted phenols and their derived 4-nitrocyclohexa-2,5-dienones. The effect the substituents have on the regioselectivity of NO_2 reaction on the phenols is examined by analysis of the types of products and in the case of 2,3,4,6-tetramethylphenol (32) it was possible to undertake ^{15}N-labelling studies to unambiguously ascertain the mode of reaction of NO_2. It is shown that the regiochemistry is dependent on the electron withdrawing or electron donating nature of the 3-substituent in the series of phenols studied, specifically 4-chloro-2,3,6-trimethylphenol (31) 2,3,4,6-tetramethylphenol (32) and 3-chloro-2,4,6-trimethylphenol (33).

The second section of this thesis is concerned with examining the reactions of 1,4,5,8-tetramethylnaphthalene (21), 1,8-dimethylnaphthalene (37), 1-methylnaphthalene (59) and as described in Appendix I the reaction of benzene with tetranitromethane in the presence of light as an activating source to generate the charge transfer complex. The photoaddition of tetranitromethane to aromatics has been shown to give nitro/trinitromethyl, nitrito/trinitromethyl, and hydroxy/trinitromethyl adducts. Also observed were some nitro or hydroxy cycloadducts in which a nitro group formally associated with a trinitromethyl group is involved in a thermal 1,3-dipolar addition across an alkene system.

Tetranitromethane in the presence of an aromatic system and light (≥ 435 nm) fragments to a trinitromethanide ion $(O_2N)_3C^-$, $^{\bullet}NO_2$, while the aromatic transfers an electron in the charge transfer process to generate a radical cation. The radical cations are then attacked initially by the very reactive trinitromethanide ion and secondly by $^{\bullet}NO_2$. This gives rise to the formation of

a variety of adducts. The nature of the radical cation is crucial in determining the position of attack of the trinitromethanide ion.

In conclusion this work has shown that the relative atomic charges of the aromatic radical cations are important in making an assessment of the likely site(s) of the trinitromethanide attack on that radical cation, but that steric interactions with *ipso*, *peri* and *vicinal* substituents to the reaction site may dictate the overall course of the reaction.

Throughout the thesis extensive use is made in product structure determination of single crystal X-ray analysis and in all 23 crystal structures are presented.

CHAPTER ONE

INTRODUCTION

1.1 ELECTROPHILIC AROMATIC SUBSTITUTION

Electrophilic substitution is one of the most extensively studied reaction types of aromatic compounds.[1-4] An aromatic ring is a site of high electron density because of the π–electrons in a cyclic conjugated system. Electrophilic species bear a formal positive charge or possess a dipole which will accept electrons donated from an electron rich species and substitute for one of the hydrogens as illustrated in Fig. 1.1. This substitution process is favoured as the stability of the aromatic ring is maintained in the substituted product as opposed to an addition reaction.

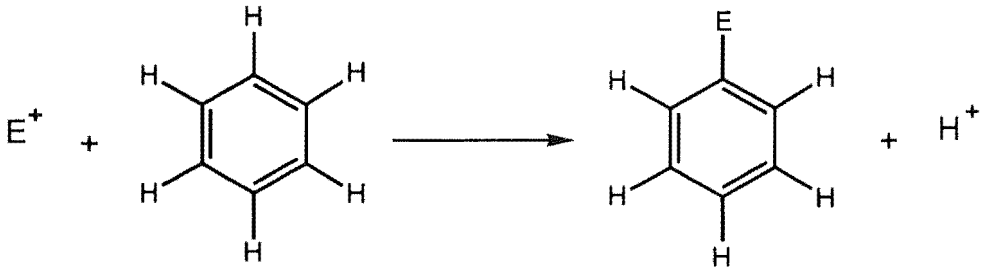

FIGURE 1.1 An electrophilic aromatic substitution where E^+ represents an electrophile.

Electrophilic aromatic substitution occurs *via* a Wheland intermediate,[5] a non aromatic carbocation intermediate which is resonance stabilised and can be represented in the following cannonical forms as illustrated in Scheme 1.1.

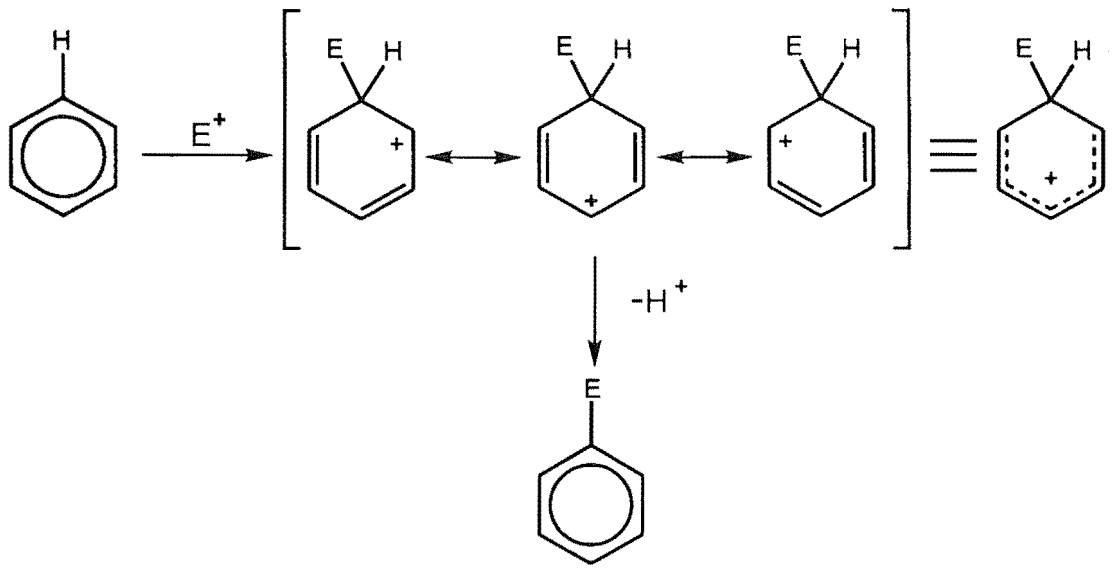

SCHEME 1.1

Monosubstituted aromatic compounds will undergo electrophilic aromatic substitution but the positions available on the Wheland intermediate for electrophilic attack are not equivalent and different substitution products are possible. The electrophile may attack at either the *ortho, meta* or *para* positions giving a corresponding Wheland intermediate, followed by loss of a proton to regenerate the aromatic ring as illustrated in Scheme 1.2.

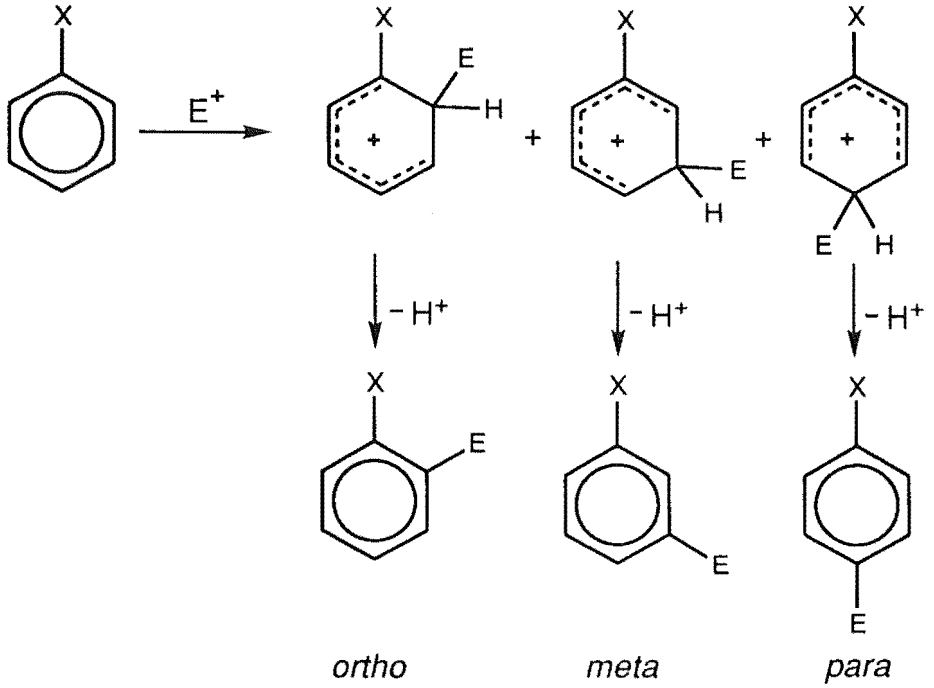

SCHEME 1.2

An alternative mode of substitution exists if the electrophile attacks at the carbon on the aromatic ring which bears the substituent X. To regain the aromaticity loss of the substituent is necessary as illustrated in Scheme 1.3. Perrin and Skinner referred to this mode of substitution as *ipso*-substitution.[6]

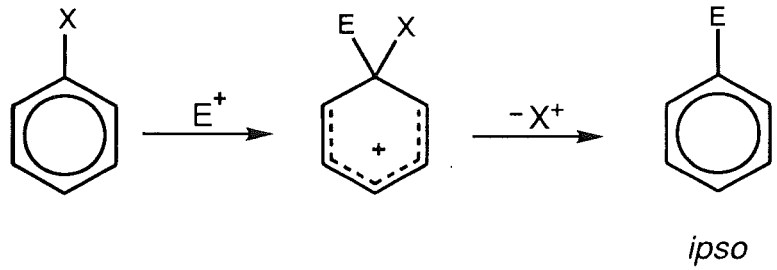

SCHEME 1.3

1.2 *IPSO* ATTACK

De la Mare and Harvey[7] demonstrated the mode of *ipso*-substitution from bromination studies of *tert*-butylbenzene and product analysis. The following product ratios were found as illustrated in Scheme 1.4.

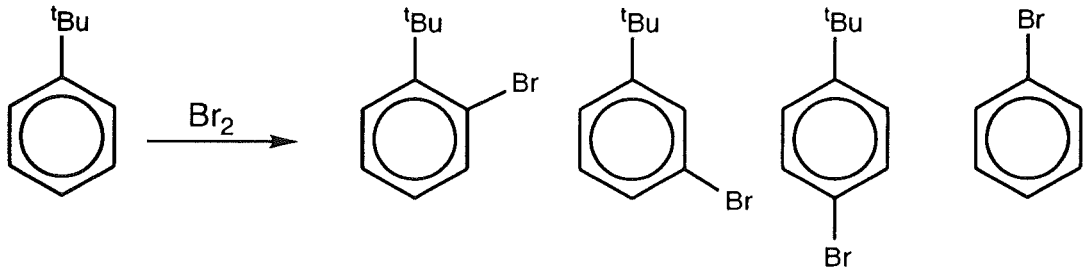

SCHEME 1.4

The formation of bromobenzene almost certainly provides evidence for electrophilic attack by bromine *ipso* to the *tert*-butyl group followed by loss of the relatively stable *tert*-butyl cation from the corresponding Wheland intermediate.

Further evidence for the formation of *ipso*-Wheland intermediates came from the observations made by Blackstock *et al.*[8] from the nitration of *o*-xylene (1) in acetic anhydride as illustrated in Scheme 1.5. The cationic nature of the Wheland intermediate makes them susceptible to nucleophilic capture if suitable species exist in the reaction medium. Formation of 4-acetoxy-*o*-xylene (2) as the major product was attributed to attack of the Wheland intermediate by the nucleophilic solvent.

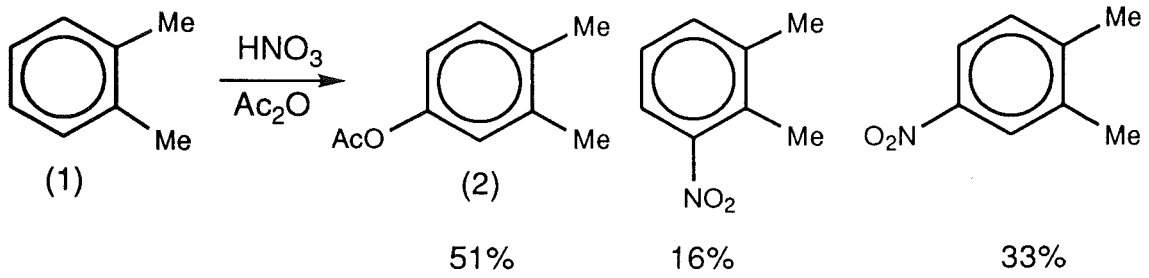

SCHEME 1.5

It was the reaction of nucleophiles particularly the acetate ion which was important in highlighting *ipso*-attack in nitration. The mechanism for the formation of the aromatic acetate (2) is illustrated in Scheme 1.6 where the acetate ion is captured by the Wheland intermediate with subsequent elimination of nitrous acid.

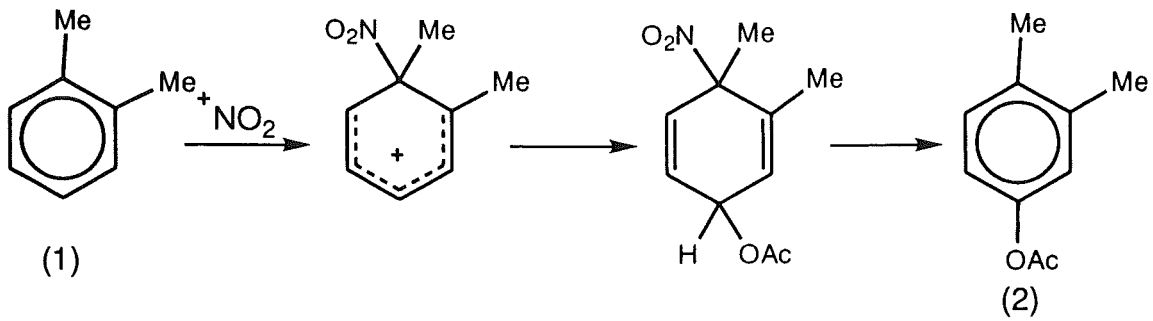

SCHEME 1.6

Further evidence supporting this mechanistic proposal was established after isolation of the two isomeric adducts (3) and (4), formed during the nitration of *o*-xylene (1).[9]

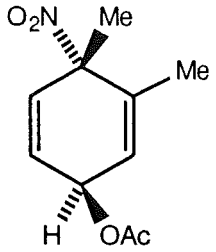

(3)

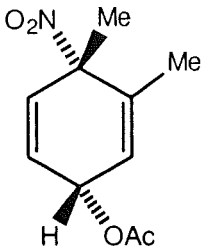

(4)

These adducts (3) and (4) were observed to undergo conversion in aqueous acid to give the aromatic acetate (2). Fisher and co-workers have observed similar products from other aromatic substrates.[10] In some situations the nitro-acetate adducts react further to give dienones as illustrated in Scheme 1.7 The yield of the dienone is dependant on the nature of the substituents.[11,12,13]

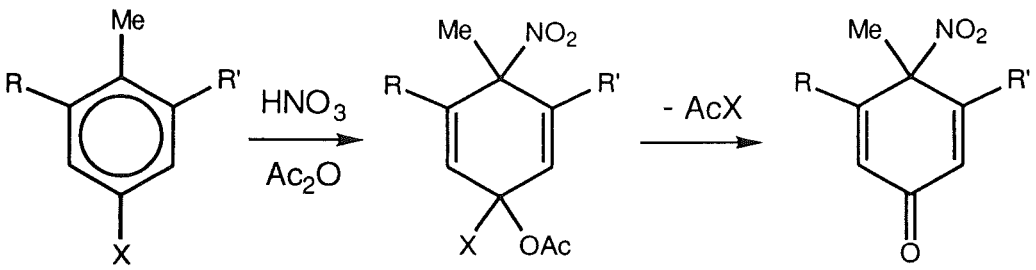

SCHEME 1.7

1.3 MIGRATION OF THE NITRO GROUP

Wheland intermediates formed in electrophilic *ipso* nitration have been observed to undergo subsequent migration of either the *ipso* substituent or the electrophile. Wheland intermediates and dienones are capable of rearrangement by migration of an *ipso*-nitro group or an *ipso*- substituent. Three modes of nitro migration have been identified and each mode has a different consequence.

These rearrangements may be separated into three categories, (i) intramolecular, (ii) extramolecular, (iii) intermolecular migrations.[14]

(i) Intramolecular migration is a process in which the nitro group never becomes sufficiently free from the carbon structure to do other than move to a position immediately adjacent to the *ipso* position, i.e. 1,2-migration occurs.

(ii) In extramolecular migration the nitro group becomes free enough to be able to distinguish and select between the positions in the carbon structure, but it does not leave the solvent cage.

(iii) In intermolecular migration the *ipso* nitro group leaves its position, diffuses into the solvent, and may react with the carbon structures other than the one to which it was attached originally.

1.3.1 INTRAMOLECULAR MIGRATION

Intramolecular 1,2-migration was first suggested by Myhre[15] as an explanation for the acidity dependence of the ratio of 3- to 4-nitro-*o*-xylene produced in the nitration of *o*-xylene in sulphuric acid.[16] Scheme 1.8 and Figure 1.2 illustrate the characteristics of this nitration.

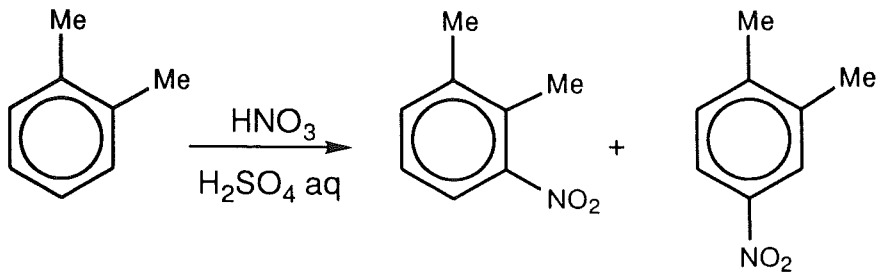

SCHEME 1.8

The proposed mechanism is illustrated in Scheme 1.9. Myhre suggested that the Wheland intermediate was captured by the nucleophilic properties of

water at low acidities but with increasing acidities 1,2-migration became more important.

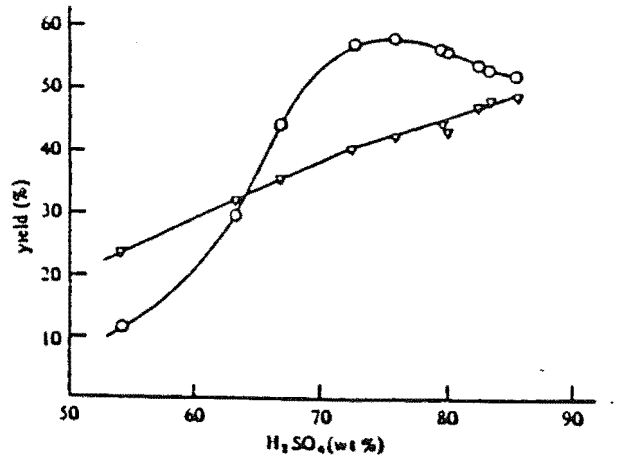

FIGURE 1.2 Nitration of *o*-xylene. Yields of 3-nitro (circles) and 4-nitro-*o*-xylene (triangles) as percentages of the starting material.

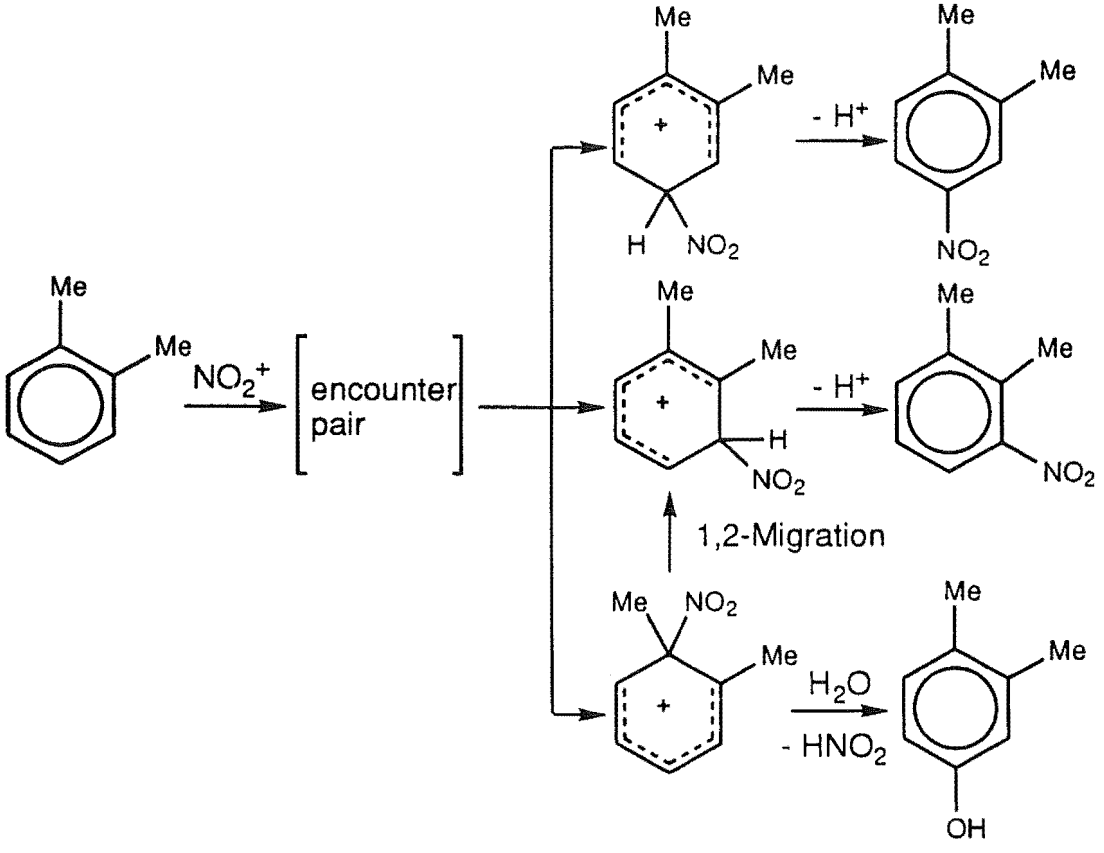

SCHEME 1.9

In accord with this mechanistic description the solvolysis of the acetoxynitrodienone adducts in sulphuric acid of several concentrations gave only the 3-nitro-*o*-xylene and 3,4-dimethylphenol as illustrated in Scheme 1.10.

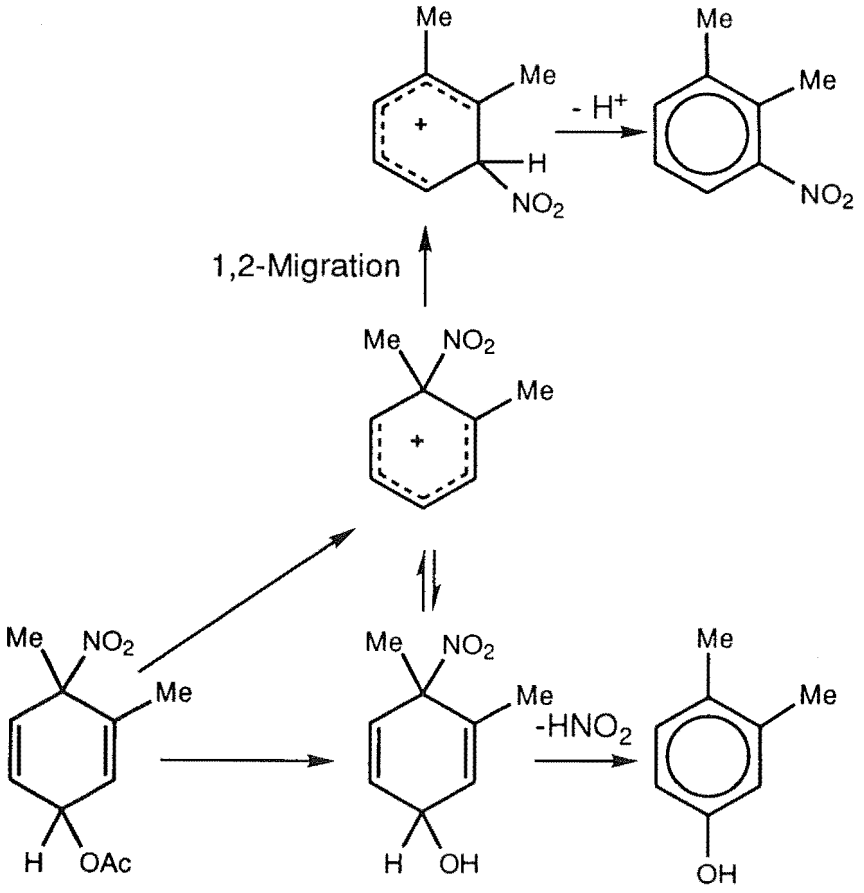

SCHEME 1.10

1.3.2 EXTRAMOLECULAR MIGRATION

Typical examples of extramolecular migration are aromatisations of 4-nitrocyclohexa-2,5-dienones by 1,3-shift of the nitro group where the *ortho* positions are not substituted to give o-nitrophenols[6,13] as illustrated in Scheme 1.11. In 1978 Barnes and Myhre[13] reported that 4-methyl-4-nitro-cyclohexa-2,5-dienones (5)-(7) re-aromatise in hexane, acetic acid, ethanol, water, and DMSO to yield products of a formal 1,3-shift of a nitro group as illustrated in Scheme 1.11.

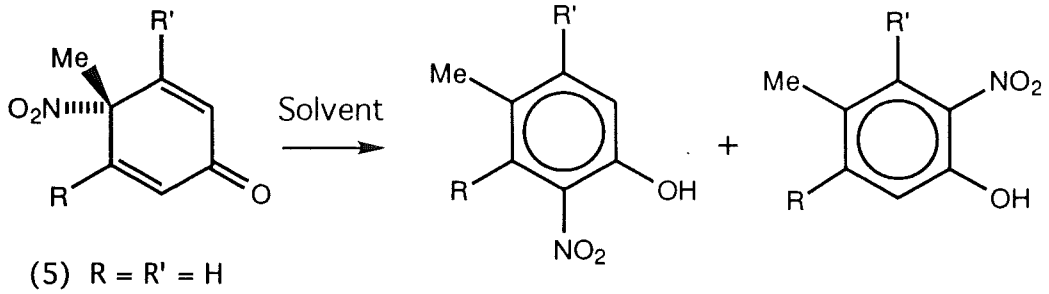

(5) R = R' = H
(6) R' = Me, R = H
(7) R = R' = Me

SCHEME 1.11

The reactions (Scheme 1.11) were followed spectrophotometrically and well-behaved first order kinetics were observed for product formation and reactant disappearance. The detailed mechanism for a 1,3-nitro migration for 4-nitro-cyclohexa-2,5-dienones is given below in Scheme 1.12. However it should be noted that the nitro migration terminus is occupied only by hydrogen. The results obtained from the kinetic study were:

(i) the reaction rates decreased as polarity or hydrogen bonding ability of the solvent increased;
(ii) the activation energies for the reactions were small but positive;
(iii) addition of radical scavengers did not alter reaction rates but did reduce the yields of nitrophenols products;
(iv) the reactivity order (5) > (6) > (7) was observed.

These results are consistent with the radical dissociation-recombination mechanism shown in Scheme 1.12, with the initial homolysis being rate determining. Consistent with the proposed mechanism is the formation of some 3,4-dimethylphenol when the 3,4-dimethyl-4-nitrodienone (6) is allowed to rearrange in the presence of the radical scavenger, hydroquinone. This clearly reflects some diffusion of the radical pair from the solvent cage.

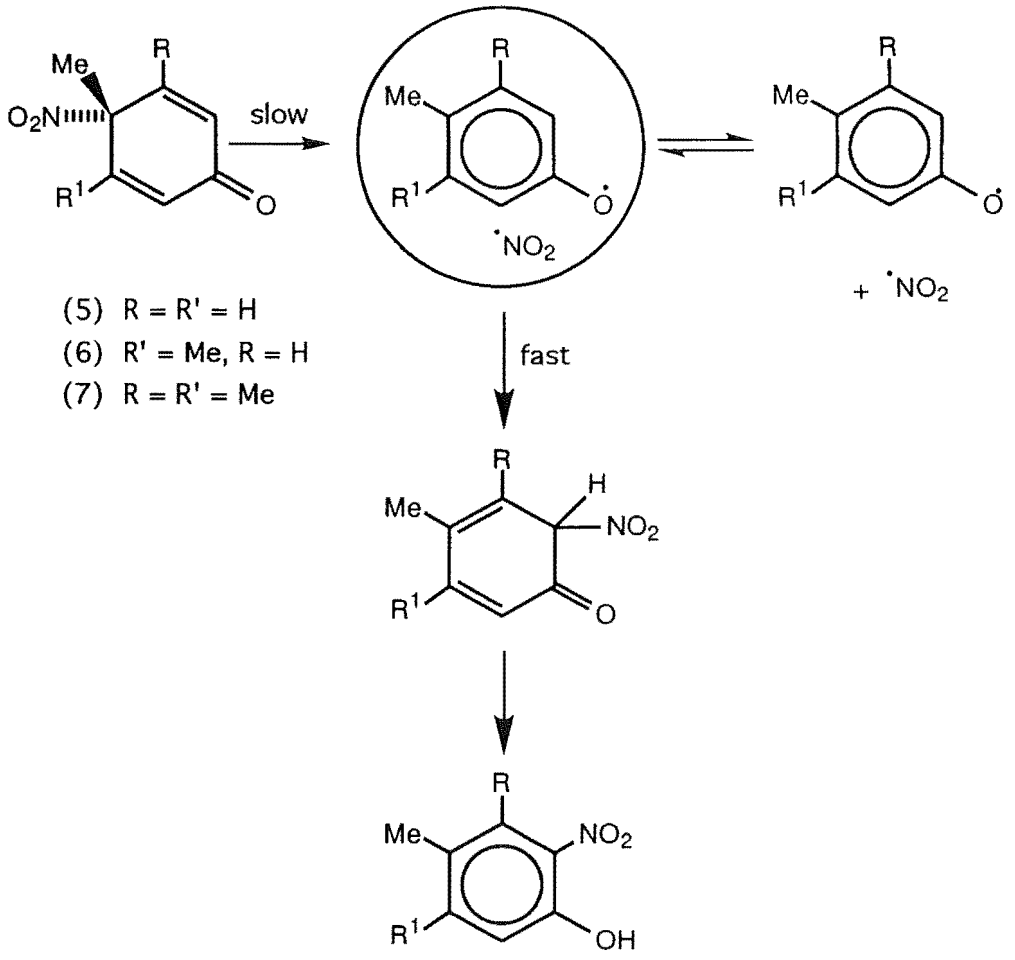

SCHEME 1.12

From isotopic labelling studies in which 3,4-dimethyl-4-nitrocyclohexa-2,5-dienone (6) was rearranged in hexane with an equal amount of the [^{15}N]-2,6-D_2 labelled dienone (6) it was found that approximately 50% scrambling was occurring as shown in Scheme 1.13.[14] This scrambling of the isotopic labels was consistent with the results obtained for reactions in the presence of radical scavengers and allowed the estimation of a recombination rate for product formation of approximately half the rate of diffusion of radical pairs from the solvent cage.

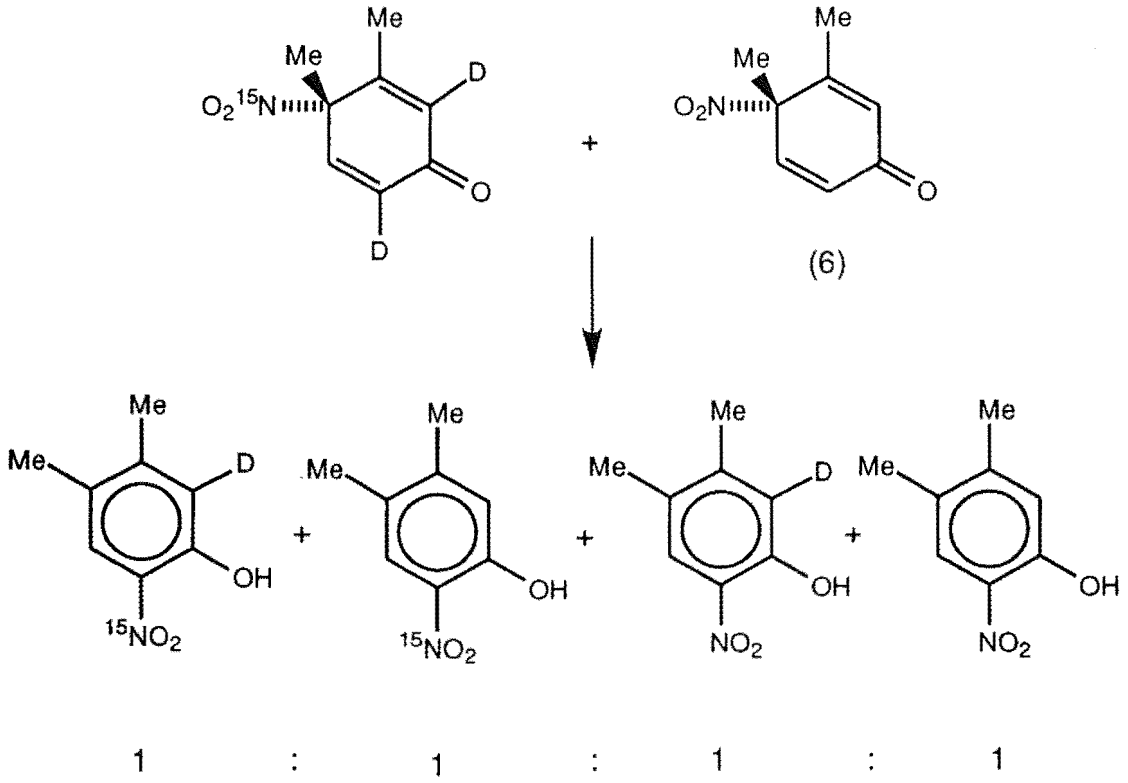

SCHEME 1.13

^{15}N-Labelling studies of 2,4,6-trisubstituted 4-nitrocyclohexa-2,5-dienones with nitrogen dioxide have also been used for circumstances in which the nitro migration terminus carries an alkyl substituent such as the 2,4,6-trisubstituted 4-nitrocyclohexa-2,5-dienones (8) and (9).

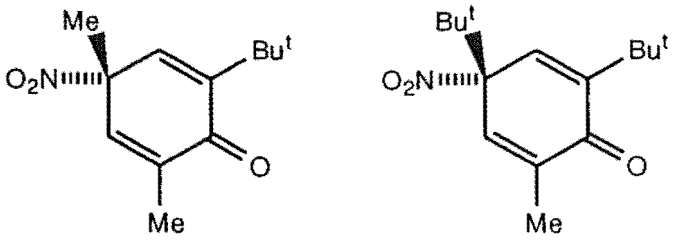

(8) (9)

For example, Jensen[14] has shown that reaction of labelled ^{15}N-4-nitrodienone (8) with excess nitrogen dioxide in benzene gives the trinitro ketones (10) and (11) in which the ^{15}N-label occurs in the nitro group at C6

with the incorporation of 40% ± 5% ^{15}N at C6 in (10) and 37% ± 7% ^{15}N at C6 in (11). The results were interpreted in terms of Scheme 1.14.

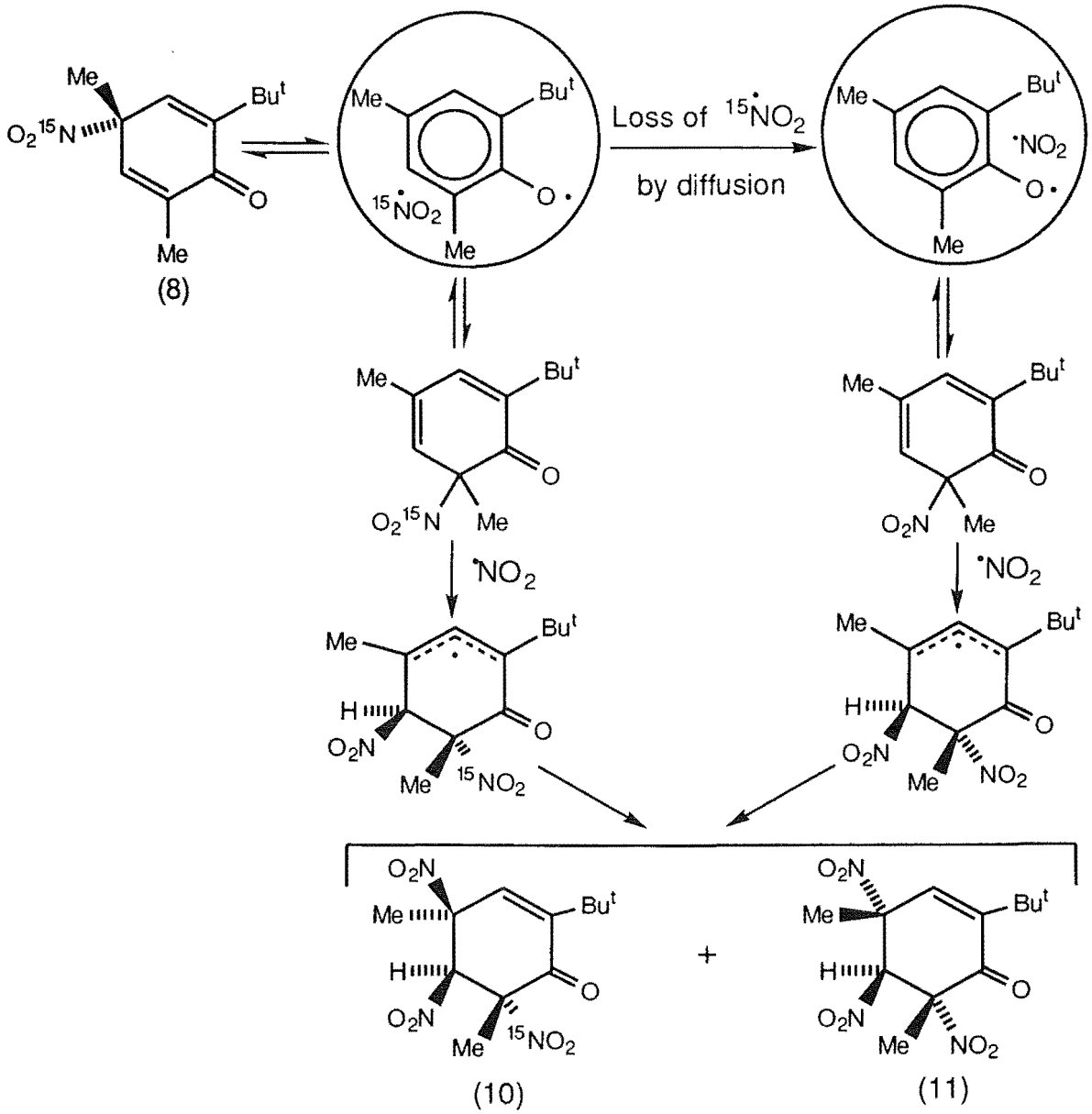

SCHEME 1.14

The initial nitro migration terminus is determined by the difference in size of the 2-t-butyl and 6-methyl groups. Subsequent addition of nitrogen dioxide to the 6-methyl-6-nitrocyclohexa-2,4-dienone is controlled by the difference in steric size of the C2 (t-butyl) and C4 (methyl) substituents.

1.4 ELECTROPHILIC ATTACK ON PHENOLS

The addition of a hydroxyl group to an aromatic ring has a marked affect on the reactivity of the system. A number of reviews cover the broad spectrum of chemistry of these compounds.[17,18] Due to the electron donating character of the -OH the aromatic ring is activated towards electrophilic attack in relation to unsubstituted benzene. The relative rates of nitration of various aromatic compounds with nitric acid are given in examples in Table 1.1.[19]

Table 1.1 Relative rates of nitration using nitric acid.

Compound	k_{rel}
Benzene	1
Toluene	25
Phenol	1000
Chlorobenzene	0.03
Nitrobenzene	6×10^{-8}

For phenols, the *ortho* and *para* positions are favoured over the *meta* positions for electrophilic attack due to delocalisation of the oxygen lone pairs into the ring as illustrated in Scheme 1.15.

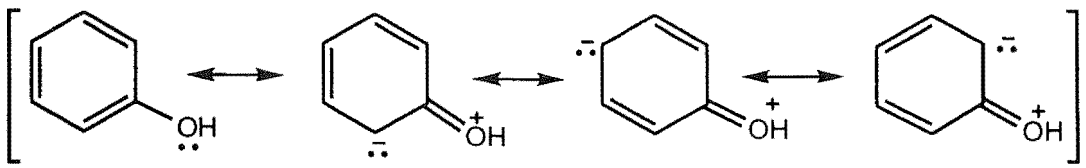

SCHEME 1.15

The phenols examined in this section of work were substituted in both the *ortho* and *para* positions, by either a halogen or a methyl group, neither of these

substituents are stable as leaving groups. Upon generation of the Wheland intermediates substitution of the substituent groups is unlikely because of their instability as leaving groups. The neutralisation of the positive charge of the Wheland intermediate will be achieved by some rearrangement process, or more likely, the loss of the hydroxy proton and rapid generation of a dienone system as illustrated in Scheme 1.16. Depending on the site of attack of the electrophile on the phenol either a linearly conjugated cyclohexa-2,4-dienone or a cross conjugated cyclohexa-2,5-dienone system is formed.

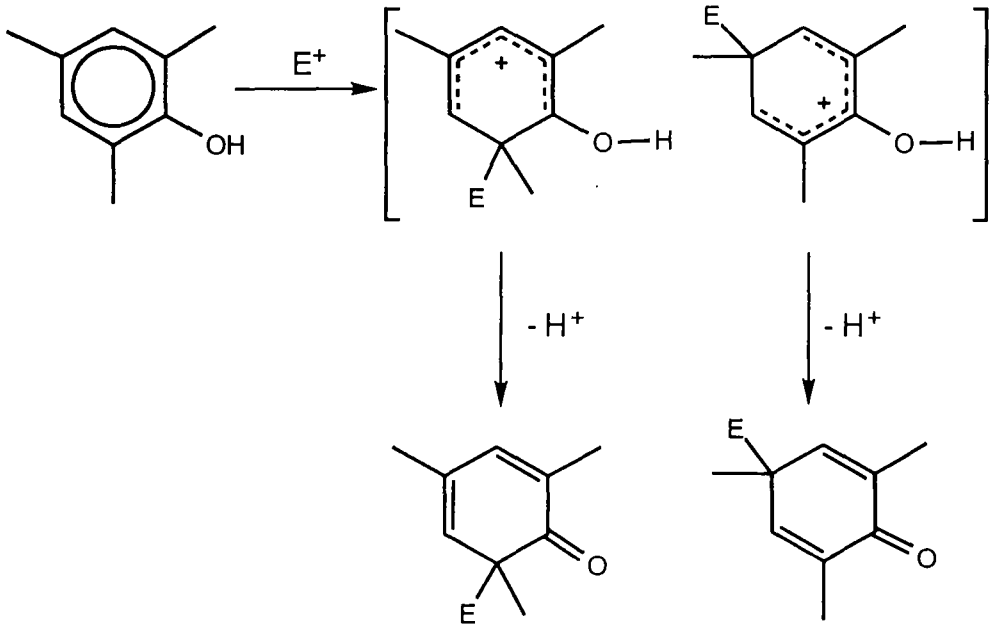

cyclohexa-2,4-dienone cyclohexa-2,5-dienone

SCHEME 1.16

4-Nitrocyclohexa-2,5-dienones are formed from phenols and nitrogen dioxide via a coupling of the corresponding phenoxy radical and nitrogen dioxide.[20,21] An illustration of this is the reaction of nitrogen dioxide with 2,6-di-t-butyl-4-methylphenol (12) as shown in Scheme 1.17.[22] This yields as a product 4-methyl-4-nitro-2,6-di-t-butylcyclohexa-2,5-dienone (14) via the corresponding phenoxy radical (13).

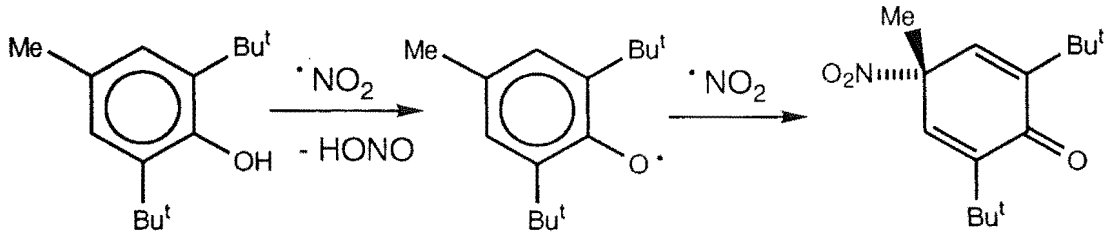

(12) (13) (14)

SCHEME 1.17

Further reaction of 4-nitrocyclohexa-2,5-dienones with nitrogen dioxide yields products identical with those of nitration of the corresponding phenols.[22] Reaction of the 2-t-butyl-4,6-dimethyl-4-nitro-cyclohexa-2,5-dienone (8), corresponding to phenol (15), with nitrogen dioxide in benzene resulted in the complete conversion into a mixture of the trinitroketones (10) and (11) as discussed previously, which was similar to that obtained when the corresponding phenol (15) was nitrated as illustrated below in Scheme 1.18.

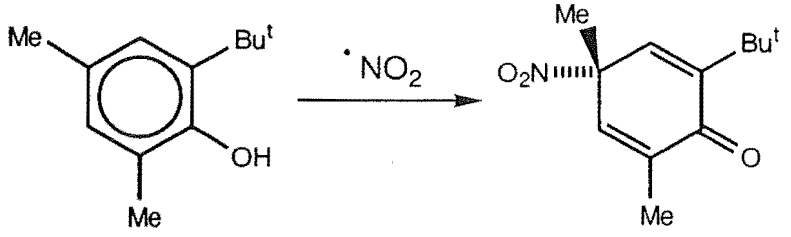

(15) (8)

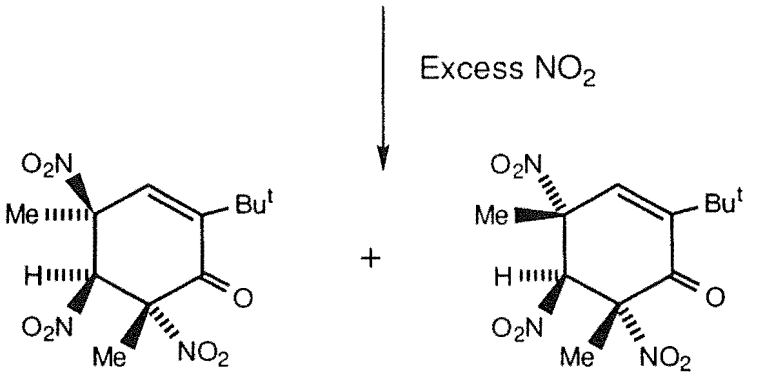

(10) (11)

SCHEME 1.18

1.5 NITRATION REACTIONS OF 2,4,6-TRIALKYLPHENOLS

The reactions of 2,4,6-trialkyl phenols with nitrogen dioxide yield a variety of compounds illustrating a diversity of reaction possibilities for this type of compound.[23,24]

The nitration of 4-t-butyl-2,6-dimethylphenol (16)[23] with nitrogen dioxide in benzene yields four 2,5,6-trinitrocyclohex-3-enones (17)-(20) and the 6-hydroxy dinitro ketone (21).

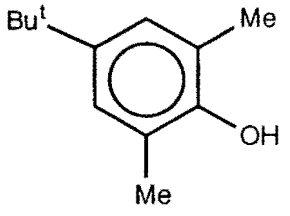

(16)

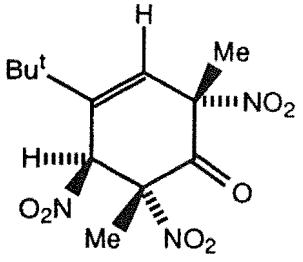

(17)

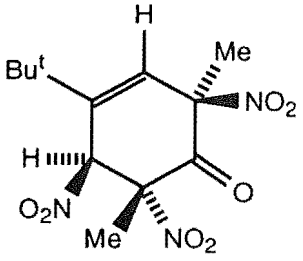

(18)

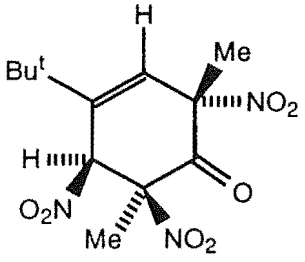

(19)

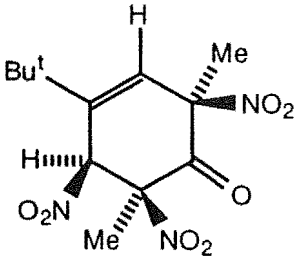

(20)

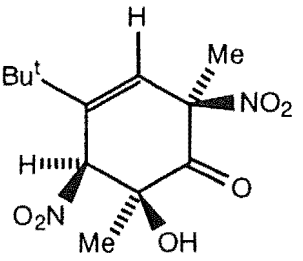

(21)

The nitration of 2,4-di-t-butyl-6-methylphenol (22) with nitrogen dioxide in benzene gives as reaction products substituted cyclohex-3-enones, 2,5,6-trinitro ketones (23)-(26), 2-hydroxy-5,6-dinitro ketones (27)-(28) and the 6-

hydroxy-2,5-dinitro ketone (29).[24] This nitration reaction illustrates how varied the reaction products can be.

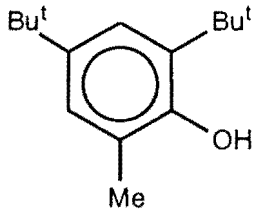

(22)

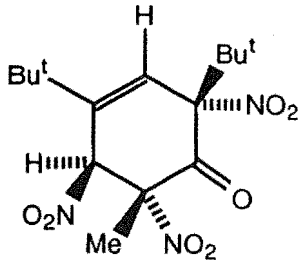

(23)

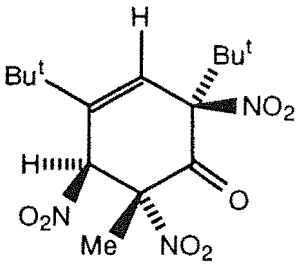

(24)

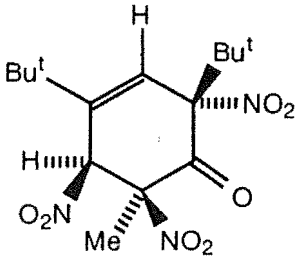

(25)

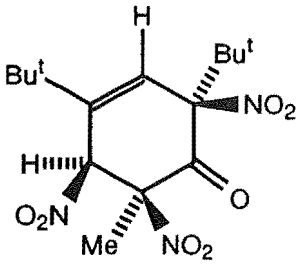

(26)

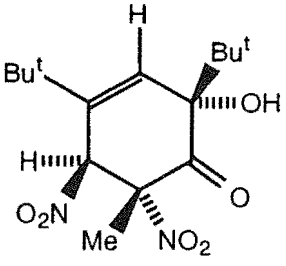

(27)

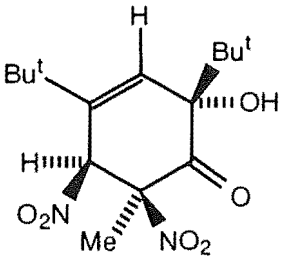

(28)

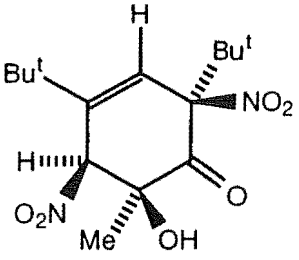

(29)

The corresponding 4-nitrocyclohexa-2,5-dienones have been established as intermediates in the above nitrations.[23,24] Similarly, nitration of 4-nitrocyclohexa-2,5-dienone (9), corresponding to phenol (22), resulted in a complete conversion into a mixture of the four trinitroketones (23)-(26), the two C6-epimeric 2-hydroxy nitro ketones (27) and (28), and the 6-hydroxy dinitro ketone (29). The ratio of products formed was similar to that found for the nitration reaction of phenol (22) in benzene, consistent with the intermediacy of the 4-nitrodienones in the reaction pathways.[25]

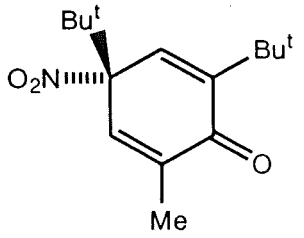

(9)

The mechanism of formation of these products can be explored by labelling the known intermediate 4-nitrocyclohexa-2,5-dienone corresponding to the phenol with ^{15}N. For example, Jensen[26] reacted the ^{15}N-labelled 4-nitrocyclohexa-2,5-dienone (9a) with pure nitrogen dioxide in benzene. The product mixture was separated into its components by chromatography.

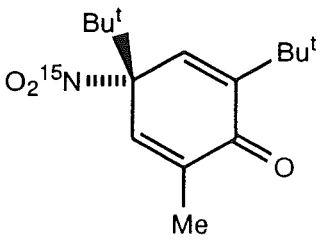

(9a)

The four isomeric trinitro ketones (23)-(26) were shown to contain ^{15}N-label located at the C6 position to the extent of *c.* 60±5%. The degree of ^{15}N incorporation is estimated from the integral for the C6-methyl in each case. These results may be rationalised in terms of the formation of the trinitro ketones (23)-(26) by a mechanistic scheme as shown in Scheme 1.19 overleaf. The trinitro ketones (23)-(26) are formed from the intermediate delocalised radicals (30) by radical coupling with nitrogen dioxide and C2-N bond formation. The C6-epimeric 2-hydroxy-5,6-dinitro ketones (27) and (28) were also shown to contain ^{15}N-label at C6 to the extent of *c.* 60±5%. These results parallel those obtained for the trinitro ketones (23)-(26) and may be rationalised in a similar fashion. Radical coupling of the delocalised radicals (30) with nitrogen

dioxide resulting in C2-O bond formation, followed by hydrolysis of the initially formed nitrite esters, would give rise to the C6-epimeric-2-hydroxy-5,6-dinitro ketones (27) and (28) with the same extent of labelling at C6 as was observed for the trinitro ketones (23)-(26)[26].

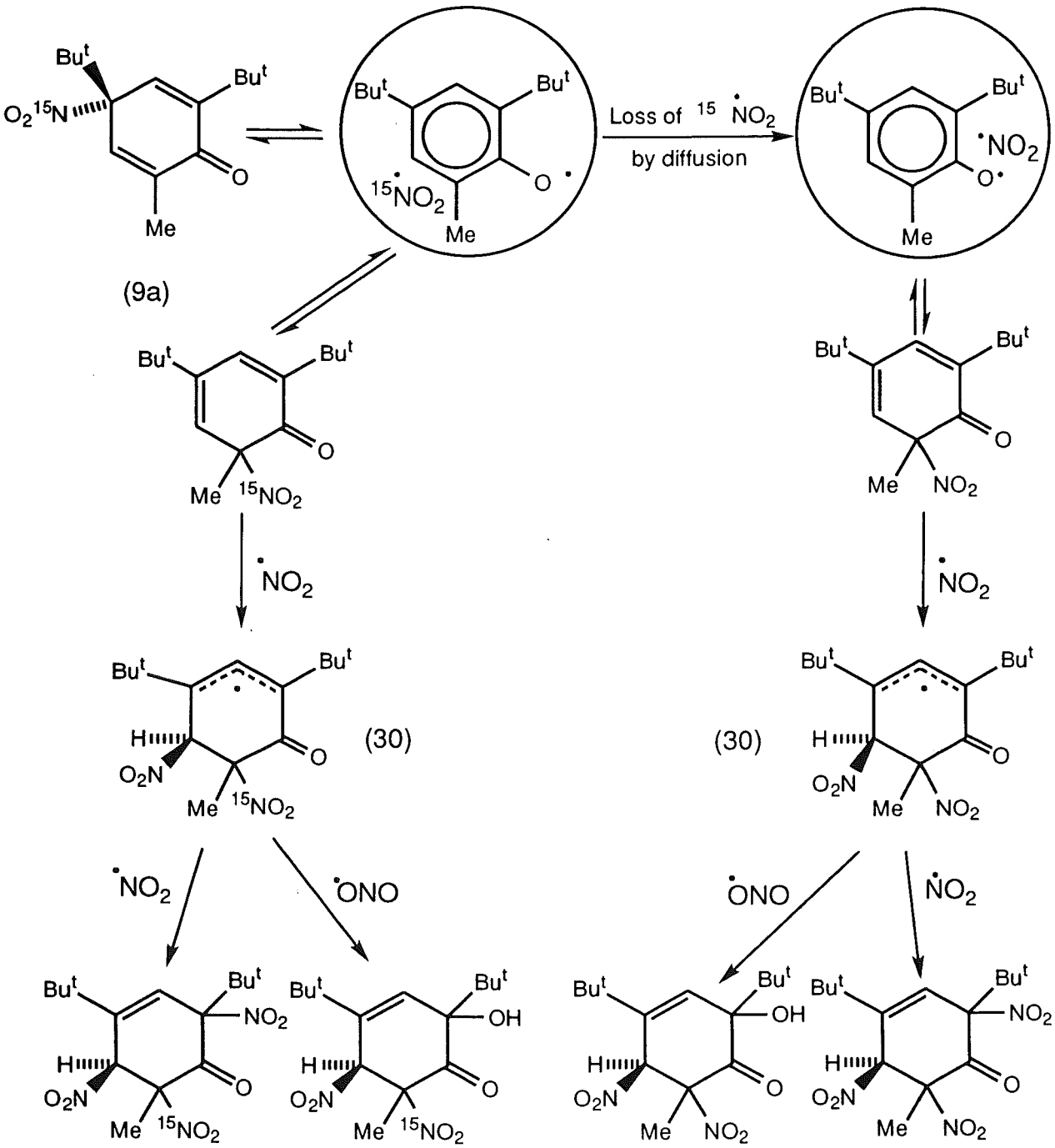

SCHEME 1.19

It is now clear, from this and earlier work, that the conversion of 2,4,6-trialkyl phenols into the corresponding 2,4,6-trialkyl-2,5,6-trinitrocyclohex-3-enones occurs *via* addition of nitrogen dioxide to the corresponding 2,4,6-trialkyl-6-nitrocyclohexa-2,4-dienone.

The major aim of this section of thesis is to explore further the mechanism of reaction with nitrogen dioxide of unsymmetrically substituted phenols and their derived 4-nitrocyclohexa-2,5-dienones. For example, the reactions with nitrogen dioxide of 4-chloro-2,3,6-trimethylphenol (31), 2,3,4,6-tetramethylphenol (32) 3-chloro-2,4,6-trimethylphenol (33) will be discussed. This investigation will involve the identification of the individual reaction products and subsequent ^{15}N-labelling studies of the reactions of the 4-nitrocyclohexa-2,5-dienone derivatives of each substituted phenol will be discussed.

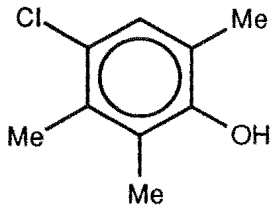

(31)

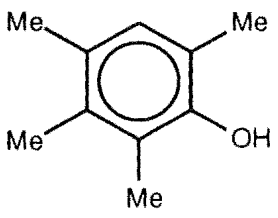

(32)

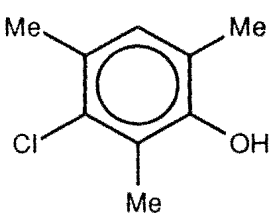

(33)

Scheme 1.20 shows the two rearrangement possibilities available to an unsymmetrical 4-nitro-2,5-dienone (34) by typical extramolecular migration of the 4-nitro group to either the C2 or C6 position giving either of the two possible 6-nitro-2,4-dienones, (35) and (36). The final nitration products would be derived either by 2,5-addition of nitrogen dioxide to (35), or by corresponding 2,5 addition of nitrogen dioxide to (36) as illustrated. The focus of this investigation will be on the effect the C3 substituent (R^{II}) has on the reaction pathway taken in the product determining extramolecular migration of nitrogen dioxide to give the 6-nitrocyclohexa-2,4-dienones (35) and (36).

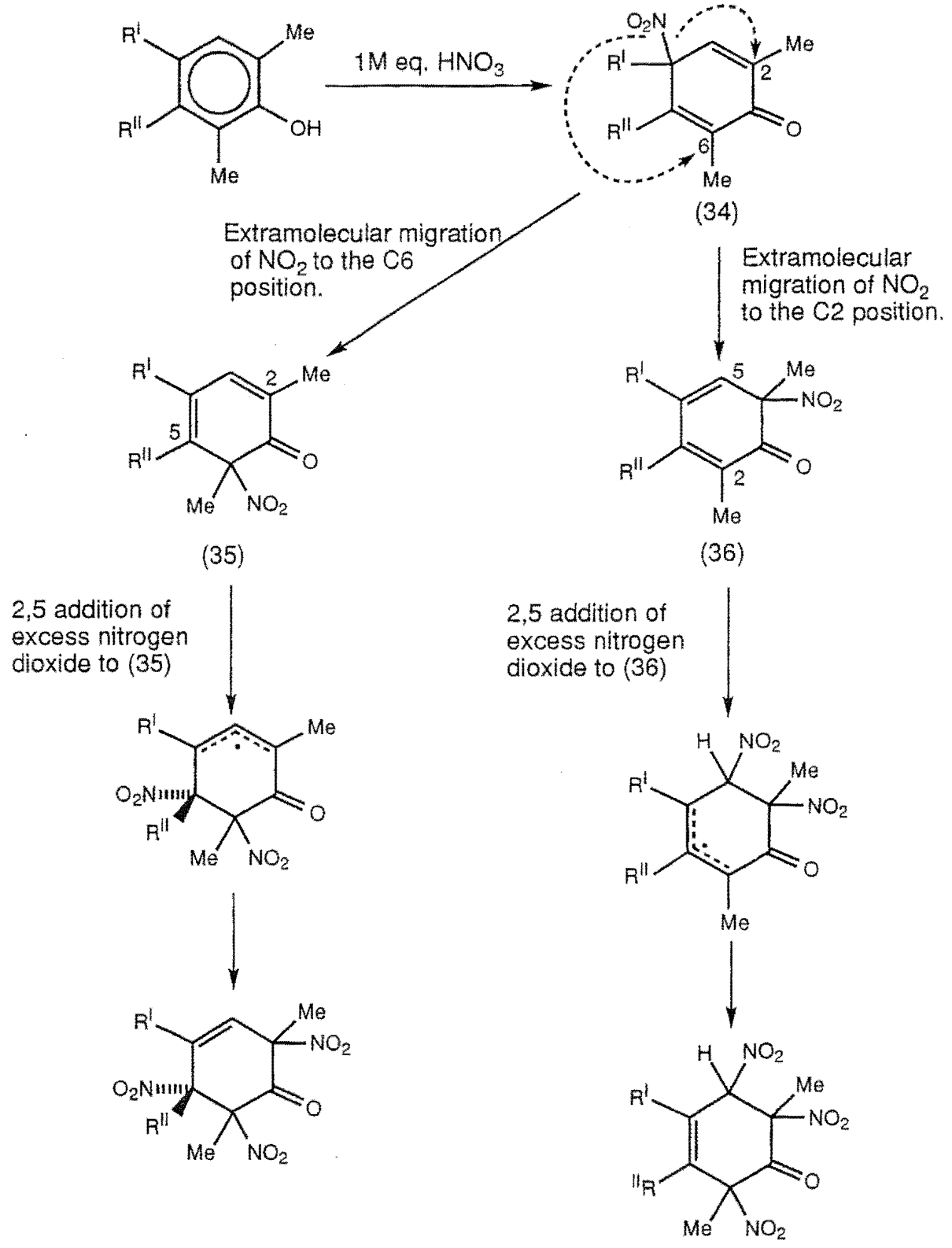
1M eq. HNO3
(34)
Extramolecular migration of NO2 to the C6 position.
Extramolecular migration of NO2 to the C2 position.
(35)
(36)
2,5 addition of excess nitrogen dioxide to (35)
2,5 addition of excess nitrogen dioxide to (36)

SCHEME 1.20

CHAPTER TWO

NITRATION OF 4-CHLORO-2,3,6-TRIMETHYLPHENOL

2.1 INTRODUCTION

As outlined in Chapter 1, investigations into the nitration of unsymmetrical phenols are being carried out to gain a better understanding of the nitration mechanism. For each substituted phenol and corresponding 4-nitrocyclohexa-2,5-dienone the products of the reaction with nitrogen dioxide will be identified and their mode of formation determined using ^{15}N-labelling techniques. It is anticipated that the results will throw further light on the effects of substituents on the reactions of phenols with nitrogen dioxide.

At an early stage of the examination of the nitration reaction products of phenol (31) with nitrogen dioxide in benzene it became apparent that a number of hydroxy dinitro ketones were present among the products. In order to more readily isolate and identify these compounds, the nitration of phenol (31) with fuming nitric acid in acetic acid was examined, a reaction known to favour the formation of hydroxy dinitro ketones rather than trinitro ketones.[27]

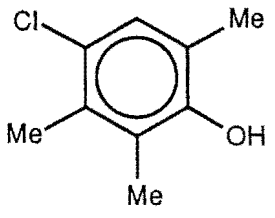

(31)

2.2 NITRATION REACTIONS OF 4-CHLORO-2,3,6-TRIMETHYLPHENOL (31)

2.2.1 The Nitration of 4-Chloro-2,3,6-trimethylphenol (31) with Fuming Nitric Acid in Acetic Acid

Fuming nitric acid was added dropwise to a stirred suspension of the phenol (31) in glacial acetic acid to give a dark orange/red solution which was stirred at 20°C for 1 min. The mixture was dissolved in ether, the organic layer washed with water, dried with magnesium sulphate and the solvent removed under reduced pressure to give a yellow residue. (Detailed reaction conditions are set out in the experimental section relating to Chapter 2.)

The product from this nitration was essentially a mixture of four hydroxy dinitro ketones (37) - (40), and 2,3,5-trimethyl-1,4-benzoquinone (41), the latter presumably being formed by loss of the elements of NOCl from the intermediate 4-nitro dienone (42). The components of this mixture were separated by fractional crystallization.

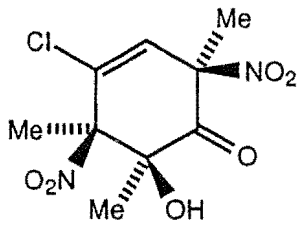

(37)

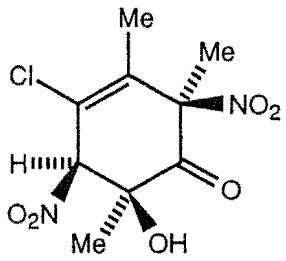

(38)

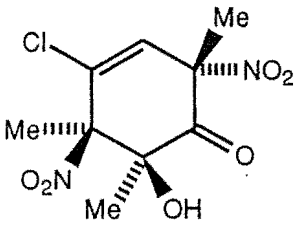

(39)

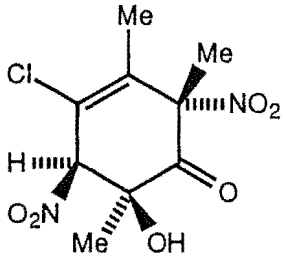

(40)

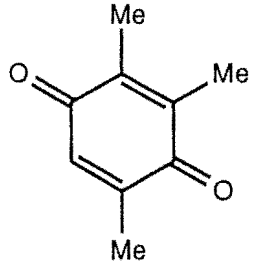

(41)

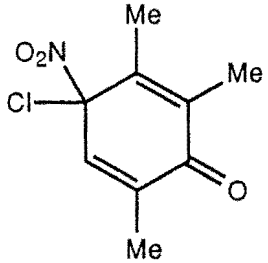

(42)

The structure of the least soluble compound (37) was determined by single crystal X-ray analysis after isolation of (37) by fractional crystallization from dichloromethane and ether mixtures of the product mixture . The perspective drawing of 4-chloro-*c*-6-hydroxy-2,5,6-trimethyl-*r*-2,*c*-5-dinitrocyclohex-3-enone (37), $C_9H_{11}ClN_2O_6$, m.p. 132-133°C, is presented in Fig. 2.1, with corresponding atomic coordinates in Table 5.1.

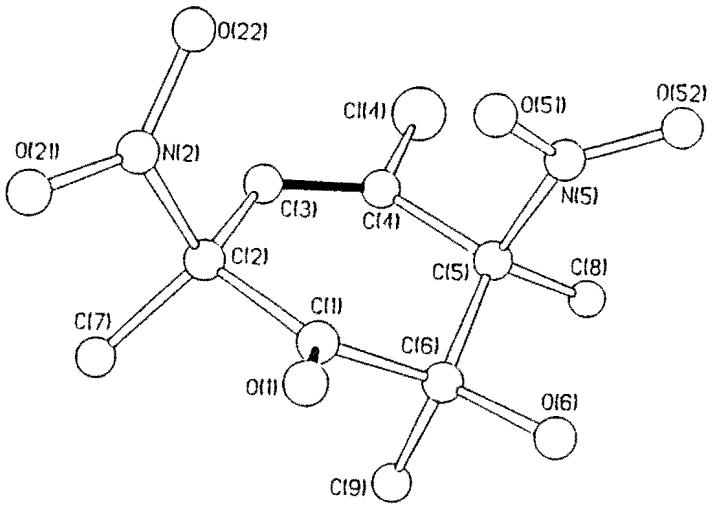

FIGURE 2.1

Perspective drawing of 4-chloro-*c*-6-hydroxy-2,5,6-trimethyl-*r*-2,*c*-5-dinitrocyclohex-3-enone (37)

In the solid state the alicyclic ring of the *cis*-dinitro ketone (37) exists in a flattened chair conformation.

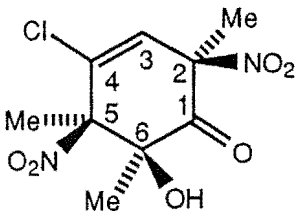

(37)

The ^1H and ^{13}C NMR spectra of adduct (37) were assigned from long range reverse detected ^1H - ^{13}C heteronuclear correlation spectra (HMBC). In particular, the ^{13}C resonances of the **C(1)**=O (δ 195.7), H-**C(3)**= (δ 129.9), and

Cl-**C(4)**= (δ 132.1) were assigned. Characteristic i.r. absorptions were observed for the functional groups associated within compound (37) as illustrated in Table 2.1.

TABLE 2.1 Characteristic i.r. absorptions ν_{max} (KBr) for compound (37).

Functional Group	Absorption (cm^{-1})
-OH	3493
C=O	1739
C=C	1637
NO_2	1569

4-Chloro-*c*-6-hydroxy-2,3,6-trimethyl-*r*-2,*c*-5-dinitrocyclohex-3-enone (38), was obtained from fractional crystallization of the product mixture using ether/pentane mixtures. Crystals were obtained that were suitable for single crystal X-ray analysis and the perspective drawing of 4-chloro-*c*-6-hydroxy-2,3,6-trimethyl-*r*-2,*c*-5-dinitrocyclohex-3-enone (38), $C_9H_{11}ClN_2O_6$, m.p. 139-141°C is presented in Figure. 2.2 with the corresponding atomic coordinates in Table 5.2.

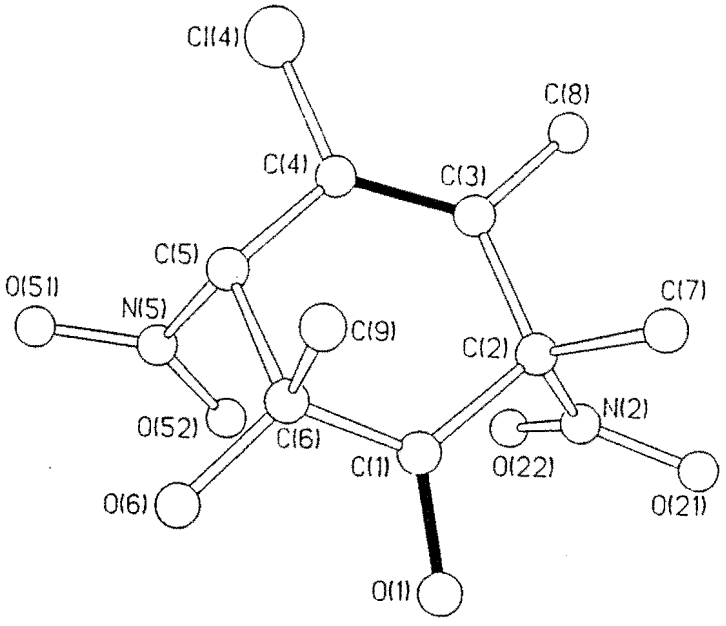

FIGURE 2.2

Perspective drawing of 4-chloro-*c*-6-hydroxy-2,3,6-trimethyl-*r*-2,*c*-5-dinitrocyclohex-3-enone (38)

In the solid state the alicyclic rings of the two *cis*-dinitro ketones (37) and (38) exist in closely similar flattened chair conformations. Table 2.2 gives a comparison of the torsion angles associated with the flattened chair conformation of (37) and (38).

Table 2.2 Comparison of torsional angles (°) of compounds (37) and (38).

Compound (37) atoms	Torsion angles	Compound (38) atoms	Torsion angles
C1-C2-C3-C4		C1-C2-C3-C4	11.0°(2.6)
C3-C4-C5-C6		C3-C4-C5-C6	27.4°(2.7)
C4-C5-C6-C1		C4-C5-C6-C1	-46.8°(2.1)
C6-C1-C2-C3		C6-C1-C2-C3	-33.8°(2.1)

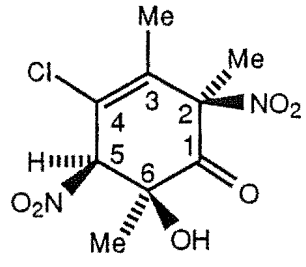

(38)

The ^{1}H and ^{13}C NMR spectra of adduct (38) were assigned from long range reverse detected ^{1}H - ^{13}C heteronuclear correlation spectra (HMBC). The ^{13}C resonances were assigned as illustrated in Table 2.3.

Table 2.3 ^{13}C NMR ($CDCl_3$) resonances for compound (38).

Chemical Shift (ppm)	Assignment
198.5	C1
132.7	C3
130.1	C4
125.0	C2
97.3	C5
75.8	C6
24.8, 23.9	2-Me, 3-Me
16.7	6-Me

4-Chloro-*t*-6-hydroxy-2,5,6-trimethyl-*r*-2,*t*-5-dinitrocyclohex-3-enone (39), was obtained from the fractional crystallization using ether and pentane mixtures. Crystals were obtained that were suitable for single crystal X-ray analysis and the perspective drawing of 4-chloro-*t*-6-hydroxy-2,5,6-trimethyl-*r*-2,*t*-5-dinitrocyclohex-3-enone (39), $C_9H_{11}ClN_2O_6$, m.p. 97-98°C is presented in Figure. 2.3 with the corresponding atomic coordinates in Table 5.3.

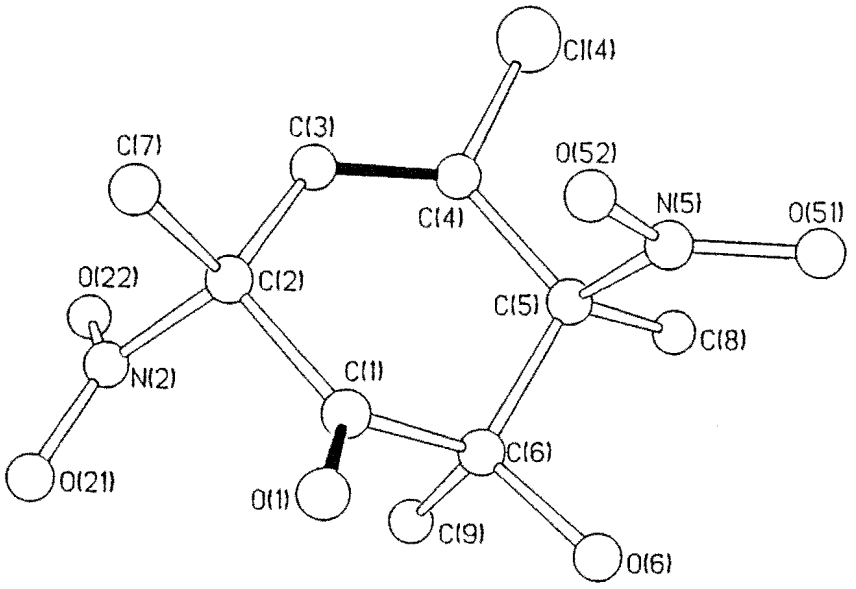

FIGURE 2.3

Perspective drawing of 4-chloro-*t*-6-hydroxy-2,5,6-trimethyl-*r*-2,*t*-5-dinitrocyclohex-3-enone (39)

In the solid state the *trans*-dinitro ketone (39) adopts a skew boat conformation.

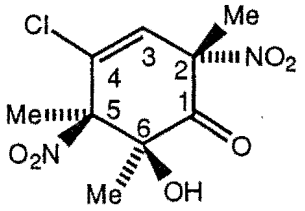

(39)

The ^{1}H and ^{13}C NMR spectra of adduct (39) were assigned from long range reverse detected 1H - 13C heteronuclear correlation spectra (HMBC). The ^{13}C resonances of the **C(1)**=O (δ 195.6), H-**C(3)**= (δ 130.3), Cl-**C(4)**= (δ 133.6) and Me-**C(6)**-OH (δ 65.3) were assigned. In particular, for the 5-methyl-dinitro ketones (37) and (39) the ^{1}H NMR. resonance for the C3-proton in the *trans*-dinitro compound (39) appeared 0.17 ppm. downfield of the chemical shift of the corresponding proton for the *cis*-dinitro compound (37), consistent with earlier stereochemistry/chemical shift correlations as illustrated in Table 2.4 and Figure 2.4.[28] For a given 5,6-stereochemistry, the H3 resonance for *r*-2,*t*-5-dinitro compounds occurs downfield (Δδ 0.10 - 0.20) from the H3 resonance for *r*-2,*c*-5-dinitro compounds.[28]

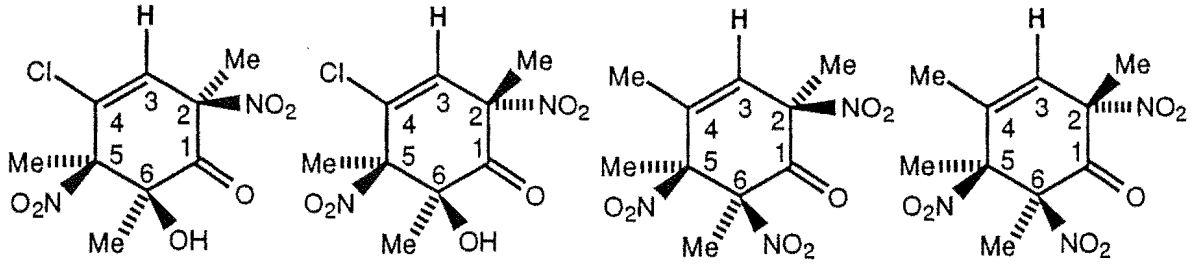

(37) *r*-2,*c*-5 (39) *r*-2,*t*-5 (43)*r*-2,*c*-5 (44) *r*-2,*t*-5

analogous tetramethyl trinitro derivatives

FIGURE 2.4

Table 2.4 ^{1}H NMR ($CDCl_3$) chemical shifts for H3 in compounds (37), (39) (43) and (44).

Compounds	r-2,t-5	r-2,c-5	Δδ
(37) and (39)	6.73	6.56	0.17
(43) and (44)	6.47	6.30	0.10

The remaining hydroxy dinitro ketone, 4-chloro-*t*-6-hydroxy-2,3,6-trimethyl-*r*-2,*t*-5-dinitrocyclohex-3-enone (40), was only obtained in the solid state co-crystallized (1:1) with 4-chloro-*t*-6-hydroxy-2,5,6-trimethyl-*r*-2,*t*-5-dinitro-cyclohex-3-enone (39). The crystals were obtained from ether and pentane mixtures and the structure was determined by X-ray crystal analysis. A perspective drawing is presented in Fig. 2.5, with corresponding atomic coordinates presented in Table 5.4.

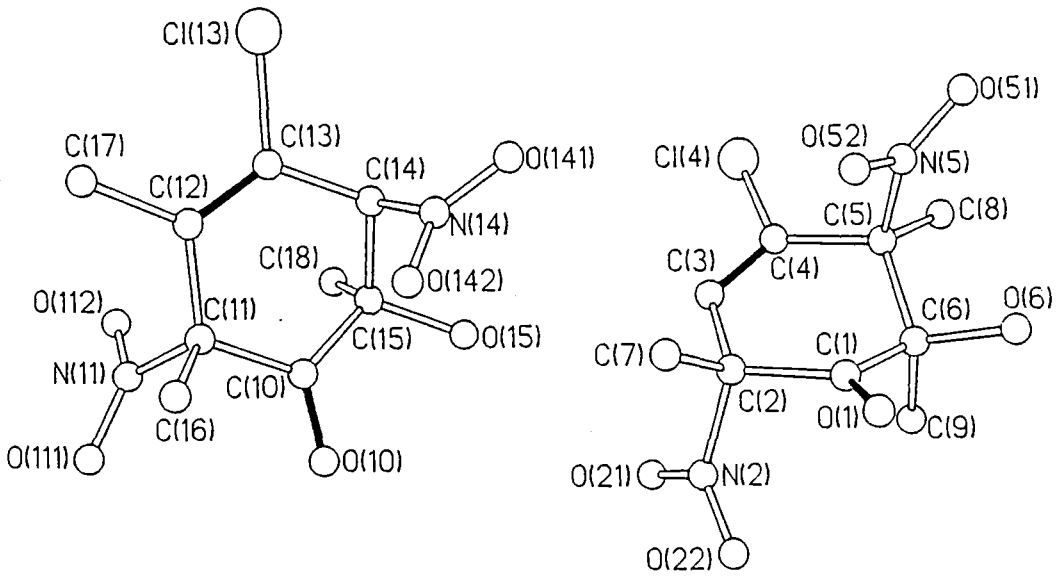

FIGURE 2.5

Perspective diagram of 4-chloro-*t*-6-hydroxy-2,3,6-trimethyl-*r*-2,*t*-5-dinitrocyclohex-3-enone (40) and 4-chloro-*t*-6-hydroxy-2,5,6-trimethyl-*r*-2,*t*-5-dinitro-cyclohex-3-enone (39).

In the solid state the structure of the *trans*-dinitro ketones (39) and (40) adopt similar skew boat conformations. The notable differences can be observed in Figure 2.6 compound (39) has been mapped onto compound (40). The molecular shape of the *trans*-dinitro 5-methyl ketone (39) is closely similar in the pure crystal and in crystalline material where it co-crystallized with the *trans*-dinitro 3-methyl ketone (40).

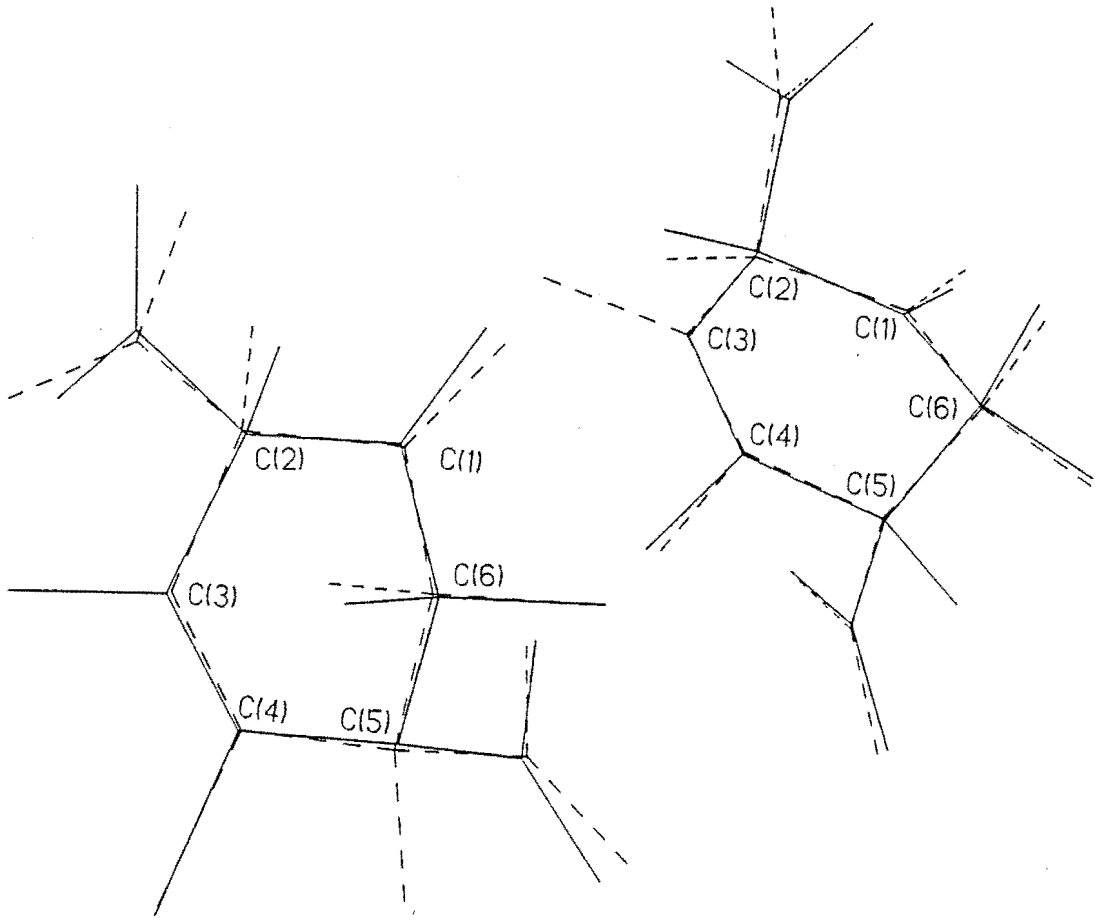

Figure 2.6 Compound (39) — mapped onto compound (40) --- in two different orientations.

A comparison of the torsional angles associated with pure compound (39) and (39) in a 1:1 mixture with compound (40) is illustrated in Table 2.5.

Table 2.5 Comparison of torsional angles (°) of compound (39) in a pure state and those associated with compound (39) in a mixture with compound (40).

Pure compound (39)	Torsion angles (°)	(39) in a 1:1 mixture with (40)	Torsion angles (°)
C3-C4-C5-C6	18.5(3)	C3-C4-C5-C6	22.7(5)
C4-C3-C2-C1	-1.0(3)	C4-C3-C2-C1	-1.0(5)
O21-N2-C2-C7	-65.8(3)	O21-N2-C2-C7	-74.4(4)
O1-C1-C6-O6	-12.5(3)	O1-C1-C6-O6	-15.3(5)
C3-C4-C5-N5	-93.4(3)	C3-C4-C5-N5	-89.4(4)
O6-C6-C5-N5	-50.5(2)	O6-C6-C5-N5	-52.7(3)

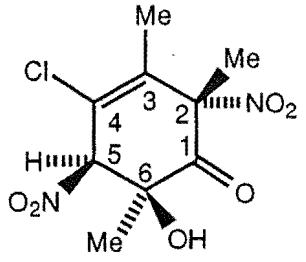

(40)

The ^{1}H and ^{13}C NMR spectra of adduct (40) were assigned from long range reverse detected ^{1}H - ^{13}C heteronuclear correlation spectra (HMBC) after subtraction of the NMR solution spectra of compound (39). In particular, the ^{13}C resonances of the **C(1)**=O (δ 197.6), H-**C(3)**= (δ 143.5), Cl-**C(4)**= (δ 130.7) and Me-**C(6)**-OH (δ 58.7) were assigned.

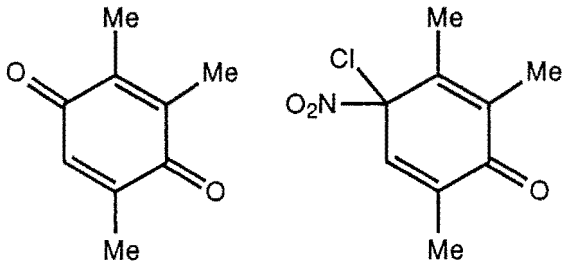

(41) (42)

2,3,5–Trimethyl-1,4-benzoquinone (41) was purified from the crude product mixture by fractional crystallization using a pentane solution. Confirmation of the presence of 2,3,5–trimethyl-1,4-benzoquinone (41) was possible with comparisons of authentic 2,3,5–trimethyl-1,4-benzoquinone being identical with the material isolated from the crude mixture by fractional crystallization.

The nitro/nitrito rearrangement of an *ipso* intermediate has been observed in chloroform to give the nitrito isomer and its corresponding hydroxy compound is assumed to be homolytic in nature.[29] The following Scheme 2.1 illustrates the reported conversion of an *ipso*-nitro to an *ipso*-hydroxy *via* an *ipso*-nitrito intermediate.[29]

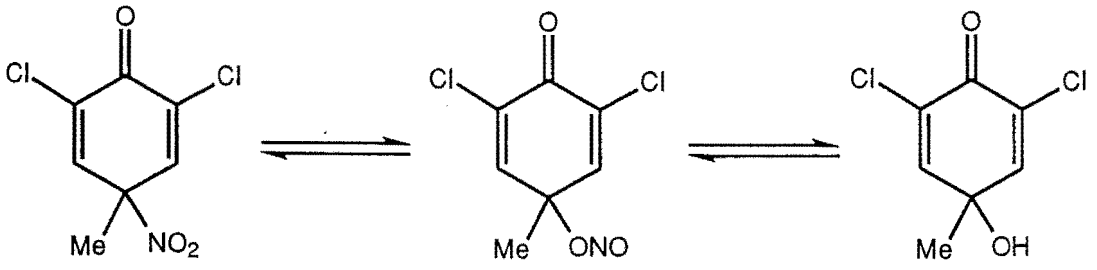

ipso -nitro *ipso* -nitrito *ipso* -hydroxy

SCHEME 2.1

Scheme 2.2 illustrates a possible mechanism for loss of NOCl from the *ipso*-nitrito intermediate to give 2,3,5–trimethyl-1,4-benzoquinone (41).

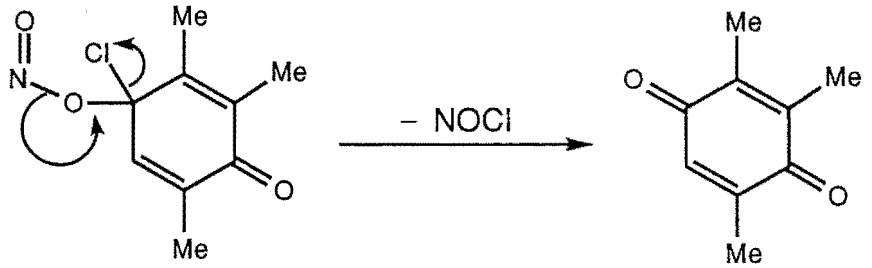

nitrito rearrangement product (41)

SCHEME 2.2

Concern that this rearrangement resulting in loss of NOCl might make the preparation of pure 4-nitrocyclohexa-2,5-dienone (42) very difficult prompted attempts to prepare the 4-nitrocyclohexa-2,5-dienone (42).

2.2.2 Attempted Preparation of 4-Chloro-2,3,6-trimethyl-4-nitrocyclohexa-2,5-dienone (42).

After isolation and characterisation of all the products from the above nitration reaction of 4-chloro-2,3,6-trinitromethylphenol the formation of the corresponding 4-nitrocyclohexa-2,5-dienone (42) was attempted.

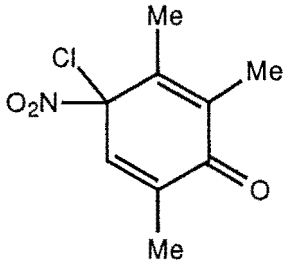

(42)

Concentrated nitric acid was added dropwise to a stirred suspension of 4-chloro-2,3,6-trimethylphenol (31) in acetic acid. The product was extracted using petroleum ether and the petroleum ether solution washed with water. The organic layer was separated, dried and the solvent removed under

reduced pressure to give a yellow residue shown to be 2,3,5-trimethyl-1,4-benzoquinone (41), identical with authentic material.

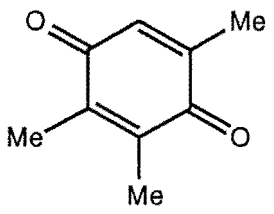

(41)

Unfortunately the attempts at preparing 4-nitrocyclohexa-2,5-dienone (42) were unsuccessful and large quantities of 2,3,6-trimethylbenzoquinone (41) were isolated. Because 4-nitrocyclohexa-2,5-dienone (42) could not be isolated from nitric acid nitration of 4-chloro-2,3,6-trimethylphenol (31) it was not possible to undertake ^{15}N-labelling studies.

2.2.3 Reaction of 4-Chloro-2,3,6-trimethylphenol (31) with Nitrogen Dioxide in Benzene

A solution of the phenol (31) in benzene was deoxygenated by a stream of pure nitrogen. Pure nitrogen dioxide was bubbled through the stirred solution at 0°C for 1 min., and the resulting solution stirred for 2 h. at 0°C under a positive pressure of nitrogen dioxide. The excess nitrogen dioxide was removed in a stream of nitrogen, and the solvent removed under reduced pressure to give a viscous pale yellow oil. This oil was shown (^1H NMR spectra) to be a mixture of four major and a number of minor components. A number of the components of this mixture were separated by chromatography on a silica gel Chromatotron plate. (Detailed reaction conditions are set out in the experimental section relating to Chapter 2.)

Chromatography on a silica gel Chromatotron plate allowed the separation of the major and some of the minor components of the mixture, with the 6-hydroxy-2,3,6-trimethyl-2,5-dinitrocyclohex-3-enones (38) and (40) being eluted together and identified from their known ^1H NMR. spectra. Similarly pure samples of the isomeric 6-hydroxy-2,5,6-trimethyl-2,5-dinitrocyclohex-3-enones (37) and (39) were obtained and identified by comparison with authentic material. 2,3,5-trimethyl-1,4-benzoquinone (41) was purified using silica gel chromatography and identified by comparison with authentic material.

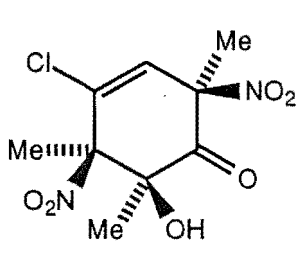

(37)

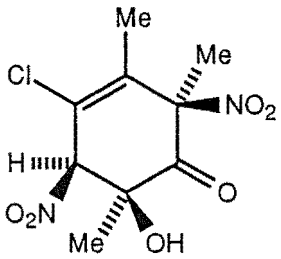

(38)

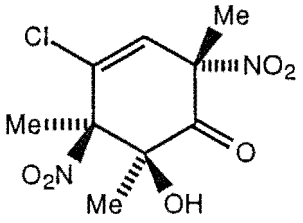

(39)

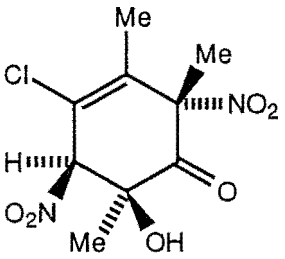

(40)

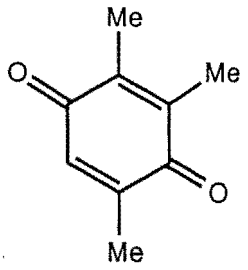

(41)

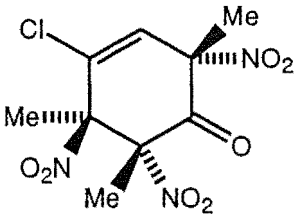

(45)

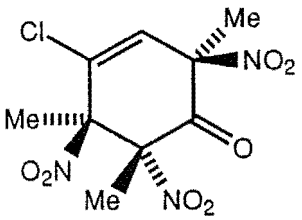

(46)

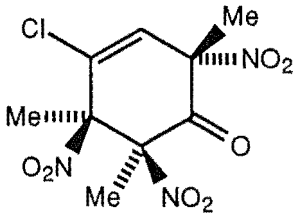

(47)

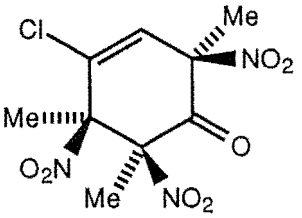

(48)

Of the four isomeric 2,5,6-trimethyl-2,5,6-trinitrocyclohex-3-enones (45 - 48) crystals of a quality satisfactory for single-crystal X-ray analysis could be obtained only for compounds (45) and (47), compound (46) proving to be

unstable and compound (48) gave only microcrystalline material. The structural assignments for these compounds (45 - 48) were based on:

(i) X-ray crystal analyses for isomers (45) and (47),

(ii) the known elution [28] order from a Chromatotron silica gel plate for 2,5,6-trinitro-cyclohex-3-enones: *r*-2,*t*-5,*c*-6-; *r*-2,*c*-5,*t*-6-; *r*-2,*t*-5,*t*-6-; *r*-2,*c*-5,*c*-6-; and

(iii) a consideration of their spectroscopic data.

Elution with pentane and ether mixtures gave 4-chloro-2,5,6-trimethyl-r-2,t-5,c-6-trinitrocyclohex-3-enone (45) the structure of which was determined by single crystal X-ray analysis. A perspective drawing of 4-chloro-2,5,6-trimethyl-*r*-2,*t*-5,*c*-6-trinitrocyclohex-3-enone (45), $C_9H_{10}ClN_3O_7$, m.p. 78-79°C, is presented in Fig. 2.7, with corresponding atomic coordinates in Table 5.5.

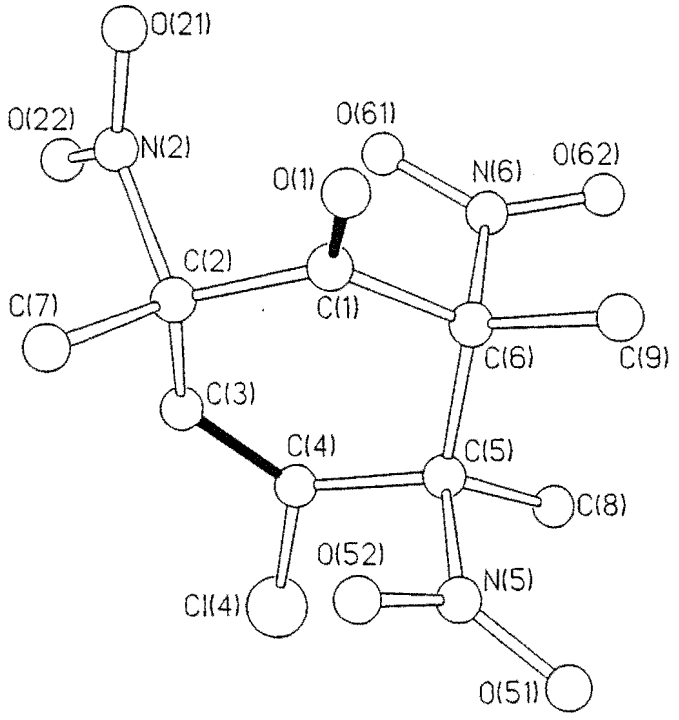

FIGURE 2.7

Perspective diagram of 4-chloro-2,5,6-trimethyl-*r*-2,*t*-5,*c*-6-trinitrocyclohex-3-enone (45)

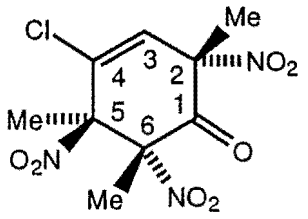

(45)

The ^{1}H and ^{13}C NMR spectra of adduct (45) were assigned from long range reverse detected ^{1}H - ^{13}C heteronuclear correlation spectra (HMBC). In particular, the ^{13}C resonances are presented in Table 2.6.

Table 2.6 ^{13}C NMR ($CDCl_3$) resonances for compound (45).

Chemical Shift (ppm)	Assignment
183.6	C1
131.9	C3
131.9	C4
96.5	C5
92.4	C2
87.4	C6
24.7, 18.6, 16.5	2-Me, 3-Me, 6-Me

Similar information is presented for 4-chloro-2,5,6-trimethyl-*r*-2,*t*-5-*t*-6-trinitrocyclohex-3-enone (47), $C_9H_{10}ClN_3O_7$, m.p. 98-100°C. A perspective drawing is presented in Figure. 2.8 with corresponding atomic coordinates given in Table 5.6.

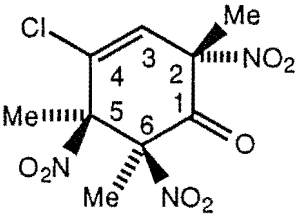

(47)

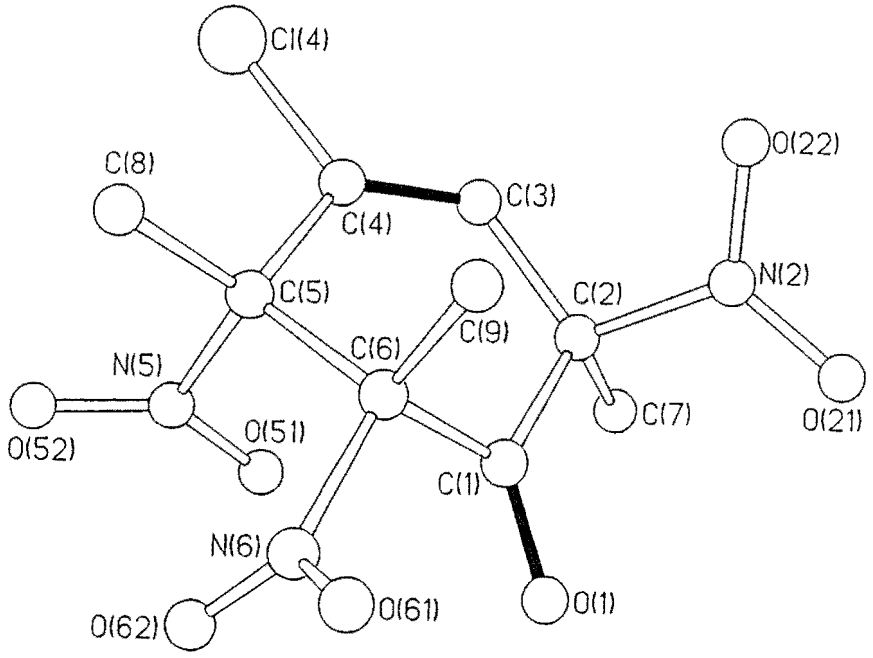

FIGURE 2.8

A perspective diagram of 4-chloro-2,5,6-trimethyl-*r*-2,*t*-5,*t*-6-trinitrocyclohex-3-enone (47)

In the solid state the alicyclic rings of compounds (45) and (47) exist in similar skew boat conformations with the planes of the 5-NO_2 and 6-NO_2 groups close to eclipsed with the C(5)-C(8) and C(6)-C(9) bonds respectively, a comparison of some torsion angles presented in Table 2.7.

Table 2.7 Comparison of torsional angles (°) of compounds (45) and (47).

Compound (45) atoms	Torsion angles	Compound (47) atoms	Torsion angles
C1-C2-C3-C4	9.7°(0.4)	C1-C2-C3-C4	-4.3°(0.5)
C3-C4-C5-C6	-18.7°(0.4)	C3-C4-C5-C6	22.3°(0.4)
C4-C5-C6-C1	37.8°(0.3)	C4-C5-C6-C1	-49.8°(0.3)
C6-C1-C2-C3	13.0°(0.4)	C6-C1-C2-C3	-25.1°(0.4)

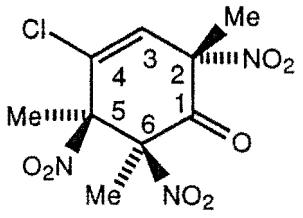

(47)

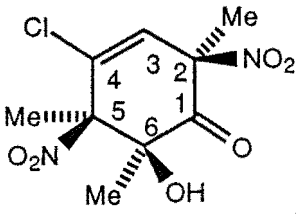

(37)

The spectroscopic data obtained for compound (47) were consistent with the established structure and compared closely to the analogous hydroxy compound (37). The ^{1}H and ^{13}C NMR spectra of adduct (47) were assigned from long range reverse detected ^{1}H - ^{13}C heteronuclear correlation spectra (HMBC). A comparison of the ^{13}C resonances of (37) and (47) in Table 2.8 illustrates the similarities the between the analogous compounds. **C(1)**=O (δ 195.7), H-**C(3)**= (δ 129.9), and Cl-**C(4)**= (δ 132.1) were assigned.

Table 2.8 ^{13}C NMR resonances for compounds (37) and (47).

Chemical Shift (ppm)	Assignment (37)	Chemical Shift (ppm)	Assignment (47)
195.7	C1	184.2	C1
129.9	C3	131.0	C3
132.1	C4	133.9	C4
97.5	C5	95.7	C5
88.7	C2	89.7	C2
23.0, 22.1	2-Me, 3-Me	23.0, 21.3	2-Me, 3-Me

4-Chloro-2,5,6-trimethyl-*r*-2,*c*-5,*t*-6-trinitrocyclohex-3-enone (46) was isolated only in low yield and was also found to be unstable. The parent ion was not visible in the mass spectrum and a satisfactory elemental analysis could not be obtained. The functionality's present in compound (46) were indicated by

characteristic absorptions illustrated in Table 2.9 and the stereochemistry of (46) was assigned on the basis of the characteristic elution order that had been established from previous studies[28] and a consideration of the spectroscopic data.

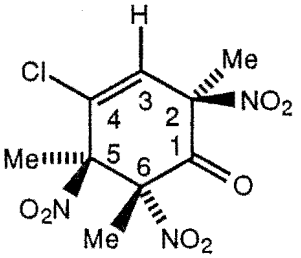

(46)

TABLE 2.9 Characteristic i.r. absorptions for compound (46).

Functional Group	Absorption (cm^{-1})
C=O	1751
C=C	1653
NO_2	1566

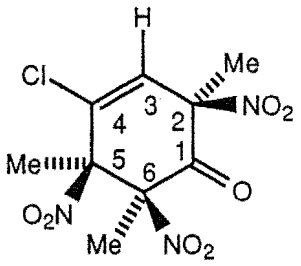

(48)

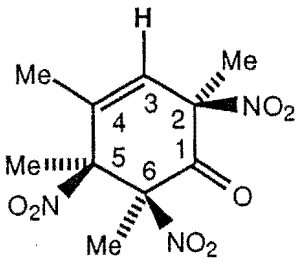

(43) *r*-2,*c*-5

analogous tetramethyl trinitro derivative

Elution with ether/methanol (99:1) gave 4-chloro-2,5,6-trimethyl-r-2,c-5,c-6-trinitrocyclohex-3-enone (48). Elemental analysis confirmed the molecular formula $C_9H_{10}ClN_3O_7$. The stereochemistry of (48) was assigned on the basis of the characteristic insolubility of the all *cis*- trinitro structure[28] and the comparison of the chemical shift data available for compound (46).

Both compounds (46) and (48) exhibited a resonance due to the vinylic H3 coupled to the 4-methyl group as illustrated in Table 2.10.

Table 2.10 ^{1}H NMR ($CDCl_3$) chemical shifts for H3 in compounds (46), (48) and the analogous tetramethyl compounds.

Compound	*r*-2,*t*-5	*r*-2,*c*-5	Δδ
(46) and (48)	6.79	6.66	0.13
Tetramethyl analogues	6.47	6.30	0.17

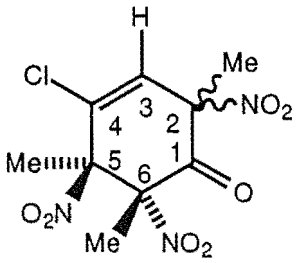

(46) and (48)

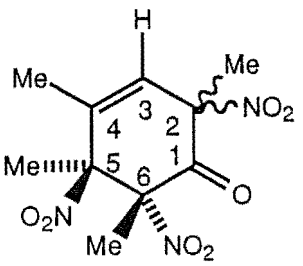

analogous tetramethyl derivatives

The C2-stereochemistry for compounds (46) and (48) were assigned on the basis of the effect of the C2-stereochemistry of such compounds on the chemical shift of the adjacent vinylic H3 resonance. For a given 5,6-stereochemistry, the H3 resonance for *r*-2,*t*-5-dinitro compounds occurs downfield (Δδ 0.10 - 0.20) from the H3 resonance for *r*-2,*c*-5-dinitro compounds.[28] Accordingly, compound (46) which exhibits a H3 resonance at δ 6.79 is assigned the *r*-2,*t*-5 stereochemistry, compared with the *r*-2,*c*-5-dinitro compound (48) (δ 6.47) (Δδ 0.13).

2.3 THE MODE OF FORMATION OF THE 6-HYDROXY-2,5-DINITRO KETONES (37-40)

Reaction of 2,4,5-tribromo-3,6-dimethylphenol (49) in cyclohexane with nitrogen dioxide was studied and observed to give only the *cis* and *trans* 6-hydroxy

dinitro ketones (50) and (51).[30] The formation of the substituted 6-hydroxy cyclohex-3-enones (50) and (51) have been accounted for previously in terms of the reaction pathway outlined in Scheme 2.3.

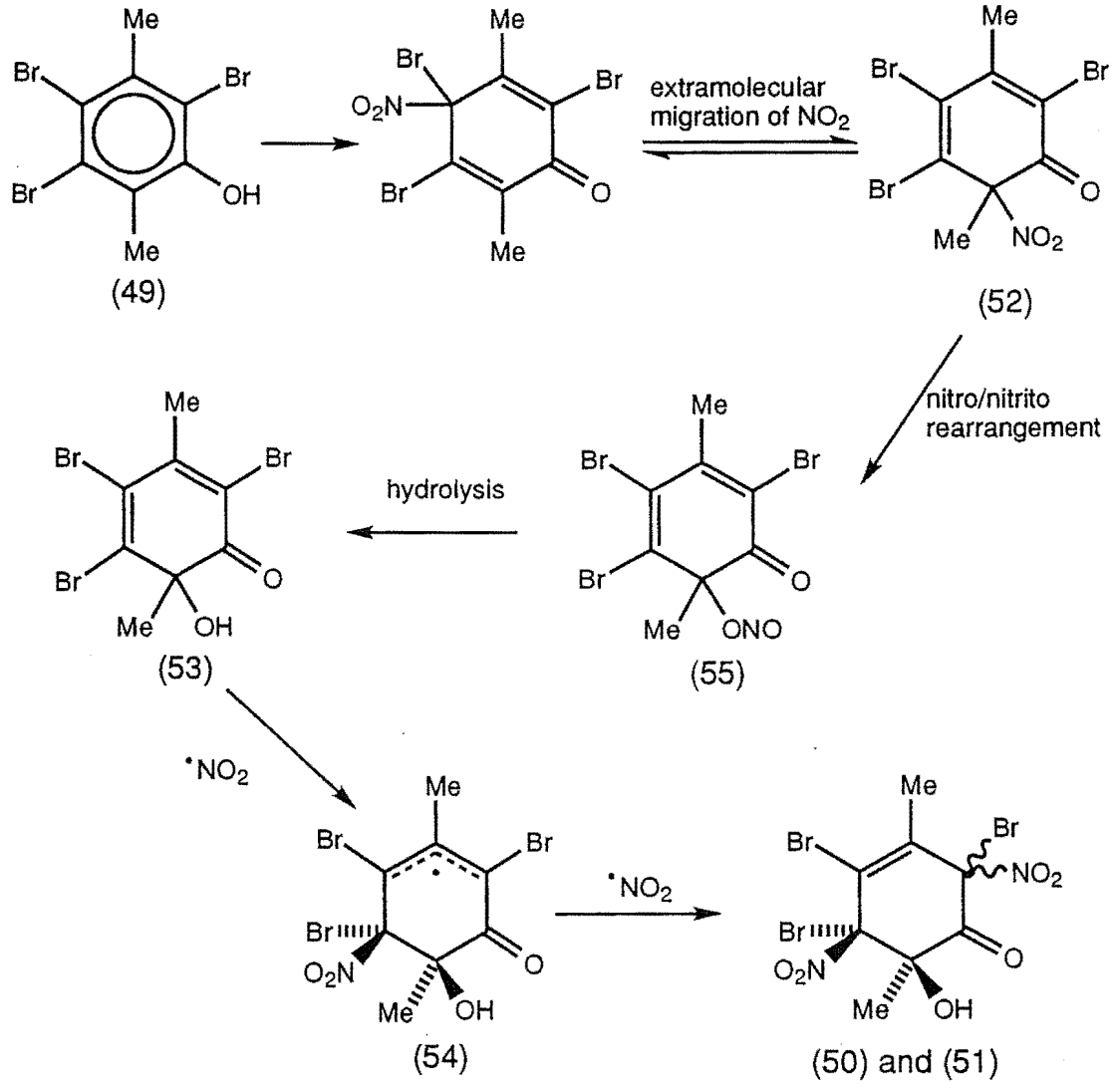

SCHEME 2.3

It was established that the mode of formation of the epimeric 6-hydroxy dinitro ketones (50) and (51) was *via* the 6-nitrodienone (52) which lead to the 6-hydroxy dienone (53) and further reaction with nitrogen dioxide gave the delocalised 6-hydroxy radical (54) with the necessary *cis*-6-hydroxy-5-nitro stereochemistry.[27] Subsequent reaction of the delocalised radical (54) would yield the observed products by reaction with $^{\bullet}NO_2$ as illustrated in Scheme 2.3.

The formation of the nitrito ketone (55) by attack of the more nucleophilic oxygen atom of $^{\bullet}NO_2$ is promoted by the presence of the electron withdrawing 5-bromo group in the phenol (49). Because of strong intramolecular carbonyl-hydroxyl bonding the conformation of the 6-hydroxy dienone (53) gives rise to the characteristic *cis*-6-hydroxy-5-nitro stereochemistry seen in the epimeric products 6-hydroxy dinitro ketones (50) and (51). The conformation is illustrated in Figure 2.9 and indicates that the C6-methyl group effectively shields the lower face of the diene system at C5.[30]

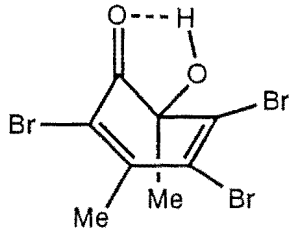

(53)

FIGURE 2.9

The nitration reaction of 2,4-dibromo-3,5,6-trimethylphenol (56) with nitrogen dioxide in cyclohexane had been studied extensively and was observed to give no hydroxy dinitro ketones species.[30] The products consisted of a series of 2,5,6-trinitrocyclohex-3-enones (57) with the rationalised mode of formation illustrated in Scheme 2.4 overleaf.

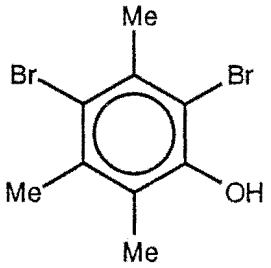

(56)

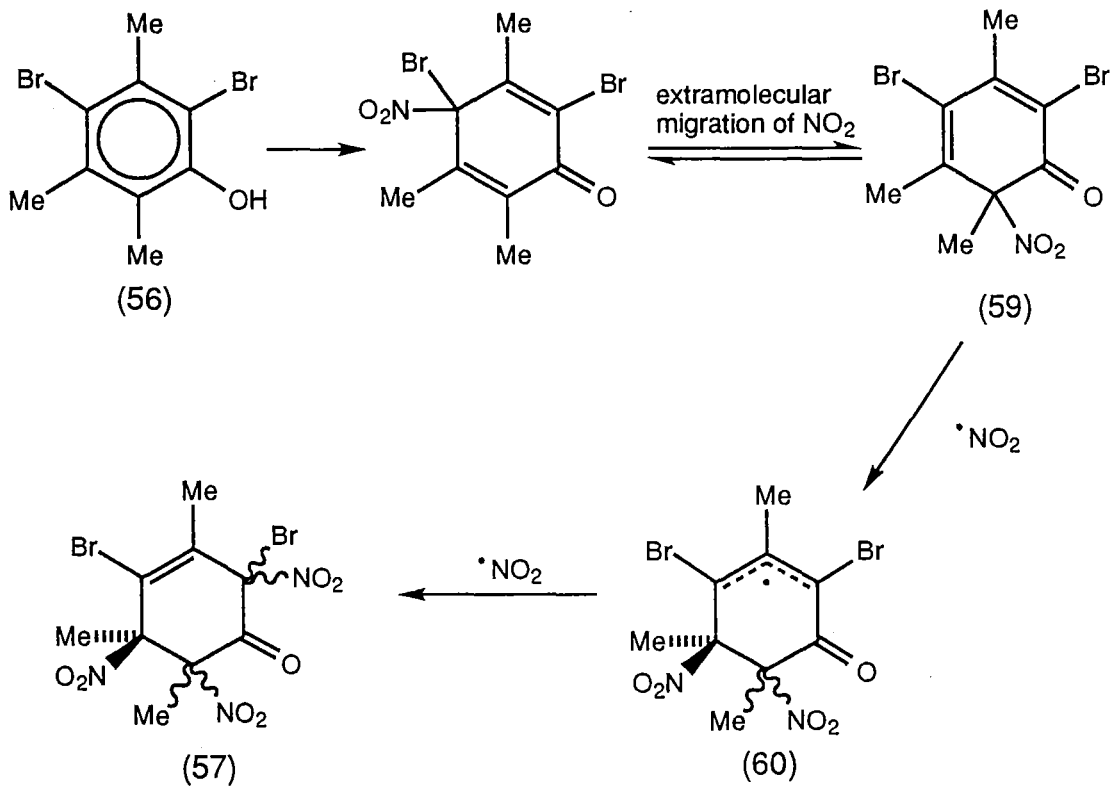

SCHEME 2.4

A comparison of the reaction products of phenols (49) and (56) with nitrogen dioxide illustrates the products are significantly different. The crucial structural feature of phenol (56) which leads to the observed reaction products is the C5-methyl group.[30] It was rationalised that the inductively electron-donating C5-methyl group in phenol (56) promotes formation of the intermediate 6-nitrodienone (59) with C-N bond formation.

The 6-hydroxy-2,5,6-trimethyl-2,5-dinitro ketones (37) and (39) and the 6-hydroxy-2,3,6-trimethyl-2,5-dinitro ketones (38) and (40) are products which have the characteristic *cis*-6-hydroxy-5-nitro stereochemistry[27]. The formation of the 6-hydroxy-2,5,6-trimethyl-2,5-dinitro ketones (37) and (39) and the 6-hydroxy-2,3,6-trimethyl-2,5-dinitro ketones (38) and (40) from the nitration reaction of 4-chloro-2,3,6-trimethylphenol will be *via* the 4-nitrodienone (42)

which, with extramolecular migration will give rise to the 6-nitrito-cyclohex-2,5-dienones (61) and (62) as illustrated in Scheme 2.5.

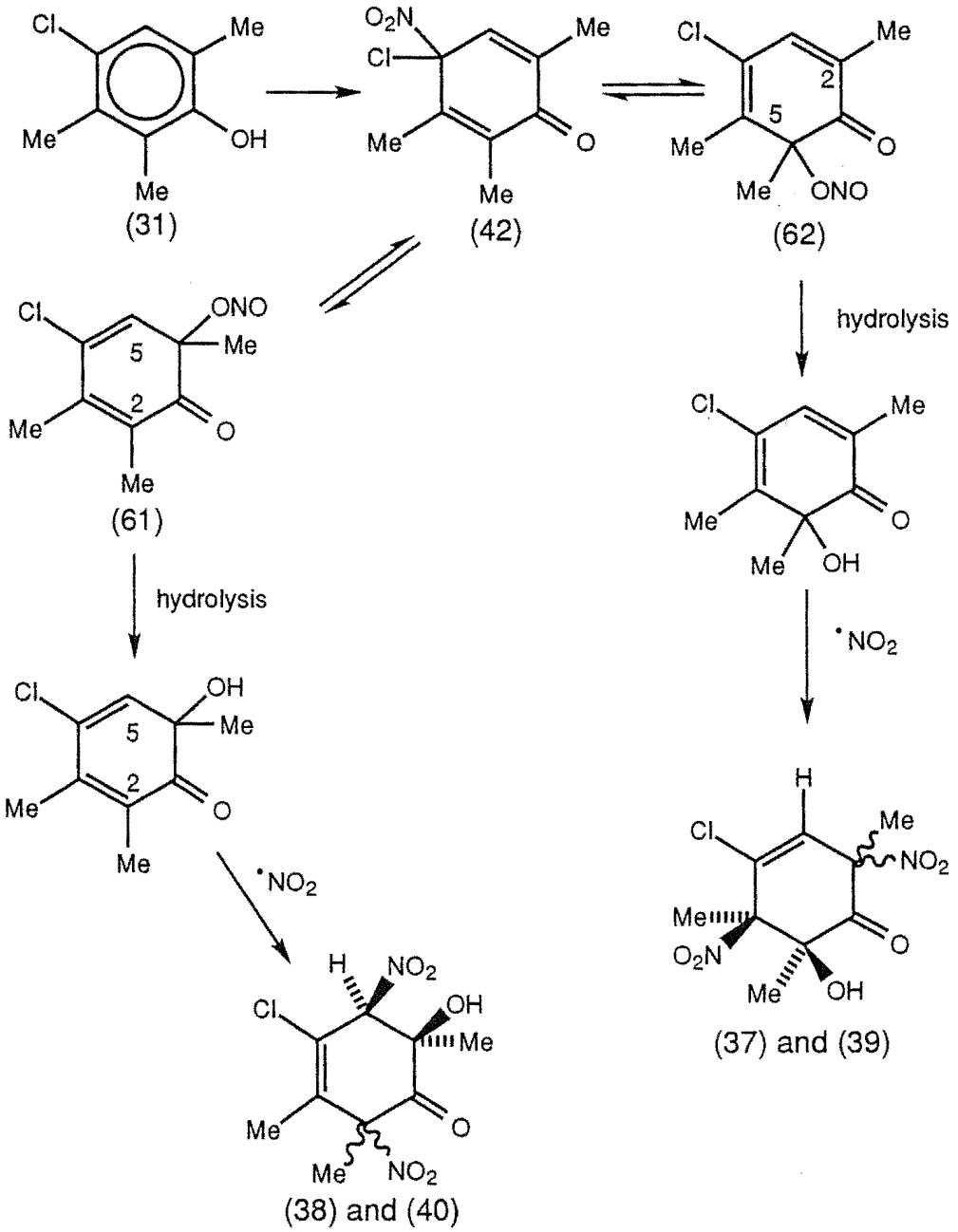

SCHEME 2.5

In keeping with the above mechanism is the isolation of 2,3,6-trimethylbenzoquinone which formed from the 4-nitrodienone (42) as shown in Scheme 2.6.

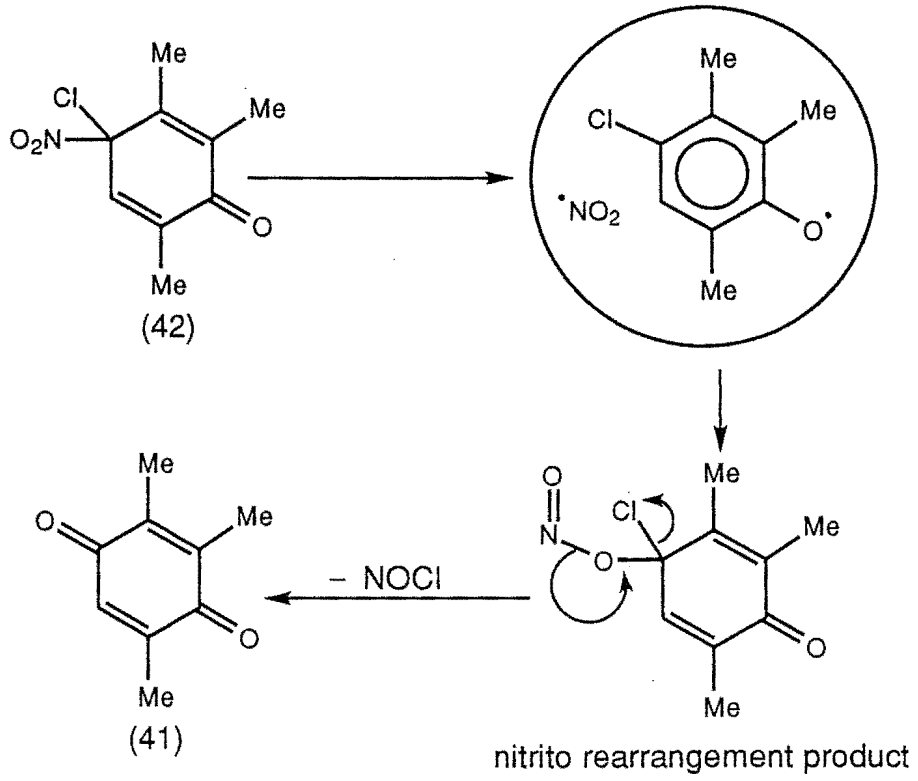

SCHEME 2.6

The products identified from the above nitration reaction of 4-chloro-2,3,6-trimethylphenol accounted for 80 % of the theoretical yield. Table 2.11 summarises the yields of compounds based on the relative integrals from the ^1H NMR ($CDCl_3$) spectrum of the crude product mixture.

Table 2.11 Yields (%) of identified products from the nitration of phenol (31) with nitrogen dioxide in benzene.

Compounds	% Yields
2,5,6-trimethyl-2,5,6-trinitrocyclohex-3-enones (45 - 48)	62%
6-hydroxy-2,5,6-trimethyl-2,5-dinitro ketones (37) and (39)	(total 12%)
6-hydroxy-2,3,6-trimethyl-2,5-dinitro ketones (38) and (40)	(total 4%)
2,3,6-trimethylbenzoquinone (41)	2%

It appears, that the presence of a 3-methyl group in 4-chloro-2,3,6-trimethylphenol (31) results in a significant preference for radical recombination to occur with the formation of the 2,5,6-trimethyl-6-nitro dienone (61). Some 74% of the observed products arise by radical coupling at C6 of the phenoxy radical (63) with nitrogen dioxide, most (62%) being formed *via* the C-N bond formation intermediate (64) and the remainder (12%) arising from the C-O bond formation intermediate (62) as illustrated in Scheme 2.7.

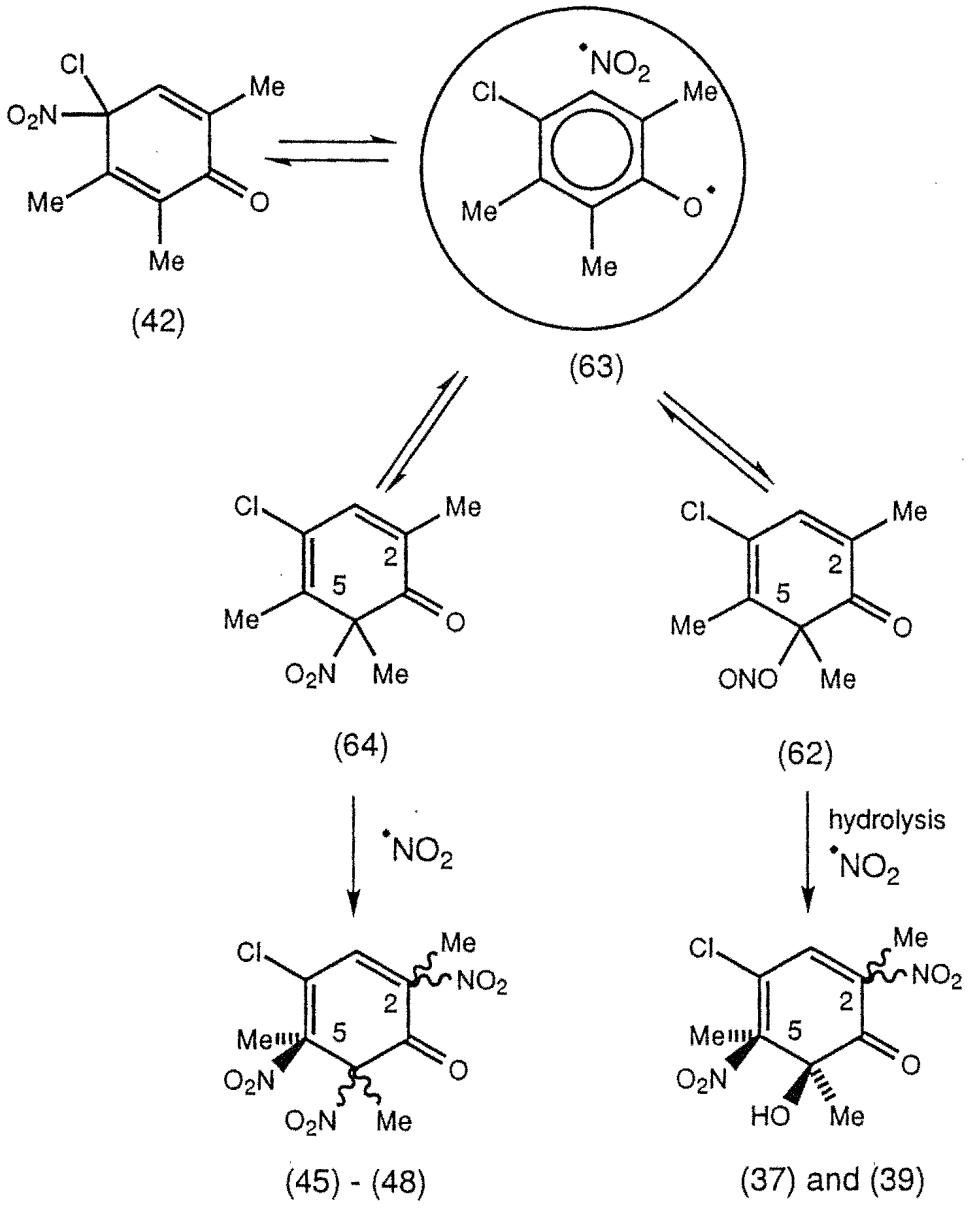

SCHEME 2.7

CHAPTER THREE

NITRATION OF 2,3,4,6-TETRAMETHYLPHENOL (32)

3.1 INTRODUCTION

The reaction of 2,3,4,6-tetramethylphenol (32) with nitrogen dioxide in benzene for 2 h has previously been reported.[28]

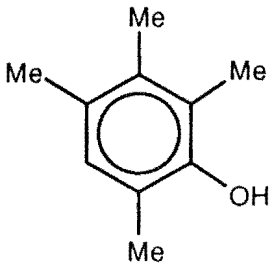

(32)

The products that were identified from the nitration reaction were the 4-hydroxy dienone (65), a compound tentatively assigned the 4-hydroxy-5,6-dinitrocyclohex-2-enone structure (66) the 2,5,6-trinitrocyclohex-3-enones (69) - (72), and the 4,5,6-trinitrocyclohex-2-enone (73).

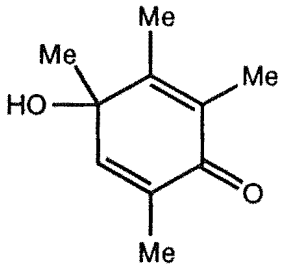

(65)

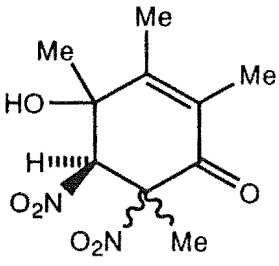

(66)

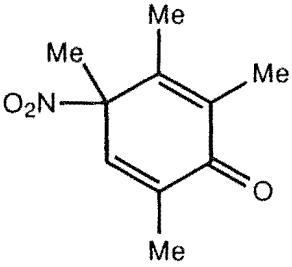

(67)

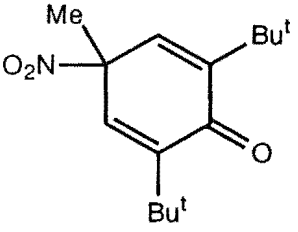

(68)

The formation of compounds (65) and (66) was suspected to occur during the isolation procedure from the intermediate 4-nitro-2,3,6-trimethylcyclohexa-2,5-

dienone (67), in a manner analogous to the known decomposition of the 2,6-di-t-butyl-4-methyl-4-nitrocyclohexa-2,5-dienone (68).[31,32]

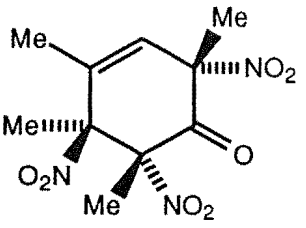

(69)

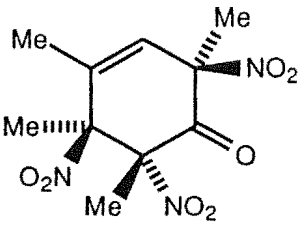

(70)

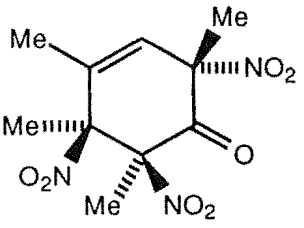

(71)

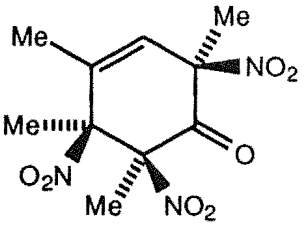

(72)

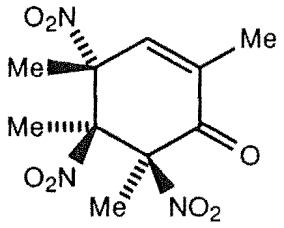

(73)

To avoid the possibility of 4-nitro-2,3,6-trimethylcyclohexa-2,5-dienone (67) decomposition it was rationalised that an increase in the reaction period from 2 h[28] to 48 h of the nitration should ensure the complete conversion of 4-nitro-2,3,6-trimethylcyclohexa-2,5-dienone (67) into nitration products.

3.2 THE NITRATION REACTION OF 2,3,4,6-TETRAMETHYLPHENOL (32)

Reaction of 2,3,4,6-Tetramethylphenol (32) with Nitrogen Dioxide

A solution of the phenol (32) in benzene was deoxygenated by a stream of pure nitrogen. Pure nitrogen dioxide was bubbled through the stirred solution at 20°C for 1 min. and the solution stirred at 20°C under an atmosphere of nitrogen dioxide for 48 h. The excess nitrogen dioxide was then removed in a stream of nitrogen and the solvent removed under reduced pressure to give a yellow oily residue. ^{1}H NMR ($CDCl_3$) indicated the presence of 4 major

components and 6 minor components. This mixture was partially separated into its components by chromatography on a silica gel Chromatotron plate, but some of the products (*c.* 30%) could not be isolated. (Detailed reaction conditions are set out in the experimental section relating to Chapter 3.)

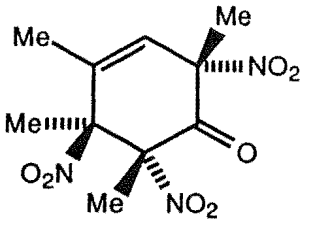

(69)

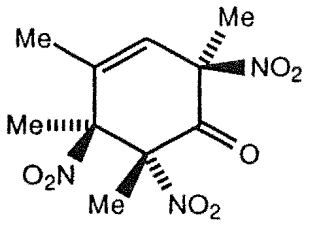

(70)

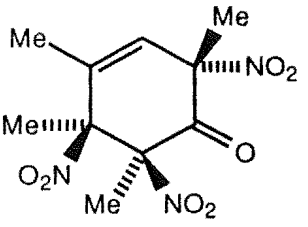

(71)

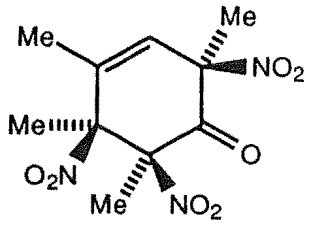

(72)

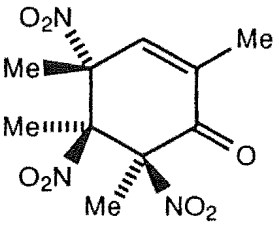

(73)

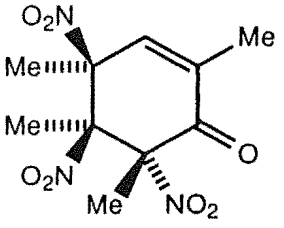

(74)

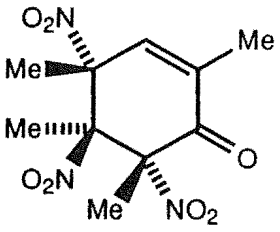

(75)

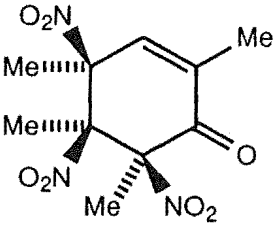

(76)

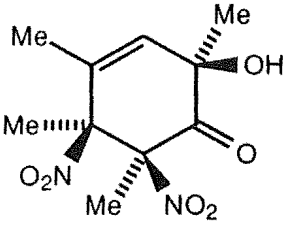

(77)

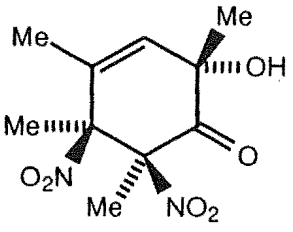

(78)

It was immediately recognised that the reaction of 2,3,4,6-tetramethylphenol (32) with nitrogen dioxide for 48h had resulted in the elimination of the two "products" (65) and (66). It was also apparent that a greater selection of

products had formed over the longer reaction period and that it was essential to characterise and identify these. The products were purified by silica gel chromatography and were eluted in the following order using solvent mixtures of pentane and ether.

2,4,5,6-Tetramethyl-*r*-4,*c*-5,*t*-6-trinitrocyclohex-2-enone (74) was obtained in a pure form and suitable crystals were obtained for the structure determination by single crystal X-ray analysis. The perspective drawing of 2,4,5,6-tetramethyl-r-4,c-5,t-6-trinitrocyclohex-2-enone (74), $C_{10}H_{13}N_3O_7$, m.p. 104-105°C, is presented in Fig. 3.1, with corresponding atomic coordinates in Table 5.7.

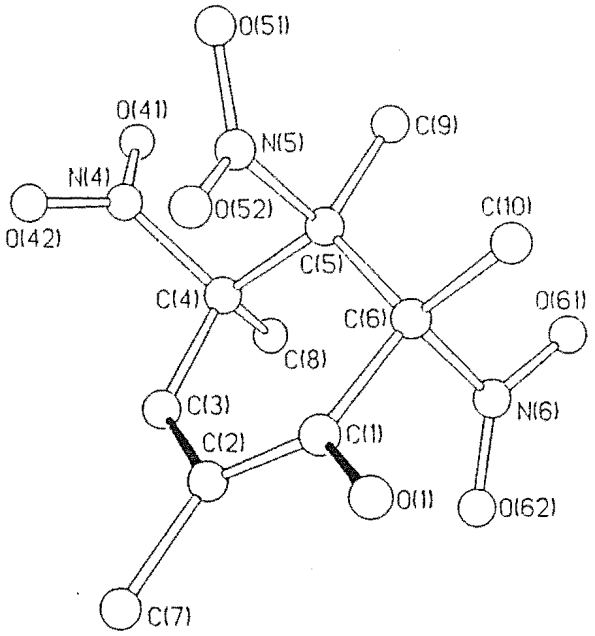

FIGURE 3.1

A perspective diagram of 2,4,5,6-tetramethyl-*r*-4,*c*-5,*t*-6-trinitrocyclohex-2-enone (74)

In the solid state the alicyclic ring of this conjugated ketone (74) exists in a flattened half-chair conformation. The spectroscopic data is consistent with the established structure. In particular characteristic i.r. absorptions were observed for the functional groups associated within compound (74) as illustrated in Table 3.1. The absorption at 1709 cm^{-1} is typical for the carbonyl stretching frequency for an α-nitro conjugated ketone.

TABLE 3.1 Characteristic i.r. absorptions ν_{max} (KBr) for compound (74).

Functional Group	Absorption (cm^{-1})
C=O	1709
NO_2	1560, 1549, 1522

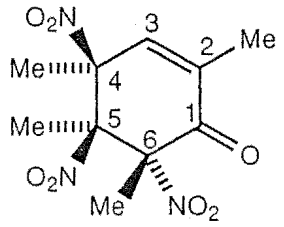

(74)

The ^1H and ^{13}C NMR spectra of adduct (74) were assigned from long range reverse detected ^1H - ^{13}C heteronuclear correlation spectra (HMBC). The ^{13}C resonances were assigned as illustrated in Table 3.2.

Table 3.2 ^{13}C NMR (C_6D_6) resonances for compound (74)

Chemical Shift (ppm)	Assignment
183.7	C1
137.4	C2
135.3	C3
91.4	C4
97.7	C5
91.9	C6
25.0, 18.1, 17.2, 16.9	Me carbons

2,4,5,6-Tetramethyl-*r*-4,*t*-5,*c*-6-trinitrocyclohex-2-enone (75) was next eluted in a small yield insufficient for elemental analysis and it was too unstable for an accurate M^+ measurement. Its structure was rationalised on the basis of

spectroscopic data and also by exclusion after the structure determinations of the closely similar compounds (76) and (77) described below.

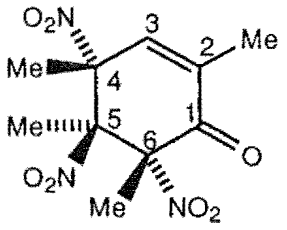

(75)

An i.r. absorption at 1707 cm^{-1} confirms the presence of an α-nitro conjugated ketone. The ^{1}H and ^{13}C NMR spectra of adduct (75) were assigned from long range reverse detected ^{1}H - ^{13}C heteronuclear correlation spectra (HMBC). A comparison between the ^{13}C resonances of compound (74) and (75) illustrated in Table 3.3 demonstrates the similarity between the isomers despite the utilisation of different solvent systems.

Table 3.3 ^{13}C NMR resonances for compound (74) and compound (75)

Chemical Shift **$CDCl_3$** (ppm)	Assignment (74)	Chemical Shift **C_6D_6** (ppm)	Assignment (75)
183.7	C1	183.2	C1
137.4	C2	140.1	C2
135.3	C3	132.3	C3
91.4	C4	88.5	C4
97.7	C5	96.9	C5
91.9	C6	88.1	C6
25.0, 18.1, 17.2,16.9	Me carbons	23.5, 18.7, 17.14, 17.10	Me carbons

2,4,5,6-Tetramethyl-*r*-2,*t*-5,*c*-6-trinitrocyclohex-3-enone (69) was eluted third in the separation of the crude product mixture. Its structure had been determined previously and the present material was identical with an authentic sample.[28]

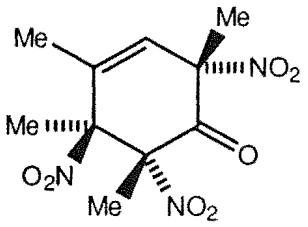

(69)

2,4,5,6-Tetramethyl-*r*-2,*c*-5,*t*-6-trinitrocyclohex-3-enone (70) was eluted following compound (69). This compound had also been identified previously and again the material isolated was identical with an authentic sample.[28] The conformation of 2,4,5,6-tetramethyl-*r*-2,*c*-5,*t*-6-trinitrocyclohex-3-enone (70) was analogous to the conformation of 4-chloro-2,5,6-trimethyl-*r*-2,*c*-5,*t*-6-trinitrocyclohex-3-enone (46) isolated from the 4-chloro-2,5,6-trimethylphenol nitration reaction described in Chapter 2. A comparison of the ^{13}C and ^{1}H NMR resonances indicates the similarities between the two compounds (46) and (70) as illustrated below in Tables 3.4 and 3.5. The ^{1}H and ^{13}C NMR spectra of adduct (70) were assigned from long range reverse detected ^{1}H - ^{13}C heteronuclear correlation spectra (HMBC). The expected minor differences between the NMR resonances of compound (46) and (70) arise from the variation in C4-substitution.

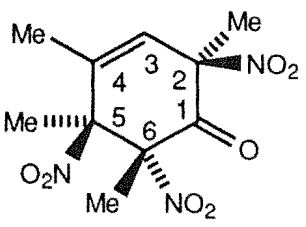

(70)

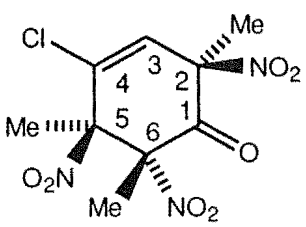

(46)

Table 3.4 ^{13}C NMR ($CDCl_3$) resonances for compounds (46) and (70).

Chemical Shift (ppm)	Assignment (46)	Chemical Shift (ppm)	Assignment (70)
185.1	C1	186.2	C1
88.7	C2	88.1	C2
131.3	C3	129.3	C3
132.9	C4	135.4	C4
93.9	C5	93.4	C5
94.5	C6	94.5	C6
27.6, 27.5, 17.6	Methyl Carbons	28.0, 20.4, 18.1, 17.4	Methyl Carbons

Table 3.5 ^{1}H NMR ($CDCl_3$) resonances for compounds (46) and (70).

Chemical Shift (ppm)	Assignment (46)	Chemical Shift (ppm)	Assignment (70)
2.01	2-Me	1.97	2-Me or 5-Me
2.13	5-Me	2.07	5-Me or 2-Me
1.91	6-Me	1.93	6-Me

Further elution gave 2,4,5,6-tetramethyl-*r*-4,*t*-5,*t*-6-trinitrocyclohex-2-enone (73). This compound had also been previously identified and its structure confirmed. The spectroscopic data obtained was identical with authentic data.[28]

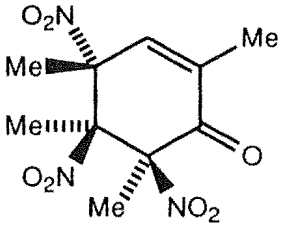

(73)

Further elution gave *r*-2-hydroxy-2,4,5,6-tetramethyl-*c*-5,*c*-6-dinitrocyclohex-3-enone (77). The structure of *r*-2-hydroxy-2,4,5,6-tetramethyl-*c*-5,*c*-6-dinitrocyclohex-3-enone (77) was assigned on the basis of its ^{1}H NMR. spectra and the results of long range HETCOR experiments. An i.r. absorption at 3469 cm^{-1} confirmed the presence of a OH functionality while the ^{13}C NMR resonance at 70.6 ppm is characteristic of a carbon bearing an oxygen atom. The ^{1}H and ^{13}C NMR spectra of adduct (77) were assigned from long range reverse detected ^{1}H - ^{13}C heteronuclear correlation spectra (HMBC).

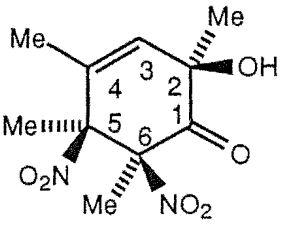

(77)

The assignment of *r*-2-hydroxy-2,4,5,6-tetramethyl-*c*-5,*c*-6-dinitrocyclohex-3-enone (77) is only tentative.

Further elution gave 2,4,5,6-tetramethyl-*r*-2,*t*-5,*t*-6-trinitrocyclohex-3-enone (71) which had also been previously identified and its structure was confirmed with comparison of spectroscopic data obtained and the available authentic data.[28]

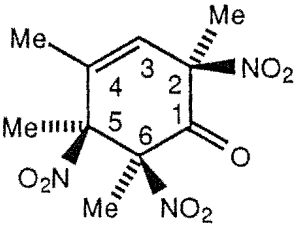

(71)

r-2-Hydroxy-2,4,5,6-tetramethyl-t-5,t-6-dinitrocyclohex-3-enone (78) was obtained in a pure form and suitable crystals were obtained for the structure determination by single crystal X-ray analysis. The perspective drawing of r-2-

determination by single crystal X-ray analysis. The perspective drawing of r-2-hydroxy-2,4,5,6-tetramethyl-t-5,t-6-dinitrocyclohex-3-enone (78), $C_{10}H_{13}N_3O_7$, m.p. 146-148°C, is presented in Fig. 3.2, with corresponding atomic coordinates in Table 5.8.

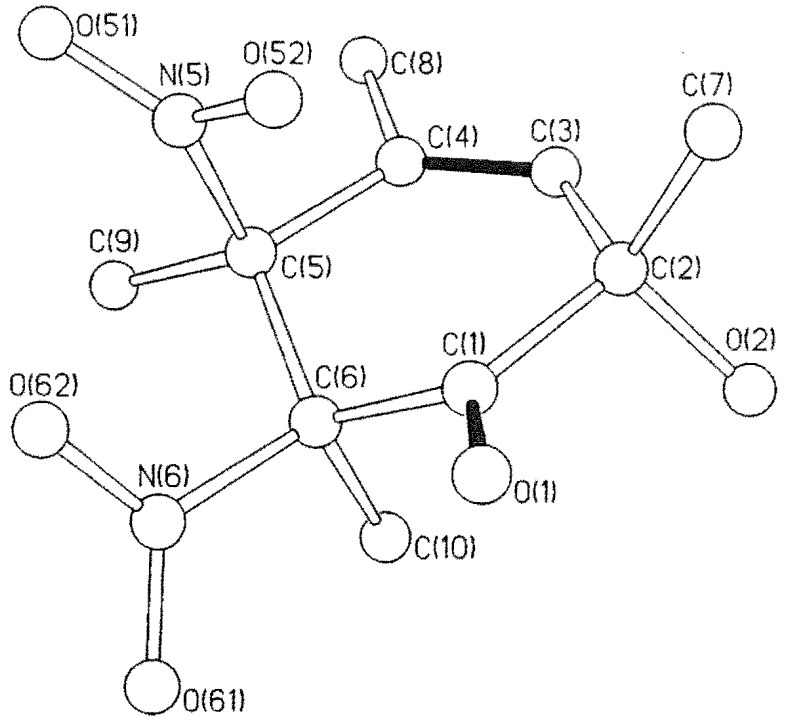

FIGURE 3.2

A perspective diagram of r-2-hydroxy-2,4,5,6-tetramethyl-t-5,t-6-dinitrocyclohex-3-enone (78)

The ring conformation for 2-hydroxy-5,6-dinitro ketone (78) is a flattened skew boat with the 5-nitro function in the flagpole orientation. The spectroscopic data for compound (78) is consistent with the established structure. The ^{1}H and ^{13}C NMR spectra of adduct (78) were assigned from long range reverse detected ^{1}H - ^{13}C heteronuclear correlation spectra (HMBC). The stereochemistry is the same as seen in compound (72) below. A comparison of the NMR resonances is given in Tables 3.6 and 3.7.

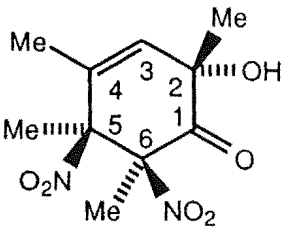

(78)

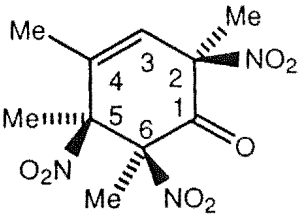

(72)

Table 3.6 ^{13}C NMR resonances for compounds (78) and (72).

Chemical Shift $CDCl_3$ (ppm)	Assignment (78)	Chemical Shift D_6-acetone (ppm)	Assignment (72)
196.2	C1	188.5	C1
72.5	C2	95.4	C2
135.5	C3	129.3	C3
132.4	C4	136.9	C4
95.3	C5	98.6	C5/C6
97.2	C6	90.2	C6/C5
23.8, 22.5, 18.9, 16.4	Me carbons	26.4, 22.3, 18.8, 16.0	Me carbons

Table 3.7 ^{1}H NMR resonances for compounds (78) and (72).

Chemical Shift $CDCl_3$ (ppm)	Assignment (78)	Chemical Shift D_6-Acetone (ppm)	Assignment (72)
1.68	2-Me	1.85	2-Me
1.82	5-Me	1.85	5-Me
2.02	6-Me	1.95	6-Me
1.92 d	4-Me	2.05 d	4-Me
5.97 q	H3	6.23 q	H3

2,4,5,6-Tetramethyl-*r*-4, *c*-5,*c*-6-trinitrocyclohex-2-enone (76) was obtained in a pure form and suitable crystals were obtained for the structure determination by single crystal X-ray analysis. The perspective drawing of 2,4,5,6-tetramethyl-*r*-4,*c*-5,*c*-6-trinitrocyclohex-2-enone (76) $C_{10}H_{13}N_3O_7$, m.p. 114-116°C (dec.), is presented in Fig. 3.3, with corresponding atomic coordinates in Table 5.9.

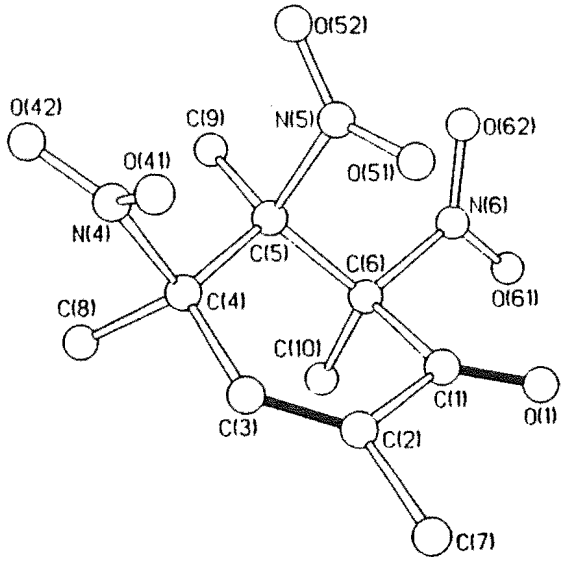

FIGURE 3.3

A perspective diagram of 2,4,5,6-tetramethyl-*r*-4, *c*-5,*c*-6-trinitrocyclohex-2-enone (76)

In the solid state the alicyclic rings of the two conjugated ketones (74) and (76) exist in closely similar flattened half-chair conformations, in contrast to the flattened skew boat conformation observed earlier for 2,4,5,6-tetramethyl-*r*-4,*t*-5,*t*-6-trinitrocyclohex-2-enone (73).[28] Table 3.8 illustrates the torsional angles observed for the ring conformations of compounds (74) and (76).

Table 3.8 Comparison of torsional angles (°) of compounds (74) and (76).

Compound (74) atoms	Torsion angles	Compound (76) atoms	Torsion angles
C1-C2-C3-C4	2.68°(2.7)	C1-C2-C3-C4	-0.63°(0.2)
C3-C4-C5-C6	34.28°(1.9)	C3-C4-C5-C6	37.67°(0.2)
C4-C5-C6-C1	-43.38°(1.8)	C4-C5-C6-C1	-54.05°(0.2)
C6-C1-C2-C3	-13.5°(2.7)	C6-C1-C2-C3	-15.98°(0.2)

The spectroscopic data is consistent with the established structure. The ^{1}H and ^{13}C NMR spectra of adduct (76) were assigned from long range reverse detected ^{1}H - ^{13}C heteronuclear correlation spectra (HMBC).

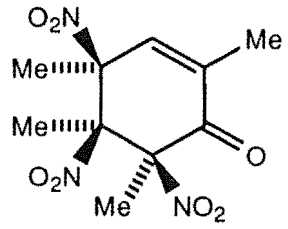

(76)

Finally elution gave 2,4,5,6-tetramethyl-*r*-2,*c*-5,*c*-6-trinitrocyclohex-3-enone (72). This compound had been identified previously and the material isolated was identical with an authentic sample.[28] The conformation of 2,4,5,6-tetramethyl-*r*-2,*c*-5,*c*-6-trinitrocyclohex-3-enone (72) was analogous to the conformation of 4-chloro-2,5,6-trimethyl-*r*-2,*c*-5,*c*-6-trinitrocyclohex-3-enone (72) isolated from the 4-chloro-2,5,6-trimethylphenol nitration reaction described in Chapter 2. A comparison of the ^{13}C NMR resonances indicates the similarities between the two compounds (48) and (72) as illustrated below in Table 3.9. The expected minor differences between the NMR resonances of compound (48) and (72) arise from the variation in C4-substitution and the necessity to use different solvent systems because of solubility differences. The ^{1}H and ^{13}C NMR spectra of adduct (75) were assigned from long range reverse detected ^{1}H - ^{13}C heteronuclear correlation spectra (HMBC).

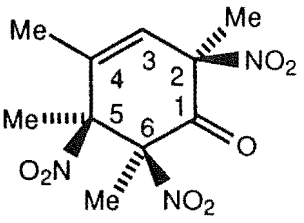

(72)

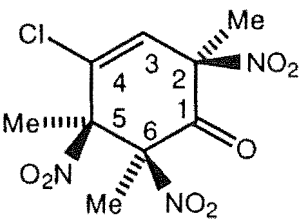

(48)

Table 3.9 ^{13}C NMR resonances for compounds (48) and (72).

Chemical Shift $CDCl_3$ (ppm)	Assignment (48)	Chemical Shift D_6-acetone (ppm)	Assignment (72)
186.8	C1	188.5	C1
89.9	C2	95.4	C2
130.5	C3	129.3	C3
130.8	C4	136.9	C4
96.1	C5	98.6	C5/C6
98.5	C6	90.2	C6/C5
27.1, 22.2, 17.6	Me carbons	26.4, 22.3, 18.8, 16.0	Me carbons

Comparison of the ^1H NMR data for the Δ2 compounds (73)-(76) reveals that the H3 resonance is affected by the C4 stereochemistry. Table 3.10 illustrates the chemical shift data for H3 in compounds (73)-(76) and the differences in the chemical shifts with respect to the stereochemistry at C4.

Table 3.10 ^1H NMR ($CDCl_3$) chemical shift data for compounds (73 - (76) .

Compound	H3 resonance (ppm)
(73) r-4, t-5, t-6	6.40
(74) r-4, c-5, t-6	6.83
(75) r-4,t-5, c-6	6.30
(76) r-4,c-5, c-6	6.74

Table 3.10 illustrates that for the C-6 epimeric compounds (73) and (75), the signal for H3 appears upfield ($\Delta\delta \approx 0.44$ppm) from the C-6 epimeric compounds (74) and (76). Comparison of the H3 signals of the *trans* -C4,C5-dinitro isomers (73) and (75), δ 6.40 and δ 6.30 respectively, reveals a difference of chemical shift ($\Delta\delta$) of 0.1ppm. Similarly for the H3 resonances of the *cis*-C4,C5-dinitro isomers (74) and (76) δ 6.83 and δ 6.74 respectively, reveals a difference of chemical shift ($\Delta\delta$) of 0.09ppm. This pattern may be significant in further attempts at assignment of similar Δ2 compounds. Similar patterns of stereochemical significance with respect to the chemical shift have been observed previously[28]

The material balance of identified products remained low (34% unidentified) but pure samples of the four 2,4,5,6-tetramethyl-2,5,6-trinitrocyclohex-3-enones (69)-(72), the four 2,4,5,6-tetramethyl-4,5,6-trinitrocyclohex-2-enones (73) - (76), and the C2-epimeric 2-hydroxy-2,4,5,6-tetramethyl-5,6-dinitro-cyclohex-3-enones (77) and (78). were obtained. Compounds (69) - (73) had been identified earlier[28], and the structure of 2,4,5,6-tetramethyl-*r*-4,*t*-5,*c*-6-trinitrocyclohex-2-enone (75) was assigned by exclusion after the structure determinations reported for isomers (74) and (76).

The products (total 66%) identified, above, were all envisaged as arising by addition of nitrogen dioxide to 2,4,5,6-tetramethyl-6-nitro dienone (79) as illustrated in Scheme 3.1.

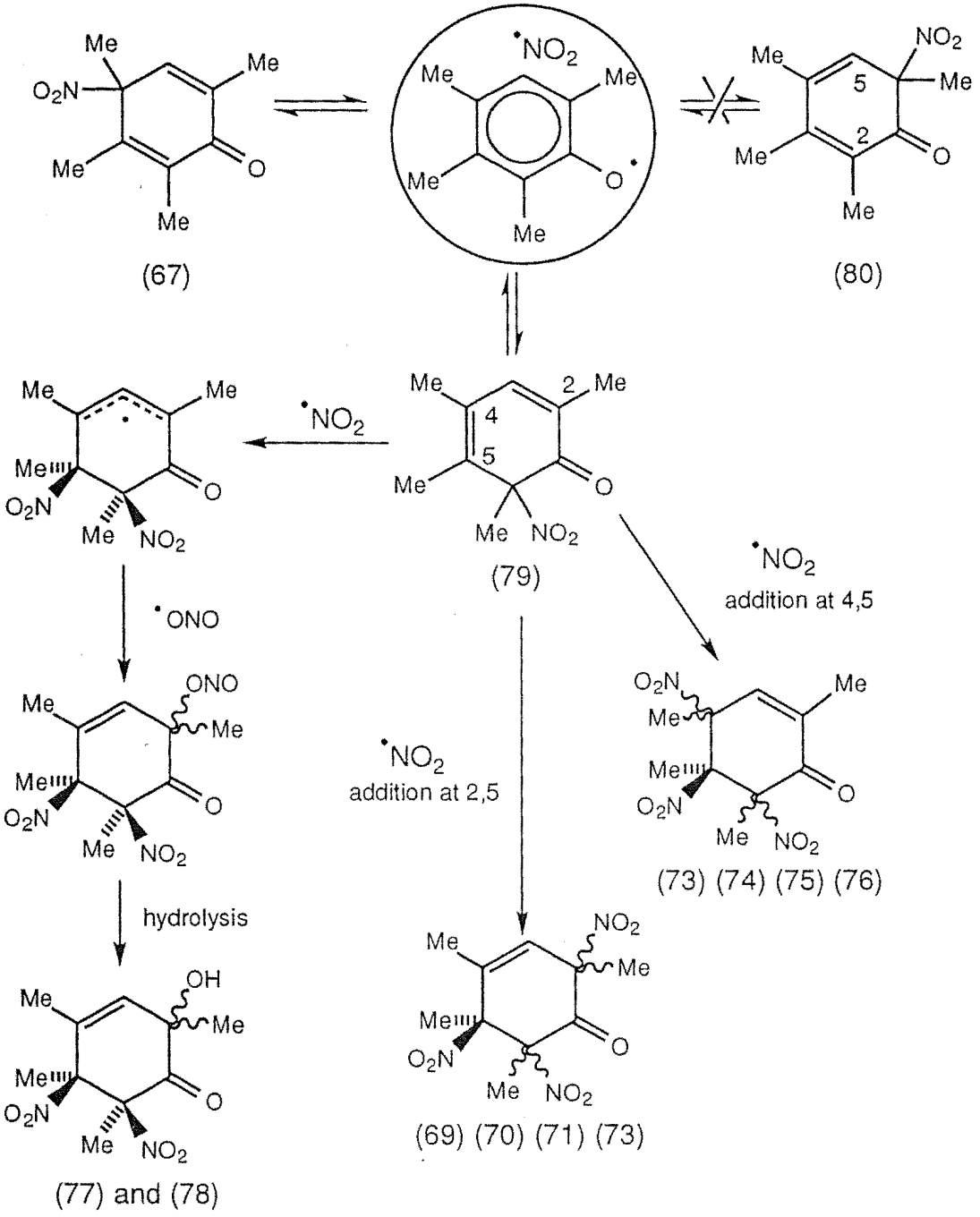

SCHEME 3.1

The 6-nitro-cyclohex-2,5-dienone (79) reacts with $^{\bullet}NO_2$, giving 2,5-addition or 4,5 addition products. The hydroxy compounds (77) and (78) are most likely formed from $^{\bullet}ONO$ attack on the delocalised radical that results after 2,5-addition of $^{\bullet}NO_2$ to the 6-nitro-cyclohexa-2,5-dienone (79) with subsequent hydrolysis in solution or upon workup to give the hydroxy functionality. It is not

possible to determine whether this is the actual pathway to formation of the hydroxy adducts. It appears from the products observed that the 6-nitro-cyclohex-2,5-dienone (80) is not involved in the formation of any observed products. To confirm the mechanism of $^{\bullet}NO_2$ addition ^{15}N-labelling studies were undertaken.

3.3 Preparation of ^{15}N-labelled 2,3,4,6-tetramethyl-4-nitrocyclo hexa-2,5-dienone (81), and its reaction with nitrogen dioxide in benzene Solution

The ^{15}N-labelled 4-nitro dienone (81) was prepared by nitration in dichloromethane at -10°C of 2,3,4,6-tetramethylphenol (32) with ^{15}N-nitric acid, obtained by distillation from a mixture of ^{15}N-sodium nitrate (95% ^{15}N) and concentrated sulphuric acid. The spectroscopic data for the ^{15}N-labelled 4-nitro dienone (81) were consistent with its assigned structure.

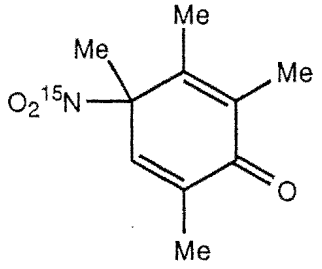

(81)

Reaction of the freshly prepared ^{15}N-labelled 4-nitro dienone (81) with nitrogen dioxide in benzene solution for 48 h gave a product mixture, the composition of which was essentially identical with the mixture obtained by the similar reaction of the 2,3,4,6-tetramethylphenol (32) with nitrogen dioxide in benzene. The ^{15}N-labelled products were separated by chromatography on a silica gel Chromatotron plate in an identical fashion as above and the location and extent of ^{15}N-labelling determined from the ^{1}H NMR spectra of the individual compounds.[26] For all compounds (69) - (78) the ^{15}N-label was located

exclusively at C6, the extent of the ^{15}N-labelling ranging from 55±5% to 62±5%. Complete experimental details are described in the experimental section relating to Chapter 3. Table 3.11 illustrates the extent of ^{15}N-labelling present in each of the isolated compounds.

Table 3.11 Extent of ^{15}N-labelling at C6 in compounds (75)-(84).

COMPOUND	^{15}N-label at C6 (%)
2,4,5,6-Tetramethyl-*r*-4,*c*-5,*t*-6-trinitrocyclohex-2-enone (74)	59±5%
2,4,5,6-Tetramethyl-*r*-4,*t*-5,*c*-6-trinitrocyclohex-2-enone (75)	62±5%
2,4,5,6-Tetramethyl-*r*-2,*t*-5,*c*-6-trinitrocyclohex-3-enone (69)	56±5%
2,4,5,6-Tetramethyl-*r*-2,*c*-5,*t*-6-trinitrocyclohex-3-enone (70)	57±5%
2,4,5,6-Tetramethyl-*r*-4,*t*-5,*t*-6-trinitrocyclohex-2-enone (73)	60±5%
r-2-Hydroxy-2,4,5,6-tetramethyl-*c*-5,*c*-6-dinitrocyclohex-3-enone (77)	61±5%
2,4,5,6-Tetramethyl-*r*-2,*t*-5,*t*-6-trinitrocyclohex-3-enone (71)	58±5%
r-2-Hydroxy-2,4,5,6-tetramethyl-*t*-5,*t*-6-dinitrocyclohex-3-enone (78)	55±5%
2,4,5,6-Tetramethyl-*r*-4,*c*-5,*c*-6-trinitrocyclohex-2-enone (76)	58±5%
2,4,5,6-Tetramethyl-*r*-2,*c*-5,*c*-6-trinitrocyclohex-3-enone (72)	60±5%

The consistency of these measurements of the extent of ^{15}N-labelling is a clear indication of the formation of these labelled products via a common ^{15}N-labelled intermediate (83) as illustrated in Scheme 3.2.

It appears, that the presence of a 3-methyl group in 2,3,4,6-tetramethylphenol (32) results in a much favoured preference for radical recombination to occur with the formation of the 2,5,6-trimethyl-6-nitro dienone (83) with 66% of the observed products having been formed *via* this 2,4,5,6-tetramethyl-6-nitro dienone intermediate (83). None of the observed product went *via* the 2,4,5,6-tetramethyl-6-nitro dienone (82). The hydroxy dinitro compounds (77) and (78) arise *via* attack of •ONO on structure (83) followed by hydrolysis to a hydroxy

functionality. The presence of the ^{15}N-label in the hydroxy compounds (77) and (78) confirms the mode of formation illustrated in Scheme 3.2.

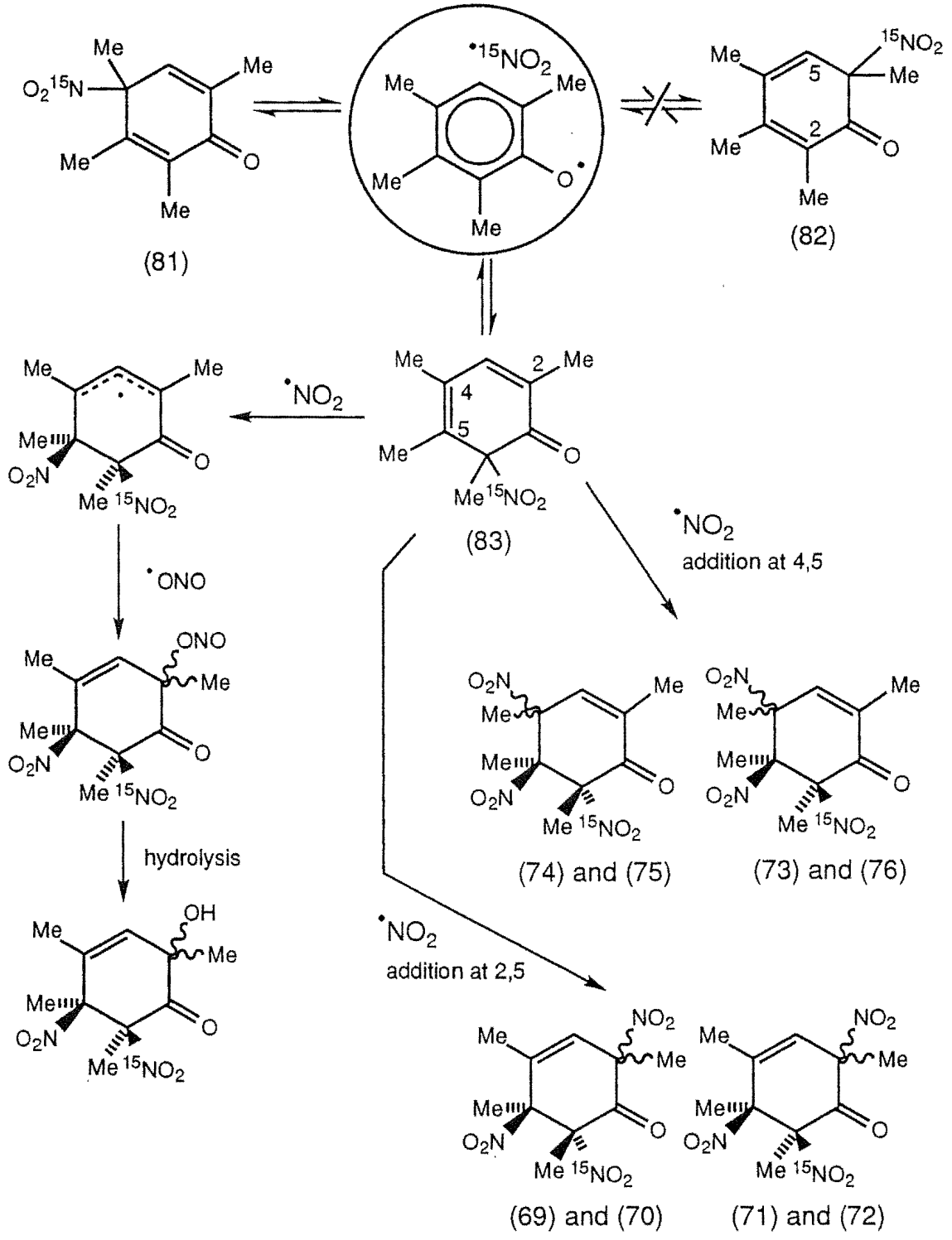

SCHEME 3.2

CHAPTER FOUR

NITRATION OF 3-CHLORO-2,4,6-TRIMETHYLPHENOL

4.1 INTRODUCTION

For the 3-methylphenols (31) and (32) reaction of the corresponding phenoxy radical with nitrogen dioxide resulted in C-N or C-O bond formation to give 6-nitro- or 6-hydroxy-5-methylcyclohexa-2,4-dienones which reacted further with nitrogen dioxide to give the final products. It was envisaged that the presence of the 3-chloro group in 3-chloro-2,4,6-trimethylphenol (33) might result in a different preference for radical recombination. It appeared likely that the coupling of nitrogen dioxide with the 3-chloro-2,4,6-trimethylphenoxy radical would occur preferentially at C6 and also with extensive C-O bond formation. The results of this study are reported below.

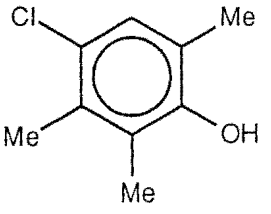

(31)

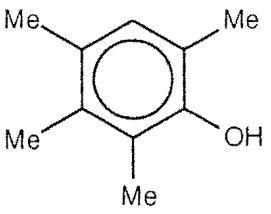

(32)

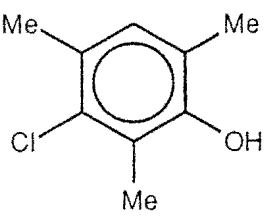

(33)

4.2 THE NITRATION OF 3-CHLORO-2,4,6-TRIMETHYLPHENOL (33)

Reaction of 3-Chloro-2,4,6-trimethylphenol (33) with Nitrogen Dioxide In Benzene Solution

A solution of the phenol (33) in benzene was deoxygenated by a stream of nitrogen. Pure nitrogen dioxide was bubbled through the stirred solution at

20° for 1 min., and the resulting mixture stirred under an atmosphere of nitrogen dioxide for 16 h. The excess nitrogen dioxide was removed in a stream of nitrogen and the solvent removed under reduced pressure to give a yellow oil, shown (^{1}H NMR) to be essentially a mixture of eight compounds. (84 - 91) with the ratios illustrated below. Two of these compounds [(84) and (85)] could be isolated by chromatography on a silica gel Chromatotron plate, the remainder being isolated by fractional crystallization. (Detailed reaction conditions are set out in the experimental section relating to Chapter 4.)

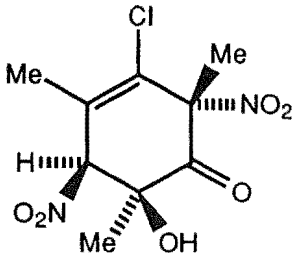

(84) 8%

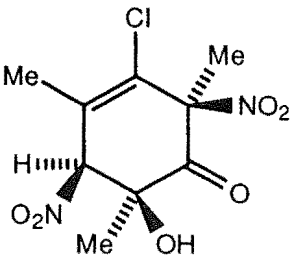

(85) 8%

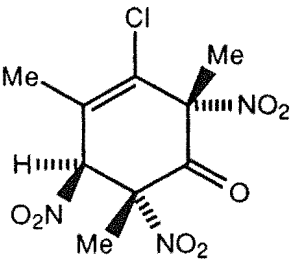

(86) 14%

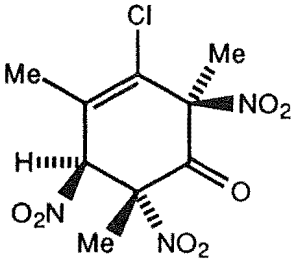

(87) 16%

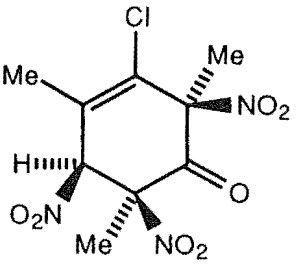

(88) 11%

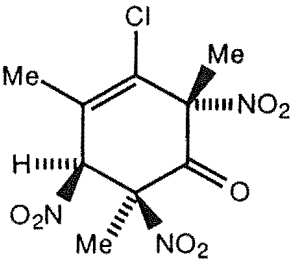

(89) 5%

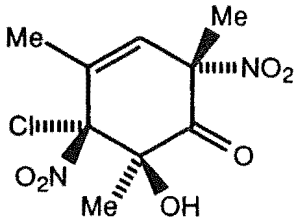

(90) 5%

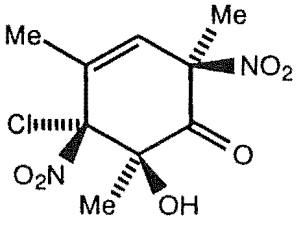

(91) 11%

3-Chloro-*t*-6-hydroxy-2,4,6-trimethyl-*r*-2,*t*-5-dinitrocyclohex-3-enone (84) was isolated and crystallised giving suitable crystals for single crystal X-ray analysis.

A perspective drawing of 3-chloro-*t*-6-hydroxy-2,4,6-trimethyl-*r*-2,*t*-5-dinitrocyclohex-3-enone (84), $C_9H_{11}ClN_2O_6$, m.p.117-118°C is presented in Fig. 4.1, with corresponding atomic coordinates in Table 5.10.

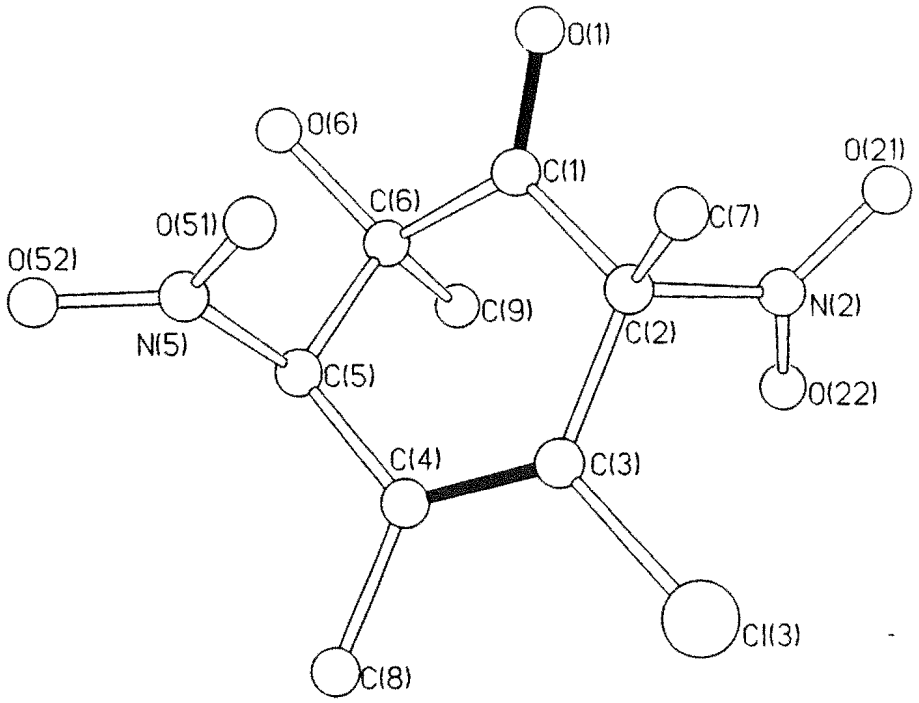

FIGURE 4.1

A perspective diagram of 3-chloro-*t*-6-hydroxy-2,4,6-trimethyl-*r*-2,*t*-5-dinitrocyclohex-3-enone (84).

Similar information is presented for 3-chloro-*c*-6-hydroxy-2,4,6-trimethyl-*r*-2,*c*-5-dinitrocyclohex-3-enone (85), although the crystal quality was low but was sufficient for the unequivocal determination of the structure of the compound. A perspective drawing of 3-chloro-*c*-6-hydroxy-2,4,6-trimethyl-*r*-2,*c*-5-dinitrocyclohex-3-enone (85), $C_9H_{11}ClN_2O_6$, m.p. 139-140°C is presented in Fig. 4.2, with corresponding atomic coordinates in Table 5.11.

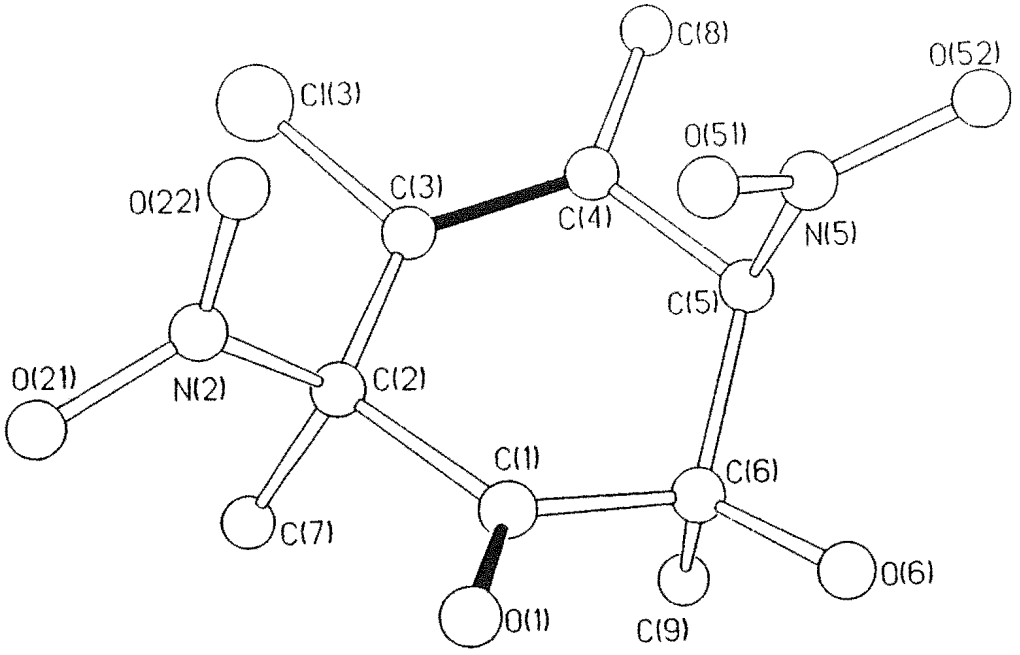

FIGURE 4.2

A perspective diagram of 3-chloro-*c*-6-hydroxy-2,4,6-trimethyl-*r*-2,*t*c5-dinitrocyclohex-3-enone (85).

The spectroscopic data for the two 3-chloro-6-hydroxy-2,4,6-trimethyl-2,5-dinitrocyclohex-3-enone compounds (84) and (85) were consistent with the structures determined. The close similarities between the ^{13}C and ^{1}H NMR data are illustrated in Tables 4.1 and 4.2 below. The assignments were made using long-range HETCOR experiments. (XCORFE).

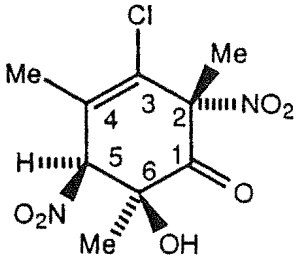

(84)

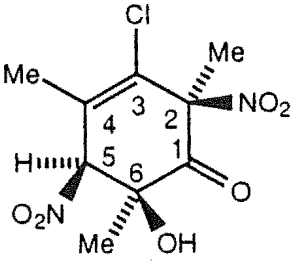

(85)

Table 4.1 ^{13}C NMR resonances for compound (84) and compound (85).

Chemical Shift $CDCl_3$ (ppm)	Assignment (84)	Chemical Shift $CDCl_3$ (ppm)	Assignment (85)
197.3	C1	197.7	C1
94.0	C2	94.4	C2
134.0	C3	132.9	C3
129.8	C4	131.0	C4
95.0	C5	95.0	C5
75.4	C6	75.4	C6
25.1, 21.5, 20.5	Me carbons	24.4, 22.9, 20.4	Me carbons

Table 4.2 ^{1}H NMR ($CDCl_3$) resonances for compounds (84) and (85).

Chemical Shift (ppm)	Assignment (84)	Chemical Shift (ppm)	Assignment (85)
5.32	H5	5.29	H5
2.14	2-Me	2.09	2-Me
2.25	4-Me	2.28	4-Me
1.65	6-Me	1.56	6-Me

Fractional crystallization of the crude product mixture enabled the separation of the three trinitro ketones (86 - 88), the structures of each of which were determined by X-ray crystal analysis.

A perspective drawing of 3-chloro-2,4,6-trimethyl-*r*-2,*t*-5,*c*-6-trinitrocyclohex-3-enone (86), $C_9H_{10}ClN_3O_7$, m.p. 112-113°C, is presented in Fig. 4.3, with corresponding atomic coordinates in Table 5.12.

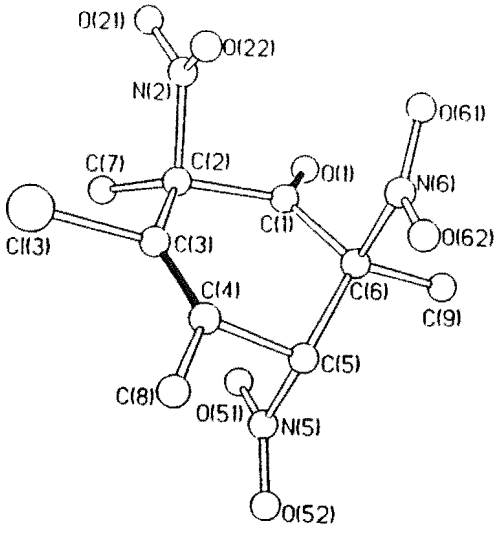

FIGURE 4.3

A perspective diagram of 3-chloro-2,4,6-trimethyl-*r*-2,*t*-5,*c*-6-trinitrocyclohex-3-enone (86)

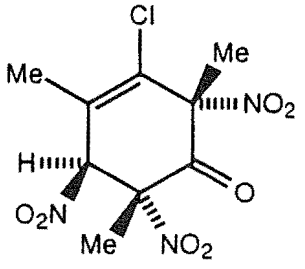

(86)

Similar information is presented for 3-chloro-2,4,6-trimethyl-*r*-2,*c*-5,*t*-6-trinitrocyclohex-3-enone (87). The structure was determined by single crystal X-ray analysis and a perspective drawing of 3-chloro-2,4,6-trimethyl-*r*-2,*c*-5,*t*-6-trinitrocyclohex-3-enone (87), $C_9H_{10}ClN_3O_7$, m.p. 112-113°C, is presented in Fig. 4.4, with corresponding atomic coordinates in Table 5.13.

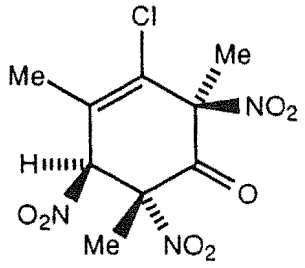

(87)

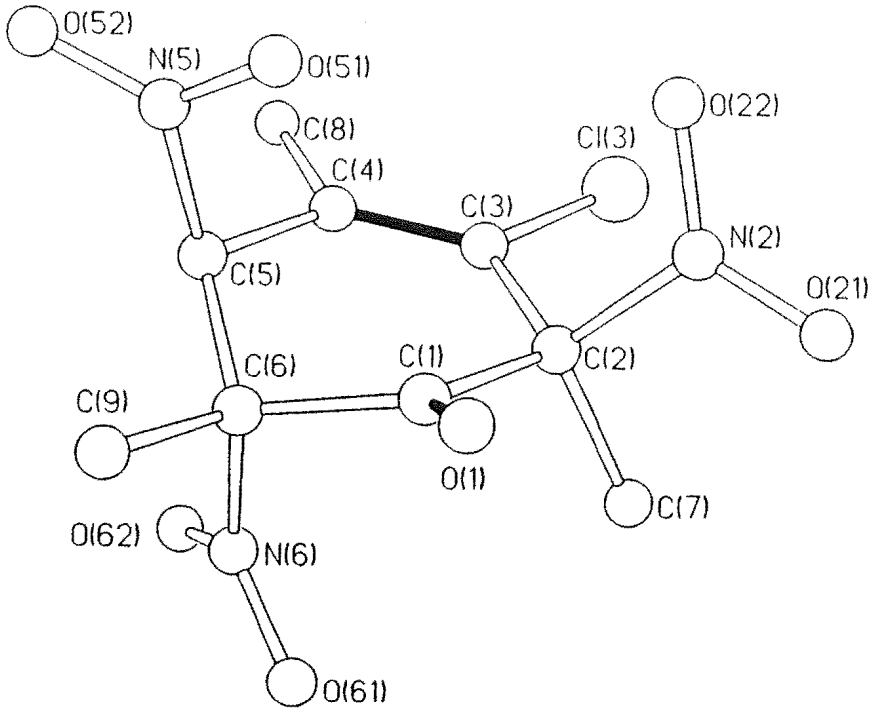

FIGURE 4.4

A perspective diagram of 3-chloro-2,4,6-trimethyl-*r*-2,*c*-5,*t*-6-trinitrocyclohex-3-enone (87)

In the solid state the alicyclic ring conformation differs for the C2-epimeric trinitro ketones (86) and (87), the *trans*-2,5-dinitro isomer (86) existing in a flattened skew boat conformation while the *cis*-2,5-dinitro isomer (87) exists as a flattened half chair conformation. A comparison of the torsional angles associated with the ring carbons indicates the different ring conformations as illustrated in Table 4.3.

Table 4.3 Comparison of torsional angles (°) of compounds (86) and (87).

Compound (86) atoms	Torsion angles	Compound (87) atoms	Torsion angles
C1-C2-C3-C4	-14.3°(1.4)	C1-C2-C3-C4	-8.6°(1.2)
C3-C4-C5-C6	31.8°(1.2)	C3-C4-C5-C6	-24.3°(1.1)
C4-C5-C6-C1	-49.5°(1.0)	C4-C5-C6-C1	45.0°(1.0)
C6-C1-C2-C3	-6.4°(1.2)	C6-C1-C2-C3	31.7°(1.0)

3-chloro-2,4,6-trimethyl-*r*-2,*c*-5,*c*-6-trinitrocyclohex-3-enone (88), $C_9H_{10}ClN_3O_7$, m.p. 120-122°. A perspective diagram is presented in Figure 4.5 and corresponding atomic coordinates in Table 5.14.

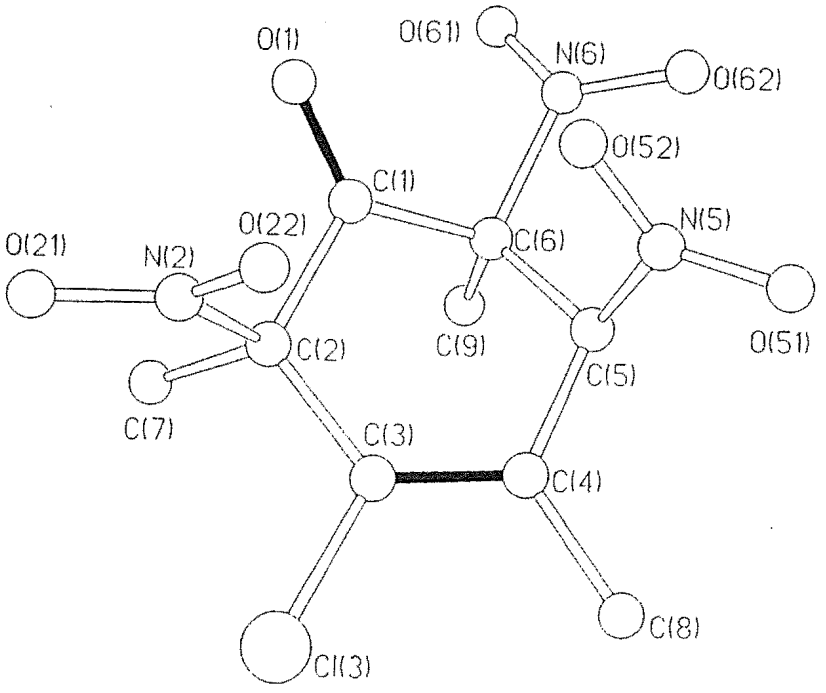

FIGURE 4.5

A perspective diagram of 3-chloro-2,4,6-trimethyl-*r*-2,*c*-5,*c*-6-trinitrocyclohex-3-enone (88)

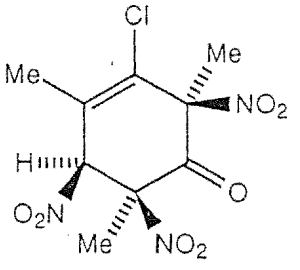

(88)

A comparison of the chemical shifts associated with the ^{13}C NMR resonances observed for the compounds (86) - (88) is presented in Table 4.4. The resonances are closely similar and in accord with the structures determined by X-ray analysis. All assignments were made from long range HETCOR experiments (XCORFE).

Table 4.4 ^{13}C NMR. ($CDCl_3$) resonances observed and assigned for (86-88).

Assignment	(86) Chemical Shifts δ	(87) Chemical Shifts δ	(88) Chemical Shifts δ
C1	183.5	184.0	183.8
C2	93.4	95.1	90.3/90.0
C3	133.7	133.4	133.3
C4	130.3	131.0	130.8
C5	91.0	90.2	90.3/90.0
C6	87.6	89.4	89.5
Me carbons	21.1, 20.2, 20.1	26.0, 22.9, 19.5	24.5, 23.0, 20.8

The fourth 2,5,6-trinitrocyclohex-3-enone (89) could be isolated only in an impure state but, given the structure determinations above and comparisons of the ^1H NMR spectra of the four isomers, the structural assignment to compound (89) appears certain. In particular, each isomer exhibits a ^1H NMR. signal in the δ 5.65 - 6.00 region characteristic of the **H**-C5-NO_2 system in such compounds as illustrated in Table 4.5.

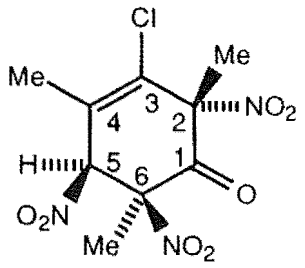

(89)

Table 4.5 ^{1}H NMR ($CDCl_3$) resonances for H5 of isomers (86-89).

Compound	H5 resonance (ppm)
(86)	5.99
(87)	5.78
(88)	5.92
(89)	5.68

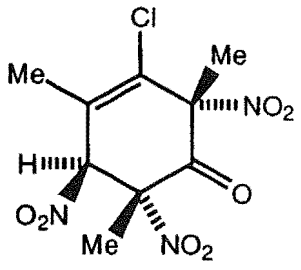

(86)

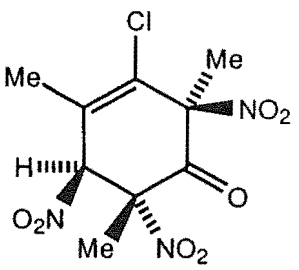

(87)

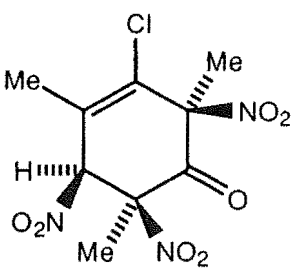

(88)

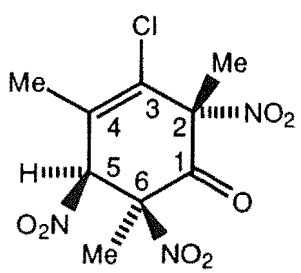

(89)

Further, it has been shown for 2,5,6-trinitrocyclohex-3-enones that the signal due to H5 appears downfield (*c.* $\Delta\,\delta$ 0.17 - 0.31) for *trans*-5,6-dinitro compounds relative to the corresponding *cis*-5,6-dinitro compounds.[28]

Comparison of the ^{1}H NMR resonances for H5 in the present series of compounds: (86) δ 5.99, (87) δ 5.78 ($\Delta\delta$ 0.21); (88) δ 5.92, (89) δ 5.68 ($\Delta\delta$ 0.24); reveals a pattern consistent with compounds (88) and (89) being the *cis*-5,6-dinitro isomers and compounds (86) and (87) being the *trans*-5,6-dinitro isomers.

Two further compounds, C2-epimeric 5-chloro-6-hydroxy-2,5-dinitro compounds (90) and (91), were also isolated in an impure state, and their structures assigned on the basis of their ^1H NMR spectra.

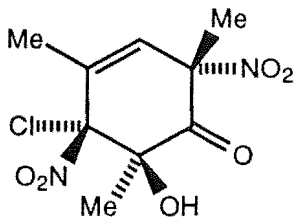

(90)

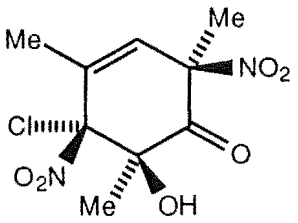

(91)

Both compounds exhibited a resonance due to the vinylic H3 coupled to the 4-methyl group, and a resonance due to the 6-methyl group reflecting the presence of the hydroxy group at C6 as illustrated in Table 4.6.

Table 4.6 ^1H NMR ($CDCl_3$) resonances for H3 and C6-Me of isomers (90) and (91).

Compound (90)	Resonance (ppm)	Compound (91)	Resonance (ppm)
H3	6.41	H3	6.23
C6-Me	1.65	C6-Me	1.61

As such 6-hydroxy-2,5-dinitro ketones characteristically have the *cis*-5-nitro-6-hydroxy stereochemistry,[27] as discussed in Chapter 2 (pg 42), compounds (90) and (91) were assigned C2-epimeric structures. The C2-stereochemistry for compounds (90) and (91) were assigned on the basis of the effect of the C2-stereochemistry of such compounds on the chemical shift of the adjacent vinylic H3 resonance. For a given 5,6-stereochemistry, the H3 resonance for *r*-2,*t*-5-

dinitro compounds occurs downfield (Δδ 0.10 - 0.20) from the H3 resonance for *r*-2,*c*-5-dinitro compounds.[28] Accordingly, compound (90) which exhibits a H3 resonance at δ 6.41 is assigned the *r*-2,*t*-5 stereochemistry, compared with the *r*-2,*c*-5-dinitro compound (91) (δ 6.23) (Δδ 0.18).

Of the products identified from the above reaction 3-chloro-2,5,6-trinitrocyclohex-3-enones (86) - (89) accounted for some 46% of the crude product, with 3-chloro-6-hydroxy-2,5-dinitro ketones (84) and (85) (total 16%), and 5-chloro-6-hydroxy-2,5-dinitro ketones (90) and (91) (total 16%) as illustrated in Table 4.7.

Table 4.7 Yields (%) of identified products from the nitration of phenol (33) with nitrogen dioxide in benzene.

Compounds	% Yields
3-chloro-2,5,6-trinitrocyclohex-3-enones (86 - 89)	46%
3-chloro-6-hydroxy-2,5-dinitro ketones (84) and (85)	(total 16%),
5-chloro-6-hydroxy-2,5-dinitro ketones (90) and (91)	(total 16%)

It appears, therefore, that the presence of the 3-chloro group in 3-chloro-2,4,6-trimethylphenol (33) results in a preference for radical recombination (Scheme 4.1) to occur with the formation of the 3-chloro-6-nitro dienone (92) or the 3-chloro-6-hydroxydienone (93) from the 4-nitrocyclohexa-2,5-dienone (94).

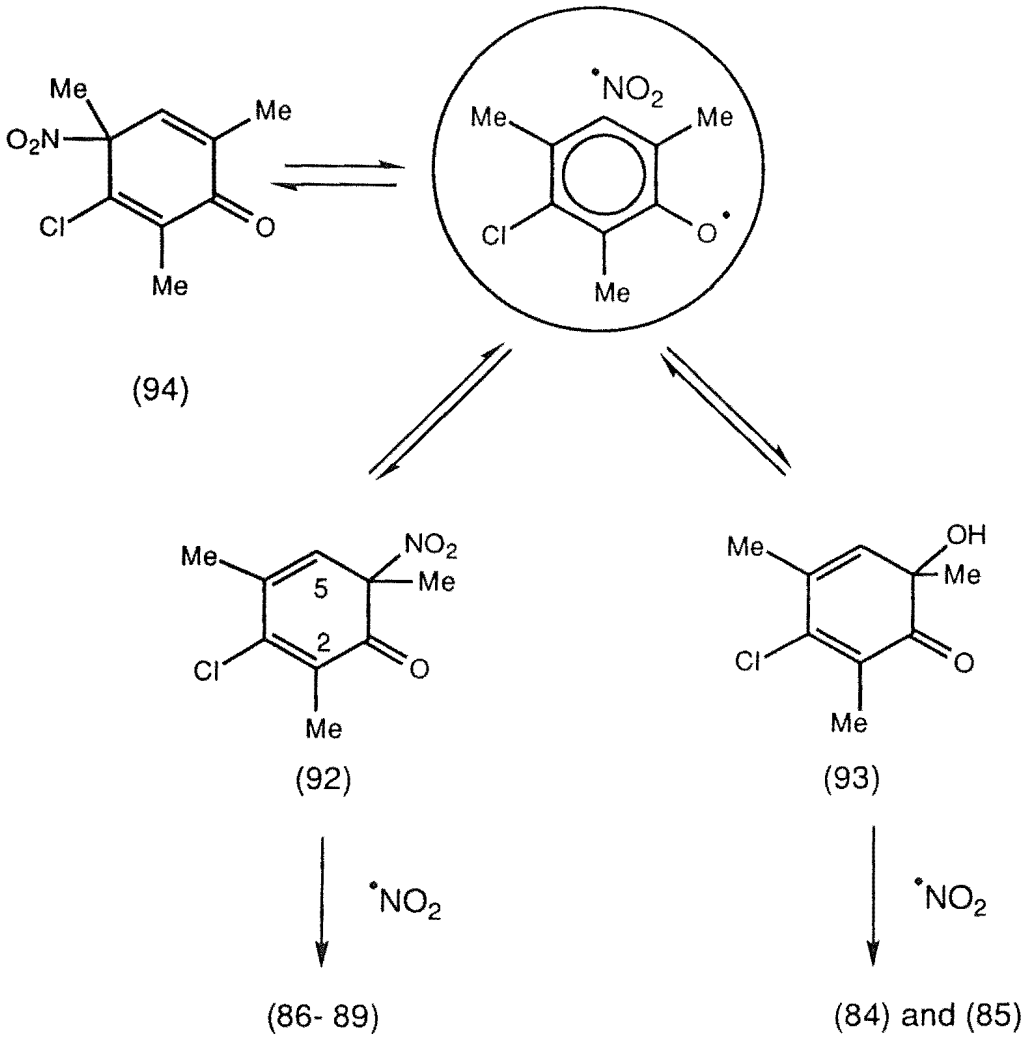

SCHEME 4.1

4.3 OVERVIEW OF THE REACTIONS OF PHENOLS (31), (32) AND (33) WITH NO_2

In the recombination of the phenoxy radical with nitrogen dioxide it is clear that the substituent X (Scheme 4.2) has a marked effect on the regiochemistry of the reaction. For the 3-methyl phenols (X = Me) (31) and (32) radical recombination with the phenoxy radical (95) resulted in C-N or C-O bond formation to give predominantly products derived from further addition of nitrogen dioxide to the 6-nitro- or 6-hydroxy- 5-methylcyclohexa-2,4-dienones (96) or (97) (Scheme 4.2). In contrast, for the 3-chloro phenol (33) radical recombination resulted in C-N or C-O bond formation to give ultimately products

derived from further addition of nitrogen dioxide to 6-nitro- or 6-hydroxy-3-chlorocyclohexa-2,4-dienones.

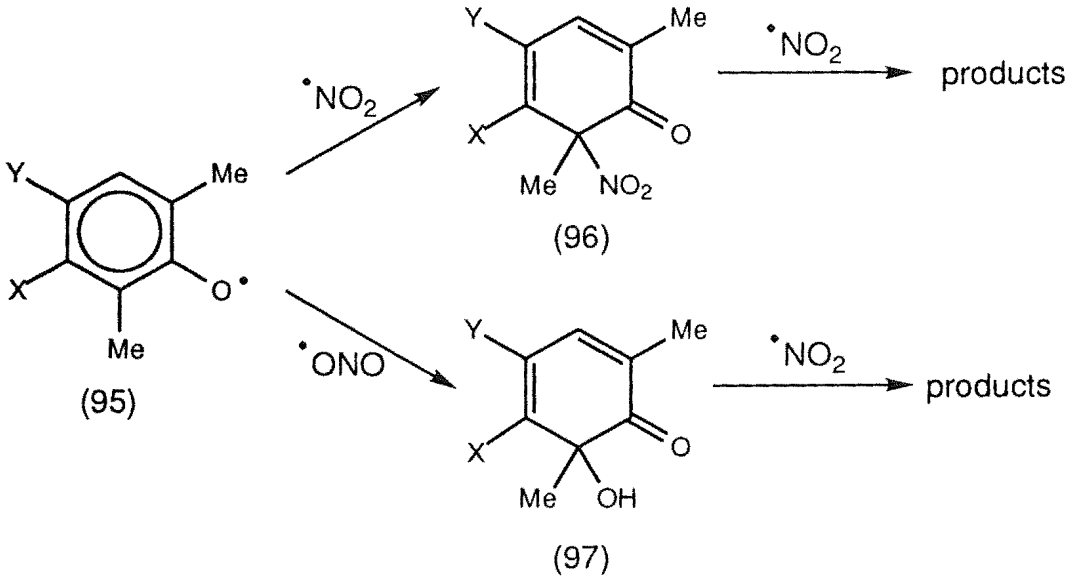

SCHEME 4.2

Apart from the above effects of substituents on the regiochemistry of radical recombination, it is clear that replacement of a methyl group by chlorine at C3 or C4 in the 2,3,4,6-tetramethylphenol (32) promotes the formation of 6-hydroxy-2,5-dinitro ketones. Although it may be tempting to attribute this effect to a favouring of radical recombination by the more nucleophilic •ONO in the presence of electron-withdrawing chlorine, it is not possible to exclude the alternative possibility that the presence of a chlorine atom facilitates the conversion of the 6-nitro- into the 6-hydroxy- group.

CHAPTER FIVE

EXPERIMENTAL, XRAY AND REFERENCES

5.1 APPARATUS. MATERIALS AND INSTRUMENTATION

Infrared spectra were recorded on a Perkin-Elmer Series 1600 FTIR for liquid films and KBr disks. ^{1}H and ^{13}C NMR. and nuclear Overhauser enhancement experiments were obtained for deutero-chloroform using TMS as an internal standard on either a Varian XL-300 or Unity 300 spectrometer. All chemical shifts are expressed as part per million (ppm) downfield from TMS and are singlets unless otherwise stated. Deutero-acetone solutions were used where solubility in deutero-chloroform was insufficient. Mass spectrometry was carried out on a Kratos MS-80. Microanalyses were carried out by Professor A. D. Campbell and associates, University of Otago. Melting points were determined on a microscope slide and are uncorrected.

Preparative scale chromatography was routinely carried out utilising a Chromatotron (a preparative scale, centrifugally accelerated, radial, thin layer chromatograph. Model 7924, Harrison Research Inc.) equipped with rotors with either Silica gel PF-254 (with $2CaSO_{4}.H_{2}O$ type 60 for tlc, Merck: E. M. laboratories Inc., Item No. 7749).

5.2 SYNTHESIS OF NITROGEN DIOXIDE

Pure nitrogen dioxide was prepared for use in a specially designed high-vacuum gas-line as illustrated in Figure 5.1. This line consisted of a 5-litre flask with a cold-finger side arm, a mercury manometer, gas inlet and a set of liquid air cooled gas traps. Pure, dry nitric oxide ('NO - Matheson & Co. 5-litre

atmospheres) was added to the main flask which had previously been evacuated by high vacuum pumping for 1 h.

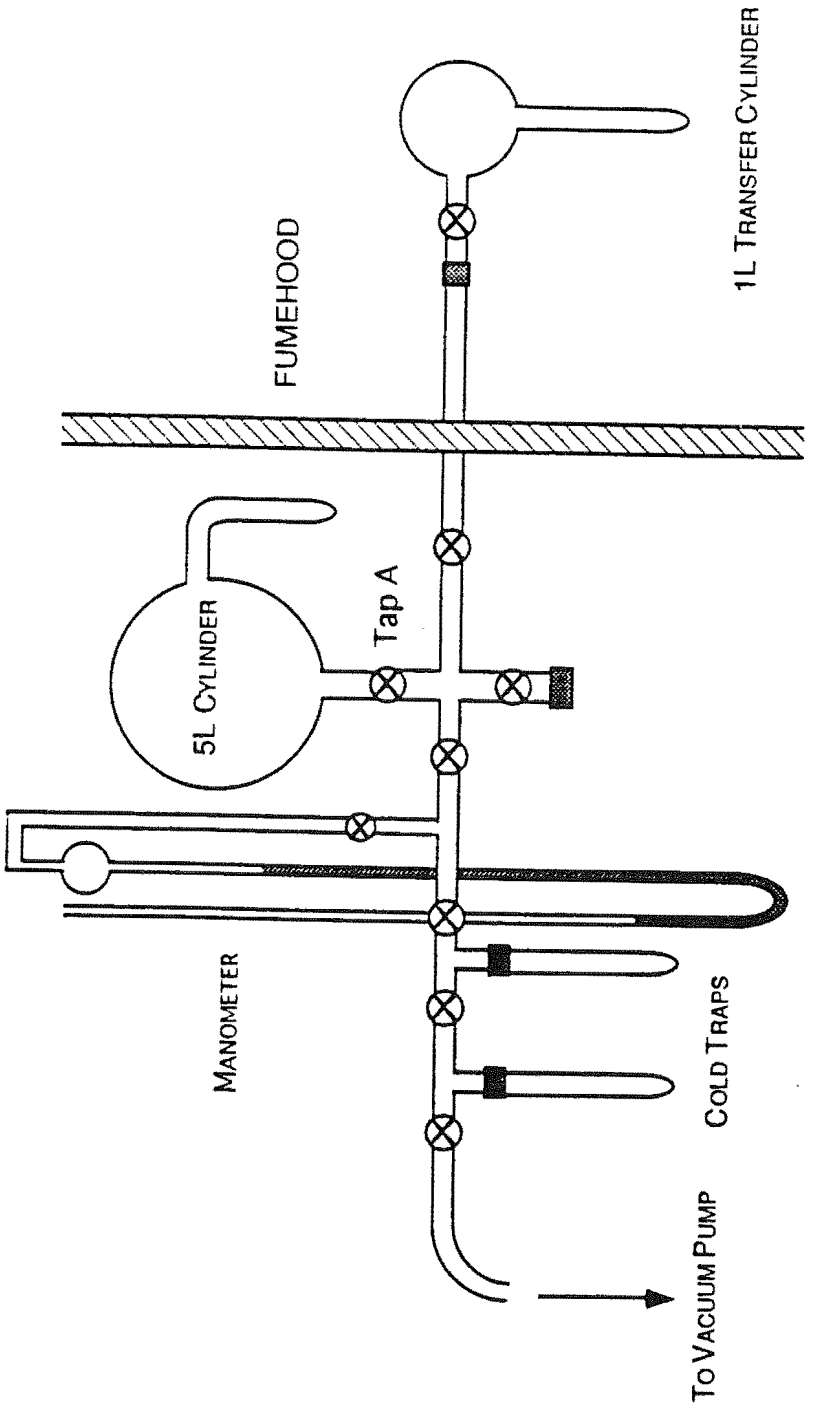

FIGURE 5.1 Nitrogen Dioxide Synthesis Apparatus

The nitric oxide was transferred by condensation at liquid air temperatures into the side arm. When the manometer indicated no residual pressure in the

vacuum line (that is all the nitric oxide condensed), pure, dry oxygen (2.5 litre atmospheres) was added rapidly to the main flask and the cold trap was removed from the side arm containing the condensed nitric oxide allowing the two gases to react. The main flask, sealed at Tap A (refer Figure 5.1), was left overnight to allow the reaction to proceed to completion. The nitrogen dioxide thus formed was transferred by condensation at liquid air temperatures into a specially designed 1-litre flask where it was stored prior to use. During the transfer of nitrogen dioxide to the smaller flask, the crystalline material deposited in the cold finger was colourless, indicating the presence of the dimeric dinitrogen tetroxide only. Other oxides of nitrogen such as dinitrogen trioxide and dinitrogen pentoxide, are coloured so their absence is implied. During the experimental work involving the use of nitrogen dioxide, the utmost care was taken to exclude atmospheric oxygen and water from the storage bulb.

5.3 Preparation of concentrated ^{15}N -labelled nitric acid

The preparation of (^{15}N) Nitric acid [95 atom % ^{15}N] was achieved by distilling under vacuum (^{15}N) sodium nitrate and excess concentrated sulphuric acid (AR). The (^{15}N) Nitric acid [95 atom % ^{15}N] was condensed into a liquid air cooled cold finger and stored at < 4°C for short intervals.

5.4 Experimental relating to chapter 2

The Nitration of 4-Chloro-2,3,6-trimethylphenol (31) with Fuming Nitric Acid in Acetic Acid

Fuming nitric acid (d 1.5, 3 ml) was added dropwise to a stirred suspension of the phenol (31) (3 g) in glacial acetic acid (8 ml) to give a dark orange/red solution which was stirred at 20°C for 1 min. The mixture was dissolved in

ether (150 ml), the organic layer washed with water (200 ml), dried with magnesium sulphate and the solvent removed under reduced pressure to give a yellow residue (4.3 g). Fractional crystallization of this residue, initially using dichloromethane/ether mixtures followed by ether/pentane mixtures for the more soluble compounds, yielded the following products in order of isolation; the yields given are those determined from the ^{1}H NMR spectrum of the product mixture, above.

4-Chloro-c-*6-hydroxy-2,5,6-trimethyl*-r-*2*,c-*5-dinitrocyclohex-3-enone* (37) (25%), m.p. 132-133°C from dichloromethane/ether mixtures (X-ray crystal structure determined, below). ν_{max} (KBr) 3493, OH; 1739, C=O; 1637, C=C; 1569 cm^{-1}, NO_2. ^{1}H NMR ($CDCl_3$) δ 6.56, s, H3; 4.00, s, OH; 2.02, s, 2-Me; 1.95, s, 5-Me; 1.48, s, 6-Me. ^{13}C NMR (D_6-acetone) δ 195.7, C1; 132.1, C4; 129.9, C3; 97.5, 88.7, C2, C5; 23.0, 22.1, 2-Me, 5-Me; 15.3, 6-Me.

4-Chloro-c-*6-hydroxy-2,3,6-trimethyl*-r-*2*,c-*5-dinitrocyclohex-3-enone* (38) (11%), m.p. 139-141°C from ether/pentane mixtures (X-ray crystal structure determined, below). ν_{max} (KBr) 3491, OH; 1743, C=O; 1653, C=C; 1560 cm^{-1}, NO_2. ^{1}H NMR ($CDCl_3$) δ 5.45, br s, H5; 4.04, s, OH; 2.02, s, 2-Me; 1.99, br s, 3-Me; 1.62, s, 6-Me. ^{13}C NMR ($CDCl_3$) δ 198.5, C1; 132.7, C3; 130.1, C4; 125.0, C2; 97.3, C5; 75.8, C6; 24.8, 23.9, 2-Me, 3-Me; 16.7, 6-Me.

4-Chloro-t-*6-hydroxy-2,3,6-trimethyl*-r-*2*,t-*5-dinitrocyclohex-3-enone* (40) (11%), which co-crystallized with 4-chloro-*t*-6-hydroxy-2,5,6-trimethyl-*r*-2,*t*-5-dinitrocyclohex-3-enone (39) below, m.p. 102-103°C from ether/pentane mixtures (X-ray crystal structure determined, below). ν_{max} (KBr) 3523, OH; 1748, C=O; 1647, C=C; 1560 cm^{-1}, NO_2. By subtraction, the NMR solution spectra for compound (16) are: ^{1}H NMR ($CDCl_3$) δ 5.45, br s, H5; 3.84, s, OH; 2.09, s, 2-Me; 2.02, br s, 3-Me; 1.68, s, 6-Me. ^{13}C NMR ($CDCl_3$) δ

197.6, C1; 143.5, C3; 130.7, C4; 97.0, C5; 84.7, C2; 58.7, C6; 25.1, 21.5, 2-Me, 5-Me; 16.9, 6-Me.

4-Chloro-t-6-hydroxy-2,5,6-trimethyl-r-2,t-5-dinitrocyclohex-3-enone (39) (26%), m.p. 97-98°C from ether/pentane mixtures (X-ray crystal structure determined, below). ν_{max} (KBr) 3505, OH; 1747, C=O; 1647, C=C; 1559 cm^{-1}, NO_2. ^1H NMR ($CDCl_3$) δ 6.73, s, H3; 2.10, s, 2-Me; 1.94, s, 5-Me; 1.40, s, 6-Me. ^{13}C NMR ($CDCl_3$) δ 195.6, C1; 133.6, C4; 130.3, C3; 98.8, 87.6, C2, C5; 65.3, C6; 23.0, 22.5, 2-Me, 5-Me; 16.3, 6-Me.

2,3,5–Trimethyl-1,4-benzoquinone (41) (22%), m.p. 32-34°C from pentane solutions. ν_{max} (liquid film) 1647, C=O; 1618 cm^{-1}, C=C; identical with an authentic sample. ^1H NMR ($CDCl_3$) δ 6.56, q, $J_{H,Me}$ 1.6 Hz, H5; 2.04, d, $J_{Me,H}$ 1.6 Hz, 6-Me; 2.02, 2.01, each q, $J_{Me,Me}$ 1.1 Hz, 2-Me, 3-Me. ^{13}C NMR ($CDCl_3$) δ 187.8, 187.4, C1, C4; 145.8, C6; 140.7, 140.8, C2, C3; 133.0, C5; 34.2, 23.5, 14.0, methyl carbons.

Reaction of 4-Chloro-2,3,6-trimethylphenol (31) with Nitrogen Dioxide in Benzene

A solution of the phenol (31) (510 mg) in benzene (5 ml) was deoxygenated by a stream of pure nitrogen. Pure nitrogen dioxide was bubbled through the stirred solution at 0°C for 1 min., and the resulting solution stirred for 2 h. at 0°C under a positive pressure of nitrogen dioxide. The excess nitrogen dioxide was removed in a stream of nitrogen, and the solvent removed under reduced pressure to give a viscous pale yellow oil (1.05 g). This oil was shown (^1H NMR spectra) to be a mixture of four major and a number of minor components. A number of the components of this mixture were

separated by chromatography on a silica gel Chromatotron plate; the yields given below are the amounts of each compound in the crude product mixture.

Elution with pentane gave 2,3,5-trimethyl-1,4-benzoquinone (41) (2%), identical with authentic material.

Elution with pentane/ether (99:1) gave *4-chloro-2,5,6-trimethyl*-r-*2*,t-*5*,c-*6-trinitrocyclohex-3-enone* (45) (16%), m.p. 78-79°C (X-ray crystal structure determined, below). ν_{max} (KBr) 1749, C=O; 1647, C=C; 1560 cm^{-1}, NO_2. ^1H NMR ($CDCl_3$) δ 6.99, s, H3; 2.10, s, 2-Me; 2.01, s, 5-Me; 1.84, s, 6-Me. ^{13}C NMR ($CDCl_3$) δ 183.6, C1; 131.9, C3 and C4; 96.5, C5; 92.4, C2; 87.4, C6; 24.7, 18.6, 16.5, methyl carbons.

Elution with pentane/ether (19:1) gave 4-chloro-2,5,6-trimethyl-*r*-2,*c*-5,*t*-6-trinitrocyclohex-3-enone (46) (20%), m.p. 83-85°C, unstable material isolated only in low yield, mass spectrum unobtainable. ν_{max} (KBr) 1751, C=O; 1653, C=C; 1566 cm^{-1}, NO_2. ^1H NMR ($CDCl_3$) δ 6.79, s, H3; 2.13, s, 5-Me; 2.01, s, 2-Me; 1.91, s, 6-Me. ^{13}C NMR ($CDCl_3$) δ 185.1, C1; 132.9, C4; 131.3, C3; 94.5, C6; 93.9, C5; 88.7, C2; 27.6, 27.5, 17.6, methyl carbons.

Elution with pentane/ether (19:1) gave 4-chloro-*c*-6-hydroxy-2,5,6-trimethyl-*r*-2,*c*-5-dinitrocyclohex-3-enone (37) (7%), m.p. 132-133°C, identical with authentic material.

Elution with pentane/ether (4:1) gave *4-chloro-2,5,6-trimethyl*-r-*2*,t-*5*,t-*6-trinitrocyclohex-3-enone* (47) (16%), m.p. 98-100°C (X-ray crystal structure determined, below). ν_{max} (KBr) 1760, C=O; 1645, C=C; 1556 cm^{-1}, NO_2. ^1H NMR ($CDCl_3$) δ 6.77, s, H3; 2.15, 2-Me; 1.97, 5-Me; 1.95, 6-Me. ^{13}C NMR

($CDCl_3$) δ 184.2, C1; 133.9, C4; 131.0, C3; 97.4, C6; 95.7, C5; 89.7, C2; 23.0, 21.3, 17.5, methyl carbons.

Elution with pentane/ether (1:1) gave 4-chloro-*t*-6-hydroxy-2,5,6-trimethyl-*r*-2,*t*-5-dinitrocyclohex-3-enone (39) (5%), m.p. 97-98°C, identical with authentic material.

Elution with ether/methanol (99:1) gave *4-chloro-2,5,6-trimethyl*-r-*2*,c-*5*,c-*6-trinitrocyclohex-3-enone* (48) (10%), m.p. 121.5-122°C (Found: C, 35.1; H, 3.3; Cl, 11.6; N, 13.8%. $C_9H_{10}ClN_3O_7$ requires C, 35.1; H, 3.3; Cl, 11.5; N, 11.5%). ν_{max} (KBr) 1756, C=O; 1638, C=C; 1560 cm^{-1}, NO_2. ^1H NMR ($CDCl_3$) δ 6.66, s, H3; 2.08, -Me; 2.00, -Me; 1.97, -Me. ^{13}C NMR ($CDCl_3$) δ 186.8, C1; 130.8, C4; 130.5, C3; 89.9, C2, 98.5, C6 96.1, C5,; 27.1, 22.2, 17.6, methyl carbons.

Also observed in the initial ^1H NMR spectrum were 4-chloro-*c*-6-hydroxy-2,3,6-trimethyl-*r*-2,*c*-5-dinitrocyclohex-3-enone (38) (2%) and 4-chloro-*t*-6-hydroxy-2,3,6-trimethyl-*r*-2,*t*-5-dinitrocyclohex-3-enone (40) (2%) but were eluted together from the silica gel plate only as an impure fraction.

Attempted Preparation of 4-Chloro-2,3,6-trimethyl-4-nitrocyclohexa-2,5-dienone (42)

Concentrated nitric acid (0.18 ml) was added dropwise to a stirred suspension of 4-chloro-2,3,6-trimethylphenol (31) (500 mg) in acetic acid (3 ml). The product was extracted using petroleum ether (2 x 10 ml) and the petroleum ether solution washed with water (3 x 50 ml). The organic layer was separated, dried and the solvent removed under reduced pressure to give a

yellow residue (354 mg) shown to be 2,3,5-trimethyl-1,4-benzoquinone (17), identical with authentic material.

5.5 EXPERIMENTAL RELATING TO CHAPTER 3

Reaction of 2,3,4,6-Tetramethylphenol (32) with Nitrogen Dioxide

A solution of the phenol (32) (500 mg) in benzene (5 ml) was deoxygenated by a stream of pure nitrogen. Pure nitrogen dioxide was bubbled through the stirred solution at 20°C for 1 min. and the solution stirred at 20°C under an atmosphere of nitrogen dioxide for 48 h. The excess nitrogen dioxide was then removed in a stream of nitrogen and the solvent removed under reduced pressure to give a yellow oily residue (1.10 g). This mixture was partially separated into its components (given below) by chromatography on a silica gel Chromatotron plate, but some of the products (*c.* 30%) could not be isolated; yields given below for the products isolated are based on integrals for the ^{1}H NMR spectrum of the yellow oily material, above.

Elution with pentane/ether (99 : 1) gave *2,4,5,6-tetramethyl*-r-*4*,c-*5*,t-*6-trinitrocyclohex-2-enone* (74) (3%), m.p. 104-105°C (X-ray crystal structure determined, below). ν_{max} (KBr) 1709, α-nitro conjugated ketone; 1560, 1549, 1522 cm^{-1}, NO_2. ^{1}H NMR ($CDCl_3$) δ 6.83, q, $J_{H3,Me}$ 1.5 Hz, H3; 2.22, s, Me; 2.16, d, $J_{Me,H3}$ 1.5 Hz, 2-Me; 1.84, s, 6-Me; 1.81, s, Me. ^{1}H NMR (C_6D_6) δ 6.09, q, $J_{H3,Me}$ 1.5 Hz, H3; 1.84, d, $J_{Me,H3}$ 1.5 Hz, 2-Me; 1.73, s, 5-Me; 1.40, s, 6-Me; 1.07, s, 4-Me. ^{13}C NMR (C_6D_6) δ 183.7, C1; 137.4, C2; 135.3, C3; 97.7, C5; 91.9, C6; 91.4, C4; 25.0, 18.1, 17.2, 16.9, methyl carbon atoms.

Elution with pentane/ether (49 : 1) gave 2,4,5,6-tetramethyl-*r*-4,*t*-5,*c*-6-trinitrocyclohex-2-enone (75) (3%), m.p. 106-108°C (Insufficient for elemental analysis; too unstable for accurate M^+ measurement). ν_{max} (KBr) 1707, α-nitro conjugated ketone; 1563 cm^{-1}, NO_2. ^1H NMR ($CDCl_3$) δ 6.30, q, $J_{H3,Me}$ 1.5 Hz, H3; 2.20, d, $J_{Me,H3}$ 1.5 Hz, 2-Me; 2.05, s, 5-Me; 1.81, s, 6-Me; 1.72, s, 4-Me. ^{13}C NMR ($CDCl_3$) δ 183.2, C1; 140.1, C2; 132.3, C3; 96.9. C5; 88.5, C4; 88.1, C6; 23.5, 18.7, 17.14, 17.10, methyl carbon atoms.

Elution with pentane/ether (49 : 1) gave 2,4,5,6-tetramethyl-*r*-2,*t*-5,*c*-6-trinitrocyclohex-3-enone (69) (11%), m.p. 104-105°C (dec.). ν_{max} (Nujol) 1758, α,α'-dinitro ketone; 1698, C=C; 1565, 1556 cm^{-1}, NO_2. ^1H NMR ($CDCl_3$) δ 6.47, q, $J_{H3,Me}$ 1.5 Hz, H3; 2.02, d, $J_{Me,H3}$ 1.5 Hz, 4-Me; 2.00, s, 2-Me; 1.92, s, 5-Me; 1.83, s, 6-Me; identical with an authentic sample.[28] ^{13}C NMR ($CDCl_3$) δ 185.2, C1; 134.2, C4; 130.1, C3; 96.3, C6; 92.2, C5; 87.2, C2; 24.4, 20.2, 17.7, 16.5, methyl carbon atoms.

Elution with pentane/ether (19 : 1) gave 2,4,5,6-tetramethyl-*r*-2,*c*-5,*t*-6-trinitrocyclohex-3-enone (72) (10%), m.p. 84-85°C (dec.). ν_{max} (Nujol) 1750, α,α'-dinitro ketone; 1570, 1555 cm^{-1}, NO_2. ^1H NMR ($CDCl_3$) δ 6.30, q, $J_{H3,Me}$ 1.5 Hz, H3; 2.08, d, $J_{Me,H3}$ 1.5 Hz, 4-Me; 2.07, s, 2- or 5-Me; 1.97, s, 5- or 2-Me; 1.93, s, 6-Me; identical with an authentic sample.[28] ^{13}C NMR ($CDCl_3$) δ 186.2, C1; 135.4, C4; 129.3, C3; 94.5, 93.4, 88.1, C2, C5, C6; 28.0, 20.4, 18.1, 17.4, methyl carbon atoms. ^1H NMR (C_6D_6) δ 5.59, q, $J_{H3,Me}$ 1.5 Hz, H3; 1.68, s, 2-Me; 1.42, s, 6-Me; 1.29, d, $J_{Me,H3}$ 1.5 Hz, 4-Me; 1.25, s, 5-Me. ^{13}C NMR (C_6D_6) δ 186.6, C1; 136.0, C4; 130.0, C3; 95.2, C6; 93.7, C5; 88.7, C2; 27.9, 19.9, 17.9, 17.4, methyl carbon atoms.

Elution with pentane/ether (9 : 1) gave 2,4,5,6-tetramethyl-*r*-4,*t*-5,*t*-6-trinitrocyclohex-2-enone (73) (3%), m.p. 108-110°C (dec.). ν_{max} (Nujol) 1715,

α-nitro conjugated ketone; 1560 cm^{-1}, NO_2. ^1H NMR ($CDCl_3$) δ 6.40, q, $J_{H3,Me}$ 1.6 Hz, H3; 2.13, d, $J_{Me,H3}$ 1.6 Hz, 2-Me; 1.92, s, 6-Me; 1.91, s, 5-Me; 1.78, s, 4-Me; identical with an authentic sample.[28] ^{13}C NMR ($CDCl_3$) δ 185.1, C1; 137.1, C2; 133.4, C3; 96.4, C6; 95.7, C5; 89.9, C4; 25.4, 21.3, 16.8, 16.7, methyl carbon atoms.

Elution with pentane/ether (22 : 3) gave *r*-2-hydroxy-2,4,5,6-tetramethyl-*c*-5,*c*-6-dinitrocyclohex-3-enone (77) (2%), an oil, ν_{max} (liquid film) 3469, OH; 1738, α-hydroxy-α'-nitro ketone; 1650, C=C; 1556,1527 cm^{-1}, NO_2. ^1H NMR ($CDCl_3$) δ 6.10, q, $J_{H3,Me}$ 1.5 Hz, H3; 1.93, d, $J_{Me,H3}$ 1.5 Hz, 4-Me; 1.91, s, 5-Me; 1.83, s, 6-Me; 1.59, s, 2-Me. ^{13}C NMR ($CDCl_3$) δ 195.6, C1; 137.0, C3; 129.7, C4; 95.3, C5; 92.0, C6; 70.6, C2; 24.1, 19.8, 18.0, 16.6, methyl carbon atoms.

Elution with pentane/ether (3 : 2) gave 2,4,5,6-tetramethyl-*r*-2,*t*-5,*t*-6-trinitrocyclohex-3-enone (71) (16%), m.p. 121-121.5°C (dec.). ν_{max} (Nujol) 1760, α,α'-dinitro ketone; 1576, 1572, 1560 cm^{-1}, NO_2. ^1H NMR ($CDCl_3$) δ 6.33, q, $J_{H3,Me}$ 1.7 Hz, H3; 2.06, s, 2-Me; 2.01, d, $J_{Me,H3}$ 1.7 Hz, 4-Me; 1.90, s, 6-Me; 1.85, s, 5-Me; identical with authentic material.[28] ^{13}C NMR ($CDCl_3$) δ 185.9, C1; 136.6, C4; 129.5, C3; 97.7, C6; 95.5, C5; 89.9, C2; 23.0, 21.5, 19.4, 16.4, methyl carbon atoms.

Elution with pentane/ether (2 : 3) gave r-*2-hydroxy-2,4,5,6-tetramethyl*-t-*5*,t-*6-dinitrocyclohex-3-enone* (78) (4%), m.p. 146-148°C (X-ray crystal structure determined, below). ν_{max} (KBr) 3492, OH; 1732, α-hydroxy-α'-nitro ketone; 1565, 1556, 1526 cm^{-1}, NO_2. ^1H NMR ($CDCl_3$) δ 5.97, q, $J_{H3,Me}$ 1.5 Hz, H3; 2.02, s, 6-Me; 1.92, d, $J_{Me,H3}$ 1.5 Hz, 4-Me; 1.82, s, 5-Me; 1.68, s, 2-Me. ^{13}C NMR ($CDCl_3$) δ 196.2, C1; 135.5, C3; 132.4, C4; 97.2, C6; 95.3, C5; 72.5, C2; 23.8, 22.5, 18.9, 16.4, methyl carbon atoms.

Elution with ether/methanol (200 : 1) gave *2,4,5,6-tetramethyl*-r-*4,* c-*5,*c-*6-trinitrocyclohex-2-enone* (76) (3%), m.p. 114-116°C (dec.) (X-ray crystal structure determined, below). ν_{max} (KBr) 1718, α-nitro conjugated ketone; 1565, 1560, 1527 cm^{-1}, NO_2. ^1H NMR ($CDCl_3$) δ 6.74, q, $J_{H3,Me}$ 1.5 Hz, H3; 2.13, d, $J_{Me,H3}$ 1.5 Hz, 2-Me; 2.10, s, Me; 2.02, s, Me; 2.00, s, 6-Me. ^1H NMR (CD_3CN) δ 6.87, q, $J_{H3,Me}$ 1.5 Hz, H3; 2.12, s, 5-Me; 2.11, d, $J_{Me,H3}$ 1.5 Hz, 2-Me; 2.09, s, 4-Me; 2.06, s, 6-Me. ^{13}C NMR (CD_3CN) δ 186.5, C1; 135.8, C3; 135.3, C2; 98.9, 98.5, C5, C6; 93.8, C4; 23.9, 22.7, 16.0, 15.9 methyl carbon atoms.

Elution with ether/methanol (49 : 1) gave 2,4,5,6-tetramethyl-*r*-2,*c*-5,*c*-6-trinitrocyclohex-3-enone (72) (11%), m.p. 133-133.5°C (dec.). ν_{max} (Nujol) 1761, α,α'-dinitro ketone; 1578, 1573, 1554 cm^{-1}, NO_2. ^1H NMR ($CDCl_3$) δ 6.23, q, $J_{H3,\ Me}$ 1.5 Hz, H3; 2.05, d, $J_{Me,H3}$ 1.5 Hz, 4-Me; 1.95, s, 6-Me; 1.85, s, Me; identical with authentic material.[28] ^1H NMR (D_6-acetone) δ 6.59, q, $J_{H3,Me}$ 1.5 Hz, H3; 2.24, s, 6-Me; 2.23, d, $J_{Me,H3}$ 1.5 Hz, 4-Me; 2.23, s, 2-Me; 2.10, s, 5-Me. ^{13}C NMR (D_6-acetone) δ 188.5, C1; 136.9, C4; 129.3, C3; 95.4, C2; 98.6, 90.2, C5, C6; 26.4, 22.3, 18.8, 16.0, methyl carbon atoms.

Preparation of ^{15}N-labelled 2,3,4,6-Tetramethyl-4-nitrocyclohexa-2,5-dienone (81)

^{15}N-nitric acid (0.148 ml, 95% ^{15}N) was added dropwise to a stirred solution of 2,3,4,6-tetramethylphenol (32) (500 mg) in dichloromethane (3 ml) at -10°C. After 5 min. the solvent was removed under reduced pressure to give a pale yellow residue (636 mg) which was shown to be essentially pure ^{15}N-2,3,4,6-tetramethyl-4-nitrocyclohexa-2,5-dienone (81), ^1H NMR ($CDCl_3$) δ

6.59, dq, $J_{H5,15\text{-}N}$ 1.1 Hz, $J_{H5,Me}$ 1.5 Hz, H5; 1.95, br s, Me; 1.94, br s, Me; 1.93, br d, $J_{Me,H5}$ 1.5 Hz, 6-Me; 1.85, d, $J_{Me,15\text{-}N}$ 3.2 Hz, 4-Me.

Reaction of ^{15}N-labelled 2,3,4,6-Tetramethyl-4-nitrocyclohexa-2,5-dienone (81) with Nitrogen Dioxide in Benzene Solution

A solution of the ^{15}N-labelled nitro dienone (81) (600 mg) in benzene (5 ml) at 4°C was deoxygenated by a stream of pure nitrogen. Pure nitrogen dioxide was bubbled through the stirred solution for 1 min. at 4°C and the resulting mixture stirred under an atmosphere of nitrogen dioxide for 48 h. The excess nitrogen dioxide was then removed in a stream of nitrogen and the solvent removed under reduced pressure to give a yellow oil shown (^{1}H NMR) to have a composition essentially identical (except for the presence of the ^{15}N-label) with the mixture obtained above from reaction of the phenol (32) with nitrogen dioxide. Chromatography on a silica gel Chromatotron plate gave the following compounds, the position and extent of the ^{15}N-label in each compound being determined by ^{1}H NMR spectra.

2,4,5,6-Tetramethyl-*r*-4,*c*-5,*t*-6-trinitrocyclohex-2-enone (74) with ^{15}N incorporation (59±5%) located at C6, ^{1}H NMR (C_6D_6) δ 6.09, q, $J_{H3,Me}$ 1.5 Hz, H3; 1.84, d, $J_{Me,H3}$ 1.5 Hz, 2-Me; 1.73, s, 5-Me; 1.40, d, $J_{Me,15\text{-}N}$ 3.0 Hz, 6-Me; 1.40, s, 6-Me; 1.07, s, 4-Me.

2,4,5,6-Tetramethyl-*r*-4,*t*-5,*c*-6-trinitrocyclohex-2-enone (75) with ^{15}N incorporation (62±5%) located at C6, ^{1}H NMR ($CDCl_3$) δ 6.30, q, $J_{H3,Me}$ 1.5 Hz, H3; 2.20, d, $J_{Me,H3}$ 1.5 Hz, 2-Me; 2.05, s, 5-Me; 1.81, d, $J_{Me,15\text{-}N}$ 3.0 Hz, 6-Me; 1.81, s, 6-Me; 1.72, s, 4-Me.

2,4,5,6-Tetramethyl-*r*-2,*t*-5,*c*-6-trinitrocyclohex-3-enone (69) with ^{15}N incorporation (56±5%) located at C6, ^1H NMR ($CDCl_3$) δ 6.47, q, $J_{H3,Me}$ 1.5 Hz, H3; 2.02, d, $J_{Me,H3}$ 1.5 Hz, 4-Me; 2.00, s, 2-Me; 1.92, s, 5-Me; 1.83, d, $J_{Me,15\text{-}N}$ 3.0 Hz, 6-Me; 1.83, s, 6-Me.

2,4,5,6-Tetramethyl-*r*-2,*c*-5,*t*-6-trinitrocyclohex-3-enone (70) with ^{15}N incorporation (57±5%) located at C6, ^1H NMR ($CDCl_3$) δ 6.30, q, $J_{H3,Me}$ 1.5 Hz, H3; 2.08, d, $J_{Me,H3}$ 1.5 Hz, 4-Me; 2.07, s, 2- or 5-Me; 1.97, s, 5- or 2-Me; 1.93, d, $J_{Me,15\text{-}N}$ 3.0 Hz, 6-Me; 1.93, s, 6-Me.

2,4,5,6--Tetramethyl-*r*-4,*t*-5,*t*-6-trinitrocyclohex-2-enone (73) with ^{15}N incorporation (60±5%) located at C6, ^1H NMR ($CDCl_3$) δ 6.40, q, $J_{H3,Me}$ 1.6 Hz, H3; 2.13, d, $J_{Me,H3}$ 1.6 Hz, 2-Me; 1.92, d, $J_{Me,15\text{-}N}$ 3.0 Hz, 6-Me; 1.92, s, 6-Me; 1.91, s, 5-Me; 1.78, s, 4-Me.

r-2-Hydroxy-2,4,5,6-tetramethyl-*c*-5,*c*-6-dinitrocyclohex-3-enone (77) with ^{15}N incorporation (61±5%) located at C6, ^1H NMR ($CDCl_3$) δ 6.10, q, $J_{H3,Me}$ 1.5 Hz, H3; 1.93, d, $J_{Me,H3}$ 1.5 Hz, 4-Me; 1.91, s, 5-Me; 1.83, d, $J_{Me,15\text{-}N}$ 3.0 Hz, 6-Me; 1.83, s, 6-Me; 1.59, s, 2-Me.

2,4,5,6-Tetramethyl-*r*-2,*t*-5,*t*-6-trinitrocyclohex-3-enone (71) with ^{15}N incorporation (58±5%) located at C6, ^1H NMR ($CDCl_3$) δ 6.33, q, $J_{H3,Me}$ 1.7 Hz, H3; 2.06, s, 2-Me; 2.01, d, $J_{Me,H3}$ 1.7 Hz, 4-Me; 1.90, d, $J_{Me,15\text{-}N}$ 3.0 Hz, 6-Me; 1.90, s, 6-Me; 1.85, s, 5-Me.

r-2-Hydroxy-2,4,5,6-tetramethyl-*t*-5,*t*-6-dinitrocyclohex-3-enone (78) with ^{15}N incorporation (55±5%) located at C6, ^1H NMR ($CDCl_3$) δ 5.97, q, $J_{H3,Me}$ 1.5 Hz, H3; 2.02, d, $J_{Me,15\text{-}N}$ 3.0 Hz, 6-Me; 2.02, s, 6-Me; 1.92, d, $J_{Me,H3}$ 1.5 Hz, 4-Me; 1.82, s, 5-Me; 1.68, s, 2-Me.

2,4,5,6-Tetramethyl-*r*-4,*c*-5,*c*-6-trinitrocyclohex-2-enone (76) with ^{15}N incorporation (58±5%) located at C6, ^1H NMR (CD_3CN) δ 6.87, q, $J_{H3,Me}$ 1.5 Hz, H3; 2.12, s, 5-Me; 2.11, d, $J_{Me,H3}$ 1.5 Hz, 2-Me; 2.09, s, 4-Me; 2.06, d, $J_{Me,15-N}$ 3.0 Hz, 6-Me; 2.06, s, 6-Me.

2,4,5,6-Tetramethyl-*r*-2,*c*-5,*c*-6-trinitrocyclohex-3-enone (72) with ^{15}N incorporation (60±5%) located at C6, ^1H NMR (D_6-acetone) δ 6.59, q, $J_{H3,Me}$ 1.5 Hz, H3; 2.24, d, $J_{Me,15-N}$ 3.0 Hz, 6-Me; 2.24, s, 6-Me; 2.23, d, $J_{Me,H3}$ 1.5 Hz, 4-Me; 2.23, s, 2-Me; 2.10, s, 5-Me.

5.6 EXPERIMENTAL RELATING TO CHAPTER 4

Reaction of 3-Chloro-2,4,6-trimethylphenol (33) with Nitrogen Dioxide In Benzene Solution

A solution of the phenol (33) (500 mg) in benzene (5 ml) was deoxygenated by a stream of nitrogen. Pure nitrogen dioxide was bubbled through the stirred solution at 20°C for 1 min., and the resulting mixture stirred under an atmosphere of nitrogen dioxide for 16 h. The excess nitrogen dioxide was removed in a stream of nitrogen and the solvent removed under reduced pressure to give a yellow oil (1.1 g), shown (^1H NMR) to be essentially a mixture of eight compounds. Two of these compounds could be isolated by chromatography on a silica gel Chromatotron plate, the remainder being isolated by fractional crystallization; yields given are based ^1H NMR integrals for the mixture. From chromatography:

3-Chloro-t-6-hydroxy-2,4,6-trimethyl-r-2,t-5-dinitrocyclohex-3-enone (84) (8%), m.p. 117-118°C (X-ray crystal structure determined, below). ν_{max} (KBr)

3526, OH; 1745, C=O; 1560 cm^{-1}, NO_2. ^1H NMR ($CDCl_3$) δ 5.32, s, H5; 4.60, OH; 2.25, s, 4-Me; 2.14, s, 2-Me; 1.65, s, 6-Me. ^{13}C NMR ($CDCl_3$) δ 197.27, C1; 133.96, C3; 129.81, C4; 94.97, C5; 93.99, C2; 75.39, C6; 25.08, 6-Me; 21.47, 2-Me; 20.49, 4-Me.

3-Chloro-c-6-hydroxy-2,4,6-trimethyl-r-2,c-5-dinitrocyclohex-3-enone (85) (8%), m.p. 139-140°C (X-ray crystal structure determined, below). ν_{max} (KBr) 3482, OH; 1745, C=O; 1647, C=C; 1560 cm^{-1}, NO_2. ^1H NMR ($CDCl_3$) δ 5.29, s, H5; 2.28, s, 4-Me; 2.09, s, 2-Me; 1.56, s, 6-Me. ^{13}C NMR ($CDCl_3$) δ 197.7, C1; 132.9, C3; 131.0, C4; 95.0, C5; 94.4, C2; 75.4, C6; 24.4, 22.9, 2-Me, 6-Me; 20.4, 4-Me.

From fractional crystallization:

3-Chloro-2,4,6-trimethyl-r-2,t-5,c-6-trinitrocyclohex-3-enone (86) (14%), m.p. 112-113°C (X-ray crystal structure determined, below). ν_{max} (KBr) 1754, C=O; 1653, C=C; 1564 cm^{-1}, NO_2. ^1H NMR ($CDCl_3$) δ 5.99, s, H5; 2.36, s, 4-Me; 2.13, s, 2-Me; 1.94, 6-Me. ^{13}C NMR ($CDCl_3$) δ 183.5, C1; 133.7, C3; 130.3, C4; 93.4, C2; 91.0, C5; 87.6, C6; 21.1, 20.2, 20.1, 2-Me, 4-Me, 6-Me.

3-Chloro-2,4,6-trimethyl-r-2,c-5,t-6-trinitrocyclohex-3-enone (87) (16%), m.p. 111-113°C (X-ray crystal structure determined, below). ν_{max} (KBr) 1760, C=O; 1555 cm^{-1}, NO_2. ^1H NMR ($CDCl_3$) δ 5.92, s, H5; 2.35, s, 4-Me; 2.08, 1.98, each s, 2-Me, 6-Me. ^{13}C NMR ($CDCl_3$) δ 184.0, C1; 133.4, C3; 131.0, C4; 95.1, C2; 90.2, C5; 89.4, C6; 26.0,22.9, 19.5, 2-Me, 4-Me, 6-Me.

3-Chloro-2,4,6-trimethyl-r-2,c-5,c-6-trinitrocyclohex-3-enone (88) (11%), m.p. 120-122°C (X-ray crystal structure determined, below). ν_{max} (KBr) 1764, C=O; 1653, C=C; 1560 cm^{-1}, NO_2. ^1H NMR ($CDCl_3$) δ 5.68, s, H5; 2.42, s, 4-

Me; 2.16, s, 2-Me; 2.03, s, 6-Me. ^{13}C NMR ($CDCl_3$) δ 183.8, C1; 133.3, 130.8, C3, C4; 90.3, 89.95, 89.45, C2, C5, C6; 24.5, 23.0, 20.8, 2-Me, 4-Me, 6-Me.

Three further compounds were detected in the ^1H NMR spectrum of the product mixture, but not isolated in a pure state, above. These were (i) the fourth trinitro ketone (89) (5%), ^1H NMR ($CDCl_3$) δ 5.78, s, H5; 2.25, 2.21, 2.03, each s, methyl groups, (ii) *c*-5-chloro-*t*-6-hydroxy-*r*-2,5-dinitro-2,4,6-trimethylcyclohex-3-enone (90) (5%), ^1H NMR ($CDCl_3$) δ 6.41, q, $J_{H3,4\text{-}Me}$ 1.5 Hz, H3; 2.08, d, $J_{Me,H3}$ 1.5 Hz, 4-Me; 2.05, s, 2-Me; 1.65, s, 6-Me, and (iii) *t*-5-chloro-*c*-6-hydroxy-*r*-2,5-dinitro-2,4,6-trimethylcyclohex-3-enone (91) (11%), ^1H NMR ($CDCl_3$) δ 6.23, q, $J_{H3,4\text{-}Me}$ 1.5 Hz, H3; 2.13, d, $J_{Me,H3}$ 1.5 Hz, 4-Me; 2.01, s, 2-Me; 1.61, s, 6-Me.

Nitration of 3-Chloro-2,4,6-trimethylphenol (33) with Nitric Acid in Acetic Acid

Concentrated nitric acid (0.123 ml) was added dropwise to a stirred solution of the phenol (33) (500 mg) in acetic acid (3 ml) and the resulting mixture stirred for 1 min. The product was extracted by means of petroleum ether and gave, after the removal of the solvents under reduced pressure, 3-chloro-2,4,6-trimethyl-4-nitrocyclohexa-2,5-dienone (94) (369 mg) , ν_{max} (liquid film) 1658, C=O; 1557 cm^{-1}, NO_2. ^1H NMR ($CDCl_3$) δ 6.64, q, $J_{H5,Me}$ 1.5 Hz, H5; 2.13, 2.00, each s, 2-Me, 4-Me; 1.98, d, $J_{Me,H5}$ 1.5 Hz, 6-Me. This nitro-dienone was unstable, with considerable decomposition being evident within 1h.

APPENDIX 1

5.7 CRYSTALLOGRAPHY

Crystal data, established from precession photographs and measured accurately, by means of a Siemens R3m/V four-circle diffractometer [molybdenum X-radiation, λ(Mo Kα) 0.71069 Å, from a crystal monochromator] are given below. The space group was, in each case, determined unambiguously as a result of the structure analyses reported below, but initially indicated by conditions limiting possible reflections. ω-Scans were used to collect reflection intensities out to a maximum Bragg angle θ, given below. The cell parameters were determined, in each case, by least-squares refinements for which the setting angles of 25 accurately centred high-angle reflections were used.

Crystal Data

4-Chloro-c-6-hydroxy-2,5,6-trimethyl-r-2,c-5-dinitrocyclohex-3-enone (37). -$C_9H_{11}ClN_2O_6$, M 278.6, monoclinic, $P\ 2_1/c$, a 12.628(6), b 8.540(3), c 10.745(5) Å, β 94.27(4)°, V 1155.6(4) Å^3, D_c 1.602 g cm^{-3}, Z 4, μ (Mo Kα) 3.5 cm^{-1}. The crystal was colourless and of approximate dimensions 0.36 by 0.34 by 0.2 mm. Data were collected at 193 K out to a maximum Bragg angle θ 26.0°. The number of independent reflections measured 2272, 1176 with $I > 3\sigma(I)$; g 0.0008; absorption corrections were not applied; R-factor 0.050; wR 0.061.

4-Chloro-c-6-hydroxy-2,3,6-trimethyl-r-2,c-5-dinitrocyclohex-3-enone (38). - $C_9H_{11}ClN_2O_6$, M 278.6, monoclinic, $P\ 2_1/c$, a 6.003(1), b 12.02(1), c 16.39(1) Å, β 98.74(7)°, V 1168.6(2) Å^3, D_c 1.584 g cm^{-3}, Z 4, μ (Mo Kα)

3.45 cm^{-1}. The crystal was colourless and of approximate dimensions 0.72 by 0.06 by 0.06 mm. Data were collected at 193 K out to a maximum Bragg angle θ 21.0°. The number of independent reflections measured 1253, 479 with $I > 3\sigma(I)$; g 0.0008; absorption corrections were not applied; R-factor 0.082; wR 0.091. The crystal was of a poor quality and gave low reflection intensities.

4-Chloro-t-6-hydroxy-2,5,6-trimethyl-r-2,t-5-dinitrocyclohex-3-enone (39). - $C_9H_{11}ClN_2O_6$, M 278.6, triclinic, space group $P\bar{1}$, a 6.302(3), b 7.593(4), c 12.911(6) Å, α 75.96(4), β 85.63(4), γ 76.02(4)°, V 581.5(5) $Å^3$, D_c 1.591 g cm^{-3}, Z 2, μ (Mo Kα) 3.5 cm^{-1}. The crystal was colourless and of approximate dimensions 0.4 by 0.42 by 0.1 mm. Data were collected at 193 K out to a maximum Bragg angle θ 29.0°. The number of independent reflections measured 3094, 1951 with $I > 3\sigma(I)$; g 0.0003; absorption corrections were not applied; R-factor 0.042, wR 0.047.

4-Chloro-t-6-hydroxy-2,3,6-trimethyl-r-2,t-5-dinitrocyclohex-3-enone (40), which co-crystallized with 4-chloro-*t*-6-hydroxy-2,5,6-trimethyl-*r*-2,*t*-5-dinitrocyclohex-3-enone (15).-$C_{18}H_{22}Cl_2N_4O_{12}$, M 557.3, triclinic, space group $P\bar{1}$, a 8.585(4), b 11.185(5), c 13.456(3) Å, α 67.03(4), β 84.13(4), γ 80.60(4)°, V 1173(9) $Å^3$, D_c 1.578 g cm^{-3}, Z 2, μ (Mo Kα) 3.44 cm^{-1}. The crystal was colourless and of approximate dimensions 0.2 by 0.56 by 0.08 mm. Data were collected at 193 K out to a maximum Bragg angle θ 27.5°. The number of independent reflections measured 5397, 3416 with $I > 2\sigma(I)$; g 0.0008; absorption corrections were not applied; R-factor 0.053; wR 0.066.

4-Chloro-2,5,6-trimethyl-r-2,t-5,c-6-trinitrocyclohex-3-enone (45) - $C_9H_{10}ClN_3O_7$, M 307.7, monoclinic, space group Pn, a 6.337(3), b 8.942(6), c 10.864(9) Å, β 95.24(5)°, V 613.0(7) $Å^3$, D_c 1.667 g cm^{-3}, Z 2, μ (Mo Kα)

3.4 cm^{-1}. The crystal was colourless and of approximate dimensions 0.48 by 0.12 by 0.10 mm. Data were collected at 173 K out to a maximum Bragg angle θ 30.0°. The number of independent reflections measured 1872, 1560 with $I > 3\sigma(I)$; g 0.0001; absorption corrections were not applied; R-factor 0.037; wR 0.036.

4-Chloro-2,5,6-trimethyl-r-2,t-5,t-6-trinitrocyclohex-3-enone (47). - $C_9H_{10}ClN_3O_7$, M 307.7, monoclinic, space group $P\,2_1/c$, a 15.323(8), b 6.5550(3), c 13.570(7) Å, β 114.47(4)°, V 1241(1) $Å^3$, D_c 1.647 g cm^{-3}, Z 4, μ (Mo Kα) 3.41 cm^{-1}. The crystal was colourless and of approximate dimensions 0.41 by 0.32 by 0.19 mm. Data were collected at 193 K out to a maximum Bragg angle θ 27.5°. The number of independent reflections measured 2853, 1929 with $I > 2\sigma(I)$; g 0.0005; absorption corrections were not applied; R-factor 0.049, wR 0.051.

2,4,5,6-Tetramethyl-r-4,c-5,t-6-trinitrocyclohex-2-enone (74). - $C_{10}H_{13}N_3O_7$, M 287.23, orthorhombic, space group $Pna2_1$, a 13.073(3), b 9.403(2), c 10.429(2) Å, V 1282.0(5) $Å^3$, D_c 1.488 g cm^{-3}, Z 4, μ(Mo Kα) 1.28 cm^{-1}. The crystal was colourless and of approximate dimensions 0.48 by 0.32 by 0.08 mm. Data were collected at 183 K out to a maximum Bragg angle θ 25°. The number of independent reflections measured 1329, 575 with $I > 2\sigma(I)$; g_1 0.1775, g_2 0.00; absorption corrections were not applied; $R_{(obs)}$-factor 0.100, $wR_{(all\ data)}$ 0.324. The crystal was of a poor quality and gave low reflection intensities.

2,4,5,6-Tetramethyl-r-4,c-5,c-6-trinitrocyclohex-2-enone (76). - $C_{10}H_{13}N_3O_7$, M 287.23, monoclinic, space group $P\,2_1/c$, a 6.8420(3), b 14.740(5), c 12.438(4) Å, β 102.56(3)°, V 1224.4(7) $Å^3$, D_c 1.558 g cm^{-3}, Z 4, μ(Mo Kα) 1.34 cm^{-1}. The crystal was colourless and of approximate dimensions 0.68 by

0.56 by 0.32 mm. Data were collected at 183 K out to a maximum Bragg angle θ 27.5°. The number of independent reflections measured 2807, 2230 with $I > 2\sigma(I)$; g_1 0.0565, g_2 0.4568; absorption corrections were not applied; $R_{(obs)}$-factor 0.041, $wR_{(all\ data)}$ 0.109.

r-2-Hydroxy-2,4,5,6-tetramethyl-t-5,t-6-dinitrocyclohex-3-enone (78). - $C_{10}H_{14}N_2O_6$, M 258.23, monoclinic, space group $P\ 2_1/n$, a 6.245(1), b 26.546(5), c 7.489(1) Å, β 104.46(3)°, V 1202.2(3) Å^3, D_c 1.427 g cm^{-3}, Z 4, μ(Mo Kα) 1.19 cm^{-1}. The crystal was colourless and of approximate dimensions 0.62 by 0.44 by 0.12 mm. Data were collected at 183 K out to a maximum Bragg angle θ 26°. The number of independent reflections measured 2360, 1547 with $I > 2\sigma(I)$; g_1 0.0412, g_2 0.6021; absorption corrections were not applied; $R_{(obs)}$-factor 0.051, $wR_{(all\ data)}$ 0.117.

3-Chloro-t-6-hydroxy-2,4,6-trimethyl-r-2,t-5-dinitrocyclohex-3-enone (84). - $C_9H_{11}ClN_2O_6$, M 278.6, monoclinic, space group $P\ 2_1/c$, a 9.844(4), b 7.077(4), c 17.043(9) Å, β 102.2(10)°, V 1161(1) Å^3, D_c 1.595 g cm^{-3}, Z 4, μ(Mo Kα) 3.47 cm^{-1}. The crystal was colourless and of approximate dimensions 0.44 by 0.36 by 0.1 mm. Data were collected at 193 K out to a maximum Bragg angle θ 27.5°. The number of independent reflections measured 2666, 1485 with $I > 3\sigma(I)$; absorption corrections were not applied; g 0.0006; R-factor 0.043, wR 0.051.

3-Chloro-c-6-hydroxy-2,4,6-trimethyl-r-2,c-5-dinitrocyclohex-3-enone (85). - $C_9H_{11}ClN_2O_6$, M 278.6, monoclinic, space group $P\ 2_1/n$, a 6.1280(4), b 11.937(11), c 16.505(14) Å, β 98.34(6)°, V 1194.6(4) Å^3, D_c 1.549 g cm^{-3}, Z 4, μ(Mo Kα) 3.37 cm^{-1}. The crystal was colourless and of approximate dimensions 0.42 by 0.12 by 0.05 mm. Data were collected at 193 K out to a maximum Bragg angle θ 23°. The number of independent reflections

measured 1648, 291 with $I > 3\sigma(I)$; absorption corrections were not applied; g 0.0006; R-factor 0.083, wR 0.085. The crystal was of a poor quality and gave low reflection intensities.

3-Chloro-2,4,6-trimethyl-r-*2*,t-*5*,c-*6-trinitrocyclohex-3-enone (86).* - $C_9H_{10}ClN_3O_7$, M 307.7, orthorhombic, space group $P\,2_12_12_1$, a 6.817(5), b 13.252(9), c 14.12(1) Å, V 1275(2) Å^3, D_c 1.602 g cm^{-3}, Z 4, μ(Mo Kα) 3.31 cm^{-1}. The crystal was colourless and of approximate dimensions 0.42 by 0.24 by 0.12 mm. Data were collected at 193 K out to a maximum Bragg angle θ 27.5°. The number of independent reflections measured 1697, 799 with $I > 2\sigma(I)$; absorption corrections were not applied; g 0.0004; R-factor 0.063, wR 0.050.

3-Chloro-2,4,6-trimethyl-r-*2*,c-*5*,t-*6-trinitrocyclohex-3-enone (87).* - $C_9H_{10}ClN_3O_7$, M 307.7, monoclinic, space group $P\,2_1/n$, a 6.281(3), b 13.076(8), c 15.264(7) Å, β 98.61(4)°, V 1240(1) Å^3, D_c 1.649 g cm^{-3}, Z 4, μ(Mo Kα) 3.41 cm^{-1}. The crystal was colourless and of approximate dimensions 0.32 by 0.28 by 0.1 mm. Data were collected at 193 K out to a maximum Bragg angle θ 25°. The number of independent reflections measured 2181, 1009 with $I > 2\sigma(I)$; absorption corrections were not applied; g 0.0006; R-factor 0.076, wR 0.079.

3-Chloro-2,4,6-trimethyl-r-*2*,c-*5*,c-*6-trinitrocyclohex-3-enone (88).* - $C_9H_{10}ClN_3O_7$, M 307.7, monoclinic, space group $P\,2_1/c$, a 13.245(6), b 8.682(4), c 11.088(4) Å, β 95.25(3)°, V 1270(1) Å^3, D_c 1.609 g cm^{-3}, Z 4, μ(Mo Kα) 3.33 cm^{-1}. The crystal was colourless and of approximate dimensions 0.3 by 0.22 by 0.1 mm. Data were collected at 193 K out to a maximum Bragg angle θ 26°. The number of independent reflections

measured 2493, 1367 with $I > 3\sigma(I)$; absorption corrections were not applied; g 0.0002; R-factor 0.039, wR 0.041.

Structure Determination

The structures were solved by direct methods and difference-Fourier syntheses. Blocked cascade least-squares[33] were employed for structures (37), (38), (39), (39/40), (45), (47), (84), (85), (86) (87) and (88), reflection weights $1/[\sigma^2(F) + g(F^2)]$ being used. The function minimized was $\Sigma w(|F_o| - |F_c|)^2$. Anomalous dispersion corrections were from Cromer and Liberman.[34]

For compounds (74), (76), and (78) full matrix least-squares refinements (SHELXL-92)[35] were employed. This program is based on intensities and uses all data. The observed threshold $I > 2\sigma(I)$ was used only for calculating $R_{(obs)}$, shown here as a comparison for the refinements based on F. Reflection weights $1/[\sigma^2(F_o^2) + (g_1P)^2 + g_2P]$, where $P = [F_o^2 + 2F_c^2]/3$, were used.

All non-hydrogen atoms were assigned anisotropic thermal parameters, except for structures (38) and (85) where only the chlorine atom was assigned the appropriate anisotropic thermal parameter. Methyl hydrogen atoms were included as rigid groups pivoting about their carbon atoms. Final Fourier syntheses show no significant residual electron density, and there were no abnormal discrepancies between observed and calculated structure factors.

Table 5.1. Fractional coordinates for atoms in 4-chloro-*c*-6-hydroxy-2,5,6-trimethyl-*r*-2,*c*-5-dinitrocyclohex-3-enone (37)

The equivalent isotropic temperature factor in Tables 5.1-5.14 is defined as one-third of orthoganalized U tensor (Å^2).

Atom	$10^4X/a$	$10^4Y/b$	$10^4Z/c$	10^3U (Å^2)
Cl(4)	133(1)	942(2)	2005(1)	39(1)
O(1)	4340(2)	-961(4)	3770(3)	26(1)
O(21)	3884(3)	-3619(4)	2005(4)	46(2)
O(22)	2331(3)	-3476(4)	2730(4)	39(1)
O(51)	2092(3)	-1212(4)	4685(4)	44(1)
O(52)	1213(4)	619(5)	5531(4)	65(2)
O(6)	3601(3)	1639(4)	4770(3)	31(1)
N(2)	3093(3)	-2905(5)	2258(4)	29(1)
N(5)	1714(3)	115(5)	4703(4)	35(2)
C(1)	3596(4)	-370(5)	3197(4)	19(1)
C(2)	3056(3)	-1115(5)	1993(4)	19(1)
C(3)	1914(3)	-622(5)	1751(5)	21(1)
C(4)	1443(3)	414(5)	2425(5)	21(1)
C(5)	1940(4)	1201(5)	3593(4)	21(2)
C(6)	3169(4)	1238(5)	3577(4)	20(1)
C(7)	3719(4)	-782(6)	896(5)	27(2)
C(8)	1495(4)	2801(6)	3832(6)	40(2)
C(9)	3489(4)	2465(5)	2617(5)	27(2)

Table 5.2. Fractional coordinates for atoms in 4-chloro-*c*-6-hydroxy-2,3,6-trimethyl-*r*-2,*c*-5-dinitrocyclohex-3-enone (38)

Atom	$10^4X/a$	$10^4Y/b$	$10^4Z/c$	10^3U (Å^2)
Cl(4)[a]	1939(10)	922(4)	4588(3)	38(2)
O(1)	-387(22)	3438(11)	7260(8)	30(4)
O(21)	1484(23)	1238(12)	8272(9)	44(4)
O(22)	-874(23)	843(11)	7197(8)	38(4)
O(51)	-3029(25)	2770(12)	4381(10)	50(5)
O(52)	-2977(22)	2103(10)	5619(8)	25(4)
O(6)	-917(22)	4436(9)	5779(7)	26(4)
N(2)	900(27)	1304(13)	7495(10)	28(5)
N(5)	-2068(29)	2493(13)	5083(11)	29(5)
C(1)	641(33)	3064(15)	6787(12)	20(5)
C(2)	2154(30)	1993(14)	6973(10)	15(5)
C(3)	2383(31)	1321(14)	6220(14)	16(5)
C(4)	1705(31)	1694(15)	5461(11)	17(5)
C(5)	371(33)	2756(15)	5248(12)	22(5)
C(6)	792(30)	3633(14)	5932(11)	15(5)
C(7)	4380(30)	2316(14)	7493(11)	18(5)
C(8)	3598(35)	206(16)	6395(12)	33(6)
C(9)	3107(29)	4202(15)	5964(11)	25(6)

a Only Cl(4) anisotropic.

Table 5.3. Fractional coordinates for atoms in 4-chloro-*t*-6-hydroxy-2,5,6-trimethyl-*r*-2,*t*-5-dinitrocyclohex-3-enone (39)

Atom	$10^4X/a$	$10^4Y/b$	$10^4Z/c$	10^3U (Å^2)
Cl(4)	2876(1)	8499(1)	-79(1)	31(1)
O(1)	-1270(3)	10338(3)	-4077(1)	26(1)
O(21)	1725(3)	13070(3)	-4722(2)	35(1)
O(22)	3827(3)	12767(3)	-3407(2)	35(1)
O(51)	-729(3)	5603(3)	-1124(2)	39(1)
O(52)	-2064(3)	8584(3)	-1716(2)	32(1)
O(6)	894(3)	6791(2)	-3445(1)	25(1)
N(2)	2202(3)	12556(3)	-3770(2)	23(1)
N(5)	-537(4)	7196(3)	-1520(2)	25(1)
C(1)	171(4)	10049(3)	-3448(2)	18(1)
C(2)	578(4)	11637(3)	-2986(2)	19(1)
C(3)	1583(4)	10904(3)	-1898(2)	21(1)
C(4)	2025(4)	9117(4)	-1398(2)	20(1)
C(5)	1797(4)	7523(3)	-1860(2)	19(1)
C(6)	1714(4)	8136(3)	-3108(2)	19(1)
C(7)	-1516(4)	13146(3)	-2980(2)	25(1)
C(8)	3480(4)	5701(4)	-1470(2)	27(1)
C(9)	4008(4)	8211(4)	-3594(2)	25(1)

Table 5.4. Fractional coordinates for atoms in 4-chloro-*t*-6-hydroxy-2,3,6-trimethyl-*r*-2,*t*-5-dinitrocyclohex-3-enone (39) co-crystallized with 4-chloro-*t*-6-hydroxy-2,5,6-trimethyl-*r*-2,*t*-5-dinitrocyclohex-3-enone (40)

Atom	$10^4X/a$	$10^4Y/b$	$10^4Z/c$	10^3U (Å^2)
Cl(4)	-6767(1)	393(1)	10792(1)	31(1)
O(1)	-4025(3)	-4428(2)	13974(2)	26(1)
O(21)	-5397(4)	-816(3)	14472(3)	43(1)
O(22)	-4630(3)	-2855(3)	15362(2)	39(1)
O(51)	-5823(4)	-3079(3)	10517(3)	44(1)
O(52)	-3990(3)	-3011(3)	11479(2)	32(1)
O(6)	-6569(3)	-4546(2)	13054(2)	24(1)
N(2)	-4837(3)	-1907(3)	14513(3)	27(1)
N(5)	-5370(4)	-2837(3)	11243(2)	25(1)
C(1)	-4834(4)	-3398(3)	13539(3)	20(1)
C(2)	-4317(4)	-2087(3)	13430(3)	22(1)
C(3)	-5070(4)	-930(3)	12523(3)	23(1)
C(4)	-6064(4)	-1015(3)	11864(3)	21(1)
C(5)	-6613(4)	-2283(3)	11947(3)	20(1)
C(6)	-6434(4)	-3328(3)	13113(3)	17(1)
C(7)	-2501(4)	-2193(4)	13362(3)	32(2)
C(8)	-8237(4)	-2121(4)	11534(3)	27(1)
C(9)	-7732(4)	-3011(3)	13886(3)	24(1)

Table 5.4. cont. Fractional coordinates for atoms in 4-chloro-*t*-6-hydroxy-2,5,6-trimethyl-*r*-2,*t*-5-dinitrocyclohex-3-enone (39) co-crystallized with 4-chloro-*t*-6-hydroxy-2,3,6-trimethyl-*r*-2,*t*-5-dinitrocyclohex-3-enone (40)

Atom	$10^4X/a$	$10^4Y/b$	$10^4Z/c$	10^3U (Å^2)
Cl(13)	647(1)	3346(1)	9839(1)	27(1)
O(10)	-1506(3)	1648(3)	14327(2)	36(1)
O(111)	669(4)	3744(3)	14283(3)	51(1)
O(112)	-222(3)	4966(3)	12713(3)	39(1)
O(141)	-1379(3)	302(2)	11256(2)	35(1)
O(142)	-91(3)	214(2)	12603(2)	29(1)
O(15)	-3389(3)	1549(2)	12891(2)	30(1)
N(11)	312(4)	3919(3)	13380(3)	29(1)
N(14)	-916(3)	806(3)	11809(2)	22(1)
C(10)	-1127(4)	2192(3)	13386(3)	24(1)
C(11)	509(4)	2700(3)	13060(3)	23(1)
C(12)	954(4)	3152(3)	11864(3)	21(1)
C(13)	87(4)	2930(3)	11200(3)	20(1)
C(14)	-1394(4)	2275(3)	11524(3)	19(1)
C(15)	-2272(4)	2463(3)	12506(3)	20(1)
C(16)	1765(5)	1651(4)	13750(3)	37(2)
C(17)	2456(4)	3767(4)	11490(3)	32(2)
C(18)	-3113(4)	3869(3)	12158(3)	30(1)

Table 5.5. Fractional coordinates for atoms in 4-chloro-2,5,6-trimethyl-*r*-2,*t*-5,*c*-6-trinitrocyclohex-3-enone (45)

Atom	$10^4X/a$	$10^4Y/b$	$10^4Z/c$	10^3U (Å^2)
Cl(4)	2547	6873(1)	3811	27(1)
O(1)	5240(4)	9282(3)	-697(2)	25(1)
O(21)	2641(5)	11762(3)	-165(3)	38(1)
O(22)	1186(5)	11554(3)	1554(3)	31(1)
O(51)	6229(4)	4722(3)	1575(3)	32(1)
O(52)	7100(4)	7069(3)	1666(3)	31(1)
O(61)	126(4)	8763(3)	1(3)	30(1)
O(62)	-119(4)	6559(3)	-820(3)	30(1)
N(2)	2450(5)	11176(3)	835(3)	22(1)
N(5)	5793(4)	6053(3)	1586(3)	21(1)
N(6)	877(4)	7558(3)	-266(3)	18(1)
C(1)	4281(5)	8895(3)	138(3)	16(1)
C(2)	4058(5)	9915(3)	1260(3)	16(1)
C(3)	3285(5)	9128(3)	2341(3)	17(1)
C(4)	3101(5)	7646(4)	2420(3)	17(1)
C(5)	3416(5)	6539(4)	1409(3)	15(1)
C(6)	3263(5)	7302(3)	109(3)	14(1)
C(7)	6142(6)	10734(4)	1618(3)	25(1)
C(8)	2033(5)	5139(3)	1449(3)	21(1)
C(9)	4153(5)	6362(4)	-891(3)	20(1)

Table 5.6. Fractional coordinates for atoms in 4-chloro-2,5,6-trimethyl-*r*-2,*t*-5,*t*-6-trinitrocyclohex-3-enone (47)

Atom	$10^4X/a$	$10^4Y/b$	$10^4Z/c$	10^3U (Å^2)
Cl(4)	1687(1)	2290(1)	3659(1)	22(1)
O(1)	2798(2)	-4306(3)	1665(2)	26(1)
O(21)	1066(2)	-2756(4)	-429(2)	40(1)
O(22)	925(2)	374(4)	-3(2)	24(1)
O(51)	2742(2)	-3164(4)	3859(2)	29(1)
O(52)	3704(2)	-1198(4)	5122(2)	35(1)
O(61)	4714(2)	-1618(4)	2259(2)	32(1)
O(62)	4543(2)	-2739(4)	3664(2)	36(1)
N(2)	1126(2)	-1426(4)	226(2)	21(1)
N(5)	3196(2)	-1591(4)	4182(2)	21(1)
N(6)	4265(2)	-1811(4)	2806(2)	19(1)
C(1)	2553(2)	-2645(5)	1825(2)	16(1)
C(2)	1476(2)	-2073(5)	1434(2)	16(1)
C(3)	1306(2)	-325(5)	2046(2)	16(1)
C(4)	1995(2)	561(5)	2883(2)	15(1)
C(5)	3062(2)	87(5)	3304(2)	14(1)
C(6)	3248(2)	-897(5)	2366(2)	14(1)
C(7)	891(2)	-3956(5)	1443(3)	26(1)
C(8)	3725(2)	1877(5)	3819(3)	22(1)
C(9)	3170(2)	710(5)	1495(2)	16(1)

Table 5.7. Fractional coordinates for atoms in 2,4,5,6-tetramethyl-*r*-4,*c*-5,*t*-6-trinitrocyclohex-2-enone (74)

Atom	$10^4X/a$	$10^4Y/b$	$10^4Z/c$	10^3U (Å^2)
O(1)	9889(7)	2130(11)	9535(15)	58(6)
O(41)	5573(9)	-990(13)	8501(15)	71(7)
O(42)	6261(11)	691(13)	7330(12)	66(9)
O(51)	7970(13)	-1517(16)	7083(13)	97(16)
O(52)	8696(9)	519(17)	7316(13)	71(7)
O(61)	8670(15)	-1111(13)	11927(12)	92(16)
O(62)	8662(11)	1119(15)	11928(13)	75(9)
N(4)	6227(11)	-8(17)	8275(14)	46(8)
N(5)	8217(12)	-505(15)	7715(13)	46(10)
N(6)	8739(11)	43(17)	11368(12)	42(8)
C(1)	9017(10)	1654(16)	9533(19)	45(7)
C(2)	8114(9)	2502(11)	9399(17)	30(6)
C(3)	7186(9)	1932(12)	9306(14)	25(7)
C(4)	6961(9)	358(12)	9384(16)	28(5)
C(5)	7935(10)	-604(14)	9275(20)	44(7)
C(6)	8905(12)	33(16)	9880(14)	34(9)
C(7)	8265(11)	4106(12)	9281(17)	39(9)
C(8)	6313(12)	111(17)	10639(17)	40(4)
C(9)	7722(12)	-2168(13)	9519(19)	48(9)
C(10)	9872(11)	-831(15)	9562(22)	57(8)

Table 5.8. Fractional coordinates for atoms in 2,4,5,6-tetramethyl-*r*-4,*c*-5,*c*-6-trinitrocyclohex-2-enone (76)

Atom	$10^4X/a$	$10^4Y/b$	$10^4Z/c$	10^3U (Å^2)
O(1)	-1727(2)	1528(1)	-1691(1)	32(1)
O(41)	-5701(2)	4470(1)	-3455(1)	34(1)
O(42)	-3522(2)	5533(1)	-3481(1)	40(1)
O(51)	-3858(2)	3352(1)	-1386(1)	28(1)
O(52)	-3051(2)	4760(1)	-1042(1)	35(1)
O(61)	1844(2)	2253(1)	-367(1)	34(1)
O(62)	-6(2)	3348(1)	2(1)	31(1)
N(4)	-3998(2)	4738(1)	-3439(1)	23(1)
N(5)	-2826(2)	4025(1)	-1445(1)	22(1)
N(6)	620(2)	2858(1)	-648(1)	23(1)
C(1)	-1796(2)	2213(1)	-2231(1)	19(1)
C(2)	-3189(2)	2335(1)	-3315(1)	17(1)
C(3)	-3383(2)	3143(1)	-3811(1)	18(1)
C(4)	-2312(2)	4001(1)	-3376(1)	17(1)
C(5)	-1167(2)	3939(1)	-2124(1)	17(1)
C(6)	-233(2)	2979(1)	-1896(1)	18(1)
C(7)	-4347(2)	1507(1)	-3777(1)	24(1)
C(8)	-1019(3)	4352(1)	-4152(1)	24(1)
C(9)	333(3)	4707(1)	-1780(1)	26(1)
C(10)	1478(2)	2776(1)	-2481(1)	25(1)

Table 5.9. Fractional coordinates for atoms in *r*-2-hydroxy-2,4,5,6-tetramethyl-*t*-5,*t*-6-dinitrocyclohex-3-enone (78)

Atom	$10^4X/a$	$10^4Y/b$	$10^4Z/c$	10^3U (Å^2)
O(1)	10127(3)	667(1)	10557(2)	31(1)
O(2)	6417(3)	98(1)	8117(3)	35(1)
O(51)	8707(3)	2247(1)	7275(3)	50(1)
O(52)	10018(3)	1490(1)	7724(3)	36(1)
O(61)	8210(3)	1412(1)	13039(3)	58(1)
O(62)	9844(3)	1831(1)	11286(3)	44(1)
N(5)	8586(3)	1808(1)	7713(3)	31(1)
N(6)	8487(3)	1524(1)	11534(3)	31(1)
C(1)	8506(4)	812(1)	9427(3)	22(1)
C(2)	7528(4)	531(1)	7615(3)	27(1)
C(3)	5812(4)	837(1)	6288(3)	29(1)
C(4)	5296(4)	1318(1)	6458(3)	26(1)
C(5)	6439(4)	1616(1)	8184(3)	24(1)
C(6)	7095(4)	1250(1)	9835(3)	21(1)
C(7)	9324(5)	366(1)	6687(4)	40(2)
C(8)	3701(4)	1601(1)	4944(4)	41(2)
C(9)	5133(4)	2070(1)	8596(4)	34(2)
C(10)	5054(4)	1027(1)	10350(3)	28(1)

Table 5.10. Fractional coordinates for atoms in 3-chloro-*t*-6-hydroxy-2,4,6-trimethyl-*r*-2,*t*-5-dinitrocyclohex-3-enone (84)

Atom	$10^4X/a$	$10^4Y/b$	$10^4Z/c$	10^3U (Å^2)
Cl(3)	7178(1)	788(1)	4921(1)	33(1)
O(1)	6629(2)	-5333(3)	3306(2)	28(1)
O(21)	4391(3)	-3174(4)	4063(2)	44(1)
O(22)	4838(3)	-606(4)	3495(2)	45(1)
O(51)	9822(2)	-3923(3)	4123(1)	28(1)
O(52)	11150(2)	-2992(4)	3327(2)	36(1)
O(6)	8263(2)	-4176(3)	2317(1)	27(1)
N(2)	5190(3)	-2039(5)	3871(2)	27(1)
N(5)	10073(3)	-2935(4)	3581(2)	21(1)
C(1)	7015(3)	-3712(5)	3377(2)	19(1)
C(2)	6772(3)	-2522(5)	4102(2)	20(1)
C(3)	7574(3)	-698(5)	4187(2)	19(1)
C(4)	8589(3)	-246(4)	3805(2)	18(1)
C(5)	8930(3)	-1585(4)	3180(2)	17(1)
C(6)	7711(2)	-2772(5)	2755(2)	21(1)
C(7)	7021(4)	-3703(5)	4860(2)	29(1)
C(8)	9422(4)	1532(5)	3935(2)	26(1)
C(9)	6671(4)	-1506(5)	2192(2)	27(1)

Table 5.11. Fractional coordinates for atoms in 3-chloro-*c*-6-hydroxy-2,4,6-trimethyl-*r*-2,*c*-5-dinitrocyclohex-3-enone (85)

Atom	$10^4X/a$	$10^4Y/b$	$10^4Z/c$	10^3U (Å^2)
Cl(3)[a]	2709(19)	120(8)	8796(6)	55(4)
O(1)	-2194(39)	3411(19)	7726(13)	38(7)
O(21)	-1198(37)	1114(19)	6893(16)	59(8)
O(22)	-2487(39)	763(18)	7971(13)	46(8)
O(51)	-3417(39)	2236(19)	9365(14)	42(7)
O(52)	-2492(32)	2862(18)	10646(12)	37(6)
O(6)	-1493(34)	4540(17)	9162(12)	38(8)
N(2)	-1080(50)	1232(26)	7652(21)	61(11)
N(5)	-2109(41)	2606(22)	9934(16)	26(8)
C(1)	-676(57)	3098(28)	8259(20)	38(11)
C(2)	560(55)	2005(26)	8130(17)	25(9)
C(3)	1397(56)	1423(28)	8893(20)	34(10)
C(4)	1445(52)	1847(27)	9690(18)	27(10)
C(5)	252(46)	2934(23)	9766(16)	11(8)
C(6)	-12(54)	3760(27)	9016(19)	27(10)
C(7)	2339(47)	2231(26)	7590(16)	34(10))
C(8)	2225(48)	1253(23)	10466(17)	29(10)
C(9)	2107(47)	4303(24)	8996(16)	15(10)

[a] Cl(3) only anisotropic.

Table 5.12. Fractional coordinates for atoms in 3-chloro-2,4,6-trimethyl-*r*-2,*t*-5,*c*-6-trinitrocyclohex-3-enone (86)

Atom	$10^4X/a$	$10^4Y/b$	$10^4Z/c$	10^3U (Å^2)
Cl(3)	819(4)	7437(2)	3377(2)	34(1)
O(1)	-2884(11)	10534(5)	2187(4)	30(2)
O(21)	-2635(14)	8322(5)	1343(4)	49(3)
O(22)	-3579(12)	7885(6)	2727(5)	52(3)
O(51)	851(13)	11082(5)	3571(5)	38(3)
O(52)	1561(11)	11048(5)	5081(6)	53(3)
O(61)	-5820(12)	9547(6)	3576(5)	53(3)
O(62)	-4545(11)	9262(5)	4941(5)	42(3)
N(2)	-2514(15)	8362(6)	2207(6)	31(3)
N(5)	558(14)	10814(6)	4374(7)	32(3)
N(6)	-4530(13)	9631(6)	4160(60	28(3)
C(1)	-2242(15)	10053(8)	2841(6)	20(3)
C(2)	-991(15)	9089(7)	2673(6)	20(3)
C(3)	-289(13)	8609(6)	3586(7)	16(3)
C(4)	-285(14)	9009(6)	4455(6)	17(3)
C(5)	-1132(14)	10071(6)	4559(6)	20(3)
C(6)	-2784(13)	10320(6)	3877(6)	13(3)
C(7)	621(16)	9328(8)	1963(6)	33(3)
C(8)	556(15)	8543(7)	5301(6)	26(3)
C(9)	-3555(15)	11412(6)	3961(7)	27(4)

Table 5.13. Fractional coordinates for atoms in 3-chloro-2,4,6-trimethyl-*r*-2,*c*-5,*t*-6-trinitrocyclohex-3-enone (87)

Atom	$10^4X/a$	$10^4Y/b$	$10^4Z/c$	10^3U (Å^2)
Cl(3)	2241(4)	6148(2)	5851(2)	49(1)
O(1)	6340(10)	9095(5)	4811(4)	44(3)
O(21)	5736(13)	8570(6)	6657(5)	73(4)
O(22)	6953(11)	7203(6)	6147(4)	47(3)
O(51)	7804(11)	6927(6)	4196(5)	57(3)
O(52)	6900(12)	6175(6)	2936(5)	64(3)
O(61)	1383(14)	9400(8)	3614(6)	102(5)
O(62)	465(14)	7980(8)	3034(6)	95(4)
N(2)	5660(14)	7889(7)	6116(5)	42(4)
N(5)	6517(14)	6681(7)	3550(6)	44(3)
N(6)	1838(15)	8543(7)	3400(6)	47(4)
C(1)	4951(14)	8486(7)	4606(5)	29(3)
C(2)	3871(15)	7903(7)	5310(6)	31(3)
C(3)	3230(13)	6845(7)	5034(6)	29(3)
C(4)	3273(13)	6445(7)	4230(6)	30(3)
C(5)	4164(14)	7027(7)	3530(6)	31(3)
C(6)	4139(14)	8190(7)	3628(6)	35(4)
C(7)	1909(15)	8527(7)	5560(6)	43(4)
C(8)	2484(15)	5389(7)	3947(6)	45(4)
C(9)	5397(13)	8753(7)	3027(5)	32(3)

Table 5.14. Fractional coordinates for atoms in 3-chloro-2,4,6-trimethyl-*r*-2,*c*-5,*c*-6-trinitrocyclohex-3-enone (88)

Atom	$10^4X/a$	$10^4Y/b$	$10^4Z/c$	10^3U (Å^2)
Cl(3)	8933(1)	2607(1)	4309(1)	35(1)
O(1)	6022(2)	5970(3)	5397(2)	27(1)
O(21)	7260(2)	2926(3)	6690(2)	47(1)
O(22)	8156(2)	5008(3)	6559(2)	34(1)
O(51)	9027(2)	8720(3)	4141(3)	35(1)
O(52)	7893(2)	7997(3)	5317(2)	40(1)
O(61)	5200(2)	7936(3)	3611(3)	44(1)
O(62)	6549(2)	9286(3)	3396(3)	38(1)
N(2)	7572(2)	4014(4)	6133(3)	27(1)
N(5)	8283(2)	7979(3)	4355(3)	26(1)
N(6)	6105(2)	8068(3)	3524(3)	27(1)
C(1)	6591(3)	5640(4)	4648(3)	19(1)
C(2)	7232(3)	4160(4)	4759(3)	20(1)
C(3)	8185(3)	4259(4)	4114(3)	21(1)
C(4)	8463(3)	5435(4)	3459(3)	22(1)
C(5)	7826(3)	6898(4)	3359(3)	22(1)
C(6)	6711(3)	6565(4)	3475(3)	19(1)
C(7)	6544(3)	2775(4)	4375(3)	28(1)
C(8)	9406(3)	5461(5)	2785(3)	36(1)
C(9)	6238(3)	5726(4)	2342(3)	26(1)

5.8 REFERENCES

1 Norman, R. O. C.; Taylor, R., *"Electrophilic Substitution in Benzoid Compounds"*, Elsevier Publishing Company, London, 1965.

2 de la Mare P. B. D.; Ridd, J. H., *"Aromatic Substitution"*, Butterworths Scientific Publications, London, 1959.

3 de la Mare P. B. D.; Bolton, R., *"Electrophilic Additions to Unsaturated Systems"*, Elsevier Publishing Company, London, 1966.

4 de la Mare P. B. D.; Bolton, R., *"Electrophilic Additions to Unsaturated Systems"*, 2nd edition, Elsevier Publishing Company, London, 1982.

5 Wheland, G. W., *J. Am. Chem. Soc.*, **64**, 900, 1942.

6 Perrin C. L.; Skinner, G. A., *J. Am. Chem. Soc.*, **93** , 3389, 1971.

7 de la Mare, P. B. D., Harvey, J. T., *J. Chem. Soc.*, 131, 1957.

8 Blackstock, D. J.; Fischer, A.; Hartshorn, M. P.; Richards, K. E.; Vaughan, J.; Wright, G. J., *Tetrahedron Lett.*, 2793, 1970.

9 Blackstock, D. J.; Fischer, A.; Richards, K. E.; Vaughan, J.; Wright, G. J., *J. Chem. Soc., Chem. Commun.*, 641, 1970.

10 Schofield, K., *"Aromatic Nitration"*, Chapter 10, pp. 175, Cambridge University Press, Cambridge, 1980.

11 Clemens, A. H.; Hartshorn, M. P.; Richards, K. E.; Wright, G. J., *Aust. J Chem.*, **30**, 113, 1977.

12 Blackstock, D. J.; Hartshorn, M. P.; Lewis, A. J.; Richards, K. E.; Vaughan, J.; Wright, G. J., *J. Chem. Soc. (B)*, 11212, 1971.

13 Barnes, C. E; Myhre, P. C., *J. Am. Chem. Soc.*, **100**, 973, 1978.

14 Jensen, R. G., M.Sc. Thesis, University of Canterbury, 19, 1987.

15 Myhre, P. C., *J. Am. Chem. Soc.*, **94**, 7921, 1972.

16 Coombes, R. C.; Russell, L. W., *J. Chem. Soc. (B)*, 2443, 1971.

17 Brittain, J. M.; de la Mare, P. B. D., ed.s Patai, S.; Rappoport, R., *"Chemistry of the Functional Groups; Supplement D: The chemistry of the Halides, Pseudo-Halides and Azides"*, John Wiley and Sons, New York, Chapter 12, pp. 481, 1983.

18 Ershov, V. V.; Volod'kin, A. A.; Bogdanov, G. N., *Russ, Chem. Rev.*, **32**, 75, 1963.

19 Sainsbury, M.,*" Aromatic Chemistry",* Oxford University Press Oxford, 1992.

20 Schofield, K., *"Aromatic Nitration"*, Chapter 10, Section 10.3, Cambridge University Press, Cambridge, 1980.

21 Brunton, G.; Cruse, H. W.; Riches, K. M.; Whittle, A.; *Tetrahedron Letters,* **20,** 1093, 1979.

22 Sutton, K. H., Ph.D Thesis, University of Canterbury, 75, 1984.

23 Hartshorn, M. P.; Penfold, B.R.; Sutton, K. H.; Vaughan, J., *Aust. J. Chem.*, **37**, 809, 1984.

24 Hartshorn, M. P.; Sutton, K. H.; Vaughan, J., *Aust. J. Chem.*, **38**, 161, 1985.

25 Sutton, K. H., Ph.D Thesis, University of Canterbury, 84, 1984.

26 Blunt, J. W.; Hartshorn, M. P.; Jensen, R. G.; Waller, G. A.; Wright, G. J., *Aust. J. Chem.*, **42**, 675, 1989.

27 Hartshorn, M. P.; Martyn, R. J.; Robinson, W. T.; Sutton, K. H.; Vaughan, J.; White, J. M., *Aust. J. Chem.*, **36**, 1589, 1983.

28 Hartshorn, M. P.; Readman, J. M.; Robinson, W. T.; Vaughan, J., *Aust. J. Chem.*, **38**, 587, 1985.

29 Amin, M. R.; Deker, L.; Hibbert, D. B.; Ridd, J. H.; Sandall, J. P. B., *J. Chem. Soc., Chem Commun.,* 566, 1992.

Hartshorn, M. P.; Martyn, R. J.; Robinson, W. T.; Sutton, K. H.; Vaughan, J.; White, J. M., *Aust. J. Chem.*, **38**, 1613, 1985.

30 Sutton, K. H.; Ph.D Thesis, University of Canterbury, 1984.

31 Coombes, R. G.; Diggle, A. W.; *Tetrahedron Lett.;* **27**, 2037, 1986.

32 Hartshorn, M. P.; Jensen, R. G.; Waller, G. A.; Wright, G. J., *Tetrahedron Lett.,* **28**, 6701, 1987.

33 Siemens SHELXTL PLUS (PC Version)

34 Cromer, D. T., and Libeman, D., *J. Chem. Phys.*, **53**, 1891, 1970.

35 Sheldrick, G. M., Unpublished data.

CHAPTER ONE

INTRODUCTION II

1.1 CHARGE TRANSFER COMPLEXES

Charge transfer complexes are characterised by one component that is electron rich (the donor) and another component that is electrophilic (the acceptor); hence, such complexes are also known as donator-acceptor complexes.[1,2]

When electron donor-acceptor complexes are characterised as reaction intermediates they exist as weakly bound species in which the donor component **D** and the acceptor moiety **A** loosely associated to retain their individual identities as illustrated in Scheme 1.1. [3,4,5]

$$D + A \underset{}{\overset{K_{assoc}}{\rightleftharpoons}} [D,A]$$

Donor-Acceptor complex

SCHEME 1.1

This donor-acceptor complex promotes reactivity by bringing the reactants together and encouraging orbital overlap for electronic re-organisation including electron transfer.[6]

In Scheme 1.1 K_{assoc} is the association constant for formation of the donor acceptor complex. K_{assoc} generally increases with the donor and acceptor strengths. The larger the value of K_{assoc} the greater the stability of the donor acceptor complex. The donor and acceptor strengths can be evaluated by the ionisation potential and electron affinity of the donor and acceptor respectively.[3,7]

1.2 CHARGE TRANSFER ABSORPTION

In 1952 Mulliken[8] reported that the coloured electron donor-acceptor complexes arose due to the electronic reorganisation involving electron promotion or charge transfer from the highest occupied molecular orbital (HOMO) primarily on the donor to an lowest unoccupied molecular orbital (LUMO) localised on the acceptor as illustrated in Fig 1.1.[8,9]

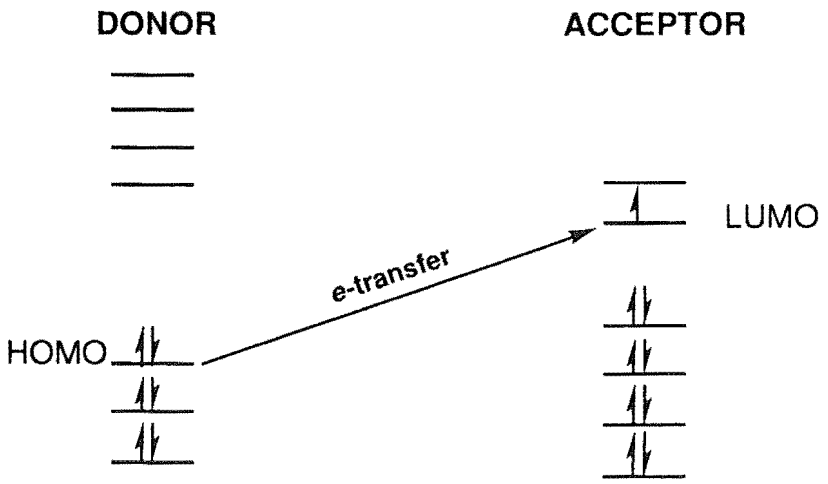

FIG 1.1

Thus the charge transfer excitation of a weakly bound electron donor-acceptor complex **[D,A]** populates an ionic state consisting of a radical ion pair as summarised in Scheme 2.[6]

$$[\mathbf{D,A}] \xrightarrow{h\nu_{CT}} [\mathbf{D}^{\bullet+}, \mathbf{A}^{\bullet-}]$$

Donor-Acceptor complex — Charge Transfer Complex

SCHEME 1.2

For example a solution of benzene and iodine in heptane forms a charge transfer complex that is violet/brown in colour. (See Schemes 1.3 and 1.4.)

SCHEME 1.3

$$C_6H_6 + I_2 \underset{}{\overset{K_{assoc}}{\rightleftharpoons}} [C_6H_6 , I_2]$$

Donor-Acceptor complex

SCHEME 1.4

$$[C_6H_6 , I_2] \xrightarrow{h\nu_{CT}} [C_6H_6^{\bullet+} , I_2^{\bullet-}]$$

Donor-Acceptor complex — Charge Transfer Complex

The charge transfer complex is attained by the absorption of visible or UV light ($h\nu_{CT}$) as shown in Scheme 1.4. The transition which accompanies the absorption of light corresponds to the transfer of the electron from the donor (C_6H_6) to the acceptor (I_2).[10,11] The high intensity absorption maximum which appears in the spectrum of iodine in a donor solvent (eg. benzene) at about 300 nm is not found in the absorption spectra of either of the components of the complex Fig 1.2.[4] The band which is considered to be characteristic of the iodine complex as a whole, is described as the charge transfer absorption with ground and excited states as defined by Mulliken.[5]

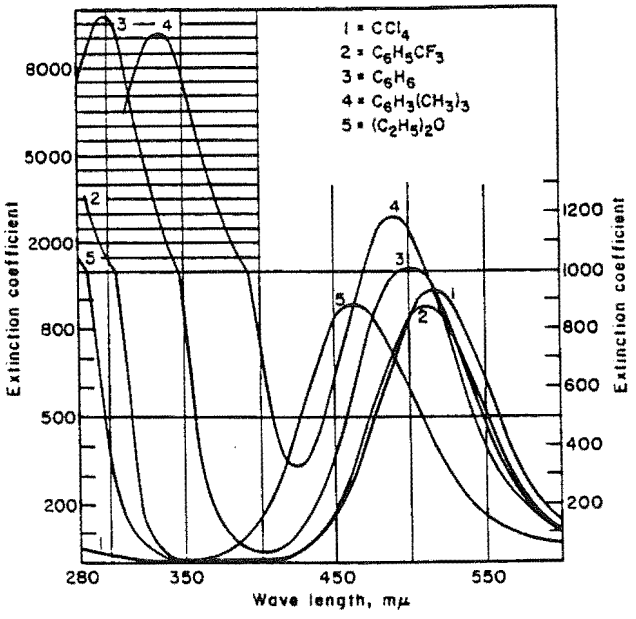

Figure 1.2 Absorption of iodine in various solvent systems.[12]

1.3 DETERMINATION OF TRANSITION ENERGIES

Qualitative evidence of the dependence of the transition energy on the donor ionisation energy is to be found in the fact that the intense UV absorption peaks for iodine complexes shift to longer wavelengths as the donors are changed from benzene ($\lambda_{max} \approx 290$ nm) to toluene ($\lambda_{max} \approx 300$ nm) and to mesitylene ($\lambda_{max} \approx 330$ nm).[4]

A number of quantitative relationships based on the frequency of the charge transfer absorption maximum (ν_{CT}), the donor ionisation potential (I_P) and the electron affinity (E_a) have been proposed. The equation describing the energy associated with the charge transfer (E_{CT}) was proposed:

$$E_{CT} = h\nu_{CT} = I_p - E_a - W$$

where h is Plancks constant, and W is the dissociation energy of the charge transfer excited state was suggested by McConnell, Ham and Platt.[13] This equation was modified to an alternative relationship by Hastings *et al.* [14] after a more detailed consideration of the energetics of the charge transfer process. The relationship provides a theoretical curve relating ν_{CT} to I_P which accommodates reasonably well the experimental values of these two variables for a group of over 30 iodine complexes as shown in Fig 1.3.

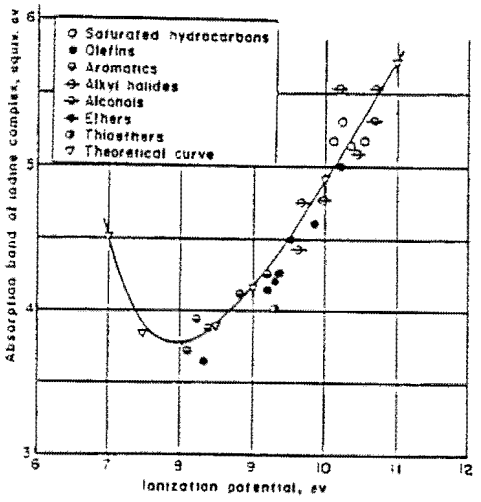

FIG 1.3 Ionisation potential vs equivalent energy of the iodine complex absorption band.[14]

Other reports have described a linear relationship between donor ionisation potential and $h\nu_{CT}$ for complexes involving components other than I_2.[15-18]

The complementary variation of ν_{CT} with electron affinity (E_a) of the acceptor has been much less widely studied, mainly due to the paucity of electron affinity data. Briegleb,[19] has attempted to make measurements of electron affinities of organic molecules and has achieved getting a similar correlation as was seen with the ionisation potential, however, this method is not preferred.

1.4 DETERMINATION OF THE EQUILIBRIUM CONSTANT K_{assoc}

Benesi and Hildebrand[20] originally reported a method commonly used in the spectrophotometric determination of the equilibrium constant K_{assoc} for a donor **D** and an acceptor **A** in solution.(See Scheme 1.5.)

$$\mathbf{D} + \mathbf{A} \underset{}{\overset{K_{assoc}}{\rightleftharpoons}} [\mathbf{D,A}] \qquad K_{assoc} = \frac{[\mathbf{D,A}]}{[\mathbf{D}]\,[\mathbf{A}]}$$

SCHEME 1.5

The assumption was made that the activity coefficients for the species **D**, **A** and **[D,A]** are all unity. Therefore, $K_{assoc} = Q_{assoc}$. Another assumption often made to simplify the determination of K_{assoc} is that only a 1:1 complex of **[D,A]** is ever formed. Generally, solutions containing interacting **D** and **A** species show not only the absorptions of **D** and **A**, sometimes noticeably modified, but also a new band or bands which are assigned to intermolecular charge transfer transition(s) of the complex. The intensity of this band is often used as a measure of the concentration of the complex in solution. Similarly the decrease in the absorption spectrum of one component as the concentration of another component is increased may be used to estimate the association constant of the complex formed. Using Beers law and knowing the extinction coefficient,

ε_λ [D,A], of [D,A] at the wavelength of measurement, λ, the K_{assoc} can be calculated from the Benesi-Hildebrand equation:

$$\frac{[A]_o}{A} = \frac{1}{K_{assoc} \cdot \varepsilon_\lambda^{DA}} \cdot \frac{1}{[D]_o} + \frac{1}{\varepsilon_\lambda^{DA}}$$

Variations of the above equation have been employed by other workers.[21]

K_{assoc} can also be determined by NMR[22], polarography[23], direct calorimetry[24], dielectric constant measurements[25], and further kinetic studies of the species involved in the initial charge transfer equilibrium.[26]

The association constant for complex formation generally increases with the donor and acceptor strengths as evaluated by the ionisation potential and electron affinity respectively.[3,7] The position of the equilibrium is very dependant on the nature of the solvent. The donor or acceptor molecules may become quite solvated affecting the size of the association constant indirectly by decreasing the intensity of the charge transfer absorption.[3] It must also be recognised that some solvents may even act as a donor or acceptor.

1.5 TETRONITROMETHANE AS AN ACCEPTOR IN COMPLEXES

Tetranitromethane (TNM) is known to form donor acceptor complexes with aromatic donors[27,28] and efficient photochemical reactions have been observed in these and related systems.[29] Kochi *et al.*[6] report mixing solutions of TNM and anthracenes, which resulted in the immediate appearance of the brown colouration of the electron donor acceptor complex as represented in Scheme 1.6.

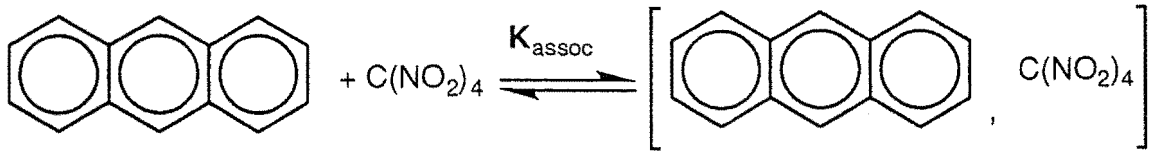

SCHEME 1.6

The electronic absorption spectrum was obtained and appears as a broad tail which extends to ≈ 700 nm as shown in Fig 1.4.

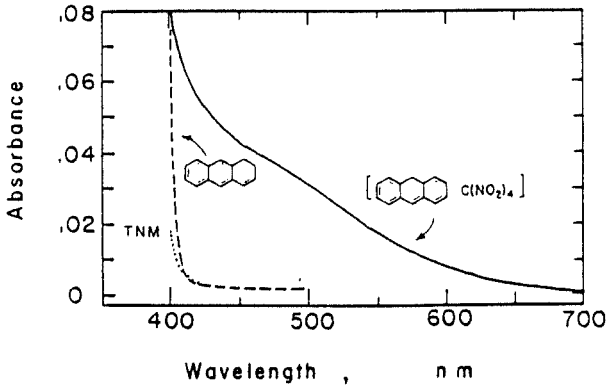

FIGURE 1.4 Charge transfer absorption spectrum of the electron donor acceptor complexes of anthracene and TNM in dichloromethane solution. The dotted lines represent the absorptions of pure anthracene and TNM in dichloromethane.[6]

The maximum of the charge transfer band is hidden under the low energy edge of the localised transitions of the uncomplexed anthracene and TNM, all the absorption at $\lambda \geq 450$ nm arises from the electron donor acceptor complex. By measuring the change in the charge transfer absorbance with increasing amounts of either anthracene or TNM, Kochi *et al.* measured the association constant and found it to be ≈ 1 M^{-1}. The magnitude of K_{assoc} is rather small for TNM as the acceptor and it was concluded that the electron donor acceptor complex is weakly bound. The electron donor acceptor complexes of the anthracenes and TNM remained unchanged for many hours if the solutions were protected from light.[6] The charge transfer spectrum in Fig 1.4 of the electron donor acceptor complex of anthracene and TNM shows that photochemical irradiation with light of wavelength > 500 nm selectively excites only the electron donor acceptor complex. The events that follow the charge transfer excitation where TNM was the acceptor were quite different from those associated with a well known acceptor tetracyanoethylene (TCNE) that was similar to TNM in its photophysical characteristics.

Kochi *et al.* observed the formation of photoproducts with TNM and a series of anthracenes (An). See Scheme 1.7.

$$An + TNM \xrightarrow{h\nu_{CT}} \text{photoproducts}$$

SCHEME 1.7

This was in strong contrast to the photoresistant behaviour in the corresponding TCNE complexes.[30] The difference between the two systems was in the nature of the acceptor anion. TCNE is known to undergo reversible back electron transfer to regenerate the original electron donor acceptor complex as demonstrated in Scheme 1.8.[30]

$$[An, TCNE] \xrightarrow{h\nu_{CT}} [An^{\bullet+}, TCNE^{\bullet-}]$$

$$[An^{\bullet+}, TCNE^{\bullet-}] \xrightarrow{< 50\ ps} [An, TCNE]$$

SCHEME 1.8

This means effectively that the activated charge transfer complex involving TCNE will not undergo any further photochemical reactions.

Kochi *et al.* believed that the electron donor acceptor complex involving TNM was not able to undergo this back electron transfer due to some form of rearrangement or decomposition of the $TNM^{\bullet-}$. The events that follow the charge transfer excitation of the electron donor acceptor complexes involving TNM were examined by Kochi *et al.* [30,31] by transient picosecond absorption techniques.[32-33] Initially, the anthracene radical cations were studied. The absorption spectra were measured after excitation of a solution of an anthracene and TNM. The excitation showed absorption bands which were assigned to the radical cations ($An^{\bullet+}$) of the respective anthracene donors

based on comparisons with the spectra of the radical cations generated by anodic oxidation.[7] See Fig 1.5.

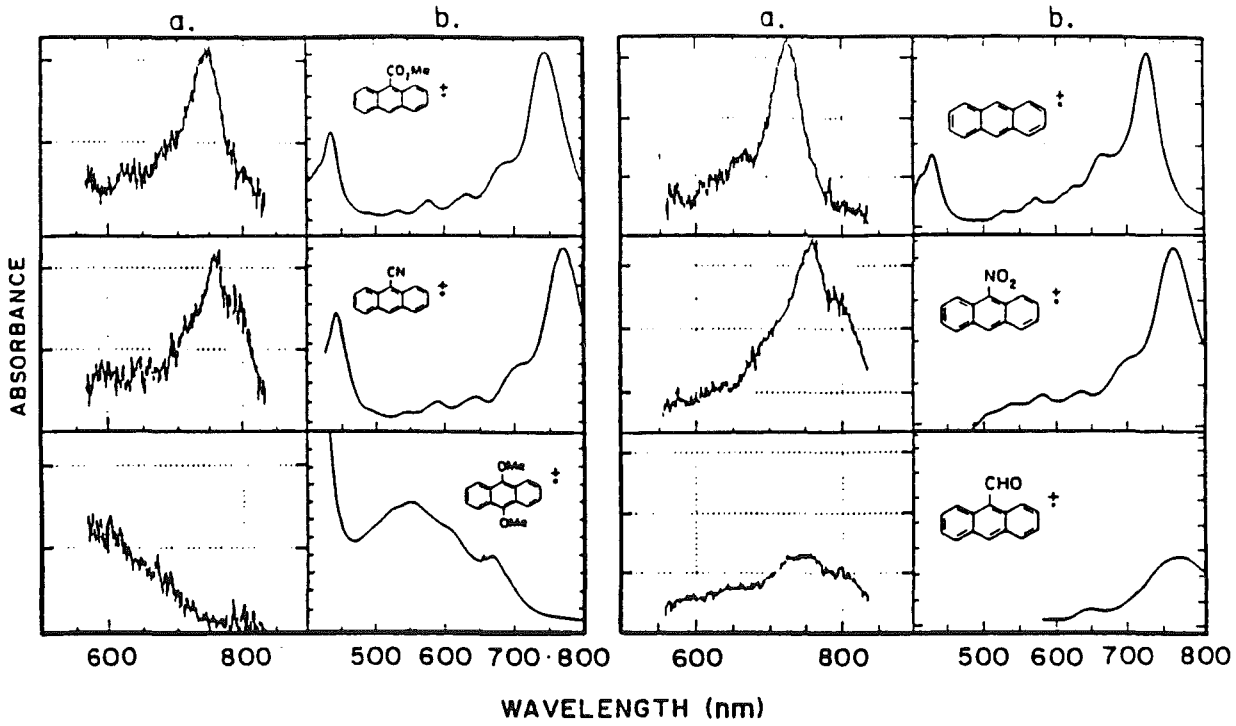

FIGURE 1.5 Picosecond absorption spectra of radical cations in (a) compared with the absorption spectra of radical cations generated by anodic oxidation in (b).

It was also noted that the transient absorption spectra of ($An^{\bullet+}$) were essentially the same as those previously reported in the time-resolved picosecond studies of the anthracene-TCNE complexes.[31]

The intense absorptions of the anthracene donors obscured the spectral region below 450 nm as shown previously in Fig 1.4. In order to observe the anion associated with tetranitromethane in the charge transfer complex Kochi *et al.* [30] used a donor such that its absorption spectrum did not interfere or absorb at wavelengths < 300 nm. Hexamethylbenzene and hexaethylbenzene were used as the donors. The absorption of an anion at ≈ 350 nm was observed upon excitation of the donor acceptor complex. See Fig 1.6. The band however, was found to correspond to the trinitromethanide anion $(O_2N)_3C^-$ and not the

tetranitromethanide anion $(O_2N)_4C^-$. The assignment was made after comparison with the absorption spectra of trinitromethanide anion $(O_2N)_3C^-$ prepared by cathodic and chemical reduction of TNM.[34,35]

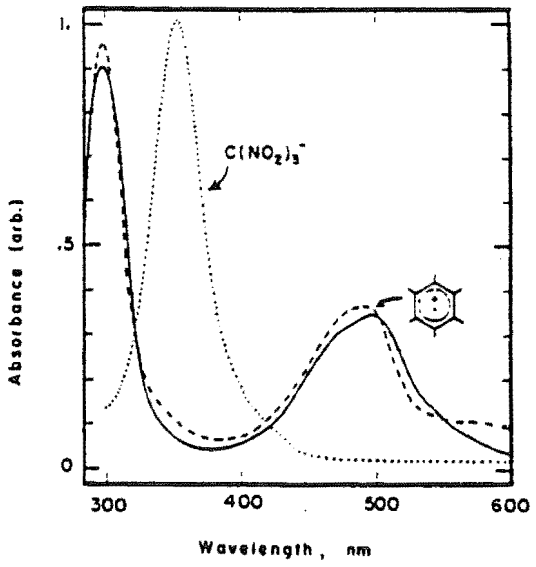

FIGURE 1.6 Absorption band of $(O_2N)_3C^-$ generated in hexamethylbenzene and TNM.

The time-resolved picosecond data obtained by Kochi *et al.* [30] demonstrated that electron transfer within the electron donor acceptor complexes of arene donors and TNM occurred effectively upon absorption of a photon. Their studies showed that the production of ion pairs from the selective excitation of the charge transfer band was correct and in agreement with the Mulliken[8] model for electron transfer upon photoexcitation of the complex. See Scheme 1.9.

$$D + A \underset{}{\overset{K_{assoc}}{\rightleftharpoons}} [D,A]$$

Donor-Acceptor complex

$$[D,A] \xrightarrow{h\nu_{CT}} [D^{+\bullet}, A^{-\bullet}]$$

Donor-Acceptor complex — Charge Transfer Complex

SCHEME 1.9

products and the principal products (1) were derived by the addition of the fragments of $(O_2N)_3C^-$ and NO_2 to the 9,10-positions of the anthracenes.

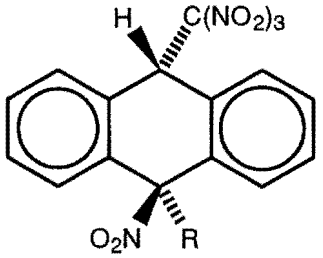

R = Br, Ph

(1)

The structures of the principal photoadduct was confirmed by X-ray crystallography in the cases of 9-phenyl and 9-bromoanthracene. Both structures indicated that the attachment of $(O_2N)_3C^-$ was regiospecific and occurred at the unsubstituted 10-position of 9-phenyl and 9-bromoanthracene. The X-ray structure of photoadduct (2) isolated from the photolysis of anthracene with TNM was also obtained showing the connectivity to be:

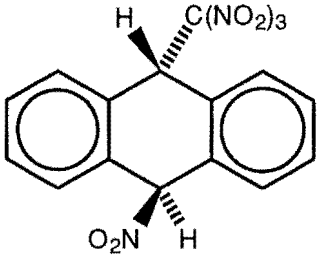

(2)

The structural elucidation of the photoproducts highlights the efficiency of ion-pair and radical pair interactions following the charge transfer excitation of the corresponding electron donor acceptor complexes. They give excellent evidence for the fragmentation of $(O_2N)_4C^{\bullet -}$, from the charge transfer complex

anthracene and the formation of some photoproducts as was previously illustrated in Scheme 1.7. The photoproducts were isolated from the reaction products and the principal products (1) were derived by the addition of the fragments of $(O_2N)_3C^-$ and NO_2 to the 9,10-positions of the anthracenes.

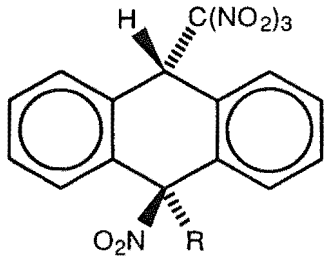

R = Br, Ph

(1)

The structures of the principal photoadduct was confirmed by X-ray crystallography in the cases of 9-phenyl and 9-bromoanthracene. Both structures indicated that the attachment of $(O_2N)_3C^-$ was regiospecific and occurred at the unsubstituted 10-position of 9-phenyl and 9-bromoanthracene. The X-ray structure of photoadduct (2) isolated from the photolysis of anthracene with TNM was also obtained showing the connectivity to be:

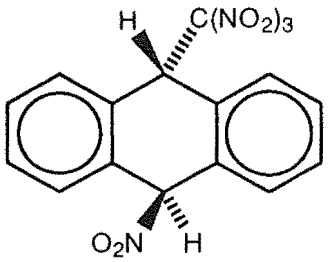

(2)

The structural elucidation of the photoproducts highlights the efficiency of ion-pair and radical pair interactions following the charge transfer excitation of the corresponding electron donor acceptor complexes. They give excellent evidence for the fragmentation of $(O_2N)_4C^{\bullet -}$, from the charge transfer complex

as the fragments are efficiently trapped as the *meso*-adducts of the corresponding anthracene.

1.7 MECHANISTIC DESCRIPTION OF THE FORMATION OF THE PRINCIPAL ADDUCTS FROM PHOTOLYSIS OF THE ANTHRACENES

Kochi *et al.* [6] described the mechanism of reaction of TNM with anthracenes by considering the nature of the principal photoadduct (1). The attachment of the trinitromethyl group to the 10-position of the anthracene series irrespective of the electron donating/withdrawing nature of the 9-substituent was consistent with the ion pair forming the most stable radical (3),[36,37] as shown in Scheme 1.12. Most substituents stabilize benzylic radicals irrespective of their electron withdrawing/donating nature.[38]

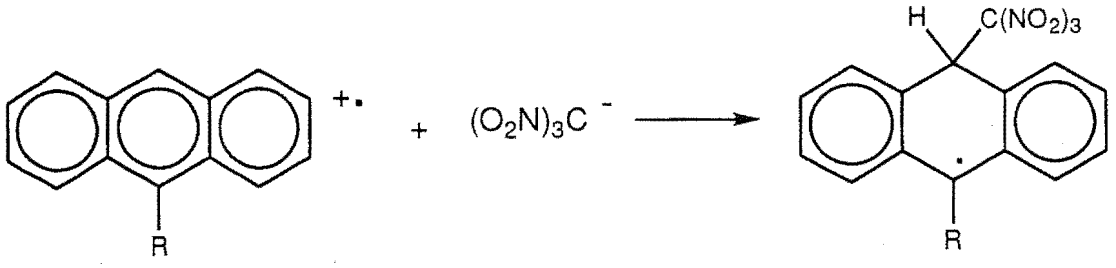

(3)

SCHEME 1.12

The presence of the radical (3) as an intermediate was confirmed by its transient absorption spectrum with λ_{max} 550 nm in a time-resolved spectroscopic study of the charge transfer irradiation of the anthracene-TNM complexes.[30,39] The coupling of the radical (3) with $^{\bullet}NO_2$ is the last stage in the formation of the photoadduct (1) as illustrated in Scheme 1.13.

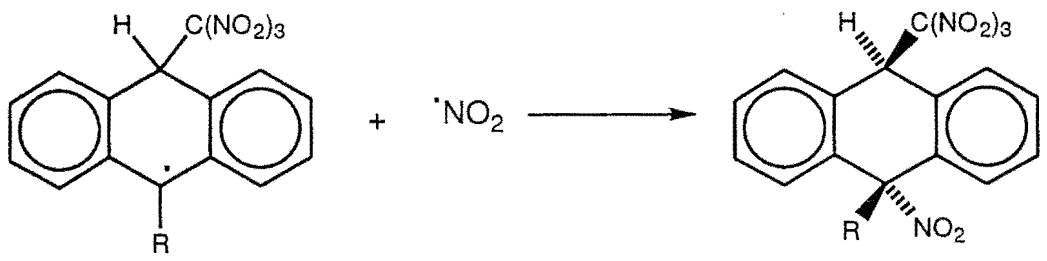

(3) (1)

SCHEME 1.13

X-ray crystallography indicated that the $^{\bullet}NO_2$ adds to the hydranthryl radical stereoselectively from the face opposite the bulky trinitromethyl group. This corresponds to an overall *anti*-addition of the TNM fragments. Steric interactions are known to play an important role in the disposition of groups in the dihydroanthracene conformations.[40]

1.8 PHOTOPRODUCTS DERIVED FROM PHOTOLYSIS OF NAPHTHALENE WITH TNM

Kenner[41] first proposed an electron transfer mechanism in nitration as an alternative to the classical Hughes-Ingold[42] mechanism involving direct electrophilic attack of nitronium ion (NO_2^+) on an aromatic substrate to give the Wheland intermediate as depicted in Scheme 1.14.

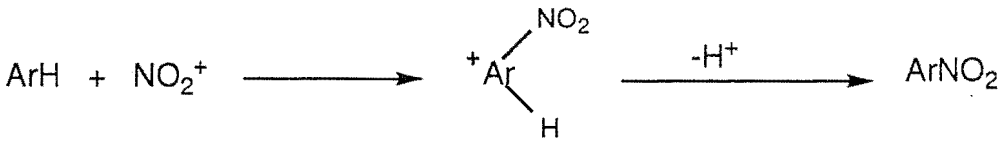

Wheland Intermediate

SCHEME 1.14

Kenner suggested that the initial step in the nitration of benzene "involves transference of a π electron , whilst the..... loss of a proton to the surrounding medium by means of the hydrogen bond mechanism is determined by the

tendency to restore the aromatic condition and neutrality of the nucleus." Kenner depicted the mechanism as shown in Scheme 1.15.

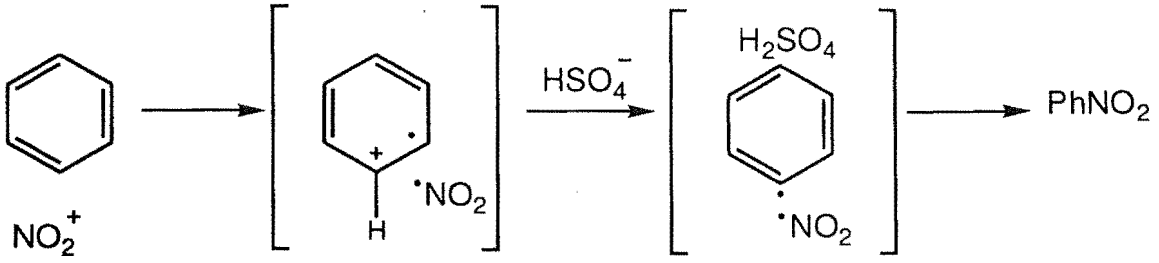

SCHEME 1.15

Thus, Kenner saw charge transfer as the essential step. As written, the subsequent step of radical coupling would not now be acceptable, for it does not include a Wheland intermediate.[43] Ingold commented on Kenner's suggestion,[44] making the point that although radicals occur in the proposed mechanism their dimerisation products were not seen as one might have expected due to radical-radical coupling.

Perrin[45] revived the electron transfer mechanism in 1957 in a bid to explain the paradox associated with strong intramolecular selectivity of nitration[46] even when there is no intermolecular selectivity[47]. Perrin suggested an encounter controlled transfer mechanism from the aromatic compound to the nitronium ion and he suggested that the intramolecular selectivity was derived from the reactions of the resulting radical cation with nitrogen dioxide as illustrated in Scheme 1.16.

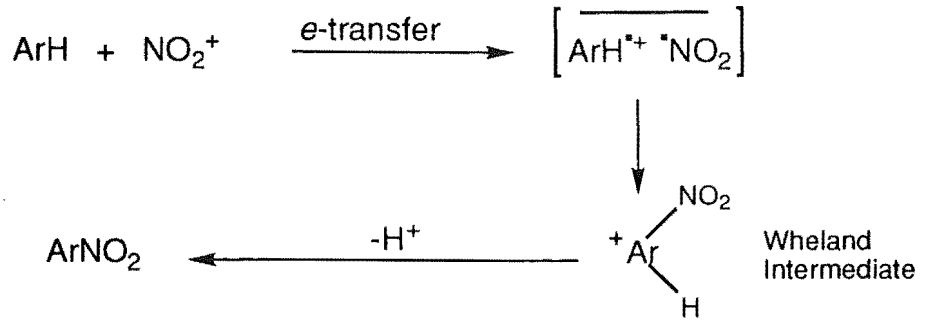

SCHEME 1.16

Perrin supported his interpretation by providing evidence that the product composition in the conventional nitration of naphthalene was the same as that observed in reactions of the electrochemically generated naphthalene radical cation with nitrogen dioxide. This is illustrated in Scheme 1.17.

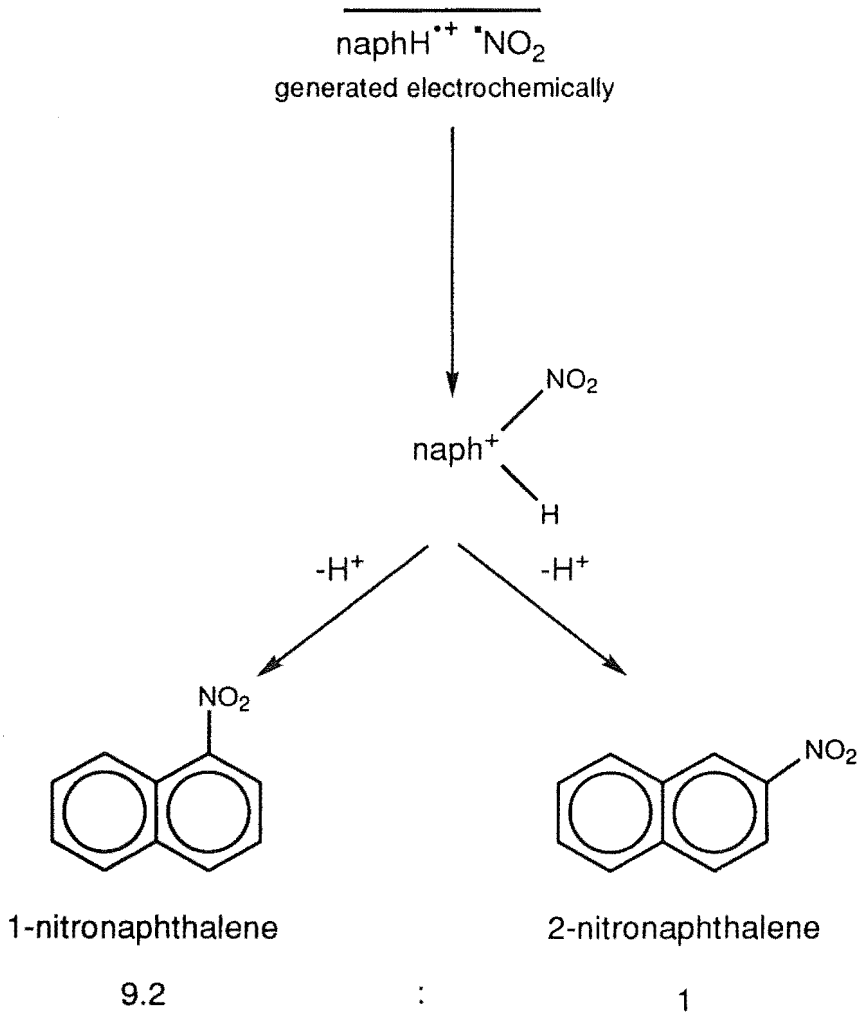

SCHEME 1.17

Perrin's ratio of 1-nitronaphthalene to 2-nitronaphthalene being 9.2 was within experimental error of the ratio of 10.9 obtained for nitration of naphthalene with NO_2^+ generated from HNO_3/H_2SO_4.[45]

Ridd *et al.* [48,49] rationalised that if Perrin were correct ^{15}N CIDNP experiments should show NMR enhancements. Only weak enhancements were seen

corresponding to no more that 9% of the Perrin mechanism in the naphH/HNO_3/H_2SO_4. reaction. Ridd *et al.* [48, 49] concluded that Perrin's idea was substantially inoperative for naphthalene.

Eberson and Radner[50] criticised the nitronaphthalene ratio obtained from the Perrin experiment involving the naphthalene radical cation and $^{\bullet}NO_2$. In their hands, reaction of the naphthalene radical cation as its hexafluorophosphate salt with a solution of $^{\bullet}NO_2$ in dichloromethane gave an almost quantitative yield of nitronaphthalenes with a very high ratio of 1-nitronaphthalene to 2-nitronaphthalene of ≈ 50. In reality coupling of $naphH^{\bullet+}$ and $^{\bullet}NO_2$ displays a high selectivity, (See Scheme 1.18), not a ratio ≈ 10 as apparently implied from Perrin's electrochemical experiment.

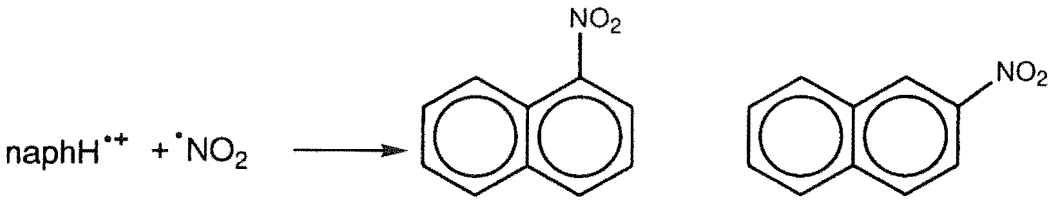

1-nitronaphthalene 2-nitronaphthalene

50 1

SCHEME 1.18

Eberson *et al.* [51] were able to demonstrate that Perrin's electrochemical experiment was flawed because of problems associated with generating $^{\bullet}NO_2$ under acid catalysed conditions with high potentials. This resulted in NO_2^+ being formed instead of the stated $^{\bullet}NO_2$. Eberson and Radner[52,53] established the following ratios for the nitronaphthalenes generated under a variety of different conditions. See Scheme 1.19.

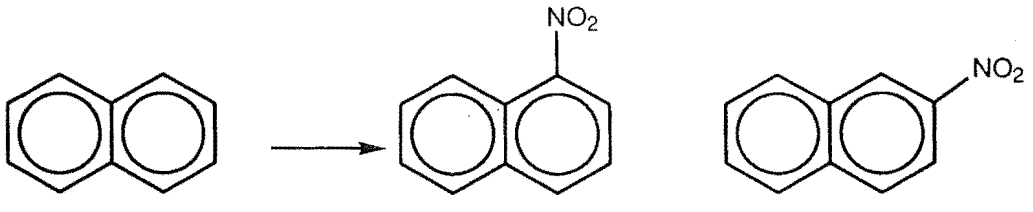

1-nitronaphthalene 2-nitronaphthalene

ArH = naphthalene

REACTION			RATIO 1/2-nitronaphthalene
$ArH^{\bullet+}$	+	$^{\bullet}NO_2$	50
ArH	+	$^{\bullet}NO_2$	20-25
ArH	+	NO_2^+	11

SCHEME 1.19

Kochi *et al.* [54] however in 1992 reported the photonitration of naphthalene with TNM in dichloromethane and acetonitrile. Their findings are summarised in Scheme 1.20.

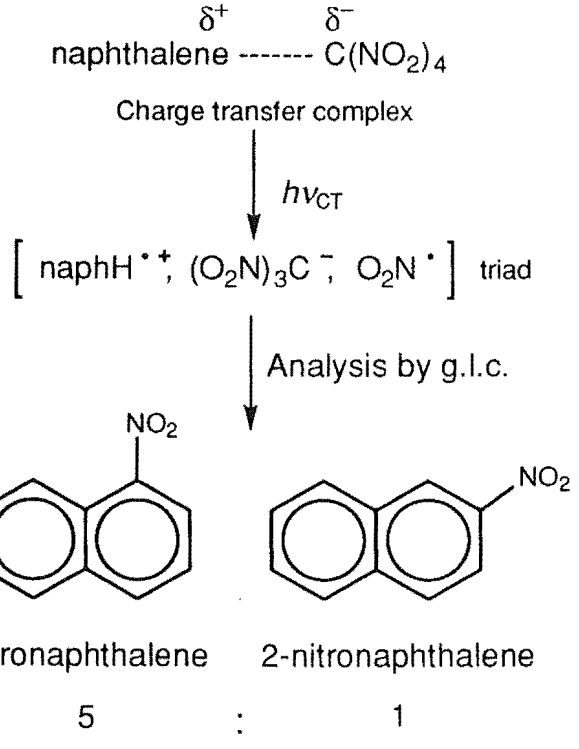

1-nitronaphthalene 2-nitronaphthalene

5 : 1

SCHEME 1.20

Kochi *et al.* [54] argued that, because their ratio of 5:1 for 1-nitronaphthalene/2-nitronaphthalene was within experimental error of Perrin's ratio of 9.2 for his

alleged electron transfer process involving naphthalene, the two mechanisms must be similar. Kochi ignored the fact that the accepted literature value (1980, 1986) for the ratio of 1-nitronaphthalene/2-nitronaphthalene generated from naphH$^{\bullet+}$ and $^{\bullet}NO_2$ was ≈ 50 and that Perrin's experiments themselves appeared critically flawed.[50] Kochi *et al.*[54] made no attempt to analyse the product mixture, other than by gas-liquid chromatography, notwithstanding his own earlier observations of the formation of unstable adducts in the photolysis of charge-transfer complexes of anthracene derivatives with TNM. Kochi appeared still to believe in Perrin's results and tried to develop further evidence for the naphthalene radical cation and $^{\bullet}NO_2$ coupling mechanism in nitronium reaction with naphthalene despite the accumulation of substantial evidence showing that Perrin's proposal was substantially inoperative.

Eberson *et al.*[55] undertook an extensive study of the nitration of naphthalene by TNM in dichloromethane and acetonitrile. They reported high yields of nitro/trinitromethyl and hydroxy/trinitromethyl adducts. Eberson *et al.*[55] isolated and/or characterised the major adducts (4), (5), (6), and(7) together with some 1-nitronaphthalene (8).

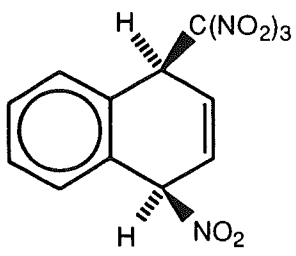

(4)

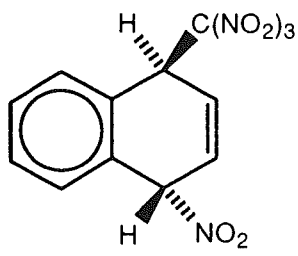

(5)

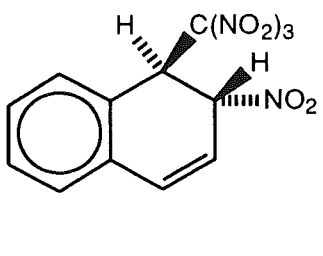

(6)

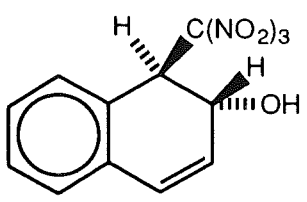

(7)

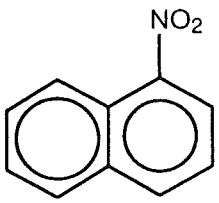

(8)

No 2-nitronaphthalene was detected giving a ratio of 1-/2-nitronaphthalenes of at least ≥ 27, consistent with nitronaphthalene formation by coupling of naphH$^{\bullet+}$ and $^{\bullet}NO_2$. The mechanism for adduct formation was assumed to involve reactions mostly with the triad formed upon photoexcitation of the charge transfer complex. How do these results fit with those observed by Kochi? Eberson *et al.* [55] observed that by taking pure adduct (4) and injecting into a g.l.c. at 100°C they obtained 1-nitronaphthalene. This is summarised in Scheme 1.21.

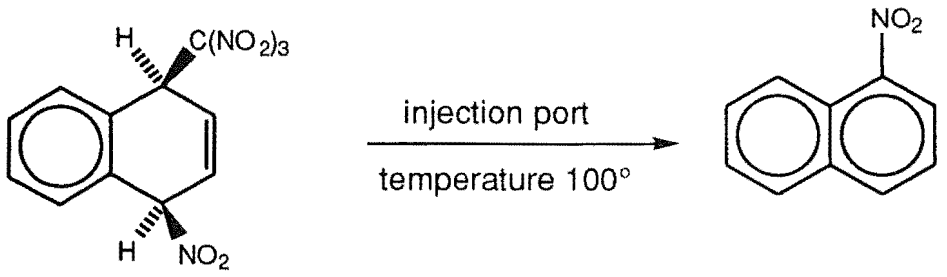

(4) 100%

SCHEME 1.21

It is clear that conclusions such as those drawn by Kochi *et al.*,[54] based on g.l.c. analysis data, are fatally flawed when the true products of reaction are thermally unstable.

In accounting for the formation of the variety of adducts in the photolysis of the naphthalene/tetranitromethane charge-transfer complex, and in particular the formation of the hydroxy/trinitromethyl adduct (7), Eberson *et al.* [55] invoked the critical first reaction step being reaction of the naphthalene radical cation with trinitromethanide ion. Subsequently this proposal was supported by experimental evidence summarised in Section 1.9.

1.9 COMPETITIVE REACTIONS OF TRINITROMETHANIDE ION AND NITROGEN DIOXIDE WITH RADICAL CATIONS

The photochemical activation of the charge transfer complex between an aromatic compound (ArH) and TNM leads within 3 ps to a triad consisting of $ArH^{\bullet+}$, $^{\bullet}NO_2$, and $(O_2N)_3C^-$ as described by Kochi [31] and as outlined in Scheme 1.22.

$$\underset{\text{CT complex}}{ArH\cdots\cdots C(NO_2)_4} \xrightarrow[< 3\ ps]{h\nu_{CT}} \underset{\text{triad}}{ArH^{\bullet+} \quad (O_2N)_3C^- \quad {}^{\bullet}NO_2}$$

SCHEME 1.22

As described above these species can combine to form primarily nitro/trinitromethyl adducts. In the formation of these adducts, the major issue which arises relates to the mechanistic nature of the first chemical step.[56]

(i) Is the first reaction step between $ArH^{\bullet+}$ and $(O_2N)_3C^-$, or $ArH^{\bullet+}$and $^{\bullet}NO_2$? [57,58] (See Scheme 1.23.)

$$ArH^{\bullet+} + (O_2N)_3C^- \xrightarrow{k_1} Ar(H)^{\bullet}C(NO_2)_3$$

$$ArH^{\bullet+} + {}^{\bullet}NO_2 \xrightarrow{k_2} Ar(H)NO_2^+$$

SCHEME 1.23

(ii) Is there any solvent effect such that the $ArH^{\bullet+}$/ $(O_2N)_3C^-$, is favoured in a less polar solvent such as dichloromethane whereas the $ArH^{\bullet+}/^{\bullet}NO_2$

reaction would occur predominantly in a polar medium such as acetonitrile?

Eberson *et al.*,[56] approached these questions by studying the effect on the lifetime of $ArH^{\bullet+}$ by removing one of the triad components as soon as it was formed. This was achieved by adding a protic acid to protonate the trinitromethanide ion $(O_2N)_3C^-$. The aromatic substrates studied are shown in Table 1.1 with the aromatic substrates listed in approximate order of decreasing $E^\circ(ArH^{\bullet+}/ArH)$. They range from those corresponding to very reactive radical cations like naphthalene and 1-methylnaphthalene to those corresponding to radical cations of high stability such as (tris(4-bromophenyl)amine). The analysis was done using EPR techniques in which the intensity of signals due to the radical cation were measured.

Solutions of the ArH and TNM in dichloromethane were photolysed with filtered light ($\lambda \geq 435$ nm) in an EPR cavity at -60°C. Only the least reactive radical cations gave any EPR signal visible above noise level. However, when TFA was added to these solutions and photolysed under identical conditions, EPR signals were observed for all the radical cations except the most reactive (naphthalene and 1-methylnaphthalene).

TABLE 1.1 EPR spectral intensities after irradiation of ArH/tetranitromethane solutions in dichloromethane with and without TFA present.

ArH	EPR Spectral Intensity		
	With $C(NO_2)_4$	With $C(NO_2)_4$ and TFA[b]	RATIO
Naphthalene	<2	<2[b] (<2)	1
1-Methylnaphthalene	<2	<2 (<2)	1
1,4-Dimethylnaphthalene	<2	10 (<1.5)	>5
1,2-Dimethylnaphthalene	<2.5	54 (<2)	>22
1,8-Dimethylnaphthalene	<2	16 (4)	>8
1,4,6,7-Tetramethylnaphthalene	<0.7	52 (3)	>74
1,4,5,8-Tetramethylnaphthalene	<1.8	100 (5)	>55
1,3,5,8-Tetramethylnaphthalene	<2	44 (2.6)	>22
1,4-Dimethoxybenzene	<2	540 (<2)	>270
9-Phenylanthracene	<1.8	100(8)	>56
9,10-Diphenylanthracene	<2.6	300(6.5)	115
Perylene	8	230(25)	106
Tris(4-bromophenyl)amine	19	181 (3.2)	9.5
9,10-Dimethylanthracene	<1	600 (4.6)	>600

Experimental details: [a]Irradiation time 6 min. (during which time 100 spectra were accumulated), $\lambda \geq 435$ nm, [ArH] =20-40 mmol dm^{-3}, $[C(NO_2)_4]$ = 0.8 mol dm^{-3}, [TFA] = 0.4 mol dm^{-3}, T = 213K.

[b]The number within parentheses refers to an identical check experiment with only TFA (0.4 mol dm^{-3}) added. [b] At [TFA] = 1 mol dm^{-3}, the naphthalene radical cation concentration was above noise level (intensity ≈ 3.5).

For dichloromethane the results were interpreted as follows.

Trinitromethanide ion is much more reactive toward $ArH^{\bullet+}$ than NO_2 , i.e. $k_1 >> k_2$ and therefore only very unreactive radical cations such as perylene$^{\bullet+}$, 9,10-diphenylanthracene$^{\bullet+}$ and (tris(4-bromophenyl)amine)$^{\bullet+}$ can be generated in a sufficient concentration above noise level in the presence of $(O_2N)_3C^-$. With the addition of a protic acid, the trinitromethanide ion is protonated rapidly , the ionic coupling reaction does not occur and the radical cation concentration increases in the presence only of the less reactive NO_2. However the radical cations of naphthalene and 1-methylnaphthalene were reactive enough, presumably with NO_2, to be undetectable under the conditions employed for the study.

1.10 PHOTOCHEMICAL NITRATION OF NAPHTHALENE BY TNM

Eberson *et al.* [55] undertook a product study of the photonitration of naphthalene by TNM in dichloromethane and acetonitrile as mentioned earlier in Section 1.8. Adduct formation is the predominant pathway in both solvents after excitation of the charge transfer complex with light.

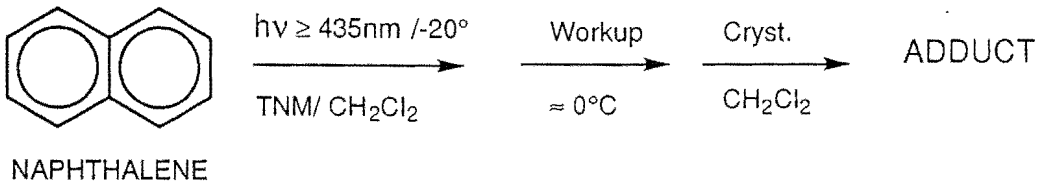

SCHEME 1.24

Only one of the addition products from the photolysis of naphthalene could be isolated (see Scheme 1.24) and characterised as cis-1,4-dihydro-1-nitro-4-

trinitromethyl-naphthalene (4) by X-ray crystallography,[59] but other adducts

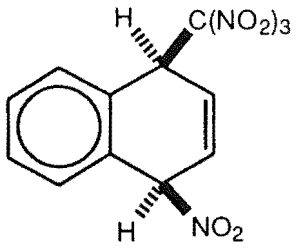

(4)

(5), (6) and (7) were identified by their NMR spectral properties. A number of other adducts were detected in the NMR spectra of the reaction product but not identified.

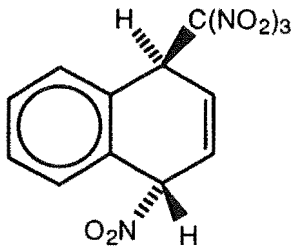

(5)

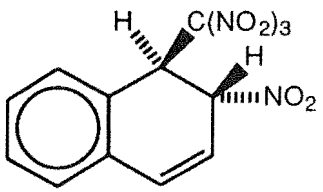

(6)

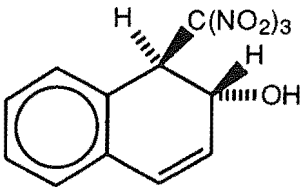

(7)

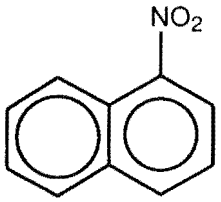

(8)

Because of the known susceptibility of such adducts to thermal decomposition the reactions were performed at two different temperatures (-20°C and 20°C). An overview of the yields of adducts for both solvents at the different temperatures are given in Tables 1.2 and 1.3.

TABLE 1.2 Overview of yields of products from the photolysis of naphthalene (1.0 mol l^{-1}) and tetranitromethane (2.0 mol l^{-1}) in dichloromethane.

		Yield(%)					
t / h	Conversion (%)	**4**	**5**	**6**	**7**	**8**	Total Adducts
At +20°C							
2	46	22.7	19.5	21.2	14.3	6.3	93.4
4	85	26.3	22.1	22.9	12.5	5.9	94.1
7.25	94	23.5	21.3	19.7	8.4	5.4	94.3
24	100	24.0	20.4	17.1	≤2[a]	4.4	95.6
At -20°C							
8.75	53	25.5	19.4	18.8	15.0	12.2	87.8
24	≈90	26.8	16.8	17.7	12.7	13.5	86.5

[a]Limit of detection

TABLE 1.3 Overview of yields of products from the photolysis of naphthalene (1.0 mol l^{-1}) and tetranitromethane (2.0 mol l^{-1}) in acetonitrile.

		Yield(%)					
t / h	Conversion (%)	**4**	**5**	**6**	**7**	**8**	Total Adducts
At +20°C							
4	40	24.1	20.7	21.9	15.0	5.9	94.1
25.5	100	26.2	24.1	17.2	≤2[a]	12.1	87.9
28.2	100	21.1	22.7	19.8	≤2[a]	10.6	87.4
At -20°C							
6.5	33	22.9	20.2	18.8	12.4	13.0	87.0
8.25	37	26.8	17.0	17.7	10.3	15.8	84.2
24	79	26.2	19.3	17.1	11.2	8.0	91.4
28.5	82	27.3	16.7	16.7	11.5	10.3	88.8

[a]Limit of detection

In the event no significant differences were observed in adduct yields between the two solvents or between the different temperatures. The adducts formed in the photolysis reaction of naphthalene and TNM represent an interesting combination. Adducts (4) and (5) are formed *via* an intermediate (9). Similarly adduct (6) can be formed via the same intermediate as shown in the following Scheme 1.25.

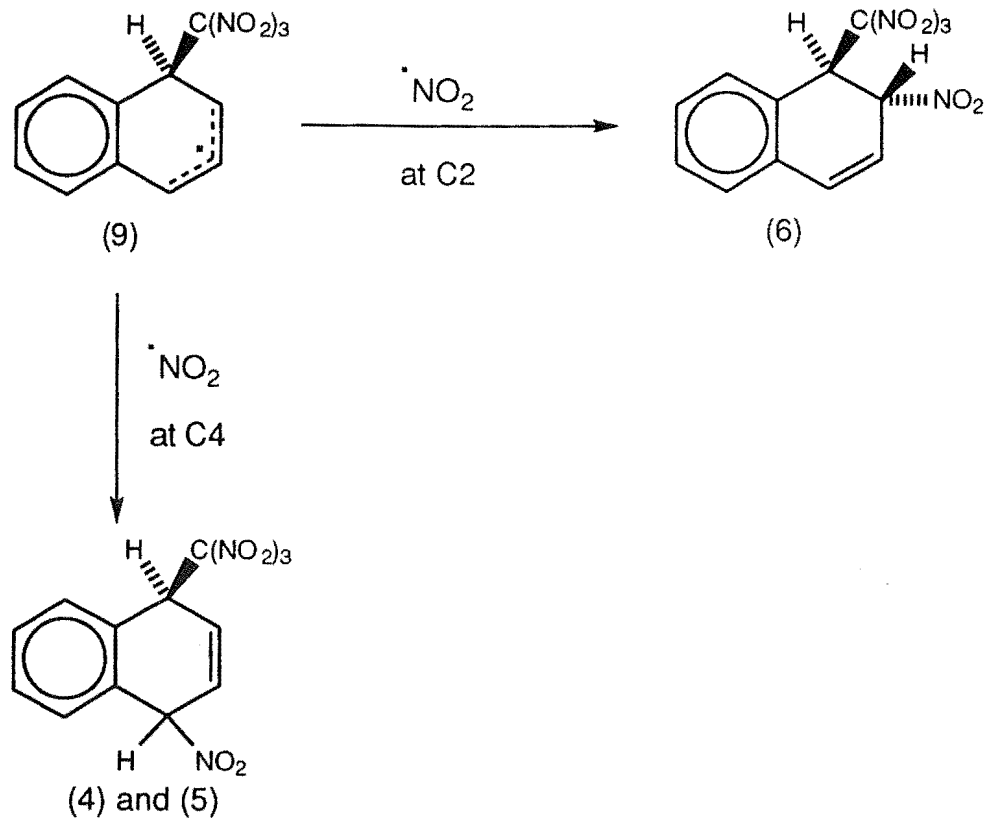

SCHEME 1.25

Adducts (4), (5) and (6) are formed by radical coupling of the delocalised carbon radical (9) with nitrogen dioxide. Attack of NO_2 at C4 would yield adducts (4) and (5), while corresponding attack at C2 would give adduct (6) The observed *trans*-stereochemistry for adduct (6) presumably arises because of the steric size of the trinitromethyl group in the delocalised carbon radical (9) which blocks attack from the *syn*- face of the ring system.

The formation of adduct (7) was seen as occurring by initial attack of NO_2 at C2 of the delocalised carbon radical (9) with C-O bond formation to yield the trinitromethyl nitrite (10), followed by hydrolysis of the nitrite ester to give the hydroxy/trinitromethyl adduct (7) either during the photolysis under the prevailing acidic conditions or during workup as illustrated in Scheme 1.26. Such C-O bond formation is a feature of reactions of NO_2 with delocalised carbon radicals when electron-withdrawing substituents are present in the structure of the carbon radical component of the reaction.

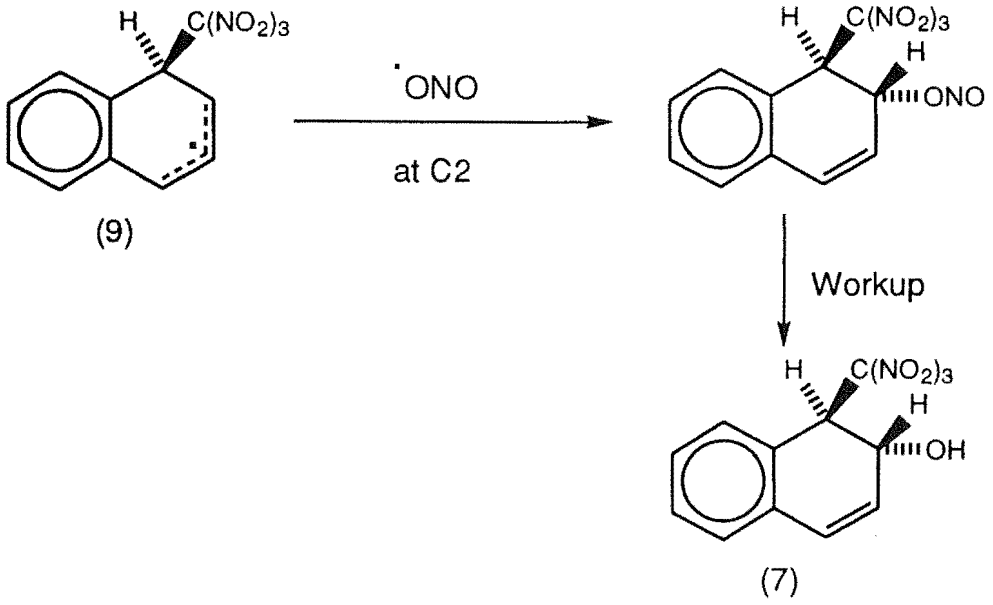

SCHEME 1.26

The formation of the 1-nitronaphthalene (8) was thought to be a direct result of $^{\bullet}NO_2$ attack on the radical cation (13) with subsequent loss of a proton to retain the aromaticity as outlined in Scheme 1.27.

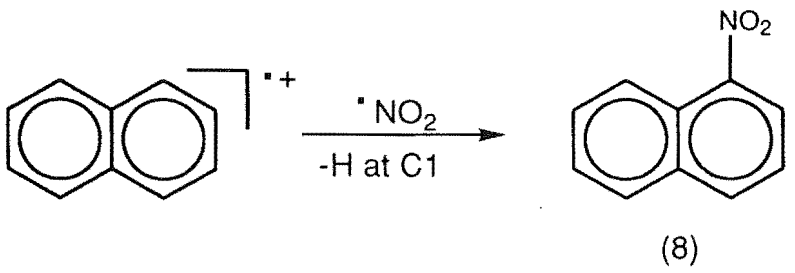

SCHEME 1.27

1.11 PHOTOCHEMICAL NITRATION OF 1,4-DIMETHYLNAPHTHALENE BY TNM

Kochi and Sankararaman[54], studied the photonitration of 1,4-dimethylnaphthalene with TNM in acetonitrile. They characterised the *syn*- and *anti*-adduct isomers (13) and (14) (total 43% at -30°C) with the structure of the predominant adduct (13) being confirmed by X-ray crystallography.

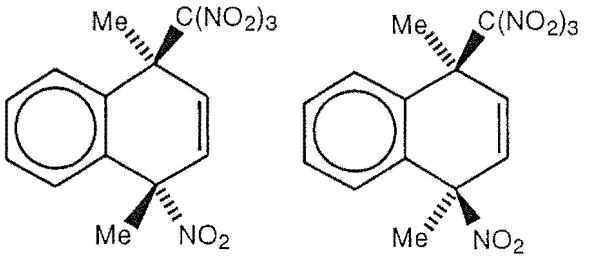

(13) (14)

Adducts (13) and (14) were observed to undergo slow decomposition in acetonitrile at room temperature to give a side chain nitro derivative (15). 1,4-Dimethyl-2-nitro-naphthalene (16) was also characterised as a minor product.

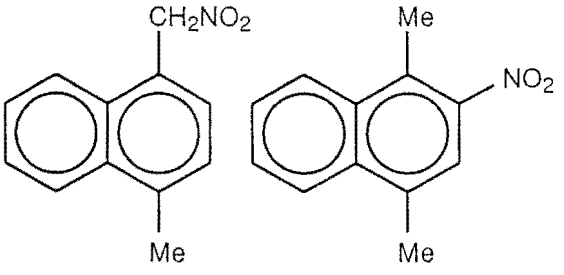

(15) (16)

Eberson *et al.* [60] also undertook an extensive product study of the photonitration of 1,4-dimethylnaphthalene by TNM in dichloromethane and acetonitrile at -50°, -20° and +20°C. They show that adduct formation is again the predominant pathway in both solvents reaching 90% at -50°C in dichloromethane. In dichloromethane adducts (13) and (14) were identified

along with the side chain nitro derivative (15) and a minor unidentified component. An overview of the product yields for the photonitration in dichloromethane at different temperatures is depicted in Table 1.4.

TABLE 1.4 Overview of yields of products from the photolysis of 1,4-dimethylnaphthalene (1.0 mol l^{-1}) and tetranitromethane (2.0 mol l^{-1}) in dichloromethane.

		Yield(%)				
t / h	Conversion (%)	**13**	**14**	**15**	**Unknown**[a]	Ratio **13:14**
At -50°C						
1	10	70	10	12	8	7
2	26	81	8	7	5	10
4	59	82	9	7	2	9
5.25	74	81	9	7	2	9
At -20°C						
1	13	68.6	4.6	19.0	7.8	15
2	34	69.9	8.1	15.9	6.1	9
4	61	70.1	10	16.9	2.9	7
5.25	81	73.3	7.7	15.4	2.6	8
At +20°C						
1	21	42.3	4.2	47.1	6.3	10
2	51	44	5.2	48	2.6	8
4	92	33	4.5	60.4	2.2	7
5.25	100	29.5	3.8	64.9	1.8	8

[a]The unknown product has CH_2-X at δ 5.691.

In acetonitrile adducts (13) and (14) were identified as well as products (15) and (16), however, two further adducts (17) and (18) were observed and assigned

as epimers of 4-hydroxy-1,4-dimethyl-1-trinitromethyl-1,4-dihydronaphthalene.

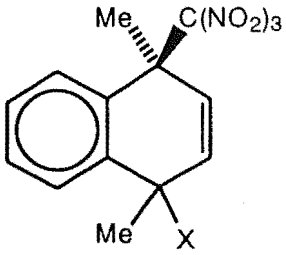

17, 18 epimers X=ONO

17a, 18a epimers X=OH after workup

(17) and (18)

The product yields from the photonitration in acetonitrile at different temperatures are shown in Table 1.5.

TABLE 1.5 Overview of yields of products from the photolysis of 1,4-dimethylnaphthalene (1.0 mol l^{-1}) and tetranitromethane (2.0 mol l^{-1}) in acetonitrile.

		Yield(%)					
t / h	Conversion (%)	**13**	**14**	**15**	**16**	**17**	**18**
At -20°							
1	8.3	61.5	11.6	6.4	-	14.8	5.7
2	24.6	68.7	15.1	6.7	-	6.4	3.2
4	45.6	71.6	15.5	7.1	-	3.9	1.8
6	60.8	71.5	17	6.8	-	3.3	1.4
At +20°C							
0.5	14.1	41.6	17.4	28	-	8.3	4.7
1	31.9	40.7	18.5	31.4	-	3.9	1.9
2	70.4	33.5	14.6	34.1	15.6	1.1	trace
3.25	97.7	33.7	9.1	43.0	14.1	trace	-

Tables 1.4 and 1.5 show that the photonitration of 1,4-dimethylnaphthalene with TNM gives apparently different outcomes in dichloromethane and acetonitrile and the adduct distribution differs between the various temperatures. Eberson *et al.* [60] explained the formation of the adducts from dichloromethane by making the assumption that adducts (13) and (14) were the primary products from the initial photochemical reaction and that the nitro substitution product (15) was formed in a secondary reaction from the primary adducts.

The experiment in dichloromethane at -50°C was run in order to minimise the occurrence of this secondary product (15). Table 1.4 illustrates that the combined yields of adducts (13) and (14) at -50°C are high. As expected on this basis, the side-chain nitro compound (15) became more prominent in both solvents as the temperature was increased and rearrangement of the initial adduct products (13) and (14) became more extensive.

The two new adducts (17) and (18) in acetonitrile were identified as the corresponding hydroxy adducts, (17a) and (18a) which must have been formed by hydrolysis of the nitrites (17) and (18) during the reaction or workup. The formation of 1,4-dimethyl-2-nitronaphthalene (16) was observed only in the latter stages of the acetonitrile reaction suggesting that it is formed from the primary product adducts (13) and (14). Eberson *et al.* suggested a possible pathway to formation could be *via* the trinitromethylcyclohexadienyl radical (19) from an acid promoted process involving NO_2 coupling at C2 with a corresponding loss of nitroform as illustrated in Scheme 1.28.

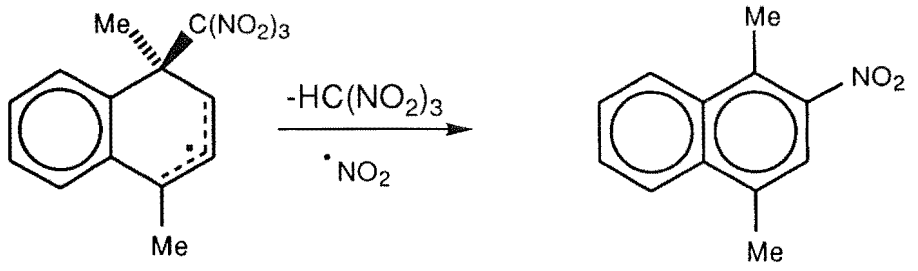

(19) (16)

SCHEME 1.28

Eberson *et al.* [60] observed that adduct (13) underwent a fast thermal rearrangement to give adduct (14) in acetonitrile. The rearrangement of (13) to (14) was assumed to be polar with the trinitromethyl group acting as the leaving group, as shown in Scheme 1.29. They report the rearrangement of adduct (14) to give adducts (17) and (18) in acetonitrile. (See Scheme 1.29.) This process was assumed to proceed *via* a trinitromethylcyclohexadienyl radical (19).

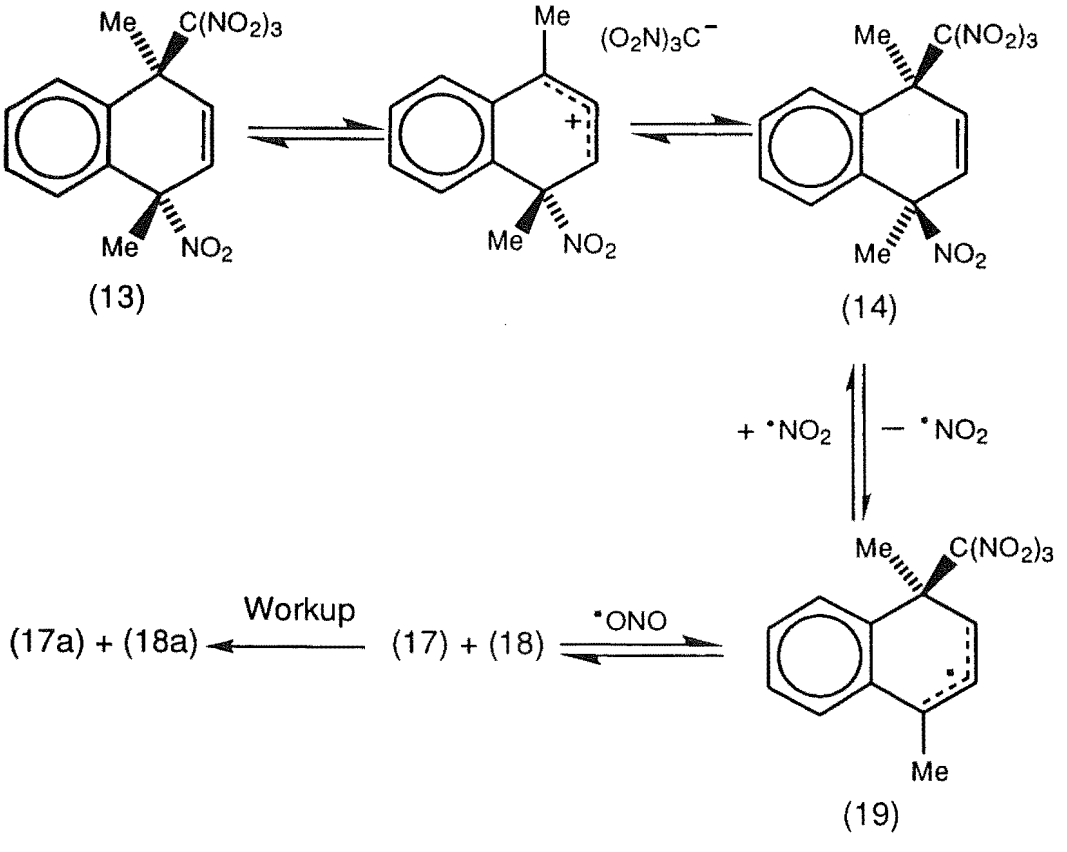

SCHEME 1.29

The formation of (15) is thought to be from the nitrocyclohexadienyl cation (20) after loss of nitroform from adducts (13) and (14). (See Scheme 1.30.)

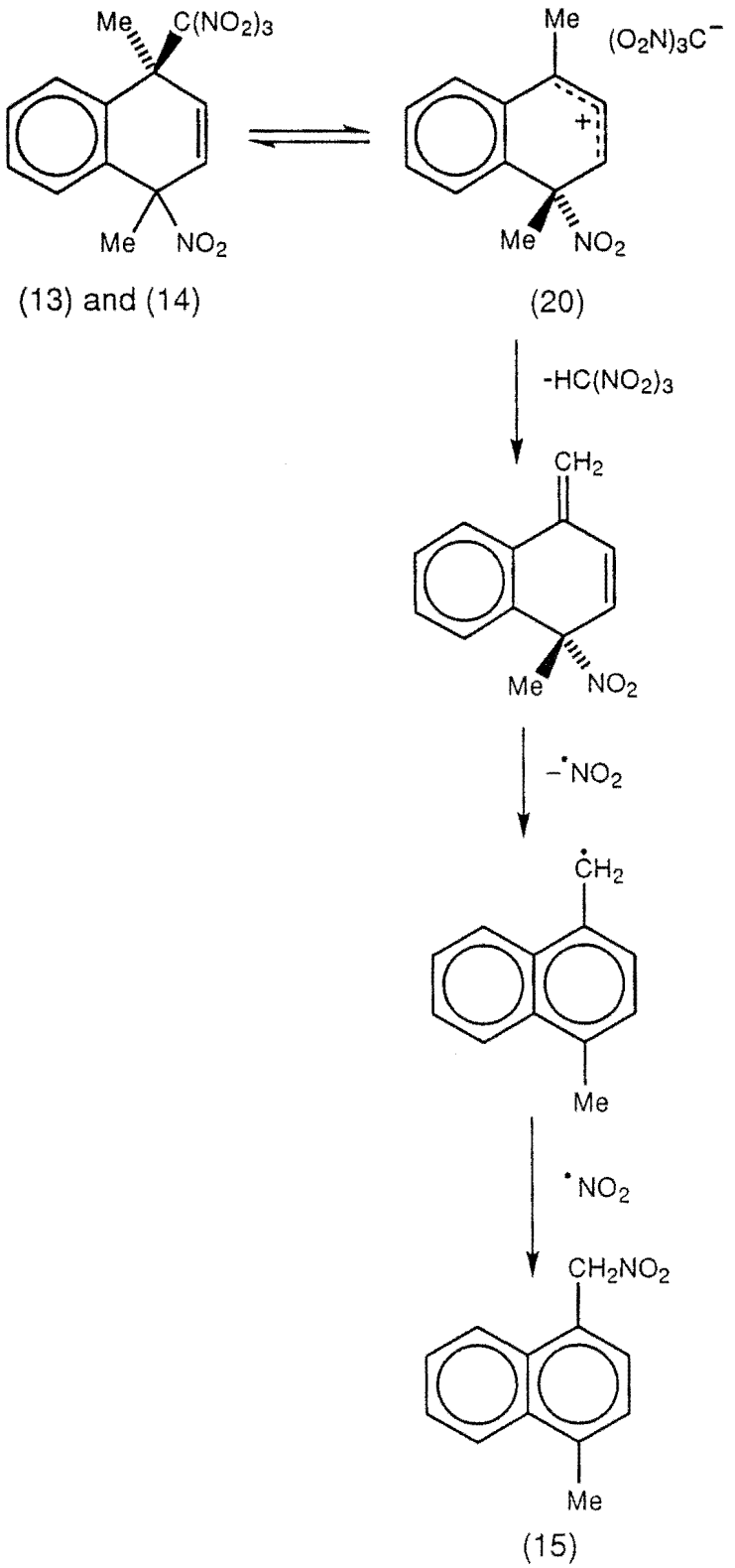

SCHEME 1.30

Analogous chemistry to give the side chain nitro product (15) is known from the chemistry of acetoxy-nitro adducts.[61]

CHAPTER TWO

PHOTONITRATION OF 1,4,5,8-TETRAMETHYLNAPHTHALENE

2.1 INTRODUCTION

As described in Chapter 1 the photoaddition of TNM to anthracenes, naphthalene and 1,4-dimethylnaphthalene has been shown to give a mixture of nitro/trinitromethyl adducts and some secondary products which are produced through a complex sequence of thermal steps. From 1,4-dimethylnaphthalene,[60] the main products in 90% yield were the *cis*- and *trans*-1,4-nitro/trinitromethyl adducts (13) and (14) when the photolysis was carried out at -50°C in dichloromethane. In addition the side-chain nitration product (15) was formed in 7% yield. For photolysis reactions at higher temperatures more extensive rearrangement of the nitro/trinitromethyl adducts (13) and (14) occurred giving the side-chain nitration product (15) in higher yield.

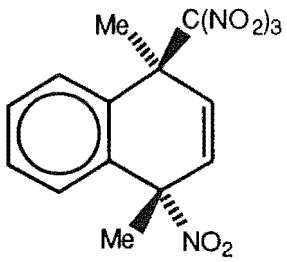

(13)

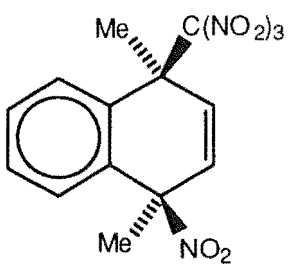

(14)

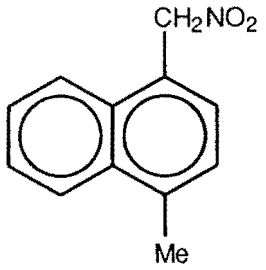

(15)

All the nitro/trinitromethyl adducts observed to date are obtained from the trinitromethyl anion attacking at C1 or the α-position of the naphthalene nucleus. 1,4,5,8-Tetramethylnaphthalene (21) however has all four of the α-positions blocked and we therefore anticipated that if 1,4-adducts analogous to (13) and (14) formed these would undergo rearrangement to give side-chain

nitro compounds even more readily because of the extensive steric compression in the 1,4,5,8-tetramethyl series.

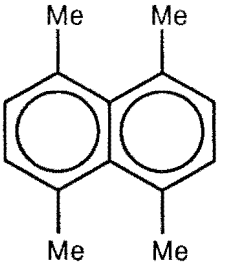

(21)

It was anticipated also that new addition modes might be induced by the higher steric congestion in transition states for trinitromethanide attack on the 1,4,5,8-tetramethylnaphthalene radical cation (22).

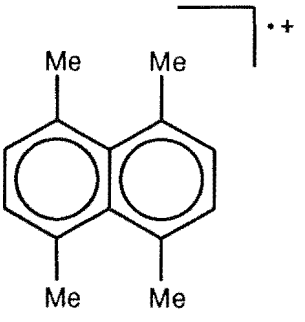

(22)

Previous work [62,63] indicated that the 1,4,5,8-tetramethylnaphthalene radical cation (22) is a relatively stable species, being observable at room temperature by EPR spectroscopy in dichloromethane containing trifluoroacetic acid (5%). Eberson *et al.*[64] have shown that $Me_4naph^{\bullet+}$ has a half life of 0.2 s in dichloromethane in the presence of tetrabutylammonium trinitromethanide, indicating a second-order rate constant of ~ 1000-2000 $M^{-1}s^{-1}$ for reaction between the radical cation and trinitromethanide ion. It was concluded that reactions between the initially formed species in the triad would most likely take

place between free solvated species. Thus it was of interest to us to undertake a study of the photonitration of 1,4,5,8-tetramethylnaphthalene (21).

2.2 THE PHOTOLYSIS OF 1,4,5,8-TETRAMETHYLNAPHTHALENE (21)

General Procedure for the Photonitration of 1,4,5,8-Tetramethylnaphthalene (21) with Tetranitromethane. - A solution of 1,4,5,8-tetramethylnaphthalene (21) (0.34 mol dm^{-3} solution) and tetranitromethane (0.68 mol dm^{-3}) in dichloromethane at -20° or acetonitrile at -20° or +20°C was irradiated with filtered light (cut-off < 435 nm). Aliquots were withdrawn at appropriate time intervals, the volatile material was removed under reduced pressure at ≤ 0°C, and the product composition determined by ^1H NMR spectral analysis. (For complete experimental details see Chapter 5.)

2.3 PHOTOCHEMISTRY OF 1,4,5,8-TETRAMETHYLNAPHTHALENE (21) IN DICHLOROMETHANE

The photolysis of a solution of 1,4,5,8-tetramethylnaphthalene (0.34 mol l^{-1}) and TNM (0.68 mol l^{-1}) in dichloromethane was carried out using filtered light (cut off ≥ 435nm) at -20°C until the strongly red colour of the charge transfer band had been bleached. Work-up at ≤ 0°C gave a residue which analysis by ^1H NMR indicated that a mixture of adducts and side-chain nitration products had formed.

The major adduct (23) was isolated by low temperature crystallisation of the crude product at -20°C and its structure was determined by single crystal X-ray analysis. A perspective drawing of 1,4,5,8-tetramethyl-*r*-1-nitro-*c*-2-trinitromethyl-1,2-dihydronaphthalene (23), $C_{15}H_{16}N_4O_8$, m.p.128-135°C (dec.), is presented in Fig. 2.1 with corresponding atomic coordinates in Table 5.1.

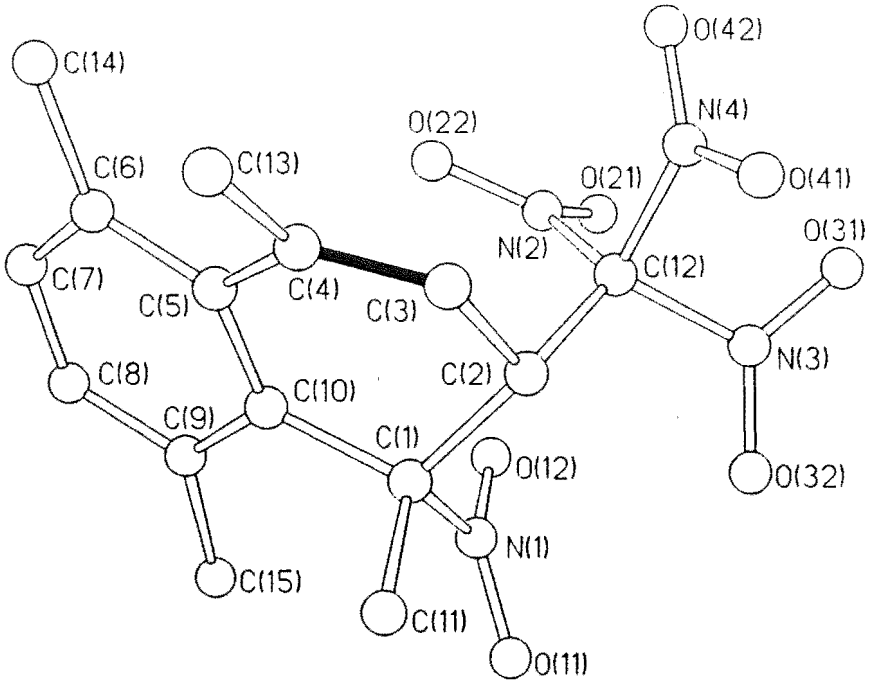

FIGURE 2.1

A perspective diagram of 1,4,5,8-tetramethyl-*r*-1-nitro-*c*-2-trinitromethyl-1,2-dihydronaphthalene (23).

In the solid state the aromatic ring in the structure is close to planar with the largest deviation being indicated by the torsional angle C(9)-C(10)-C(5)-C(6) -9.9°. In contrast the alicyclic ring, effectively a substituted cyclohexa-1,3-diene system, is considerably puckered. The relief of one of the *peri*-interactions is evident in the twisting of the "diene" system, torsional angles: C(3)-C(4)-C(5)-C(10) 25.8°, C(6)-C(5)-C(4)-C(13) 31.9°. The second *peri*-interaction present in 1,4,5,8-tetramethylnaphthalene is also relieved in adduct (23) as a consequence of C(1) being a sp^3 carbon atom; the conformation adopted is revealed by the torsional angles: C(9)-C(10)-C(1)-C(11) -85.3°, C(9)-C(10)-C(1)-N(1) 33.7°. The orientation of the trinitromethyl group relative to the ring systems is indicated by the torsional angle: C(11)-C(1)-C(2)-C(12) 155.8°, the C(2)-C(12) bond being close to perpendicular to the mean plane of the carbon atoms of the bicyclic system.

The ^1H and ^{13}C NMR spectra of adduct (23) were assigned from long range reverse detected ^1H - ^{13}C heteronuclear correlation spectra (HMBC). In

particular, the ^{13}C resonances of the Me-**C(1)**-NO_2 (δ 92.39), H-**C(2)**-$C(NO_2)_3$ (δ 48.03), H-**C(3)**= (δ 114.14), and Me-**C(4)**= (δ 145.02) were assigned. The NMR spectroscopic data for adduct (23) are consistent with the established structure. In particular, the observed H(2)-H(3) coupling constant (*J* 7.9 Hz) corresponds closely to that derived from the Karplus equation and the torsional angle of H(2)-C(2)-C(3)-H(3), 35.3° (*J* 7.84 Hz).

A minor adduct (24) was isolated in a slightly impure state (*c.* 95%) by HPLC on a cyanopropyl column using hexane/dichloromethane mixtures as eluting solvents. The structure of adduct (24) was established on a comparison of the NMR spectra of the two adducts (23) and (24). (See Table 2.1.)

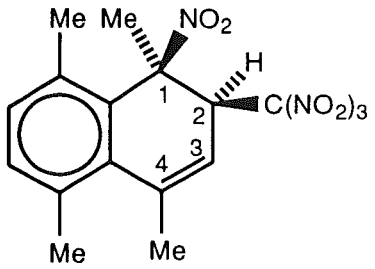

(23)

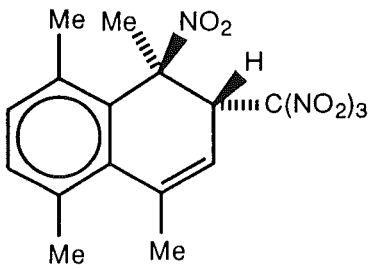

(24)

TABLE 2.1 Comparisons between ^{13}C NMR data and ^{1}H NMR data for adducts (23) and (24) in ppm.

ADDUCT (23)		ADDUCT (24)	
C1	92.4	C1	94.7
C2	48.0	C2	47.0
C3	114.0	C3	116.5
C4	145.0	C4	143.8
CH_3-1	2.17, s	CH_3-1	2.19, s
H2	4.38, d, *J* = 7.9 Hz	H2	5.34, d, *J* = 6.7 Hz
H3	5.76, dq *J* = 7.9, *J'*= 1.5 Hz	H3	5.96, dq *J* = 6.7, *J'*= 1.5 Hz
CH_3-4	2.22, d, *J* = 1.5 Hz	CH_3-4	2.09, d, *J* = 1.5 Hz

HMBC spectra allowed the unambiguous assignment of the ^{13}C resonances of adducts (23) and (24). For sp^3 carbons directly connected to a trinitromethyl group (eg. C2) the ^{13}C shift was always between 40-50 ppm. Similarly, for sp^3 carbons directly connected to a nitro group (eg. C1) the ^{13}C shift was ≈ 90 ppm.

The two side-chain nitration products (25) and (26) were isolated in pure form using silica gel chromatography.

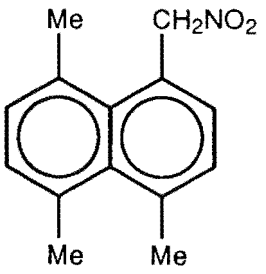

(25)

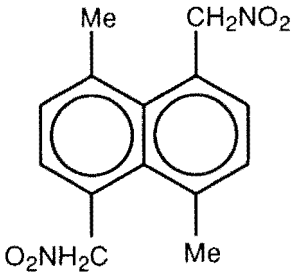

(26)

The structure of 4,5,8-trimethyl-1-nitromethylnaphthalene, (25), m.p.101-103°C (Lit.[51] 101-103) was determined from its NMR and infrared data. In particular, the NMR data indicated an aromatic derivative of 1,4,5,8-tetramethylnaphthalene. The very characteristic ^1H resonance at δ 5.47 ppm for the CH_2NO_2 function along with a characteristic infrared absorption at 1540 cm^{-1} for a $-NO_2$ substituent provided evidence for product (25). Unambiguous assignment of compound (25) came with comparison of NMR data available in the literature.[52,53]

The structure of 1,5-dinitromethylnaphthalene (26) was determined from its ^1H NMR spectra and nuclear Overhauser enhancement experiments. In particular, the ^1H resonances of H2 and H3, and H6 and H7, appeared as identical AB quartets (δ 7.74 and 7.61, $J_{H,H}$ 9.8 Hz), and irradiation at δ 2.98 (4-Me, 8-Me) gave enhancements of the signals due H3/H7 (δ 7.61) and the 1- and 5-

CH_2NO_2 groups (δ 6.44); irradiation at δ 6.44 gave enhancements of the signals due to 4-Me/8-Me (δ 2.98) and H2/H6 (δ 7.74) as illustrated in Fig 2.2. Elemental analysis established the empirical formula $C_7H_7NO_2$.

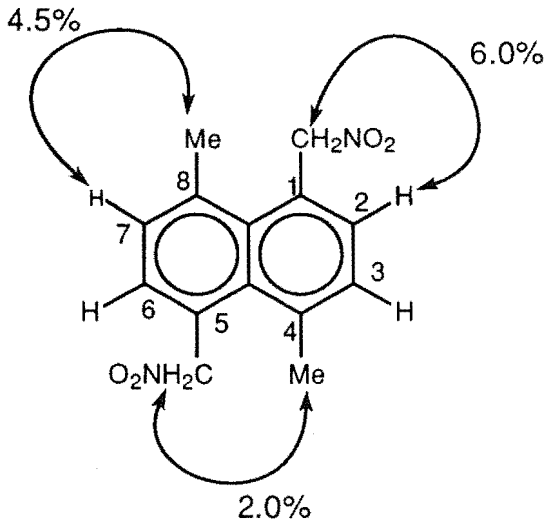

(26)

FIGURE 2.2 Indicating the enhancements % from nOe experiments.

When the reaction was monitored with time, two new adducts were detected by ^1H NMR during the first hour of the photolysis after workup at ≤ 0°C and they disappeared during the following hour. (See Table 2.2)

TABLE 2.2 Overview of yield of products from the photolysis at -20°C of 1,4,5,8-tetramethylnaphthalene (0.34 mol dm^{-3}) and tetranitromethane (0.68 mol dm^{-3}) in dichloromethane.

	Relative Yield (%)						
t / h	**(23)**	**(24)**	**(25)**	**(26)**	**(27)**	**(28)**	**Unidentified** [a]
0.5	21	8	58	-	8	5	-
1	24	9	58	-	4	3	-
2	24	10	27	11	-	-	24
8	16	8	24	11	-	-	41

[a] These are products of further photonitration of 4,5,8-trimethyl-1-nitromethylnaphthalene (25).

These were assigned the structures of the two 1,4-hydroxy/trinitromethyl adducts (27a) and (28a) on the basis of ^1H NMR spectral analysis and comparison with the hydroxy/trinitromethyl adducts found in the 1,4-dimethylnaphthalene system. (See Fig. 2.3.)

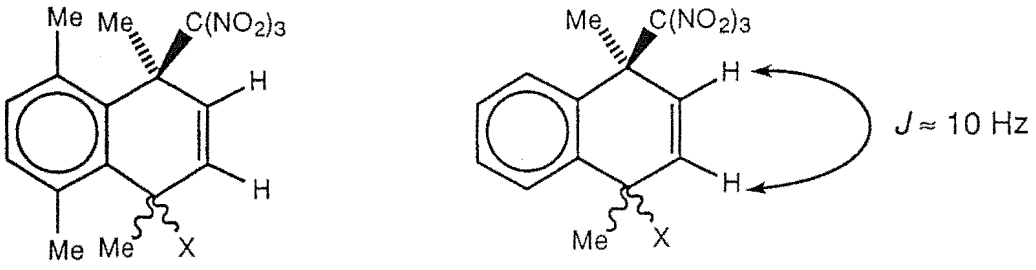

(27) and (28) epimers X = ONO (17), (18) epimers X=ONO

(27a) and (28a) epimers X = OH (17a), (18a) epimers X=OH

FIGURE 2.3

These adducts (27a) and (28a) are formed by hydrolysis of the nitrites (27) and (28) during the workup of the reaction mixture. Such nitrites would be expected to be susceptible to hydrolysis under the prevailing acidic conditions[62] which arise from the formation of nitroform during the photolysis reaction.[55,59,60] The presence of adducts arising by 1,4-addition to a 1,4-dimethylnaphthalene is readily recognised by the appearance of the characteristic coupling of ≈ 10 Hz between two vinylic hydrogens.[60] (See Table 2.3.)

Table 2.3 Chemical Shifts δ and coupling constants ($J_{H2,H3}$ H2) of the vinylic hydrogens of 1,4-adducts derived from 1,4-dimethylnaphthalene.

1,4-dimethylnaphthalene		1,4,5,8-Tetramethylnaphthalene	
(13)	δ 6.26,6.68 *J*= 10.5 Hz		
(14)	δ 6.49,6.66 *J*= 10.5 Hz		
(17a)	δ 5.95,6.36 *J*= 10.1 Hz	(27a)	δ 5.79,6.10 *J*= 10.0 Hz
(18a)	δ 5.97,6.29 *J*= 10.2 Hz	(28a)	δ 5.80,6.14 *J*= 9.8 Hz

Thus the 1,4-nitro/trinitromethyl adducts of 1,4-dimethylnaphthalene (13) and (14) had resonances at: δ 6.26, 6.68, ($J_{H2,H3}$ 10.5 Hz), δ 6.49, 6.66, ($J_{H2,H3}$ 10.5 Hz), respectively and the corresponding 1,4-hydroxy/trinitromethyl adducts (17a) and (18a), derived from reaction workup of the 1,4-nitrito/trinitromethyl adducts (17) and (18), had resonances at δ 5.95, 6.36, ($J_{H2,H3}$ 10.1 Hz) and δ 5.97, 6.29, ($J_{H2,H3}$ 10.2 Hz). The NMR spectra of (17a) and (18a) also had singlets at δ 1.65 and 1.57, respectively, assigned to the HC(O)C**H**$_3$ function.

The photolysis of the TNM/1,4,5,8-tetramethylnaphthalene charge-transfer complex was also carried out at -50°C in dichloromethane in an attempt to limit the conversion of adducts (27) and (28) into secondary products [eg. the side-chain nitro product (25)]. However, the reaction at -50°C resulted in a similar product distribution, comprising of (23) (24%), (24) (9%), (25) (51%), (26) (<5%) and some unidentified material (16%).

2.4 PHOTOCHEMISTRY OF 1,4,5,8-TETRAMETHYLNAPHTHALENE IN ACETONITRILE

The photolysis of a solution of 1,4,5,8-tetramethylnaphthalene (0.34 mol l^{-1}) and TNM (0.68 mol l^{-1}) in acetonitrile was carried out using filtered light (cut off ≥ 435nm) at -20°C and monitored with time. (See Table 2.4.) At the completion of the reaction the same products (23) to (26) were formed as in dichloromethane but with a higher yield of rearrangement products of (25) and (26) and markedly lower yields of adducts (23) and (24). The labile adducts (27) and (28) were present in a total yield of 53% after 1 h but absent from the product mixture after 4 h some unidentified products of the same nature as those formed in dichloromethane were also detected. These have been shown

to arise by further photonitration of the side-chain nitro compound (25). (See experimental section for details.)

TABLE 2.4 Overview of yield of products from the photolysis at -20°C of 1,4,5,8-tetramethylnaphthalene (0.34 mol dm^{-3}) and tetranitromethane (0.68 mol dm^{-3}) in acetonitrile.

	Relative Yield (%)						
t / h	**(23)**	**(24)**	**(25)**	**(26)**	**(27)**	**(28)**	**Unidentified** [a]
1	7	2	38	-	29	24	-
2	7	2	68	2	7	12	2
4	6	2	64	7	-	-	21
8	7	2	52	11	-	-	28

[a] These are products of further photonitration of 4,5,8-trimethyl-1-nitromethylnaphthalene (25)

From Table 2.4 evidence for the conversion of the 1,4-nitrito/trinitromethyl adducts (27 and (28) to the side-chain nitro derivative is obtained in the first two hours of the reaction. The significant drop in the relative yields of (27) and (28) in the second hour of the photolysis is reflected by a corresponding increase in the relative yield of the side-chain nitro derivative (25) as illustrated in Scheme 2.1. This is compelling evidence for the presence of the nitrito/trinitromethyl adducts (27) and (28) in the reaction mixture, with hydroxy/trinitromethyl adducts (27a) and (28a) being formed during the workup procedure.

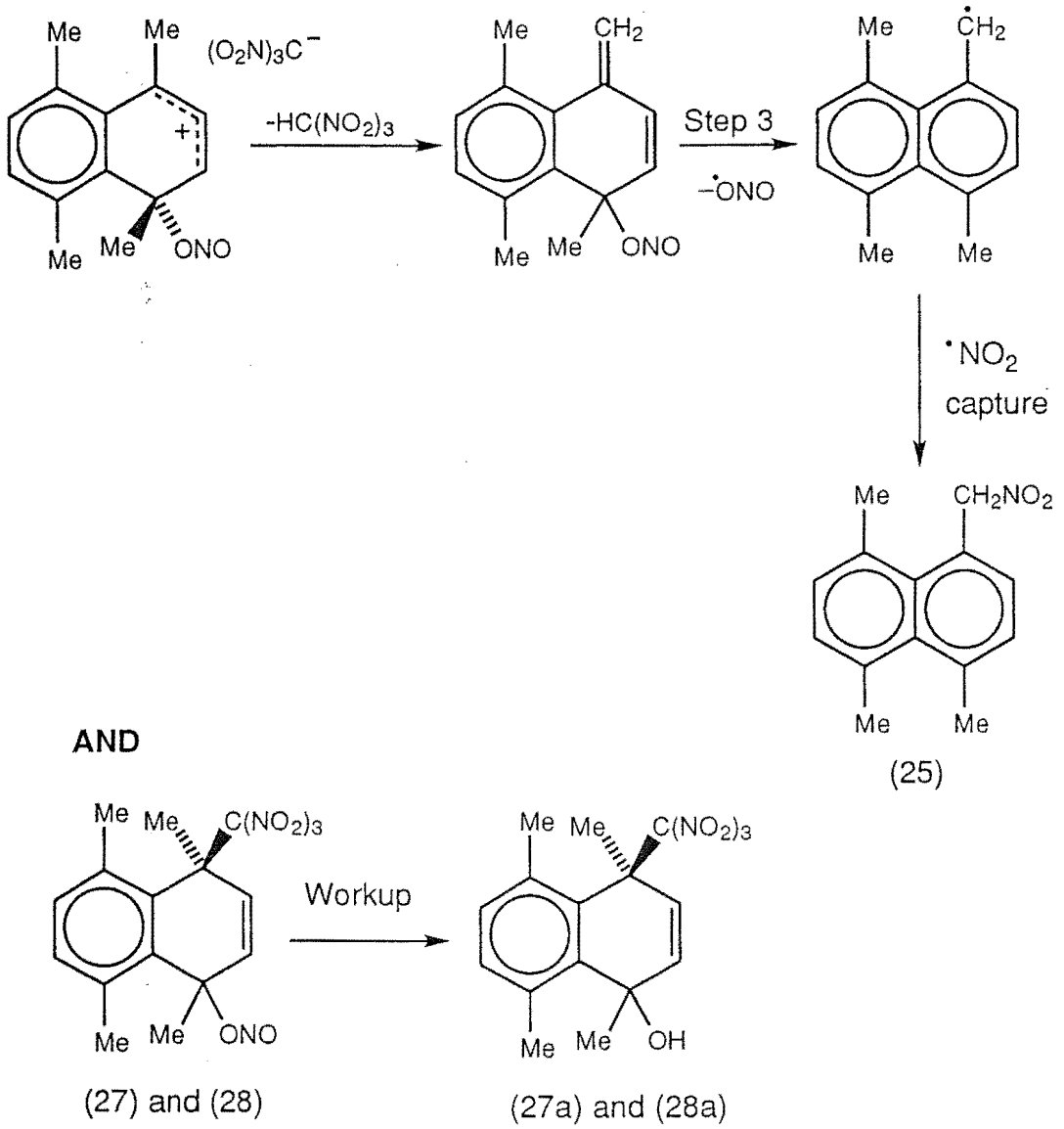

SCHEME 2.1

A photolysis carried out at +20°C for 8 h. gave the two nitromethyl derivatives (25) and (26) in 17% and 53% yield, respectively, none of the adducts (23) and (24) being detected. This was not simply a reflection of the instability of adduct (23) in acetonitrile at +20°C as a control experiment was conducted which showed that a solution of adduct (23) in acetonitrile-d_3 was unchanged after 48 h

at +23°C. Tables 2.3 and 2.4 show clearly that the formation of adducts (23) and (24) is less favoured in acetonitrile as opposed to dichloromethane. It is envisaged that the more polar solvent acetonitrile more effectively stabilises the trinitromethanide ion by solvation and leads to selective reaction at the α-position of 1,4,5,8-tetramethylnaphthalene radical cation (22), the ring position carrying the higher cationic charge. (See Section 2.5 below.)

2.4.1 Photonitration of 4,5,8-Trimethyl-1-nitromethylnaphthalene (25) with Tetranitromethane in Acetonitrile at +20°C.

Reaction of 4,5,8-trimethyl-1-nitromethylnaphthalene (25) and tetranitromethane in acetonitrile at +20°C, as above, gave after 2 h. a residue which was shown by ^{1}H NMR spectra to be a mixture (*c.* 1 : 1) of 4,5,8-trimethyl-1-nitromethyl-naphthalene (25) and 4,8-dimethyl-1,5-dinitromethylnaphthalene (26) (total 35%), together with considerable amounts (*c.* 65%) of unidentified material, similar to that obtained in the photonitration of 1,4,5,8-tetramethylnaphthalene in acetonitrile at +20°C, above. From this control experiment it was clear that the 1,5-dinitromethyl-4,8-dimethylnaphthalene (26) arises by further photonitration of the 1-nitromethyl-4,5,8-trimethylnaphthalene (25).

2.5 Overview of the Photochemical Nitrations and Discussion Relating to the Mode of Formation of Products

The products formed in the photolysis of the 1,4,5,8-tetramethylnaphthalene (21) / tetranitromethane charge-transfer complex are significantly different from those formed in analogous reactions of naphthalene and 1,4-dimethylnaphthalene. Adducts (23) and (24) are of different regiochemistry with the trinitromethyl group placed in the 2-position. No 1,4-nitro/trinitromethyl

adducts are detectable, but instead labile 1,4-nitrito/trinitromethyl adducts (27) and (28) have been identified.

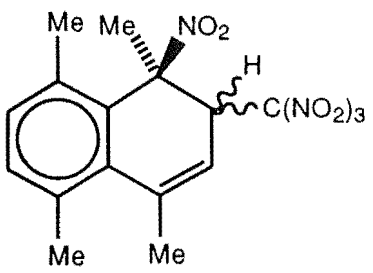

(23) and(24)

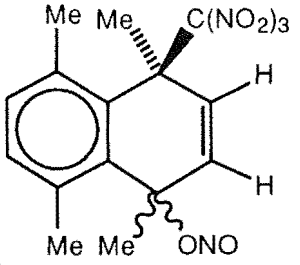

(27) and (28)

The initial step is envisaged as being attack of trinitromethanide on the radical cation of 1,4,5,8-tetramethylnaphthalene (22). Evidence for this was established in Chapter 1 where Eberson *et al.* [56] found that the trinitromethanide ion combines more rapidly than nitrogen dioxide with the aromatic radical cation. We must now, however, explain why trinitromethanide attack occurs at both the 1- and 2-positions of the 1,4,5,8-tetramethylnaphthalene radical cation (22). .

The 1-position is highly favoured by the atomic charge distribution of the radical cation, as is found for other naphthalene derivatives. See Figure 2.4.

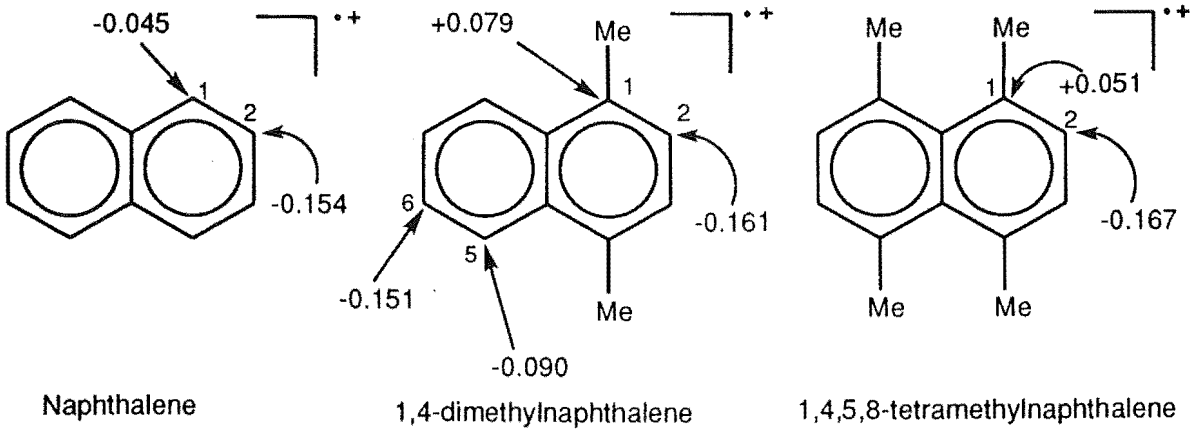

Naphthalene 1,4-dimethylnaphthalene 1,4,5,8-tetramethylnaphthalene

FIGURE 2.4 Atomic charges on ring C atoms for the radical cations.

However, the formation of adducts (23) and (24) indicates that attack at C2 is a significant pathway and we suggest that the steric effects due to the methyl substitution in the radical cation (22) are the origin of this apparent anomaly. The structure of 1,4,5,8-tetramethylnaphthalene (21) has been determined by X-ray crystallography[66] and the molecule was shown to be non-planar in the solid state because of the strong *peri* methyl/methyl interactions.

The first step involving reaction of trinitromethanide and the radical cation (21) can lead to either of the two possible intermediates (29) and (30). From radical (30) reaction with $^{\bullet}NO_2$ will give adduct (23) and its epimer (24). Reaction of radical (29) with nitrogen dioxide at C4 with C-O bond formation will give the observed epimeric 1,4-nitrito/trinitromethyl adducts (26) and (27).

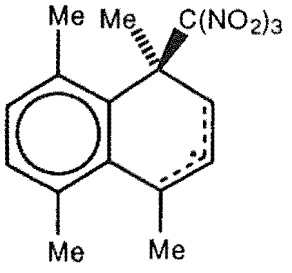

(29)

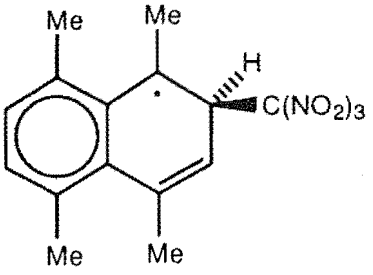

(30)

The 1,4,5,8-tetramethylnaphthalene reaction can best be viewed as being qualitatively analogous to that of the 1,4-dimethylnaphthalene, yet with significant differences. The following Scheme 2.2 summarises the likely pathways to formation of adducts and product (25) after coupling of the radical cation (22) with the trinitromethanide ion.

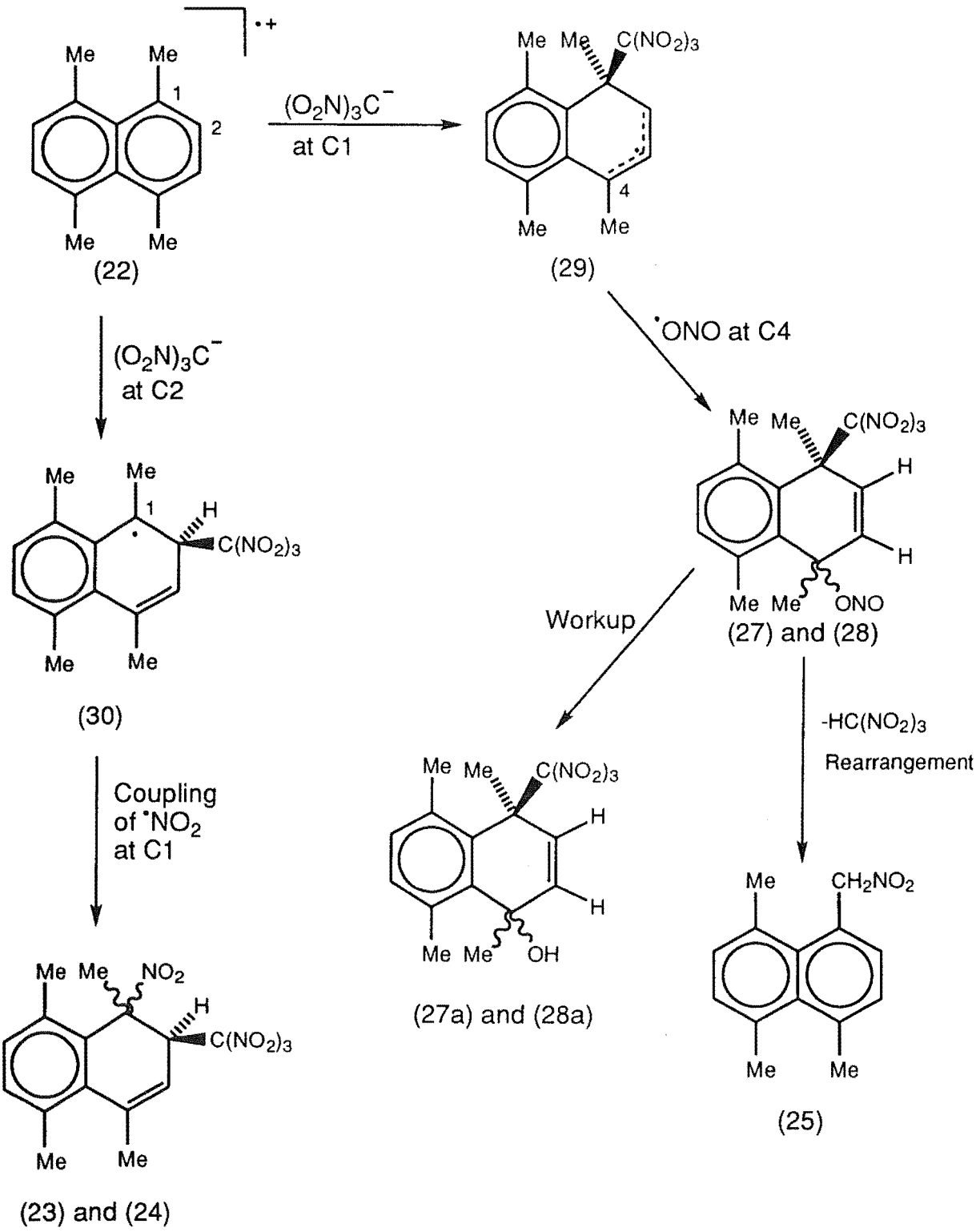
Me
Me
1
2
Me
Me
(22)
$(O_2N)_3C^-$
at C1
Me Me $C(NO_2)_3$
4
Me
Me
(29)
$(O_2N)_3C^-$
at C2
Me
Me
1
H
$C(NO_2)_3$
Me
Me
(30)
•ONO at C4
Me Me $C(NO_2)_3$
H
H
Me Me ONO
(27) and (28)
Workup
Coupling
of $•NO_2$
at C1
Me Me NO_2
H
$C(NO_2)_3$
Me
Me
(23) and (24)
Me Me $C(NO_2)_3$
H
H
Me Me OH
(27a) and (28a)
$-HC(NO_2)_3$
Rearrangement
Me
CH_2NO_2
Me
Me
(25)

SCHEME 2.2

This new addition mode leading to formation of the relatively stable 1-nitro-2-trinitromethyl adducts (23) and (24) with different regiochemistry from all previous adducts is presumably dictated by the steric properties of the 1,4,5,8-tetramethylnaphthalene radical cation. The ratio of C1 to C2 attack by the trinitromethanide ion on the radical cation varied with the solvent used. In dichloromethane the extent of attack at C2 was higher than that found in acetonitrile. This suggests that the more polar solvent, acetonitrile, is stabilising the trinitromethanide ion thus rendering it more selective than the less polar medium (dichloromethane).

No 1,4-nitro/trinitromethyl adducts were identified as products from the reactions of 1,4,5,8-tetramethylnaphthalene and only the very labile 1,4-nitrito/trinitromethyl adducts were observed. Although the intermediacy of 1,4-nitro/trinitromethyl adducts in the formation of the side-chain nitro compound (25) can not be excluded, it is clear that this nitro compound (25) is formed by further reaction of the labile 1,4-nitrito/trinitromethyl adducts (27) and (28). Elimination of nitroform from adducts (27) and (28) would give the diene (31) which on C-O bond homolysis would yield the benzylic radical and NO_2 within a solvent cage (Scheme 2.3). Recombination of this radical pair (32) would give the side chain nitro compound (25).

However, it must be remembered that adduct decomposition would not be the only pathway available to formation of product (25). It has been shown that even in the more reactive systems such as naphthalene, nitrogen dioxide leaks from the triad and builds up to significant concentrations during photolysis.[67]

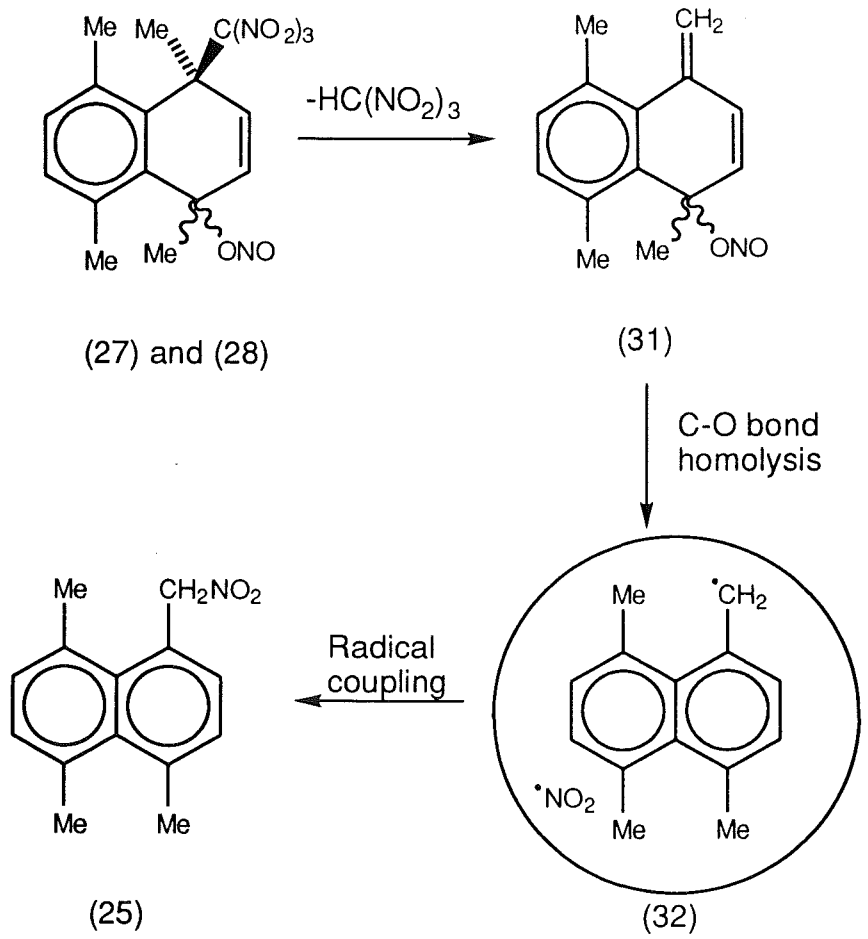

SCHEME 2.3

This suggests that simple nitration of 1,4,5,8-tetramethylnaphthalene by NO_2, which is known[50,52] to give solely (25) under conditions resembling those prevailing during photolysis in dichloromethane at room temperature, may account for part of the observed yield of (25) in runs at +20°C but is likely to be insignificant at -20°C and -50°C.

The bis-nitromethyl compound (26) was shown to arise from further photonitration of the mono-nitromethyl compound (25). Given the established structure of the bis-nitromethyl compound (26) and the mode of formation of side-chain nitro compounds, it seems certain that much, if not all, of compound (26) is formed as shown in Scheme 2.4. The transformation of adducts (33) follows a sequence of reaction steps analogous to those in the formation of

side-chain nitro compound (25) (Scheme 2.3), i.e. loss of nitroform to give the nitrito nitro diene (34) which on C-O bond homolysis gives the radical pair (35), the recombination of which gives the bis-nitromethyl product (26) as illustrated in Scheme 2.4.

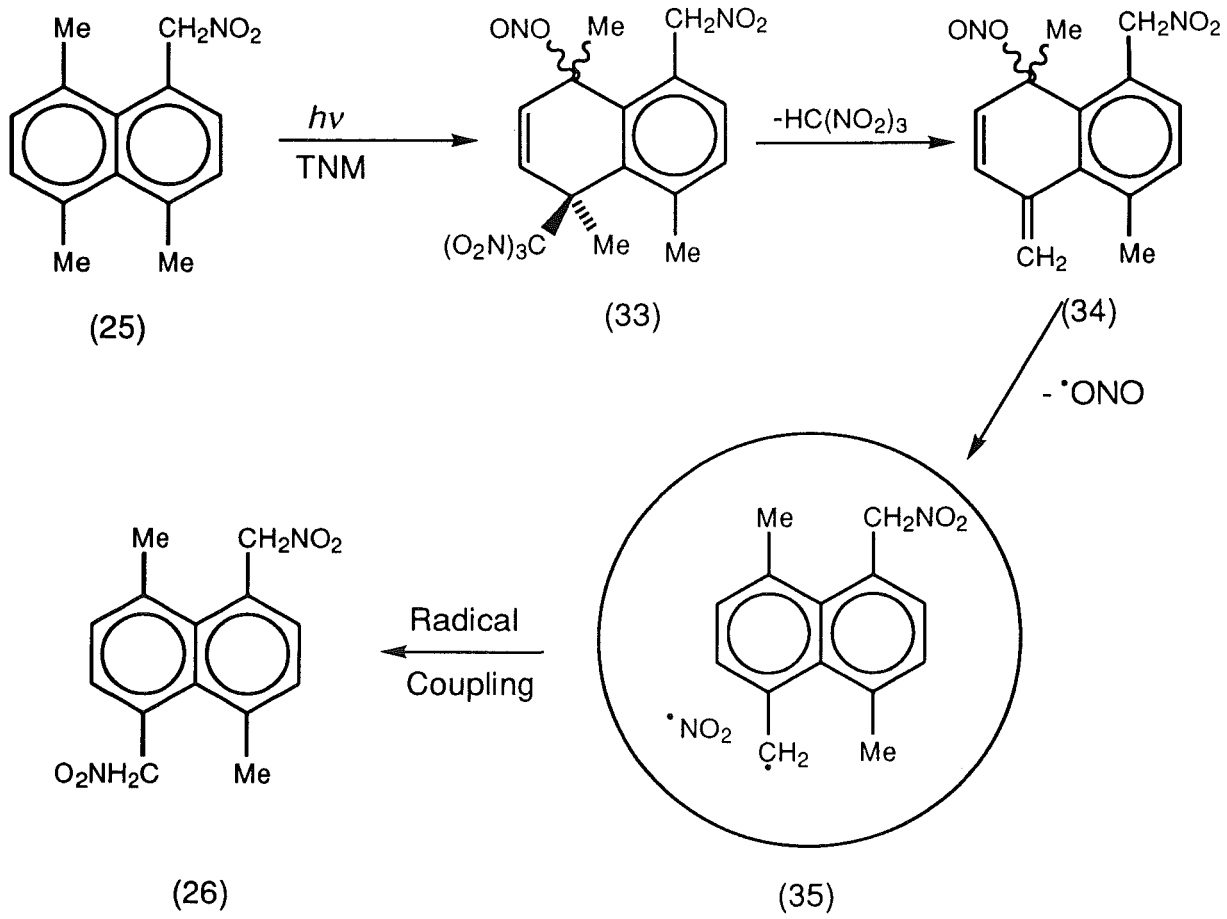

SCHEME 2.4

CHAPTER THREE

PHOTONITRATION OF 1,8-DIMETHYLNAPHTHALENE

3.1 INTRODUCTION

In the photonitration of naphthalene[55] and 1,4-dimethylnaphthalene[60] with TNM the initial bond formation between $ArH^{\bullet+}$ and trinitromethanide ion occurs at the α-position of the naphthalene nucleus, and *ipso* to a methyl group in 1,4-dimethylnaphthalene. In these cases the attack of trinitromethanide ion occurs at the favourable ring position in the corresponding aromatic radical cation, as judged by the calculated (AM1)[68] atomic charges on the respective ring carbon atoms (Figure. 3.1).

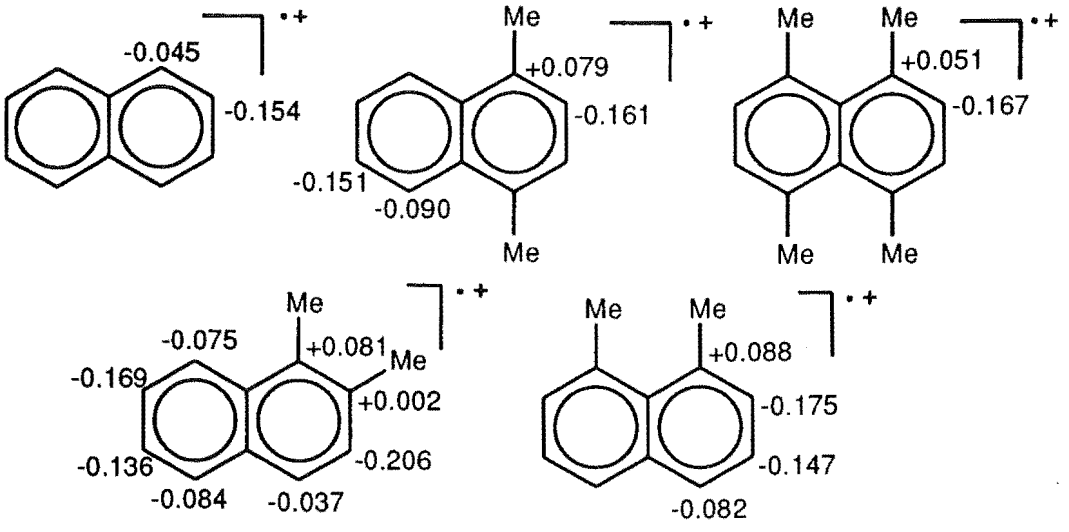

FIGURE 3.1 Calculated (AM1) atomic charges on the respective ring carbon atoms of some aromatic radical cations.

In the photonitration of 1,4,5,8-tetramethylnaphthalene, the bond formation of the trinitromethanide ion with the corresponding aromatic radical cation occurs at the favourable ring position (C1) as calculated and also at the less favourable ring position (C2). This deviation from expectation based on

calculated atomic charges has been rationalized in terms of steric hindrance to attack of the bulky trinitromethanide ion on the (C1) ring position. (Chapter 2).

Reaction of the trinitromethanide ion with the 1,2-dimethylnaphthalene radical cation yields nitro/trinitromethyl and hydroxy/trinitromethyl adducts (total 80%; at +20°C in dichloromethane) arising from trinitromethanide ion attack not at the carbon centres, C1 and C2, apparently favoured by their calculated atomic charges (Figure. 1) but instead at C4.[69] This deviation from expectation based on calculated atomic charges has been rationalized in terms of trinitromethanide ion attack at C1 or C2 of the 1,2-dimethylnaphthalene radical cation being blocked sterically by the presence of a methyl group at the respective β-positions (C2 or C1), leaving attack of trinitromethanide ion at the unhindered C4 as the only viable alternative.[69]

Having established that attack of trinitromethanide ion on the radical cation of 1,4-dimethylnaphthalene is not prohibited by the presence of an *ipso*-methyl substituent[60] and in the light of information gained from the reaction of the radical cations of 1,4,5,8-tetramethylnaphthalene and 1,2-dimethylnaphthalene with trinitromethanide ion, we examined the photochemical reaction of 1,8-dimethylnaphthalene (36) with TNM in the expectation that steric crowding due to the *peri*-methyl substituent might suppress trinitromethanide ion attack at C1(C8) of the 1,8-dimethylnaphthalene radical cation (37) despite this position being significantly favoured by the atomic charge density. (Figure 3.1)

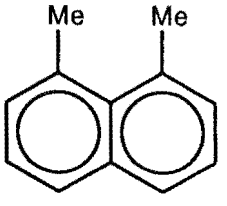

(36)

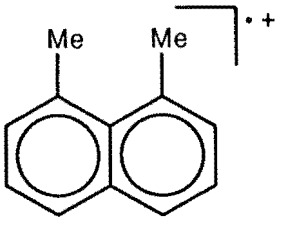

(37)

3.2 THE PHOTOLYSIS OF 1,8-DIMETHYLNAPHTHALENE (36)

General Procedure for the Photonitration of 1,8-Dimethylnaphthalene (36) with Tetranitromethane.

A solution of 1,8-dimethylnaphthalene (500 mg, equal to a 0.4 mol l^{-1} solution) and tetranitromethane (0.8 mol l^{-1}) in dichloromethane or acetonitrile (8 ml) was irradiated at +20 or -20°C with filtered light (cut-off <435 nm). Aliquots were withdrawn from the reaction mixture at appropriate time intervals, the volatile material removed under reduced pressure at 0°C, and the product composition determined by ^1H NMR spectral analysis. (For complete experimental details see Chapter 5.)

3.3 PHOTOCHEMISTRY IN DICHLOROMETHANE OF 1,8-DIMETHYLNAPHTHALENE

The photolysis of a solution of 1,8-dimethylnaphthalene (0.4 mol l^{-1}) and TNM (0.8 mol l^{-1}) in dichloromethane at -20 and +20°C was carried out with filtered light (cut-off at 435 nm) until the red colour of the CT band had been bleached. Isolation of the reaction mixtures at ≤ 0°C gave a mixture of adducts (38)-(43), 1,8-dimethyl-4-nitronaphthalene (44), and an unidentified mixture of other aromatic compounds. The adducts (38) - (43) were partially separated in small quantities by h.p.l.c. on a cyanopropyl column using hexane/dichloromethane mixtures as the eluting solvent.

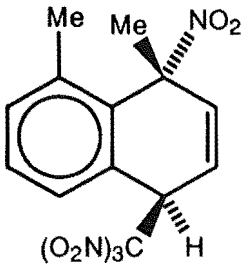

(38)

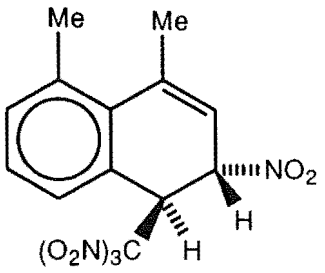

(39)

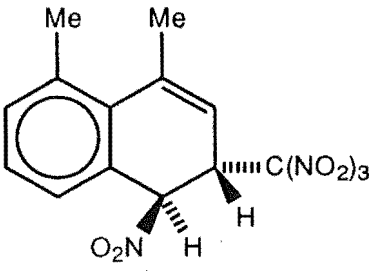

(40)

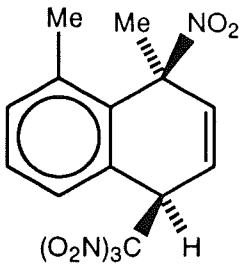

(41)

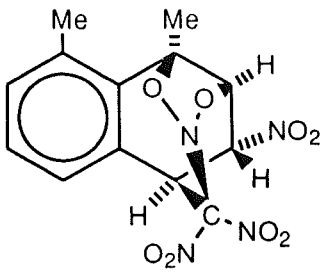

(42)

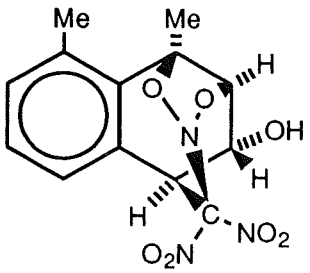

(43)

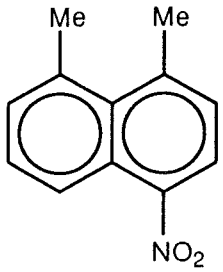

(44)

The structure of adduct (38) was determined by single crystal X-ray analysis. A perspective drawing of 1,8-dimethyl-*r*-1-nitro-*t*-4-trinitromethyl-1,4-dihydronaphthalene (38), $C_{13}H_{12}N_4O_8$, m.p. 119-121°C, is presented in Figure. 3.2, and the corresponding atomic coordinates are given in Table 5.2. In the solid state the alicyclic ring exists in a somewhat flattened boat conformation with the 1-methyl and 4-trinitromethyl groups in the flagpole orientation [torsional angles: C(2)-C(3)-C(4)-C(9) -13.3(4)°; C(3)-C(2)-C(1)-C(10) 15.3(5)°; C(8)-C(10)-C(1)-C(11) -70.7(4)°; C(8)-C(10)-C(1)-N(11) 50.4(4)°; C(5)-C(9)-C(4)-C(12) 73.5°]. The 8-methyl group [C(13)] is somewhat displaced from the plane of the aromatic ring, presumably as a result of differences in the steric interactions with the methyl and nitro groups at C(1) [torsional angles: C(6)-C(7)-C(8)-C(13) -177.1(3)°; C(9)-C(10)-C(8)-C(13) 177.9(3)°].

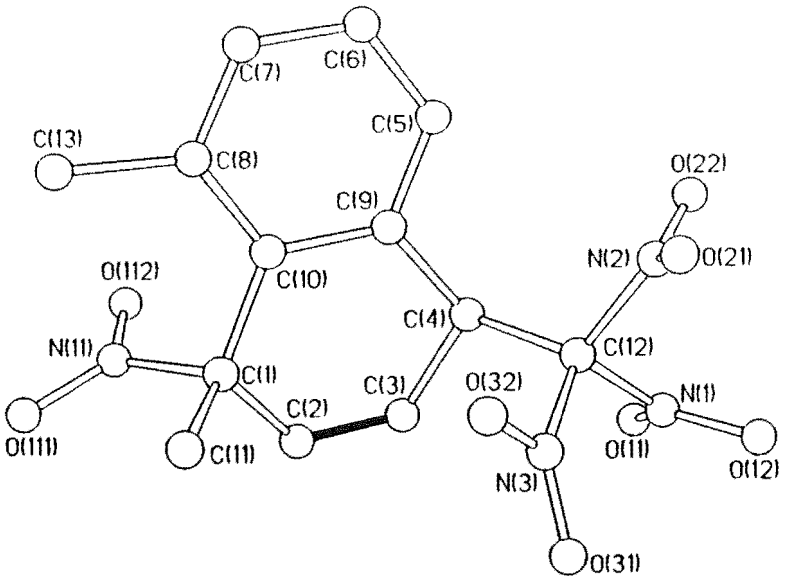

FIGURE 3.2

A perspective diagram of 1,8-dimethyl-*r*-1-nitro-*t*-4-trinitromethyl-1,4-dihydronaphthalene (38).

The spectroscopic data for adduct (38) were in accord with the established structure. In particular, the **C**H-C$(NO_2)_3$ resonance appeared at δ 45.5, while the **C**Me-NO_2 resonance appeared at δ 88.2, these assignments being confirmed by long range reverse detected heteronuclear correlation spectra (HMBC). The ^{1}H NMR coupling constants for adduct (38) were as expected for the established structure and consistent with the existence of the molecule in the same conformation in the solid state and in solution. See Figure 3.3.

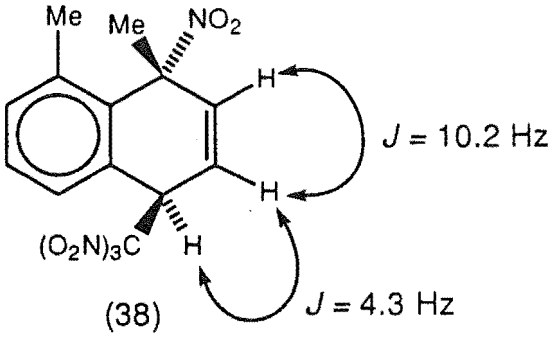

FIGURE 3.3 Illustrating the coupling constants associated with adduct (38).

The second adduct (39) eluted was obtained only in admixture with adduct (38) above. This adduct (39), identified as 1,8-dimethyl-*r*-3-nitro-*t*-4-trinitromethyl-

3,4-dihydronaphthalene, was unstable in solution and underwent thermal cycloaddition of a nitro group of the trinitromethyl group with the C(1) / C(2) alkene function to give the nitro cycloadduct (42), the structure of which is determined below by single crystal X-ray analysis. The structure of adduct (39) is therefore assigned (i) on the basis of its ^{1}H NMR spectrum, determined by subtraction of the spectrum of adduct (38) from the spectrum of the mixture of the two adducts, (38) and (39), and (ii) the cycloaddition reaction to give the nitro cycloadduct (42) (see below).

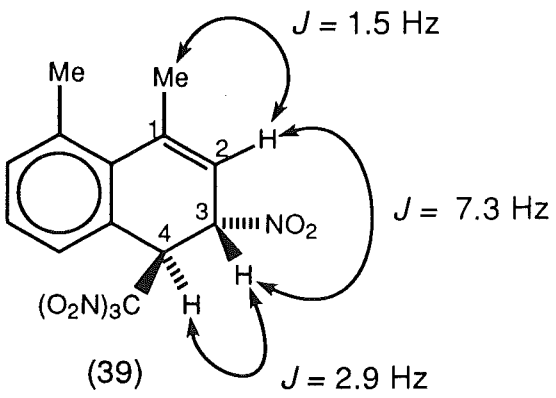

FIGURE 3.4 Illustrating the coupling constants associated with adduct (39).

Characteristic ^{1}H NMR resonances were observed for: C**H**(NO_2) as a broad doublet at δ 5.64; C**H**[$C(NO_2)_3$] appeared as a doublet at δ 5.61 and the olefinic C**H**= appeared at δ 5.80 ppm as a doublet of quartets. The coupling constants for adduct (39) as illustrated in Figure 3.4 can be analysed using the Karplus equation to gain information about the likely conformation of the trinitromethyl and nitro groups. The coupling constant $J_{H3/H4}$ = 2.9 Hz suggests that the dihedral angle between H3 and H4 is ≈ 65°. This implies that the trinitromethyl group must be axial to the plane of the ring and similarly the nitro group must also be in the axial orientation. If the trinitromethyl and nitro group were both in the equatorial conformation the expected coupling constant would be much larger as the angle between H3/H4 would be ≈180° and by the Karplus equation this would correspond to J = 8 Hz. The coupling constant $J_{H3/H2}$ =

7.3 Hz indicates that the corresponding dihedral angle between H2 and H3 must be smaller than between H3/H4 and a value of ≈ 20° by the Karplus equation would correspond to the observed coupling constant.

The isomeric adduct, 1,8-dimethyl-*t*-4-nitro-*r*-3-trinitromethyl-3,4-dihydro-naphthalene (40), was identified from its spectroscopic data, the compound yielding only microcrystalline material unsuitable for single crystal X-ray analysis. The assignments of the ^{1}H and ^{13}C NMR. spectra were confirmed by long range reverse detected heteronuclear correlation spectra (HMBC), and necessitated the location of the trinitromethyl function at C3 and *trans* to the nitro function at C4. Thus, the **C**H-C$(NO_2)_3$ structure gave a ^{13}C NMR. resonance at 40.3 which is significantly different from resonances observed in situations where the trinitromethyl group is at C1 or C4. Typically these resonances would occur at δ 45. The ^{1}H NMR assignments were further confirmed by nuclear Overhauser enhancement experiments. In particular, irradiation at δ 7.19 (H5) gave an enhancement at δ 5.77 (H4), irradiation at δ 2.30 (1-Me) resulted in an enhancement of the signal at δ 5.64 (H2), and irradiation at δ 5.77 gave an enhancement of the signal at δ 5.30 (H3) as illustrated in Figure 3.5.

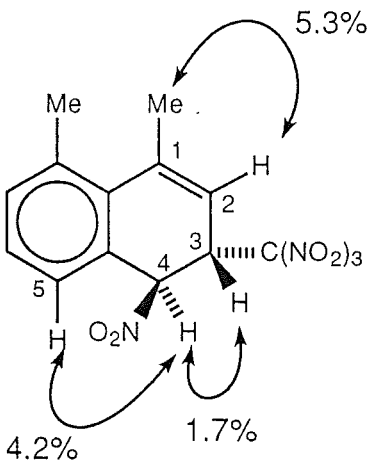

(40)

FIGURE 3.5 Indicating the enhancements (%) from nOe experiments.

In the ^1H NMR spectrum the C**H**-$C(NO_2)_3$ resonance was observed at δ 5.30, while the **CH**-NO_2 structure gave resonances at δ 83.4 and at δ 5.77 in the ^{13}C and ^1H NMR spectra respectively. Unlike the thermally labile 3-nitro-4-trinitromethyl adduct (39), the 4-nitro-3-trinitromethyl adduct (40) was relatively stable and did not undergo a cycloaddition reaction, as expected given the relative positions of the trinitromethyl and alkene functions in the latter compound. The stereochemistry of adduct (40) was assigned as the *trans*-nitro/trinitromethyl adduct from a comparison of the coupling constants of adduct (39) as illustrated in Figure 3.6.

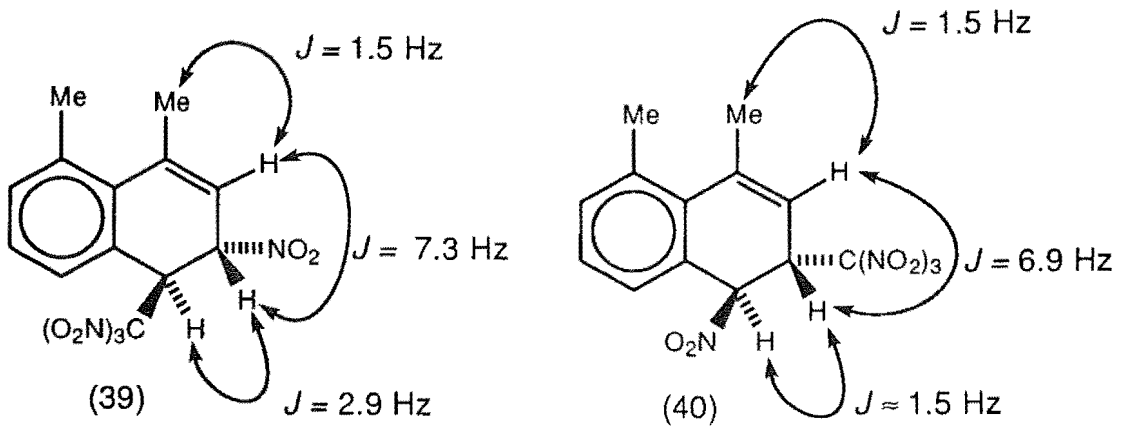

FIGURE 3.6 Comparison of the coupling constants of adducts (39) and (40).

The similarity in the coupling constants of adducts (39) and (40) indicate that the dihedral angles between the protons H2/H3 and H3/H4 are very similar and by the Karplus equation relate to similar coupling constants. This implies that the conformation of the trinitromethyl and nitro substituents must both be in the axial orientations. Unambiguous assignment of the trintromethyl group to the C3 position was possible with HMBC data.

The fourth adduct eluted from the h.p.l.c. column was identified as 1,8-dimethyl-*r*-1-nitro-*c*-4-trinitromethyl-1,4-dihydronaphthalene (41), epimeric with the *r*-nitro-*t*-4-trinitromethyl adduct (38) the structure of which has been

determined above by single crystal X-ray analysis. The structure of adduct (41) was determined from a consideration of the ^{1}H and ^{13}C NMR data, the assignments of which were confirmed by long range reverse detected heteronuclear correlation spectra (HMBC), and comparison with similar data for its epimer (38). The two sets of spectroscopic data for adducts (38) and (41) were closely similar and consistent with their assignment as epimers. Some of the characteristic data is compared in Figure 3.7.

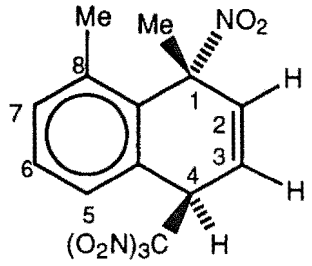

(38)

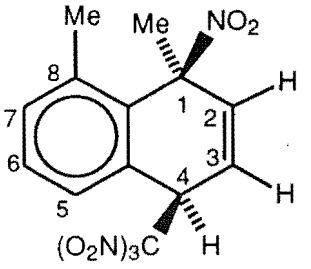

(41)

C1	88.2	C1	86.8
C2	125.3	C2	125.6
C3	120.7	C3	120.4
C4	45.5	C4	44.5
C5	129.9	C5	129.6
Me-1	2.13	Me-1	1.97
H2	6.33	H2	6.37
H3	6.45	H3	6.37
H4	5.51	H4	5.46

FIGURE 3.7 Comparison of the characteristic ^{13}C and ^{1}H NMR resonances for adducts (38) and (41) in ppm.

The structure of the fifth adduct eluted from the h.p.l.c. column was determined by single crystal X-ray analysis. A perspective drawing of the nitro cycloadduct (42), $C_{13}H_{12}N_4O_8$, m.p. 180°C (sublimed), is presented in Figure. 3.8, and the corresponding atomic coordinates in Table 5.3. In the formation of the

heterocyclic cage structure it is clear that the nitrogen atom of the planar nitro group involved in the cycloaddition reaction assumes a trigonal geometry in the cycloadduct (42). This will account for some of the changes that are observed in the bond lengths of the nitrocycloadduct which are illustrated below.

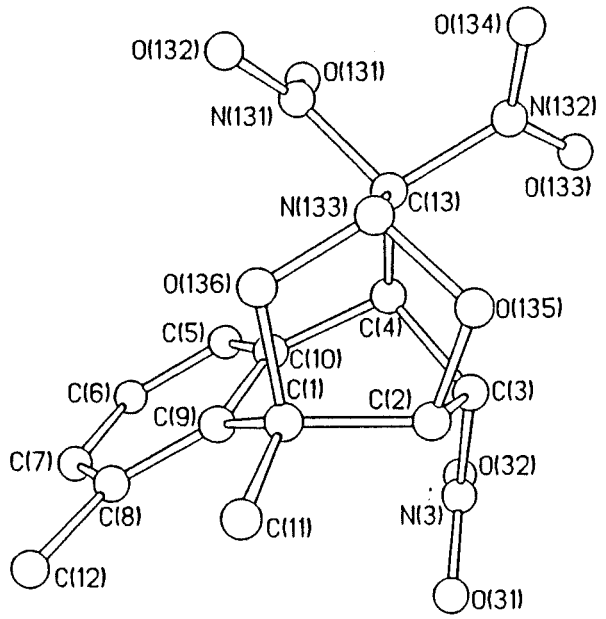

FIGURE 3.8

A perspective diagram of the nitro cycloadduct (42)

Some of the bond lengths are of interest and are shown in Table 3.1. In particular we note the substantial lengthening of the N(133)-O(136) and N(133)-O(135) bonds (which is the nitro group involved in the cycloaddition) increasing from the typical nitro group N-O length of 1.203(3) to ≈1.406(6). This indicates that these N-O bonds have lost their partial double bond character and have become sp^3 in character. Similarly the C(13)-N(133) bond length is shortened in comparison with the normal C-NO_2 bond length.(eg. C(13)-N(133) 1.468(3) whereas the typical C-NO_2 bond length can be compared to C(13)-N(132) 1.535(4) and C(13)-N(131) 1.510(4). The shortening of this bond suggests that the now tetragonal N(133) with its lone pair of electrons is moving towards the carbon C(13) in a bid to stabilise the electron withdrawing effect of the two nitro groups on C(13) involving N(131)

and N(132). The bond length from O(135)-C(2) of 1.442(3) is typical for a C-O bond.

TABLE 3.1 Selected Bond Lengths of the nitro cycloadduct (42).

BONDS	BOND LENGTHS (Å)	BONDS	BOND LENGTHS (Å)
O(131)-N(131)	1.212(3)	C(1)-C(2)	1.545(4)
O(132)-N(131)	1.203(3)	C(1)-O(136)	1.483(3)
O(133)-N(132)	1.204(3)	C(2)-O(135)	1.442(3)
O(134)-N(132)	1.211(3)	C(13)-C(4)	1.517(4)
O(135)-N(133)	1.409(3)	C(1)-C(11)	1.502(4)
O(136)-N(133)	1.403(3)	C(2)-C(3)	1.496(4)
N(131)-C(13)	1.510(4)	C(3)-C(4)	1.522(4)
N(132)-C(13)	1.535(4)	C(3)-N(3)	1.488(4)
N(133)-C(13)	1.468(3)	C(4)-C(13)	1.517(4)

Confirmation of the *anti*-stereochemistry of the trinitromethyl and nitro group also provided confirmation of the stereochemistry for adduct (39) which was the precursor to the cycloadduct. Indirectly the stereochemistry of adduct (40) could also be confirmed from the X-ray analysis of the cycloadduct (42) because of the close similarity between their coupling constants of the cycloadduct precursor (39) and adduct (40).

The spectroscopic data for the nitro cycloadduct (42) were consistent with the established structure. Some of the ^{1}H NMR resonances are summarised in Table 3.2. Notable among the spectroscopic data are the observed $J_{H,H}$ coupling constants, including W-coupling between H2 and H4. (See Table 3.2) The coupling constants observed are in agreement with the dihedral angles obtained from the measured dihedral angles from the X-ray analysis.

TABLE 3.2 ^{1}H NMR data associated with the nitro cycloadduct (42).

^{1}H NMR Assignment	Chemical Shift (δ)	Coupling Constants (Hz)
H2	5.46 dd	$J_{H2,H4}$ 2.9; $J_{H2,H3}$ 2.0
H3	5.66 dd	$J_{H3,H4}$ 3.9; $J_{H3,H2}$ 2.0
H4	5.20 dd	$J_{H4,H3}$ 3.9; $J_{H4,H2}$ 2.9

Characteristic ^{13}C NMR resonances were observed as illustrated in Table 3,3. These resonances agreed with the structure obtained for the cycloadduct (42) from single crystal X-ray analysis.

TABLE 3.3 ^{13}C NMR data associated with the nitro cycloadduct (42).

^{13}C NMR Assignment	Chemical Shift (δ)
C1	78.7
C2	83.2
C3	90.1
C4	45.9
C5	129.8

The above assignments were confirmed by long range reverse detected heteronuclear correlation spectra (HMBC).

Finally, a small quantity of an oil was eluted which could not be induced to crystallize, but which has been identified as the hydroxy cycloadduct (43) from a consideration of its spectroscopic data. An i.r absorption was observed at 3544 cm^{-1} indicating the presence of an -OH function. Nuclear Overhauser experiments confirmed the assignment of the ^{1}H NMR resonances to H2, H3

and H4, the various coupling constants for which were similar to those for the related nitro cycloadduct (42). See Table 3.4.

TABLE 3.4 ^{1}H NMR data associated with the hydroxy cycloadduct (43).

^{1}H NMR Assignment	Chemical Shift (δ)	Coupling Constants (Hz)
H2	4.65 dd	$J_{H2,H4}$ 2.0; $J_{H2,H3}$ 2.0
H3	4.86 dd	$J_{H3,H4}$ 4.0; $J_{H3,H2}$ 2.0
H4	4.73 dd	$J_{H4,H3}$ 4.0; $J_{H4,H2}$ 2.0

The ^{13}C NMR resonances for the two cycloadducts (42) and (43) were closely similar, except for the expected differences arising from the presence of the nitro or hydroxy functions in the two compounds. (See Figure 3.9). The spectroscopic assignments were again confirmed by HMBC spectra.

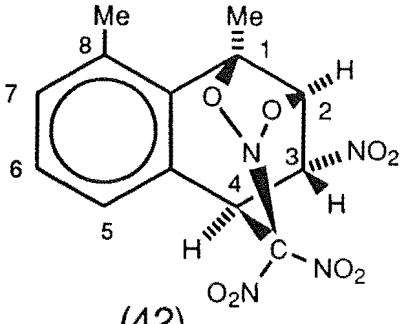

(42)

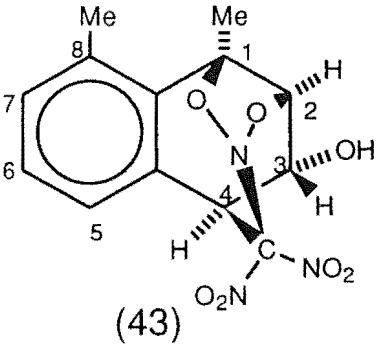

(43)

C1	78.7	C1	88.5
C2	83.2	C2	87.3
C3	90.1	C3	66.4
C4	45.9	C4	49.6
C5	129.8	C5	129.5

FIGURE 3.9 Comparison of the characteristic ^{13}C NMR resonances for adducts (42) and (43) in ppm.

A pure sample of 1,8-dimethyl-4-nitronaphthalene (44) was isolated by chromatography on a silica gel Chromatotron plate and the structure was confirmed by comparison of its melting point and NMR data with available literature values.[70] The other unidentified aromatic compounds could not be separated by chromatography.

When the reaction at +20°C was monitored with time (Table 3.5), one further adduct (45) could be detected among the reaction products, giving a ^{1}H NMR spectrum ($CDCl_3$) δ 4.85, d, $J_{H4,H3}$ 2.4 Hz, H4; 5.07, dd, $J_{H3,H2}$ 7.8 Hz, $J_{H3,H4}$ 2.4 Hz, H3; 5.68, d, $J_{H2,H3}$ 7.8 Hz, H2; the remainder of the spectrum for this compound was obscured by signals from other components of the mixture. At no time was this adduct detected among the materials eluted from the h.p.l.c. column, above. This additional adduct (45) is seen as the precursor of the hydroxy cycloadduct (43). The assignment was made from a comparison of the spectroscopic data for the nitro cycloadduct (42) and its precursor (39).

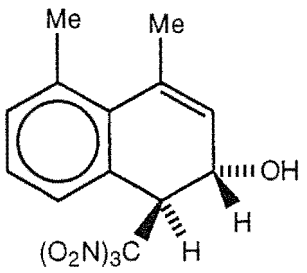

(45)

When the reaction at -20°C was monitored with time, the extent of conversion of 1,8-dimethylnaphthalene into adducts was much reduced (Table 3.5), and 1,8-dimethyl-4-nitronaphthalene became a major product under these reaction conditions. These results indicate that the cycloaddition in the 3-nitro-4-trinitromethyl adduct (44) does not occur significantly in the duration of the reaction (2 h), in contrast to the similar reaction at +20°C. (Table 3.5)

TABLE 3.5 Overview of yields of products from the photolysis of 1,8-dimethylnaphthalene (0.4 mol l^{-1}) and tetranitromethane (0.8 mol l^{-1}) in dichloromethane

		Yield (%)								
t / h	Conversion (%)	(38)	(39)	(40)	(41)	(42)	(43)	(45)	Total Adducts	(44)
At +20°C										
0.5	88	18.2	23.8	trace	6.7	3.1	2[a]	2[a]	55.8	14.4
2	100	25.3	19.7	6.6	4.0	15.0	1[a]	1[a]	72.9	trace
At -20°C										
1	52	7.7	6.5	5.4	13.1	0	0	0	32.7	34.6
2	92	10.2	5.3	7.2	10.2	0	0	0	32.9	31.0

[a] Integrals unreliable because of overlapping signals.

This observation is consistent with the separate demonstration, below, that this cycloaddition reaction is *thermal* and not *photochemical* in character. Hydroxy adducts (43) and (45) were not detected in the ^1H NMR spectra of the product mixtures from reaction at -20°C. Finally, it became clear that in photolyses at +20°C (but more slowly, if at all at -20°C) 1,8-dimethyl-4-nitronaphthalene reacted further to give a mixture of unidentified aromatic compounds which could not be separated by chromatography.

Thermal Cycloaddition of 1,8-Dimethyl-r-3-nitro-t-4-trinitromethyl-3,4-dihydronaphthalene (39) *in (D)-chloroform.*

A solution of a mixture of 1,8-dimethyl-*r* -3-nitro- *t*-4-trinitromethyl-3,4-dihydronaphthalene (39) and 1,8-dimethyl-*r*-1-nitro-*t*-4-trinitromethyl-1,4-

dihydronaphthalene (38) in D-chloroform was stored at 22°C in the dark and the ^{1}H NMR spectrum monitored at appropriate time intervals. Under these conditions the 1-nitro-4-trinitromethyl adduct (38) was unchanged during the period of observation but the 3-nitro-4-trinitromethyl adduct (39) was slowly transformed (half-life ~ 12 h.) into the nitro cycloadduct (42). (Scheme 3.1) The material isolated by removal of the (D)-chloroform under reduced pressure was shown (^{1}H NMR) to be a mixture (*c.* 1 : 1) of the 1-nitro-4-trinitromethyl adduct (43) and the nitro cycloadduct (42).

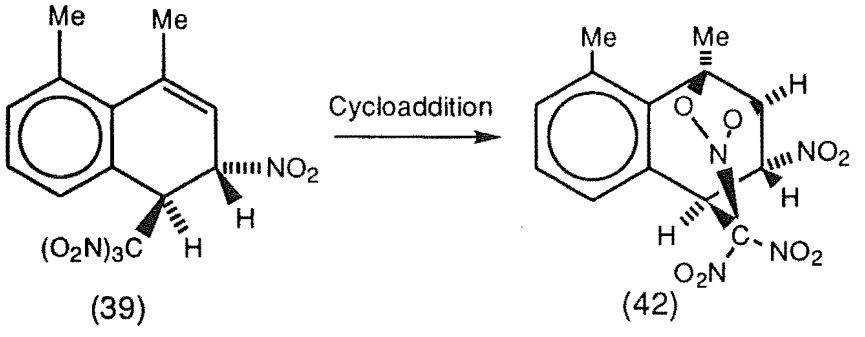

SCHEME 3.1

A graph of the conversion of adduct (39) into the cycloadduct (42) with time is shown in Figure 3.10.

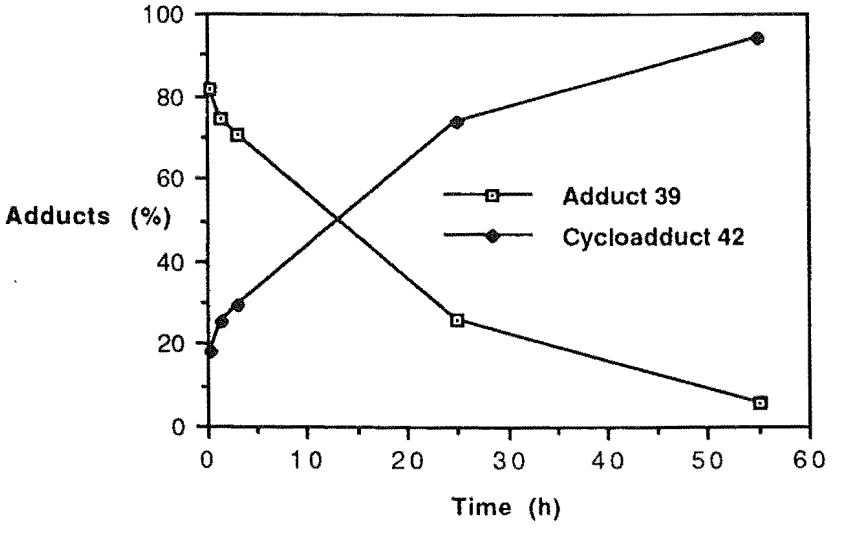

FIGURE 3.10 Kinetics of cycloaddition of adduct (39) to adduct (42) in deutero-chloroform at 22°C.

This observation established that the cycloaddition was *thermal* rather than *photochemical* in character.

3.4 THERMAL CYCLOADDITIONS OF NITRO GROUPS ACROSS ALKENE SYSTEMS

The nitro group according to the Huisgen's classification,[71] belongs to the allylic type of 1,3 dipoles, which are well stabilised by resonance and show little tendency to undergo cycloadditions. However, the intramolecular 1,3-cycloaddition of a nitro group across a double bond has been observed in compounds where the carbon atom bearing the nitro group also has other electron withdrawing substituents directly bound to it. The following cycloadditions observed by Simonyan *et. al.*[72] shown in Scheme 3.2 illustrate the thermal intramolecular reaction.

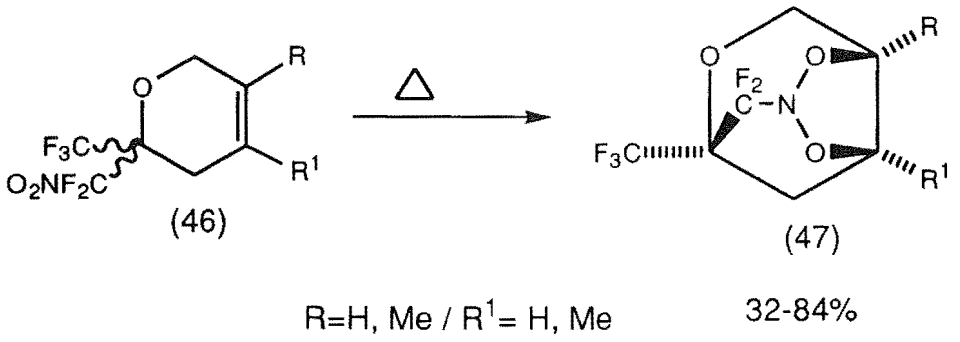

R=H, Me / R^1= H, Me 32-84%

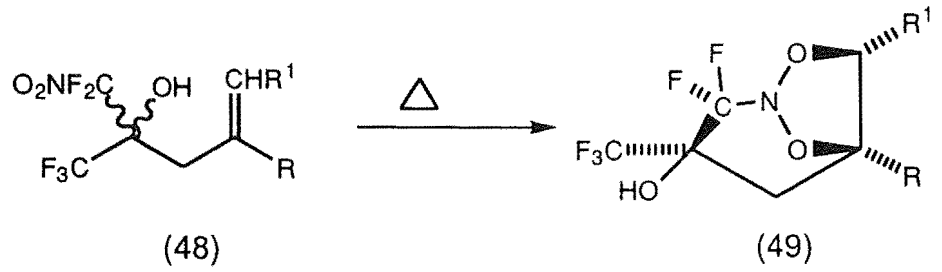

R=H, Me / R^1= H, Me 42-59%

SCHEME 3.2

There is one published example of thermal intermolecular cycloaddition of nitro-compounds to alkenes, which was observed with nitrobenzene derivatives bearing electron-withdrawing groups and the highly reactive (*E,Z*)-cycloocta-1,5-diene (50) to give the product (52) as illustrated in Scheme 3.3.[73]

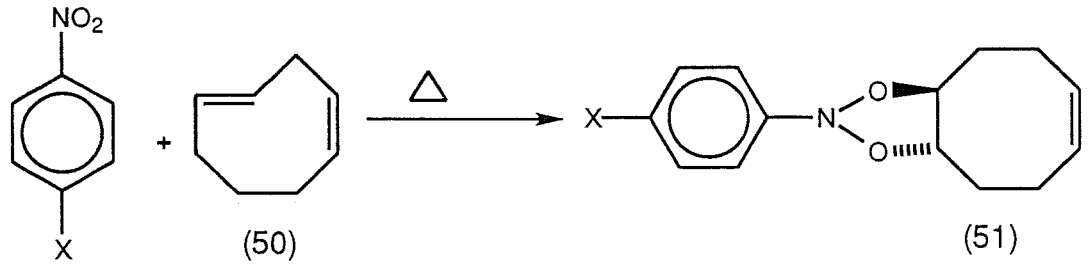

X = CN, NO_2

SCHEME 3.3

Joule *et al.* [74] have recently described the reaction of 2-methoxy-1,6,8-trinitronaphthalene (52) with fuming nitric acid to give the tricyclic 1,3,2-dioxazolidine (53) after single crystal X-ray analysis as illustrated in Scheme 3.4.

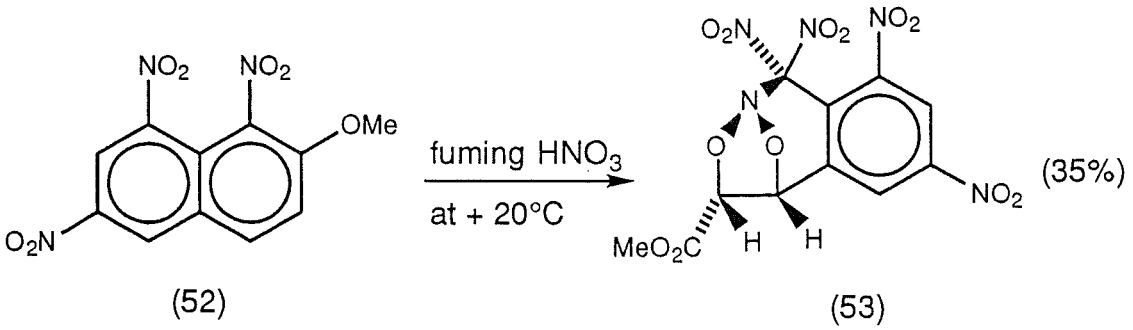

SCHEME 3.4

Joule *et al.*[74] concluded that the method of preparation, the disposition of nitrogen and oxygens in the dioxazolidine ring strongly suggested that (53) was formed *via* an intramolecular cycloaddition of one of the nitro groups across an alkene. With respect to the mode of formation of (53) Joule *et al.* [74]

rationalised a fragmentation process of the aromatic ring containing the methoxy group with further nitration and finally the intramolecular cycloaddition.

The cycloaddition adducts (42) and (43) observed as products of the 1,8-dimethylnaphthalene photonitration are formed under analogous conditions to those featured above and as illustrated in Scheme 3.5.

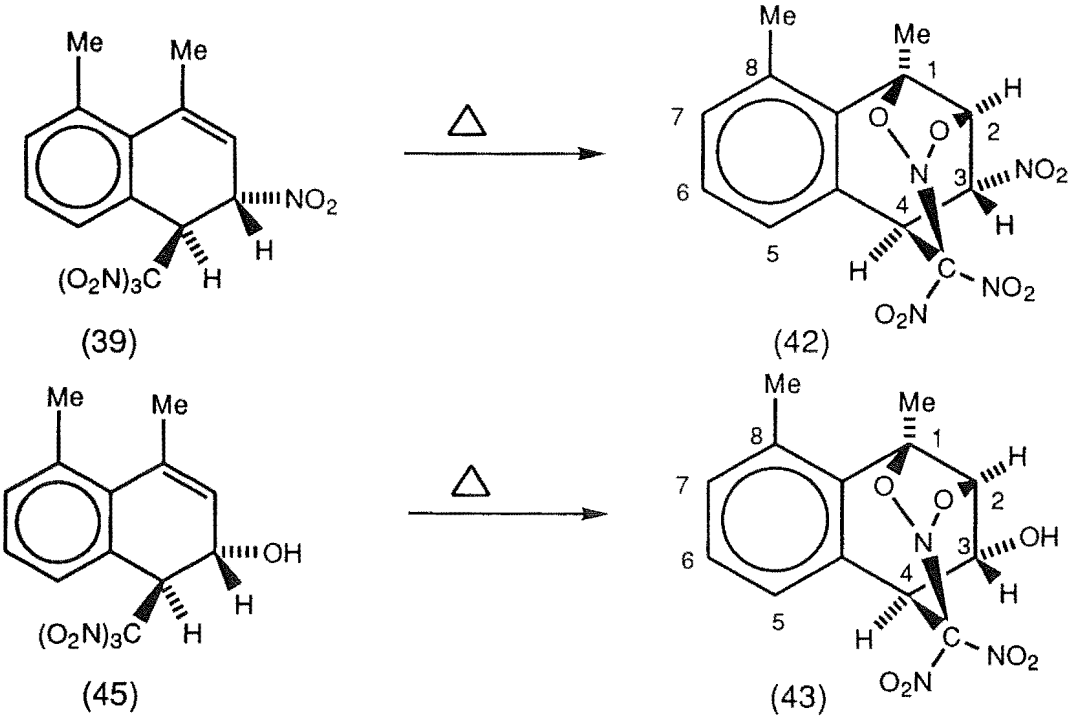

SCHEME 3.5

Butts *et al.* have reported analogous nitro-cycloaddition adducts (54) and (55) arising from the reaction of 1,2-dimethylnaphthalene with TNM.[69]

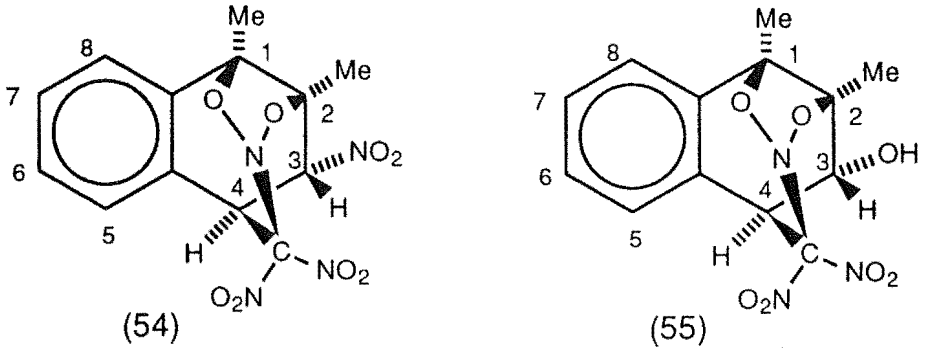

Although the structures of adducts (54) and (55) were determined by single crystal X-ray analysis no direct demonstration of *thermal* cycloaddition was possible for the reactive cycloaddition precursors (56) and (57).[69]

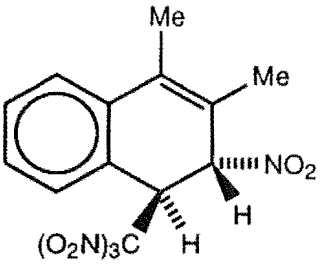

(56)

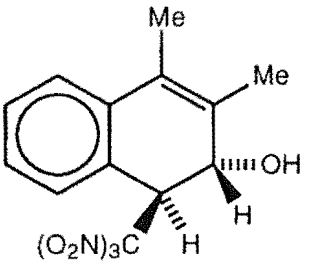

(57)

Even in the 1,8-dimethylnaphthalene system it was not possible to isolate pure samples of cycloaddition precursors (39) and (45). However, it was possible to isolate a mixture of adducts (38) and (39), adduct (38) being stable in solution in (D)-chloroform. The cycloaddition of adduct (39) in (D)-chloroform in the dark at 22°C occurred to give the nitro cycloadduct (42) with a half-life of approximately 12 h., giving the first direct evidence that the cycloaddition of adducts such as (39), (45), (46), and (47) are thermal reactions. (See Figure 3.10.)

3.5 PHOTOCHEMISTRY IN ACETONITRILE

Photolyses of solutions of 1,8-dimethylnaphthalene (0.4 mol l^{-1}) and TNM (0.8 mol l^{-1}) in acetonitrile were carried out at +20 and -20°C as for the reactions in dichloromethane, above. The results of these reactions, monitored with time, are summarized in Table 3.6. The yields of 1,8-dimethyl-4-nitronaphthalene (44) are significantly higher in acetonitrile than in dichloromethane, the yields of adducts being correspondingly reduced. Otherwise the same general pattern of formation of adducts (38) - (43) and (45) is observed in acetonitrile at +20 and -20°C as was found for the corresponding reactions in dichloromethane.

TABLE 3.6 Overview of yields of products from the photolysis of 1,8-dimethylnaphthalene (0.4 mol l^{-1}) and tetranitromethane (0.8 mol l^{-1}) in acetonitrile.

		Yield (%)								
t / h	Conversion (%)	(38)	(39)	(40)	(41)	(42)	(43)	(45)	Total Adducts	(44)
At +20°C										
0.5	77	9.0	3.0	2.2	4.2	1.6	1[a]	trace[a]	21.1	55.9
1	94	14.4	6.2	3.2	4.1	1.1	2[a]	2[a]	32.8	57.9
2	97	16.7	2.8	4.4	1.0	2.3	3[a]	1[a]	30.8	38.4
At -20°C										
1	72	12.2	2.1	2.7	3.6	0	0	0	20.6	56.5
2	94	14.7	3.7	3.3	3.7	0	0	0	25.4	44.5

[a] Integrals unreliable because of overlapping signals.

3.6 OVERVIEW OF THE PHOTONITRATION OF 1,8-DIMETHYLNAPHTHALENE

As noted above the yields of identified adducts are high (up to 73%) for the photolysis of the 1,8-dimethylnaphthalene/TNM charge-transfer complex in dichloromethane at +20°C, but much reduced (25-33%) in dichloromethane at -20°C or in acetonitrile at both temperatures. For the reaction in dichloromethane at +20°C the notable feature of the adducts which have been identified is that the majority (66%) are formed by attack of the trinitromethanide ion at C4 of the 1,8-dimethylnaphthalene radical cation, the

remainder (7%) arising by attack of trinitromethanide ion at C3 on that radical cation. This is illustrated in Figure 3.11.

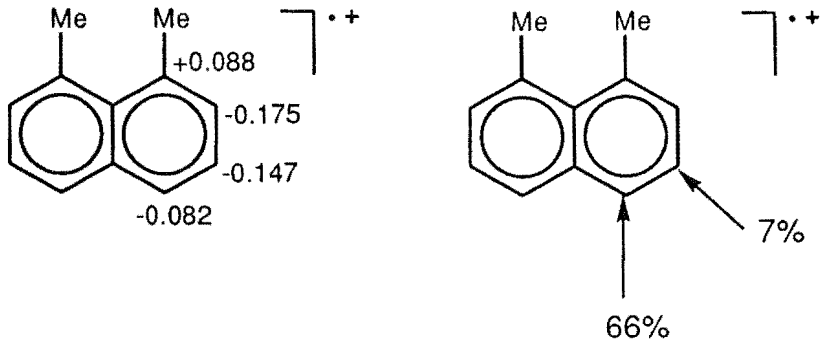

FIGURE 3.11 Comparison of the atomic charge densities on the ring carbons of the radical cation and the adducts (%) identified corresponding to attack of the trinitromethanide ion.

Although attack of trinitromethanide ion on the 1,8-dimethylnaphthalene radical cation might have been expected to occur at C1(C8) on the basis of the relative atomic charges on the naphthalene nucleus, it is clear that steric interactions between the bulky trinitromethanide ion and the 1,8-dimethyl system discourages C1(C8) attack. However, we cannot exclude the possibility that some attack by trinitromethanide ion at C1 may occur giving unstable adducts. In all probability such adducts would be epimeric 4-nitro-1-trinitromethyl compounds (58) which might be expected to lose the acidic proton at C4, *ipso* to the nitro group, and trinitromethanide ion to form 1,8-dimethyl-4-nitronaphthalene (44) and nitroform as illustrated in Scheme 3.6. It seems likely that some 1,8-dimethyl-4-nitronaphthalene (44) is formed in this manner, but an alternative mode of formation could involve reaction of the 1,8-dimethylnaphthalene radical cation (37) with free NO_2 which would have leaked from the triad during the course of the reaction.[67]

In conclusion, it is clear that the attack of the trinitromethanide ion on the radical cation occurs substantially at unhindered ring positions where the relative atomic charges do not prohibit reaction.[75] (See Figure. 3.11.)

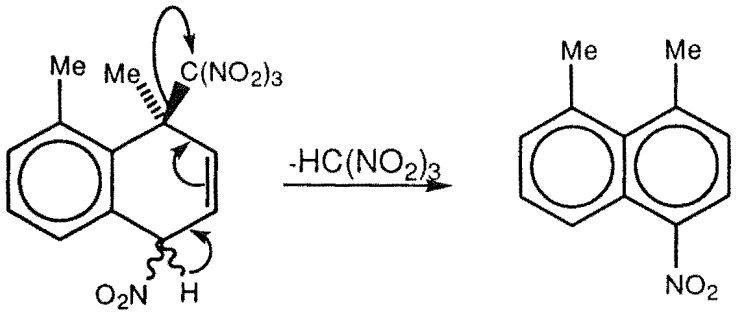

(58) (44)

SCHEME 3.6

CHAPTER FOUR

PHOTONITRATION OF 1-METHYLNAPHTHALENE

4.1 INTRODUCTION

In determining the structures of the adducts formed from the photonitration of aromatics with TNM it has been determined that the first bond formation involving reaction of trinitromethanide ion with $ArH^{\bullet+}$ is crucial. The subsequent coupling of the delocalized carbon radical, so formed, with nitrogen dioxide then yields either nitro/trinitromethyl adducts or labile nitrito/trinitromethyl adducts, the latter being hydrolysed during either the reaction or the work-up procedure to give hydroxy/trinitromethyl adducts as illustrated in the generalised Scheme 4.1.

$$ArH^{\bullet+} + (O_2N)_3C^- \longrightarrow ArHC(NO_2)_3^{\bullet}$$

$$ArHC(NO_2)_3^{\bullet} + NO_2 \longrightarrow \text{adducts}$$

SCHEME 4.1

Some adducts with suitable stereochemistry can undergo intramolecular cycloaddition to give cyclo-adducts as found in the 1,8-dimethylnaphthalene[75] and 1,2-dimethylnaphthalene[69] series.

We noted previously that attack on the radical cation of 1,8-dimethyl-naphthalene by trinitromethanide ion occurred at C4(C5) to the extent of at least 66% in dichloromethane at +20°C, and even at C3(C6) (6.6%),[75] although substantial attack of trinitromethanide ion at C1(C8) might have been expected on the basis of the calculated atomic charges[68] (Figure 4.1).

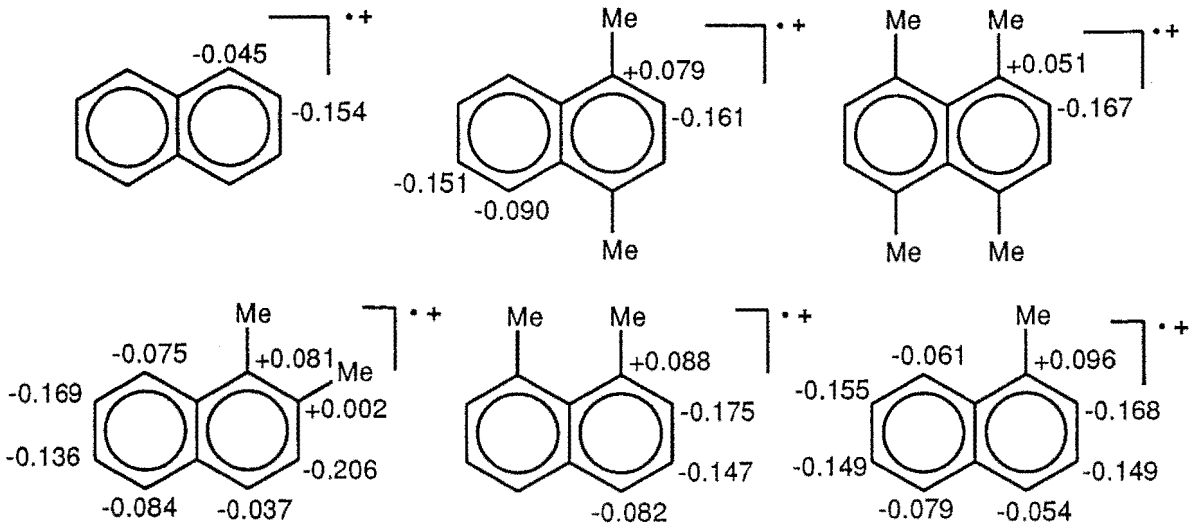

FIGURE 4.1 Calculated (AM1) atomic charges on the respective ring carbon atoms of some aromatic radical cations.

This deviations from expectation based on the calculated atomic charges has been rationalized in terms of steric hindrance to attack of the bulky trinitromethanide ion on some of the ring positions, i.e. C1/C8.

As discussed in Chapter 1, attack of the trinitromethanide ion on the radical cation of 1,4-dimethylnaphthalene is not prohibited by the presence of an *ipso*-methyl substituent.[60] It has been postulated that in the reactions of the 1,8-dimethylnaphthalene radical cation the attack of the trinitromethanide ion at C1(C8) is suppressed by the presence of the *peri*-methyl group.[75] Further, it has been proposed that for the 1,2-dimethylnaphthalene radical cation the trinitromethanide ion attack at either C1 or C2 is blocked sterically by the presence of a methyl group at the respective β-positions (C2 or C1), leaving attack of trinitromethanide ion at the unhindered C4 as the only viable alternative.[69]

The above discussion makes the assumption that the presence of an *ipso*-methyl group does not interfere prohibitively with the attack of the

trinitromethanide ion. This assumption is based on the evidence of the reaction products from photonitration of 1,4-dimethylnaphthalene. However, it should be noted that the most likely alternative point of attack on the 1,4-dimethylnaphthalene radical cation, on the basis of the calculated atomic charges, is at C5(C8), *peri-* to the 1-(4-)-methyl group.

In the light of this information we examined the photochemical reaction of 1-methylnaphthalene (59) with tetranitromethane. It was anticipated that it would be possible to assess the consequences of attack of the trinitromethanide ion on the 1-methylnaphthalene radical cation (60) in the uncomplicated presence of a potential *ipso*-methyl substituent.

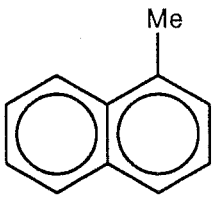

(59)

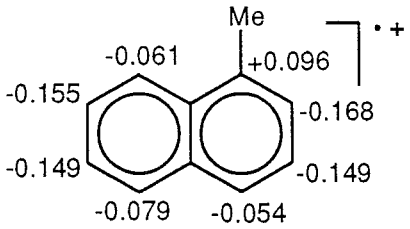

(60)

4.2 THE PHOTOLYSIS OF 1-METHYLNAPHTHALENE (59)

General Procedure for the Photonitration of 1-Methylnaphthalene (59) with Tetranitromethane.

A solution of 1-methylnaphthalene (500 mg, equal to a 0.4 mol l^{-1} solution) and tetranitromethane (0.8 mol l^{-1}) in dichloromethane or acetonitrile (8 ml) was irradiated at +20° or -20°C with filtered light (cut-off <435 nm). Aliquots were withdrawn from the reaction mixture at appropriate time intervals, the volatile material removed under reduced pressure at 0°C, and the product composition determined by ^1H NMR spectral analysis. (For complete experimental details see Chapter 5.)

4.3 PHOTOCHEMISTRY IN DICHLOROMETHANE OF 1-METHYLNAPHTHALENE (59)

The photolysis of a solution of 1-methylnaphthalene (0.4 mol l^{-1}) and TNM (0.8 mol l^{-1}) in dichloromethane at +20°C was carried out with filtered light (cut-off at 435 nm) until the red colour of the CT band had been bleached. Isolation of the reaction mixture at ≤ 0°C gave a mixture of adducts (61) - (68), and an unidentified mixture of nitroaromatic compounds. These adducts (61) - (67) were partially separated in small quantities by h.p.l.c. on a cyanopropyl column using hexane/dichloromethane mixtures.

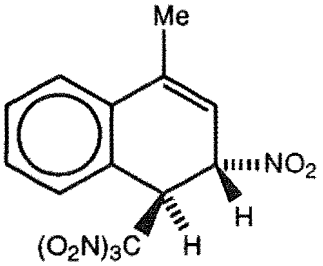

(61)

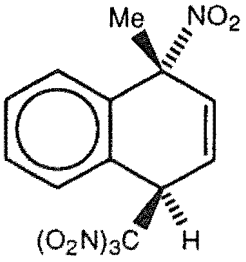

(62)

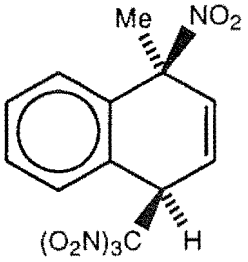

(63)

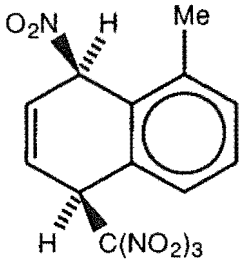

(64)

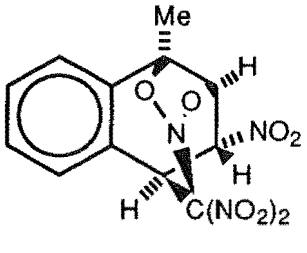

(65)

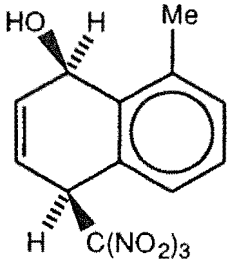

(66)

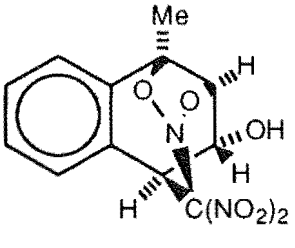

(67)

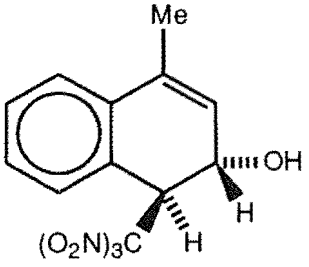

(68)

The structure of adduct (61) was determined by single crystal X-ray analysis. A perspective drawing of 1-methyl-*r*-3-nitro-*t*-4-trinitromethyl-3,4-dihydronaphthalene (61), $C_{12}H_{10}N_4O_8$, m.p. 89-91°C, is presented in Figure 4.2, and the corresponding atomic coordinates are given in Table 5.4.

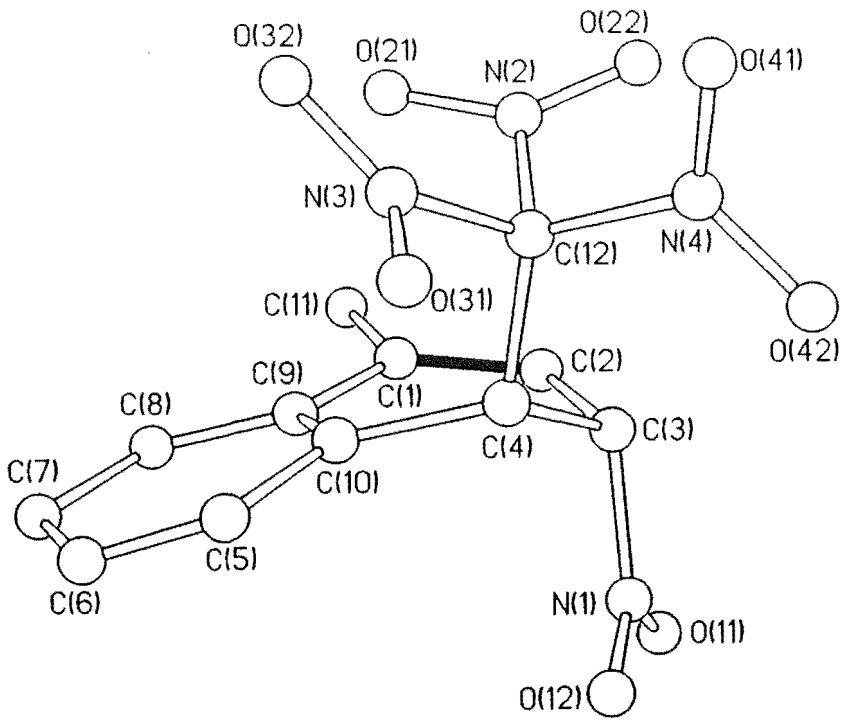

FIGURE 4.2

A perspective diagram of 1-methyl-*r*-3-nitro-*t*-4-trinitromethyl-3,4-dihydronaphthalene (61).

In the solid state the conformation of the alicyclic ring is such that the nitro and trinitromethyl substituents are close to *anti* to each other with the C4-$C(NO_2)_3$ bond close to perpendicular to the plane of the aromatic ring [torsional angles: N(61)-C(63)-C(4)-C(12) 160.0(63)°; C(12)-C(4)-C(10)-C(9) 91.4(4)°]. The spectroscopic data for adduct (61) were in accord with the established structure. In particular, the **C**H-$C(NO_2)_3$ resonance appeared at δ 43.8, while the **C**H-NO_2 resonance appeared at δ 88.6, these assignments were confirmed by long range reverse detected heteronuclear correlation spectra (HMBC). A comparison of the spectral features with the analogous adduct formed in the 1,8-dimethylnaphthalene series is illustrated in Figure 4.3.

Adduct (61) was unstable and underwent cycloaddition to form the cycloadduct (65), see below.

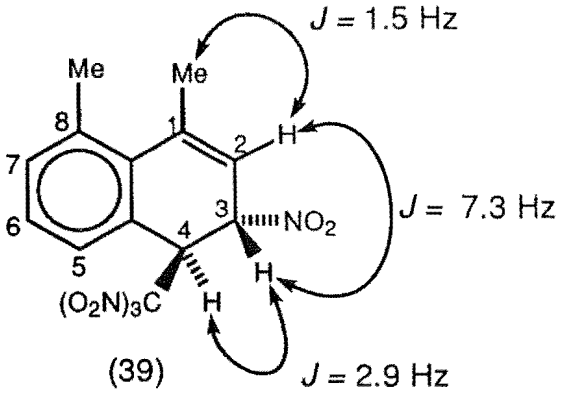

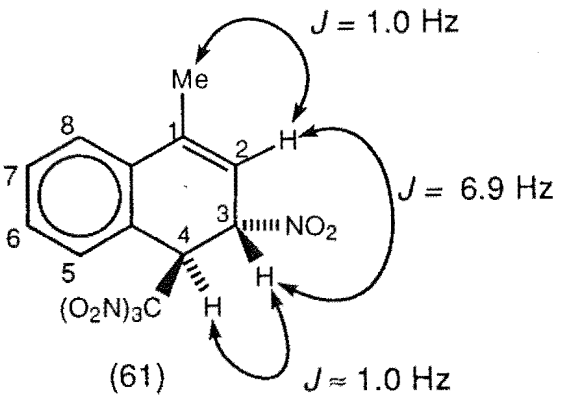

Me-1	2.30	Me-1	2.20
H2	5.80	H2	5.85
H3	5.64	H3	5.73
H4	5.61	H4	5.63
		C1	141.9
^{13}C NMR not obtainable		C2	113.0
		C3	88.6
		C4	43.8
		C5	131.5

FIGURE 4.3 NMR characteristics between adduct (39) and adduct (61)

Adducts (62) and (63) were eluted next from the h.p.l.c. column and in that order. While adduct (62) could not be obtained in a crystalline form it was characterised by NMR data and compared with the spectral features of adduct (63). See below.

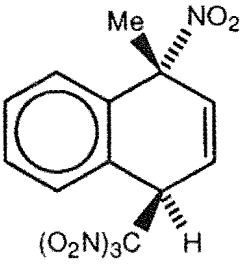

(62)

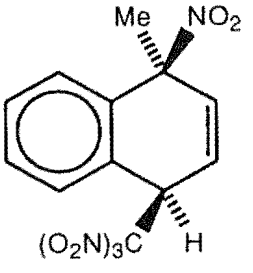

(63)

Adduct (63) gave crystals of adequate quality for its structure determination by single crystal X-ray analysis. A perspective drawing of 1-methyl-*r*-1-nitro-*c*-4-trinitromethyl-1,4-dihydronaphthalene (63), $C_{12}H_{10}N_4O_8$, m.p.88-89°C, is presented in Figure 4.4, and the corresponding atomic coordinates in Table 5.5.

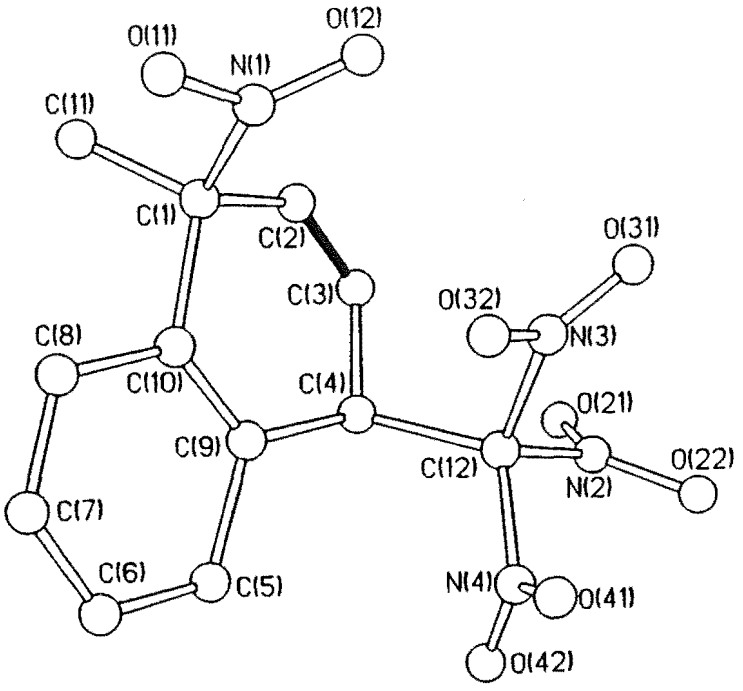

FIGURE 4.4

A perspective diagram of 1-methyl-*r*-1-nitro-*c*-4-trinitromethyl-1,4-dihydronaphthalene (63).

In the solid state the alicyclic ring exists in a somewhat flattened boat conformation with the nitro and trinitromethyl groups in the flagpole orientation [torsional angles: C(63)-C(62)-C(61)-C(10) -4.8(8)°; C(62)-C(63)-C(4)-C(9) 14.5(8)°; C(5)-C(9)-C(4)-C(12) -75.5(7)°; N(61)-C(61)-C(10)-C(8) 71.1(7)°]. Given the established structure of adduct (63), adduct (62) was assigned the epimeric structure on the basis of the close similarity between the spectroscopic data for the two compounds and the analogous adduct identified in the 1,8-dimethylnaphthalene series (38) as illustrated in Figs 4.5 and 4.6. The coupling coupling constants for adducts (38) and (62) agree very closely and this implies that the conformations of the two adducts are closely similar.

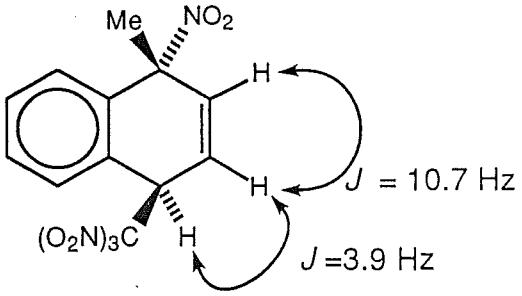

(62)

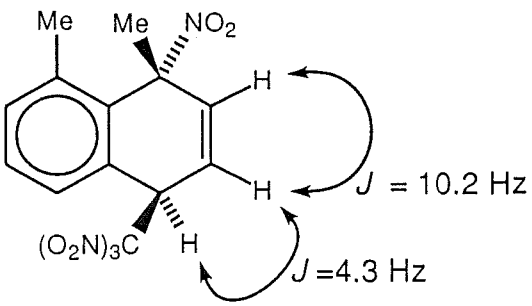

(38)

FIGURE 4.5 Comparison of the coupling constants of adducts (38) and (62)

Figure 4.6 illustrates the characteristic ^{13}C NMR and ^{1}H NMR resonances associated with the adducts (62) and (63).

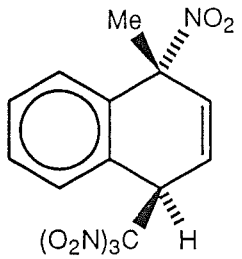

(62)

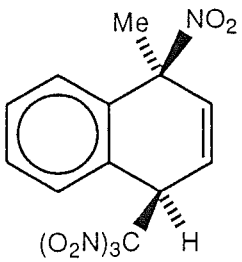

(63)

Me-1	2.08	Me-1	2.03
H2	6.44	H2	6.59
H3	6.51	H3	6.59
H4	5.51	H4	5.33
C1	86.9	C1	87.2
C2	127.1	C2	127.5
C3	121.3	C3	122.1
C4	44.3	C4	44.5

FIGURE 4.6 Characteristic NMR resonances for adducts (62) and (63)

The fourth adduct (64) eluted from the h.p.l.c. column was identified by single crystal X-ray analysis. A perspective drawing of 8-methyl-*r*-1-nitro-*c*-4-trinitromethyl-1,4-dihydronaphthalene (64), $C_{12}H_{10}N_4O_8$, m.p. 129-131°C, is presented in Figure 4.7, and the corresponding atomic coordinates are given in Table 5.6.

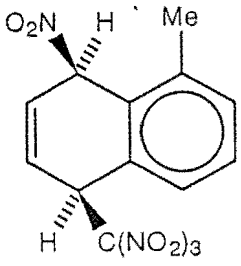

(64)

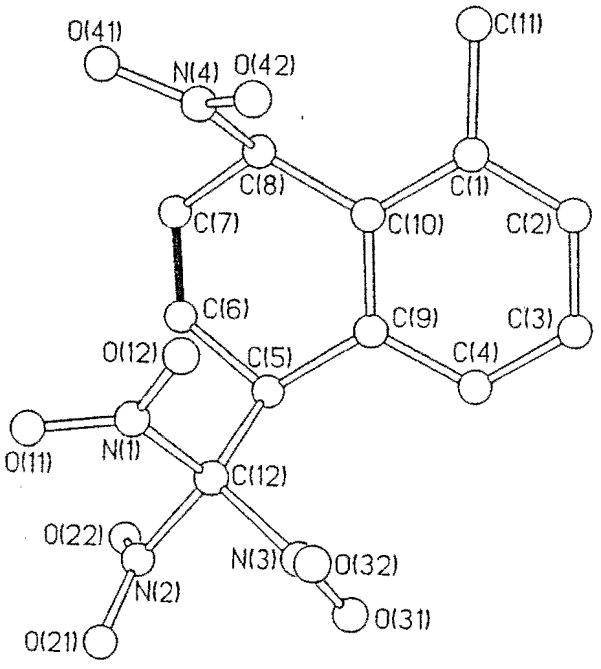

FIGURE 4.7

A perspective drawing of 8-methyl-*r*-1-nitro-*c*-4-trinitromethyl-1,4-dihydronaphthalene (64).

In this structure also the alicyclic ring exists in a flattened boat conformation with the nitro / trinitromethyl substituents in flagpole orientations [torsional angles: C(7)-C(6)-C(5)-C(9) -17.6(4)°; C(6)-C(7)-C(8)-C(10)13.3(4)°; N(4)-C(8)-C(10)-C(1) -75.9(3)°; C(12)-C(5)-C(9)-C(4) 77.5(3)°]. The notable feature of adduct (64) is that the photoaddition of the trinitromethanide ion to the 1-methylnaphthalene radical cation (59) has occurred to the non-methylated ring and with a regiochemistry which implies initial attack of the trinitromethanide ion on the 1-methylnaphthalene radical cation at the α-position most remote from the 1-methyl substituent. The spectroscopic data for adduct (64) were consistent with the existence of the molecule in the same

conformation in the solid state and in solution. In particular, the coupling constants indicated the 1/4-substitution with J = 10.2 Hz for H2/H3 as illustrated in Figure 4.8.

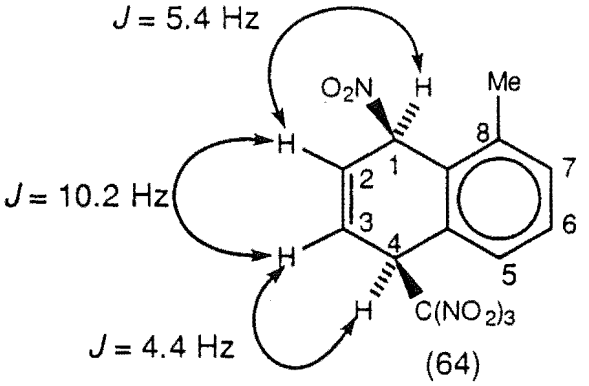

FIGURE 4.8

The structure of the fifth adduct eluted from the h.p.l.c. column was also determined by single crystal X-ray analysis, and a perspective drawing of the nitro cycloadduct (65), $C_{12}H_{10}N_4O_8$, m.p. 159-160°C, is presented in Figure 4.9, and the corresponding atomic coordinates are given in Table 5.7.

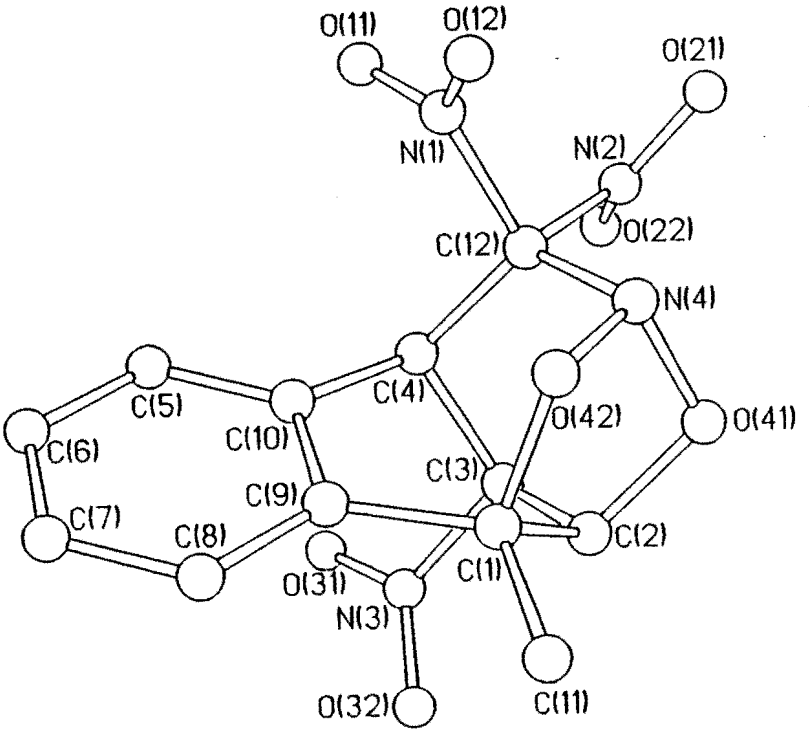

FIGURE 4.9

A perspective diagram of the nitro cycloadduct (65).

In the structure N(4) is clearly trigonal and bond length differences are observed for the C(12)-N bonds [C(12)-N(4) 1.490(3) Å; C(12)-N(1) 1.534(3) Å; C(12)-N(2) 1.550(3) Å], similar to those observed earlier [69,75] (pages 183, 192) for analogous heterocyclic cage structures. As expected, given the mode of genesis of the nitro cycloadduct (65) by cycloaddition in the *r*-3-nitro-*t*-4-trinitromethyl adduct (61), the C(2)-NO_2 bond is *anti* to the C(4)-$C(NO_2)_3$ bond. The spectroscopic data for the nitro cycloadduct (65) are consistent with the established structure. In particular, in the ^1H NMR spectrum the W-coupling, $J_{H2,H4}$ 2.0 Hz, is as expected given the near-coplanarity of the C(2)-H(2) / C(4)-H(4) bonds as illustrated in Fig 4.10. The same ^1H NMR features were observed in the 1,8-dimethylnaphthalene series with the analogous nitro-cycloadduct (42). These similarities are summarised in Table 4.1.

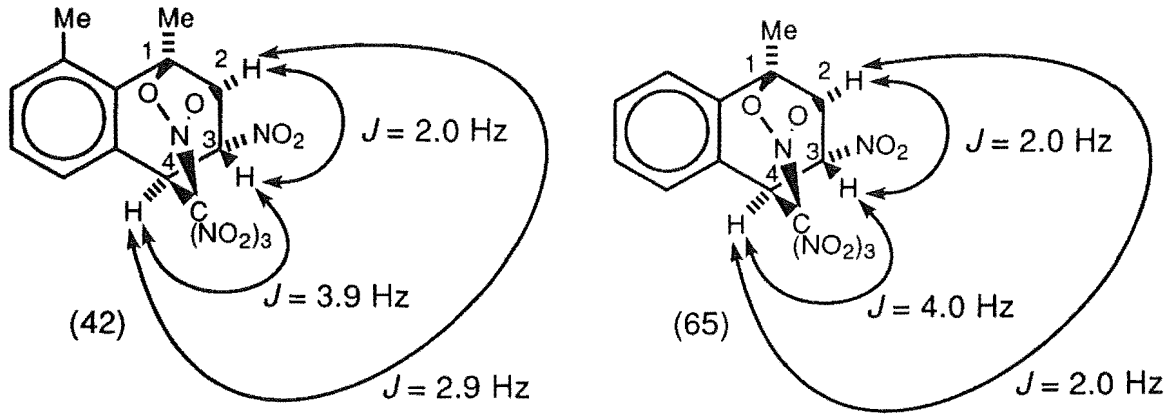

FIGURE 4.10 Coupling constants associated with adducts (42)and (65).

TABLE 4.1 ^{1}H NMR data associated with the nitro cycloadducts (42) and (65).

^{1}H NMR Assignment (42)	Chemical Shift (δ)	Coupling Constants (Hz)
H2	5.46 dd	$J_{H2,H4}$ 2.9; $J_{H2,H3}$ 2.0
H3	5.66 dd	$J_{H3,H4}$ 3.9; $J_{H3,H2}$ 2.0
H4	5.20 dd	$J_{H4,H3}$ 3.9; $J_{H4,H2}$ 2.9

^{1}H NMR Assignment (65)	Chemical Shift (δ)	Coupling Constants (Hz)
H2	5.51 dd	$J_{H2,H4}$ 2.0; $J_{H2,H3}$ 2.0
H3	5.72 dd	$J_{H3,H4}$ 4.0; $J_{H3,H2}$ 2.0
H4	5.26 dd	$J_{H4,H3}$ 4.0; $J_{H4,H2}$ 2.0

^{13}C NMR resonances were observed as illustrated in Table 4.2. These resonances are very similar to those observed for the nitrocycloadduct (42) observed in the 1,8-dimethylnaphthalene series.

TABLE 4.2 ^{13}C NMR data associated with the nitro cycloadducts (42) and (65).

ADDUCT (42)		ADDUCT (65)	
^{13}C NMR	Chemical Shift (δ)	^{13}C NMR	Chemical Shift (δ)
C1	78.7	C1	79.3
C2	83.2	C2	81.1
C3	90.1	C3	87.2
C4	45.9	C4	45.5
C5	129.8	C5	≈130

The next adduct (66) eluted from the h.p.l.c. column was obtainable only in microcrystalline form and its identification is based on a consideration of its

spectroscopic data. From its ^1H NMR spectrum it could be defined as a 1,4-adduct in the non-methylated ring. The presence of a broad doublet upfield of the normal range for aromatic protons at δ 7.00, assigned to H5, is characteristic of an aromatic proton *peri* to a C4-$C(NO_2)_3$ function.[69] N.O.e. experiments confirmed the proximity of H5 (δ 7.00) and the C**H**-$C(NO_2)_3$ (δ 5.25), the latter proton appearing as expected somewhat upfield of the corresponding proton signal (δ 5.39) in the nitro trinitromethyl adduct (64). The ^1H NMR resonances and nOe enhancements are illustrated in Figure 4.11.

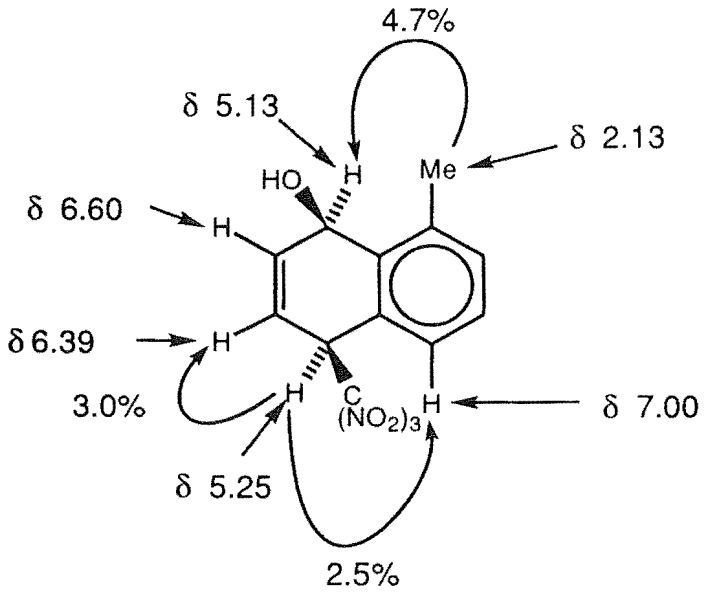

(66)

FIGURE 4.11 ^1H NMR resonances (δ) and nOe enhancements (%)

Given the closely similar coupling constants, $J_{H1,H2}$ and $J_{H3,H4}$, for the two adducts (64) and (66), (as illustrated in Figure 4.12) it is assumed that the two compounds have the same 1,4-stereochemistry and that the difference between the structures lies only in the nature of the C1-substituent. An i.r. absorption was observed at 3447 cm^{-1} indicating the presence of an -OH function. In the nitro adduct (64) the ^1H NMR signal for H1 appears at δ 6.04, but that for H1 in the hydroxy adduct (66) is located upfield at δ 5.13, consistent with the difference in the *ipso* substituent.

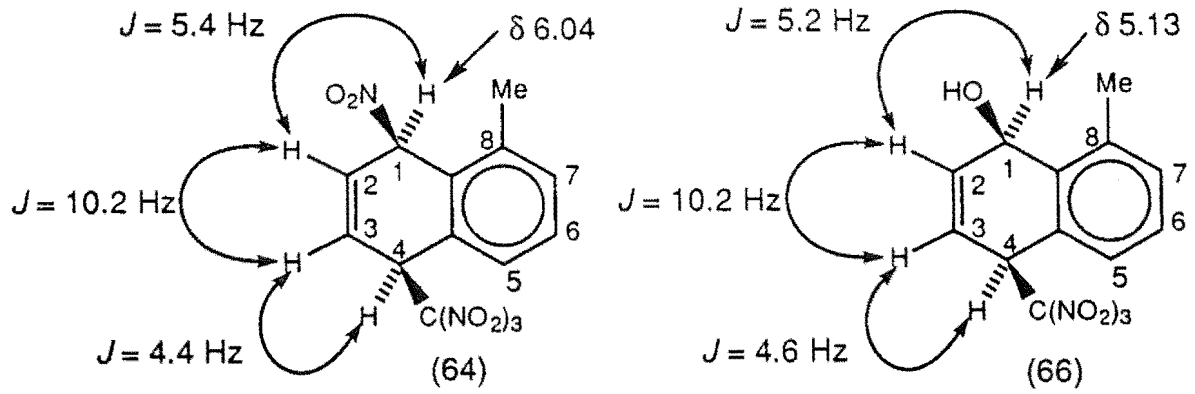

FIGURE 4.12 Comparison of coupling constants (Hz) and chemical shifts (δ) for the characteristic spectral features of adducts (64), and (66).

The structure of the last adduct eluted from the h.p.l.c. column was determined by single crystal X-ray analysis to be the hydroxy cycloadduct (67), $C_{12}H_{11}N_3O_7$, m.p. 182-184°C. A perspective drawing is presented in Figure 4.13 and the corresponding atomic coordinates are given in Table 5.8.

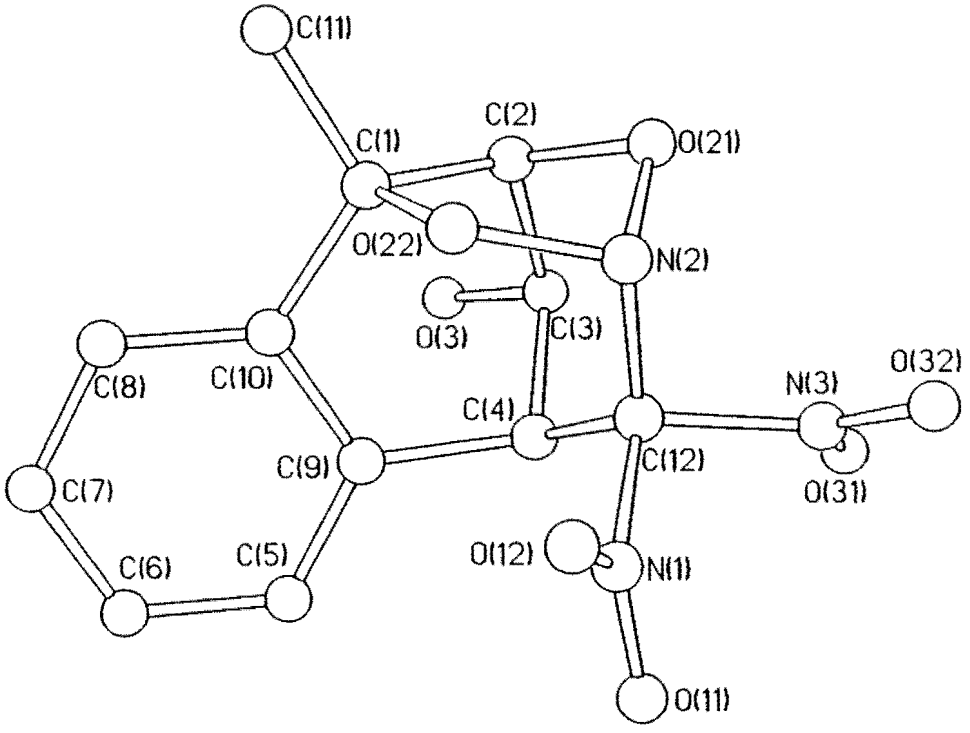

FIGURE 4.13

A perspective diagram of the hydroxy cycloadduct (67).

As for the nitro cycloadduct (65), the nitrogen atom in the heterocyclic cage structure of hydroxy cycloadduct (67) is trigonal and the pattern of bond lengths is similar: C(12)-N(2) 1.493(63) Å, C(12)-N(1) 1.528(2) Å, C(12)-N(2) 1.546(2) Å.

The spectroscopic data for the hydroxy cycloadduct (67) are in accord with the established structure. An i. r. absorption was observed at 3541 cm^{-1} which is characteristic for an -OH function. N.O.e. experiments confirmed the assignment of the chemical shifts for the protons. Irradiation at Me-1 gave enhancements at H2 (6.3%) and H8 (3.7%) while irradiation at H5 gave an enhancement at H4 (2.3%).

The similarities in the ^{13}C NMR spectra of characteristic absorptions between the analogous hydroxycycloadduct (42) isolated from the 1,8-dimethylnaphthalene series and adduct (67) are illustrated in Figure 4.14.

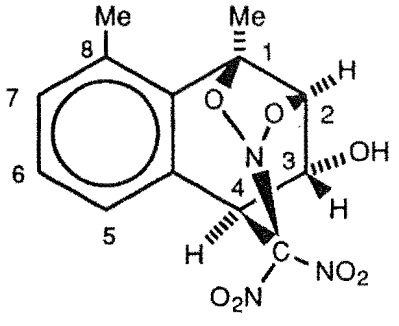

(42)

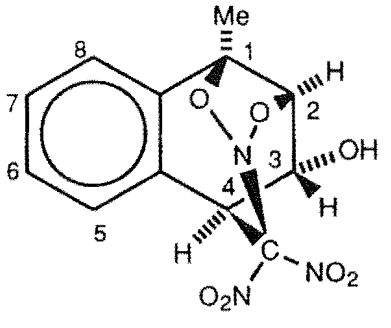

(67)

C1	88.5	C1	85.8
C2	87.3	C2	85.0
C3	66.4	C3	66.9
C4	49.6	C4	49.0
C5	129.5	C5	131.8

FIGURE 4.14 ^{13}C NMR charateristic resonances for analogous adducts (42) and (67).

Although the precursor (68) of the hydroxy cycloadduct (67) could not be isolated by h.p.l.c., it could be detected among the reaction products with a partial ^1H NMR spectrum ($CDCl_3$) δ 4.76, br s, H4; 4.83, d, $J_{H3,H2}$ 6.8 Hz, H3; 5.78, d, $J_{H2,H3}$ 6.8 Hz, H2; the remainder of the spectrum was obscured by signals from other components of the mixture. The coupling constant of 6.8 Hz for H_2/H_3 indicates that the addition is of the 1,2-type and compares closely with those of the related adducts (39) and (61) implying the same stereochemistry for the three compounds. See Figure 4.15.

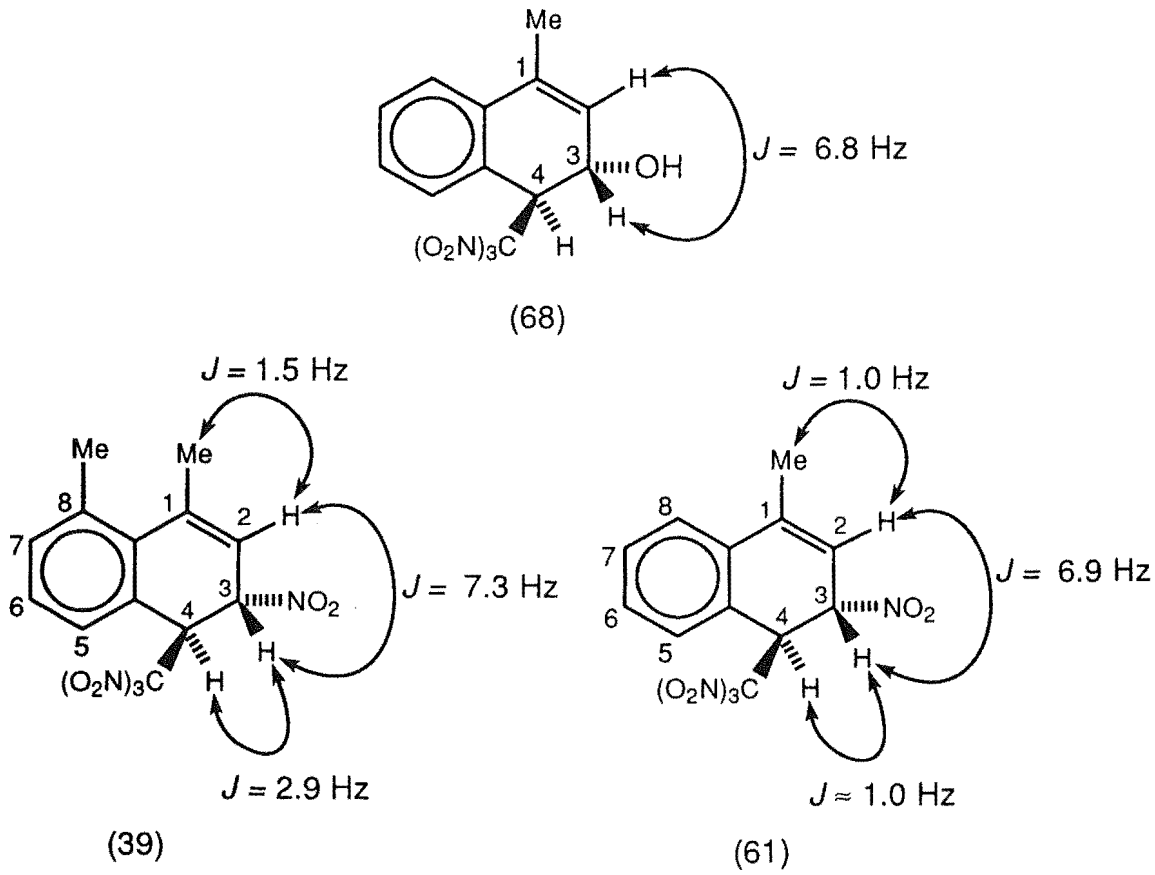

FIGURE 4.15 Comparison of coupling constants between related adducts (39), (61) and (68).

The photolysis of the 1-methylnaphthalene/TNM charge transfer complex in dichloromethane at -20°C resulted in a similar pattern of adduct formation as

observed in the photolysis at +20°C. An overview of the yields is presented in Table 4.3.

Table 4.3. Overview of yields of products from the photolysis of 1-methylnaphthalene (0.4 mol l^{-1}) and tetranitromethane (0.8 mol l^{-1}) in dichloromethane.

		Yield (%)									
t / h	Conversion (%)	(61)	(62)	(63)	(64)	(65)	(66)	(67)	(68)	Total Adducts	(69)[b]
At +20°C											
1	76	19.6	16.9	7.0	2.1	1.7	0.7	2.1	2.8	52.9	4.2
2	97	22.3	24.5	10.3	3.4	3.8	0.5	4.9	3.3	73.0	7.1
3	100	19.4	20.8	9.5	3.0	7.8	0.9	5.9	2.1	69.4	8.6
At -20°C											
1	42	22.9	14.2	8.4	4.8	trace	1.4	trace	10[a]	61.7	9.1
2	80	16.8	14.6	8.4	3.9	8.4	1.1	trace	7.8	61.0	10.0
4	96	15.7	14.4	7.0	2.7	6.9	1.0	trace	5.7	53.4	10.2

[a] Unreliable integral due to overlapping signals

[b] Unidentified nitroaromatics

4.5 PHOTOCHEMISTRY IN ACETONITRILE

Photolyses of solutions of 1-methylnaphthalene (0.4 mol l^{-1}) and TNM (0.8 mol l^{-1}) in acetonitrile were carried out at +20° and -20°C as for the reactions in dichloromethane, above. The results of these reactions, monitored with time, are summarized in Table 4.4. The same general pattern of formation of adducts

is observed in acetonitrile at +20° and -20°C as was found for the corresponding reactions in dichloromethane except that adducts (65) and (66) were not detectable among the products in the acetonitrile reaction at -20°C. Table 4.4 gives an overview of the yields of products in acetonitrile.

Table 4.4. Overview of yields of products from the photolysis of 1-methylnaphthalene (0.4) mol l^{-1}) and tetranitromethane (0.8 mol l^{-1}) in acetonitrile.

		Yield (%)									
t / h	Conversion (%)	(61)	(62)	(63)	(64)	(65)	(66)	(67)	(68)	Total Adducts	(69)[b]
At +20°C											
1	58	19.9	12.9	1.9	3.1	trace	trace	trace	4.2	42.0	10.9
5	100	15.4	20.5	13.7	2.3	17.1	2.6	4.1	4.3	80.0	9.4
At -20°C											
2	40	14.1	7.1	7.5	trace	0	0	trace	7.1	35.8	9.4
5	85	8.8	8.2	6.4	1.2	0	0	1.0	7.0	32.6	10.0

[b] Unidentified nitroaromatics

4.5 The Thermal Cycloaddition of Adduct (61) to Give the Nitro Cycloadduct (65)

The isolation of the *r*-3-nitro-*t*-4-trinitromethyl adduct (61) in a pure state afforded the opportunity to study its cycloaddition reaction. A solution of adduct

(61) in (D)-chloroform was stored in the dark and the ^1H NMR spectrum monitored at appropriate time intervals. The precursor adduct (61) was slowly transformed into the nitro cycloadduct (65). (See Scheme 4.2 and Figure 4.16).

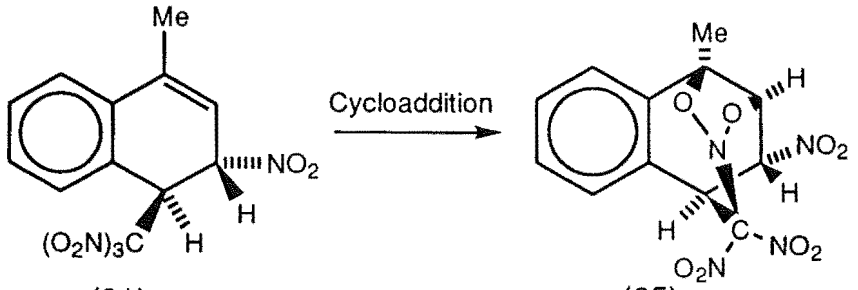

(61) (65)

SCHEME 4.2

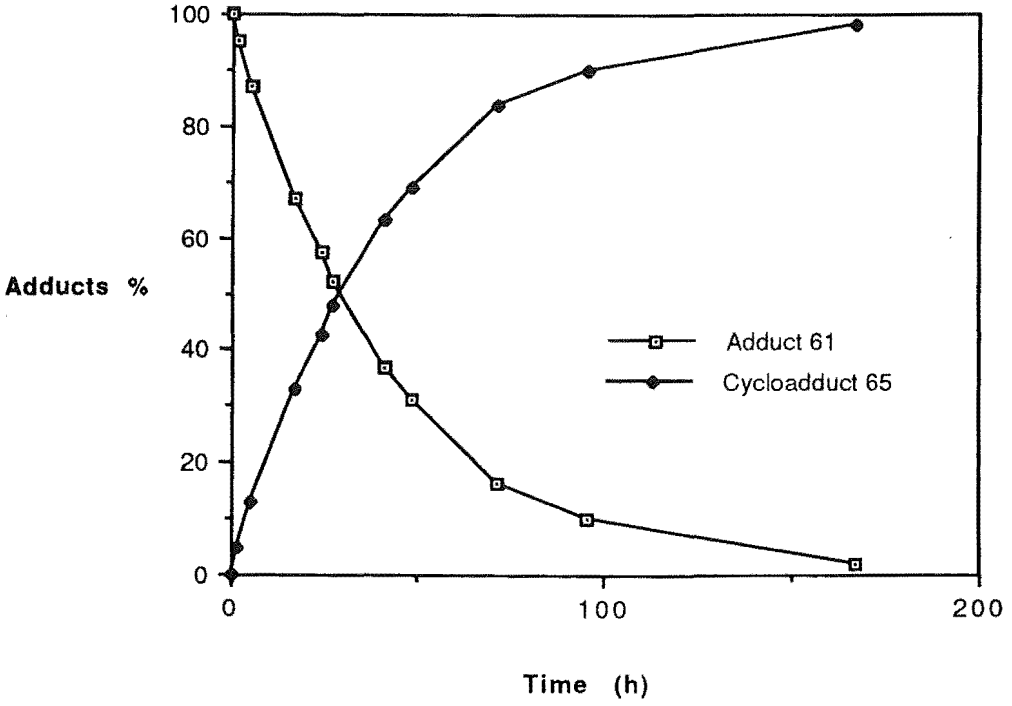

FIGURE 4.16 Kinetics of cycloaddition of adduct (61) to adduct (65) in deutero-chloroform at 22°C.

The half-life for the cycloaddition (61) → (65) (Scheme 4.2) is *c.* 29 h, compared with a half-life of *c.* 12 h for the analogous cycloaddition in the 1,8-dimethylnaphthalene series, i.e. (39) → (42) as illustrated in Scheme 4.3.[75] (See Chapter 3.)

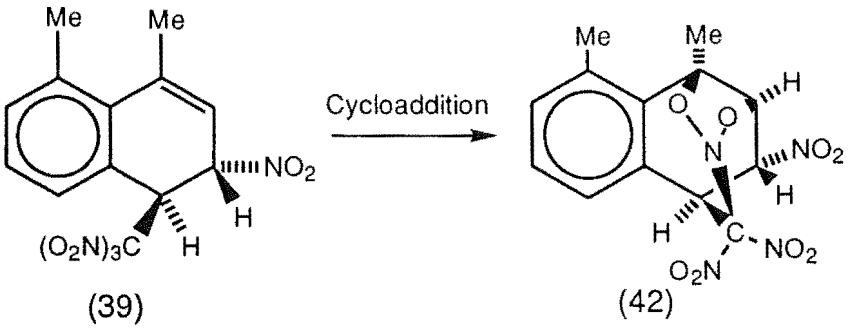

(39) (42)

SCHEME 4.3

The differences between the rate of the two cycloaddition reactions presumably arises from the greater electron availability in the alkene function of the precursor (67) due to the presence of the additional methyl group.

4.6 Overview of the Photonitration of 1-Methylnaphthalene.

The yields of identified adducts are high (up to 80%) for the photolysis of the 1-methylnaphthalene/TNM charge-transfer complex in dichloromethane or acetonitrile at +20°C, but somewhat reduced for reactions in either solvent at -20°C. For the reaction in dichloromethane at +20°C, of the total adducts identified (69%) the majority (65%) are formed by attack of the trinitromethanide ion at C4 of the 1-methylnaphthalene radical cation, the remainder (4%) arising by attack of trinitromethanide ion at C5 on that radical cation. (See Figure 4.17.)

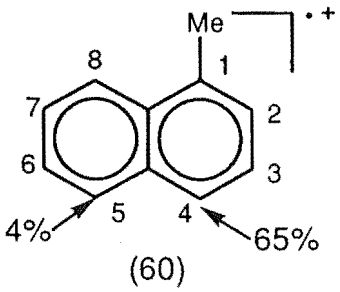

(60)

FIGURE 4.17

Although attack of trinitromethanide ion on the 1-methylnaphthalene radical cation might have been expected to occur *ipso* to the 1-methyl group on the

basis of the relative atomic charges on the aromatic nucleus, such attack by the bulky trinitromethanide ion is clearly restricted by the considerable steric compression in attack at that position. Of the remaining three α-positions (C4, C5, and C8) of the 1-methylnaphthalene radical cation (60), the position *peri* to the methyl group (C8) would be disfavoured by the steric interaction between the attacking trinitromethanide ion and the *peri*-methyl group. This rationalization leaves C4 and C5 as the only likely sites for trinitromethanide ion attack, of which C4 would be apparently preferred on the basis of the calculated relative atomic charges in the 1-methylnaphthalene radical cation (60), (See Figure 4.1). This argument of attack of the trinitromethanide ion fits with the observed pattern of the adducts isolated and identified in the 1-methylnaphthalene series[76] and also the 1,8-dimethylnaphthalene[75] and 1,2-dimethylnaphthalene series.[69]

Attack of the trinitromethanide ion on the 1-methylnaphthalene radical cation thus gives mainly the delocalized carbon radical (70) but also some of the isomeric radical (71). See Schemes 4.4 and 4.5.

The final adduct-forming steps involve coupling of these delocalized carbon radicals with nitrogen dioxide. Coupling with C-N bond formation occurs with radical (70) at C1 to give the epimeric nitro/trinitromethyl adducts (62) and (63), and at C3 to give the *r*-3-nitro-*t*-4-trinitromethyl adduct (61) (Scheme 4.4), the formation of the epimeric *r*-3-nitro-*c*-4-trinitromethyl adduct being blocked by the bulky trinitromethyl group in the radical (70). Alternatively, coupling with C-O bond formation can occur to give the nitrito/trinitromethyl adduct which on hydrolysis, either in the prevailing acidic conditions of the reaction or on work-up, gives the *r*-3-hydroxy-*t*-4-trinitromethyl adduct (68).

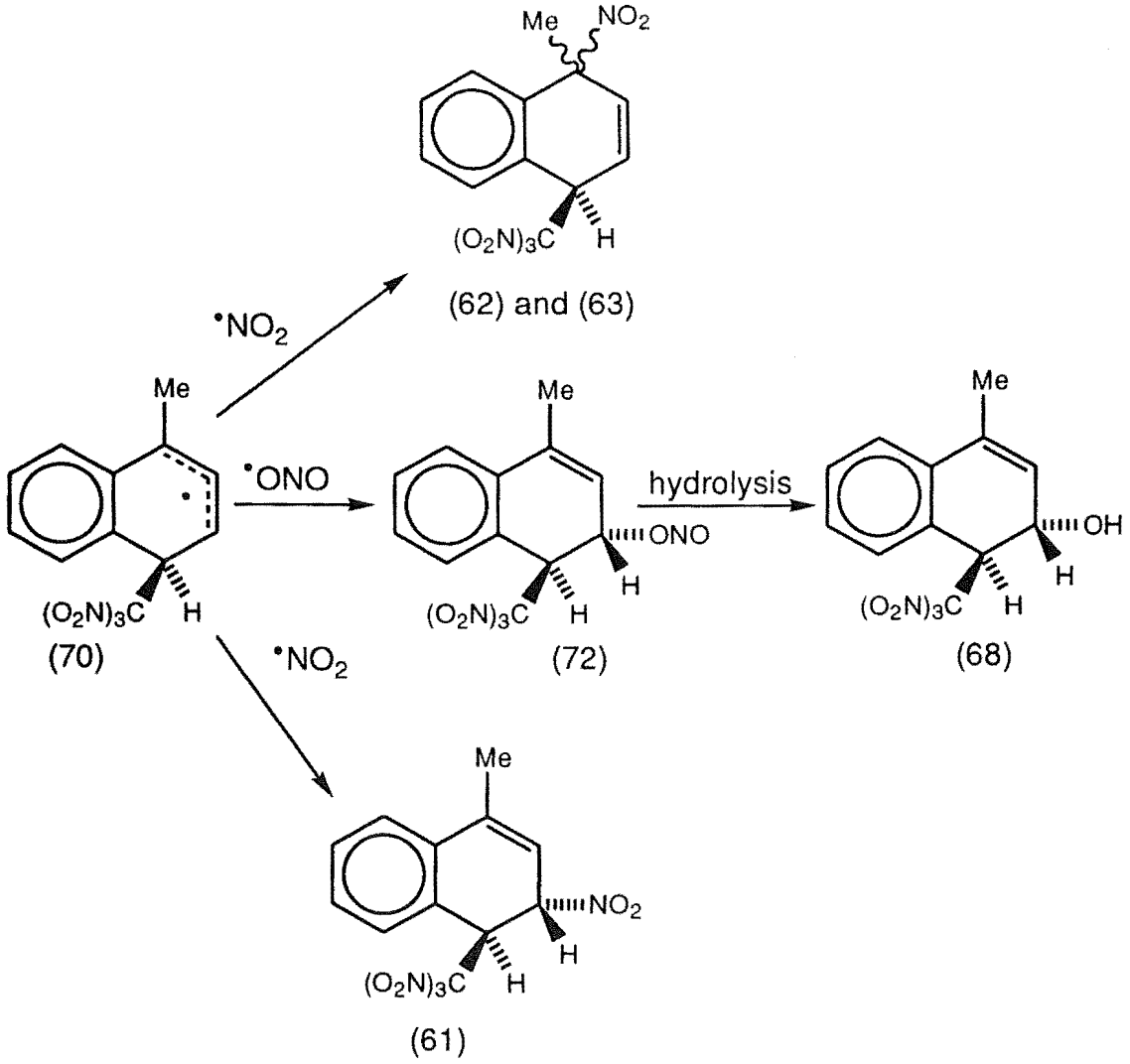

SCHEME 4.4

Analogous reactions of nitrogen dioxide with the delocalized carbon radical (71) can occur at C1 with C-N and C-O bond formation to give the nitro/trinitromethyl adduct (64) and the nitrito/trinitromethyl adduct (72), the latter yielding the hydroxy/trinitromethyl adduct (66) on hydrolysis (Scheme 4.5). Subsequently, the nitro/trinitromethyl and hydroxy/trinitromethyl adducts, (61) and (68), undergo thermal cycloaddition of one nitro group of the trinitromethyl function with the alkene system to give the cycloadducts (65) and (67).

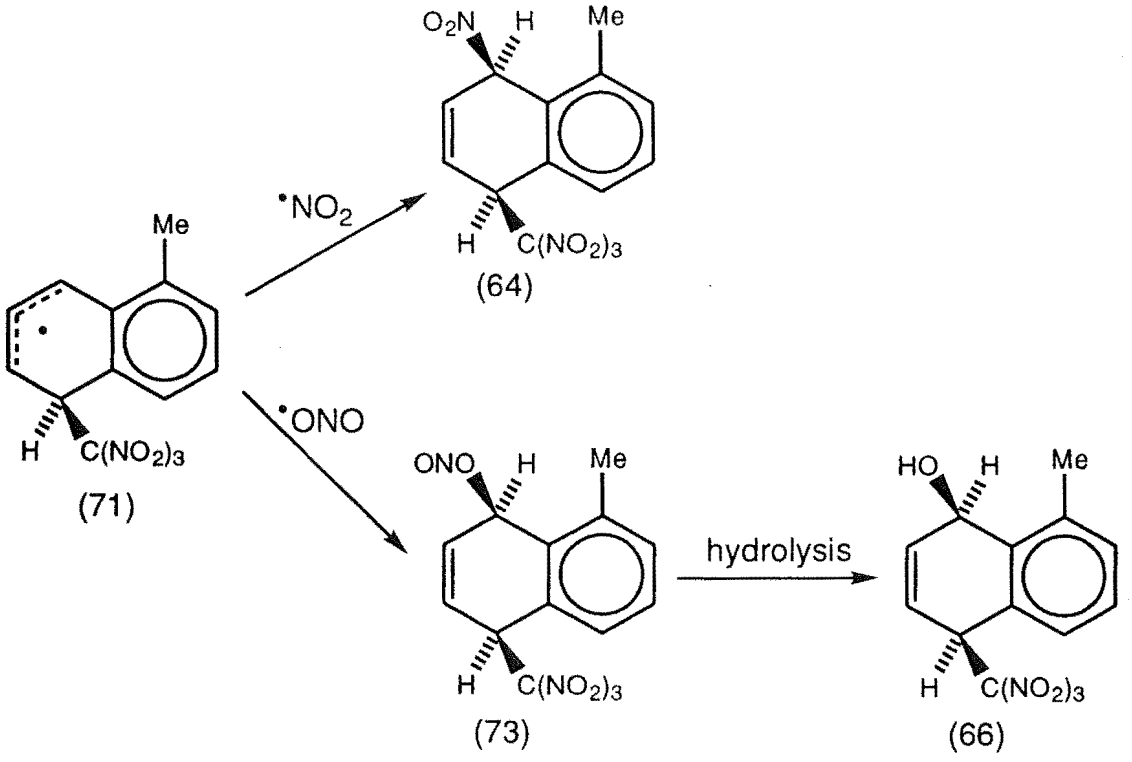

SCHEME 4.5

In view of the results and their rationalization reported in the previous Chapters it is now appropriate to reconsider the possible reasons for the almost exclusive formation of adducts in 1,4-dimethylnaphthalene derived by attack on the corresponding radical cation by trinitromethanide ion *ipso* to a methyl group.[60]

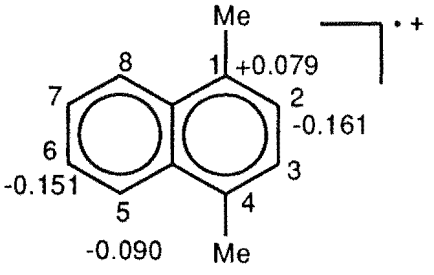

FIGURE 4.18

Given the calculated relative atomic charges (Figs. 4.1 and 4.18) it appears that the only conceivable alternative ring position(s) for attack by trinitromethanide ion on 1,4-dimethylnaphthalene radical cation is C5(C8) which is a position *peri*

to a methyl group shown to be disfavoured on steric grounds as for C8-attack in the 1-methylnaphthalene radical cation reaction with trinitromethanide ion.
It appears therefore that *ipso*-attack of trinitromethanide ion on the 1,4-dimethylnaphthalene radical cation occurs by default with the atomic charge at C1(C4) being sufficient to offset the energetic disadvantage of the steric compression encountered in the attack.

In conclusion, it is now clear that the relative atomic charges of the aromatic radical cation are important in making an assessment of the likely sites(s) of the trinitromethanide ion attack on that radical cation, but that steric interactions with substituents *ipso*, *peri*, and *vicinal* to the reaction site may dictate the course of the reaction.

EXPERIMENTAL

5.1 APPARATUS. MATERIALS AND INSTRUMENTATION

Infrared spectra were recorded on a Perkin-Elmer Series 1600 FTIR for liquid films and KBr disks. ^{1}H and ^{13}C NMR and nuclear Overhauser enhancement experiments were obtained for deutero-chloroform using TMS as an internal standard on either a Varian XL-300 or Unity 300 spectrometer. All chemical shifts are expressed as part per million (ppm) downfield from TMS and are singlets unless otherwise stated. Deutero-acetone solutions were used where solubility in deutero-chloroform was insufficient. Mass spectrometry was carried out on a Kratos MS-80. Melting points were determined on a microscope slide and are uncorrected.

Preparative scale chromatography was routinely carried out utilising a Chromatotron (a preparative scale, centrifugally accelerated, radial, thin layer chromatograph. Model 7924, Harrison Research Inc.) equipped with rotors with either Silica gel PF-254 (with $2CaSO_{4}.H_{2}O$ type 60 for tlc, Merck: E. M. laboratories Inc., Item No. 7749).

Tetranitromethane $C(NO_2)_4$ was purchased from Aldrich or synthesised using the procedure described by Poe and Liang in Organic Synthesis Collective volume 3 pg 803-805.

WARNING while no incident was experienced in working with tetranitromethane, is should be noted that its mixtures with hydrocarbons are detonative within certain concentration limits and that due care should be taken in handling mixtures of TNM and organic compounds.

H.p.l.c. separation was achieved using a Varian 5000 liquid chromatograph equipped with an Alltech cyanopropyl column and Varian UV-50 detector, eluting with hexane/dichloromethane mixtures.

The photonitration apparatus are illustrated below in Figures 5.1-5.3.

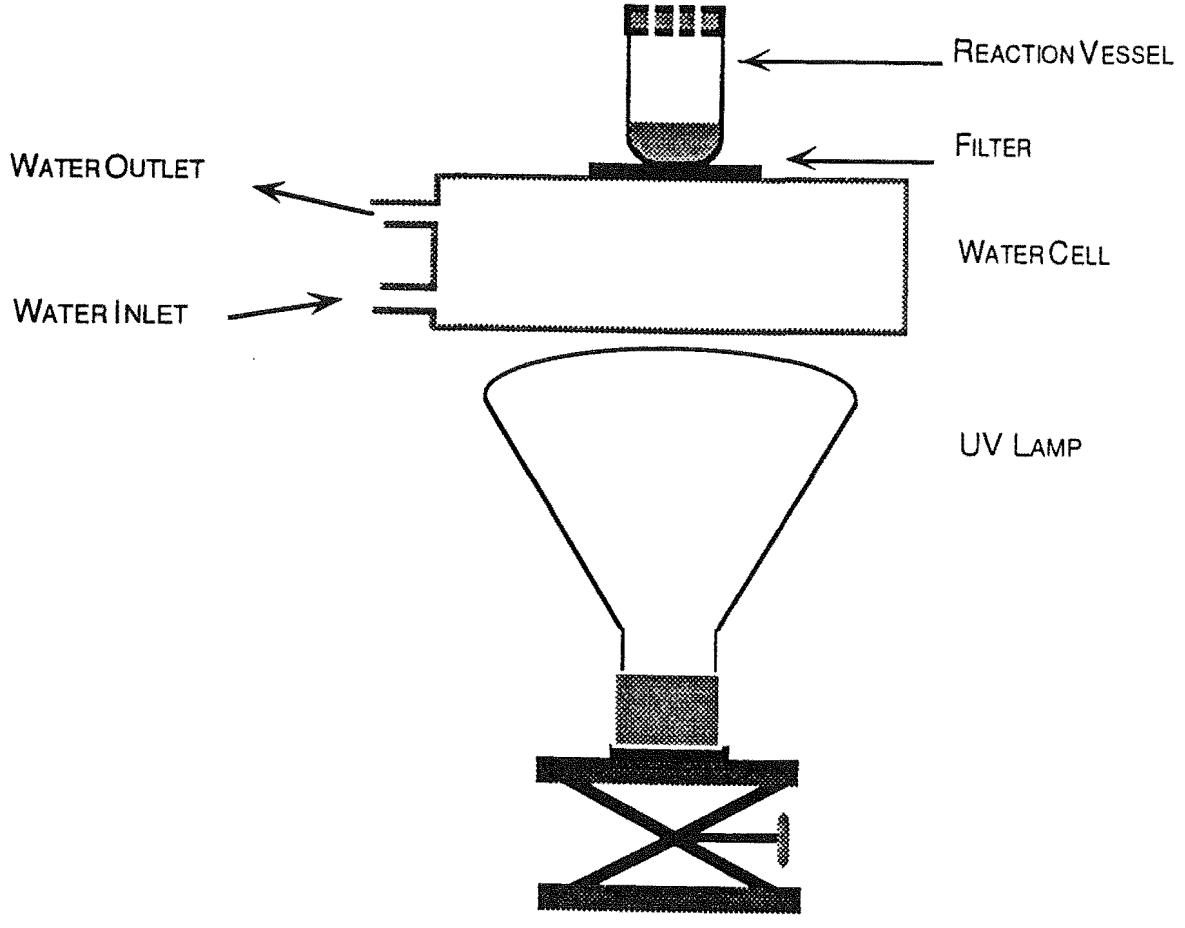

FIGURE 5.1 Apparatus used for photonitrations at +20°C.

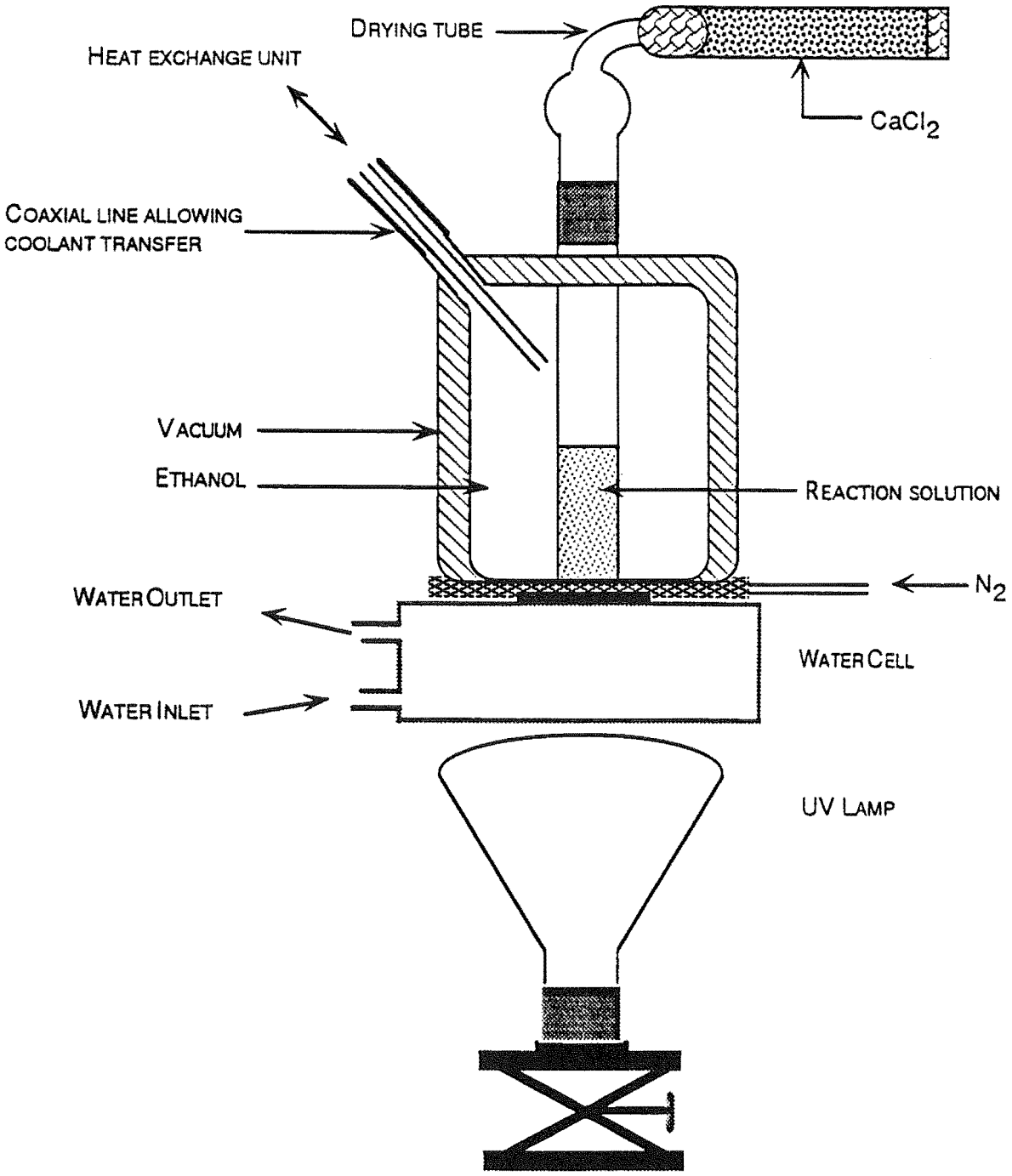

FIGURE 5.2 Apparatus used for photonitrations at -20°C

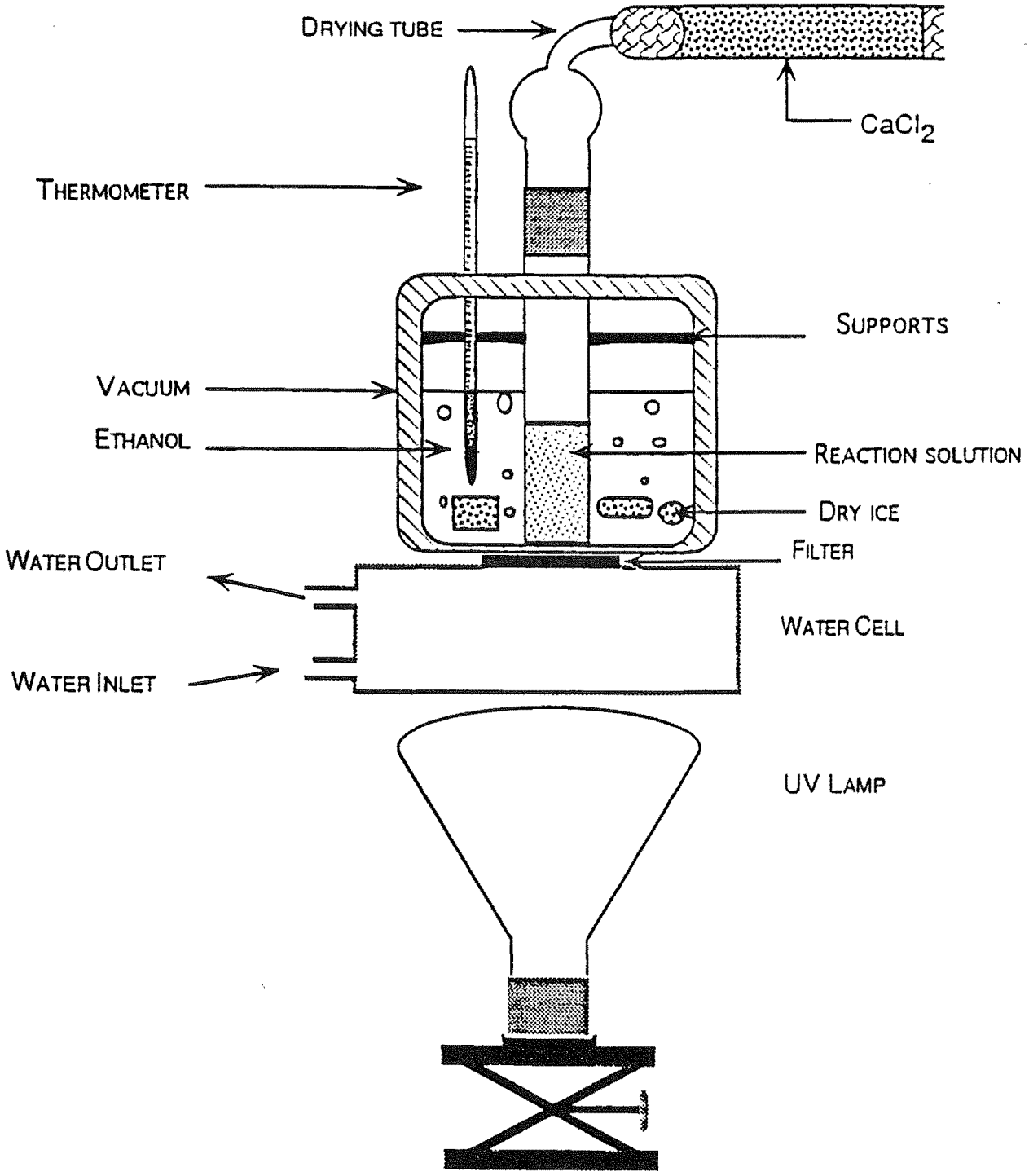

FIGURE 5.3 Apparatus used for -20° to -50°C photonitrations.

5.2 EXPERIMENTAL RELATING TO CHAPTER TWO

General Procedure for the Photonitration of 1,4,5,8-Tetramethylnaphthalene (21) with Tetranitromethane.

A solution of 1,4,5,8-tetramethylnaphthalene (0.34 mol dm^{-3} solution) and tetranitromethane (0.68 mol dm^{-3}) in dichloromethane at -20°C or acetonitrile at -20°C or +20°C was irradiated with filtered light (cut-off < 435 nm). Aliquots were withdrawn at appropriate time intervals, the volatile material removed under reduced pressure at ≤ 0°C, and the product composition determined by ^1H NMR spectral analysis.

5.2.1 Photonitration of 1,4,5,8-Tetramethylnaphthalene in Dichloromethane

Reaction in Dichloromethane at -20°C *and the identification of Products.* - Reaction of 1,4,5,8-tetramethylnaphthalene-tetranitromethane(21) at -20°C, as above, gave, after bleaching of the CT band, a product which was shown by ^1H NMR spectra to be a mixture of adducts (23) (20 %) and (24) (10%), 4,5,8-trimethyl-1-nitromethylnaphthalene (25) (30%), 4,8-dimethyl-1,5-dinitro-methylnaphthalene (26) (27%), and unidentified material (*c.* 13%). The major adduct (23) was isolated by crystallization of the crude product from dichloromethane/pentane at -20°C to give:

1,4,5,8-tetramethyl-r-1-nitro-c-2-trinitromethyl-1,2-dihydronaphthalene, (23) (20 %) m.p.128-135°C (dec.) (Found: C, 47.2; H, 4.2; N, 14.5. $C_{15}H_{16}N_4O_8$ requires C, 47.4; H, 4.2; N, 14.7%) (X-ray crystal structure determined, below). υ_{max} (KBr) 2919, aromatic C-H stretch; 1599, $C(NO_2)_3$; 1552 cm^{-1}, NO_2. ^1H NMR ($CDCl_3$) δ 7.11, d, $J_{H6,H7}$ 7.9 Hz, H6; 7.00, d, $J_{H7,H6}$ 7.9 Hz, H7; 5.76, dq,

$J_{H3,H2}$ 7.9Hz, $J_{H3,Me}$ 1.5Hz, H3; 4.38, d, $J_{H2,H3}$ 7.9Hz, H2; 2.45, s, 5-Me; 2.22, d, $J_{Me,H3}$ 1.5 Hz, 4-Me; 2.17, s, 3H, 1-Me; 2.05, s, 3H, 8-Me. ^{13}C NMR ($CDCl_3$) δ 145.0, C4; 133.7,C6 ; 133.6 , C10; 133.2, C6; 132.9, C7; 132.2, C8; 132.1, C9; 114.4, C3; 92.4, C1; 48.0, C2; 25.6, 1-Me; 23.9, 4-Me; 23.2, 5-Me; 19.4, 8-Me. The above assignments were confirmed by long range reverse detected ^1H - ^{13}C heteronuclear correlation spectra (HMBC).

The two nitromethylnaphthalene derivatives were isolated by chromatography on a silica gel Chromatotron plate (Harrison & Harrison) and gave:

4,8-dimethyl-1,5-dinitromethylnaphthalene, (26), m.p. 173 -175°C (sublimed) (Found: C, 60.7; H, 5.1; N 10.1. $C_{14}H_{14}N_2O_4$ requires C, 61.3; H, 5.1; N, 10.2%). υ_{max} (KBr) 2950, aromatic C-H stretch; 1597, aromatic C=C; 1539 cm^{-1}, NO_2. ^1H NMR (D_6-acetone) δ 7.74, d, $J_{H2,H3}$, $J_{H6,H7}$ 9.8Hz, 2H, H2, H6; 7.61, d, $J_{H3,H2}$, $J_{H7,H6}$ 9.8Hz, 2H, H3, H7; 6.44, s, 4H, 1-CH_2NO_2, 5-CH_2NO_2; 2.98, s, 6H, 4-Me, 8-Me. N.O.e. experiments gave the following results: irradiation at δ 6.44 gave enhancements at δ 2.98 (4%) and 7.74 (4%); irradiation at δ 2.98 gave enhancements at δ 6.44 (7%) and 7.61 (6%). ^{13}C NMR (D_6-acetone) δ 137.3, C4.; 134.6, C9/C10; 134.2, C2/C6; 130.5, C3/C7; 126.6, C1; 80.7, 4-CH_2NO_2, 8-CH_2NO_2; 24.5, 1-Me, 5-Me.

4,5,8-Trimethyl-1-nitromethylnaphthalene, (25), m.p.101-103°C (Lit.101-103).[52,53] υ_{max} (KBr) 2924, aromatic C-H stretch; 1616, aromatic C=C; 1540 cm^{-1}, NO_2. ^1H NMR (D6-benzene) δ 6.95-7.05, m, 3H, H3, H6, H7;6.89, d, $J_{H2,H3}$ 7.4 Hz, H2; 5.47, s, 2H, -CH_2NO_2; 2.60, s, 6H, 4-Me, 5-Me; 2.51, s, 3H, 8-Me. N.O.e. experiments gave the following results: irradiation at δ 5.47 gave enhancements at δ 6.89 (6%) and 2.51 (2%). ^{13}C NMR ($CDCl_3$) δ 139.7; 135.6; 134.9; 134.0; 133.2; 131.5; 130.8; 129.8; 128.6; 124.6; 80.9, CH_2NO_2; 26.8, 26.5, 25.0, methyl carbons.

H.p.l.c. separation of the crude mixture eluting with hexane/dichloromethane mixtures gave the nearly pure (*c* . 90% by ^{1}H NMR)) minor adduct assigned structure 1,4,5,8-tetramethyl-*r*-1-nitro-*t*-2-trinitromethyl-1,2-dihydronaphthalene, (24) (10%), ν_{max} (Nujol) 1607, $C(NO_2)_3$; 1556 cm^{-1}, NO_2. ^{1}H NMR ($CDCl_3$) δ 7.17, d, $J_{H6,H7}$ 9.8 Hz, H6; 7.15, d, $J_{H7,H6}$ 9.8 Hz, H7; 5.96, dq, $J_{H3,H2}$ 6.7 Hz, $J_{H3,Me}$ 1.5 Hz, H3; 5.34, d, $J_{H2,H3}$ 6.7 Hz, H2; 2.47, s, 8-Me; 2.34, s, 5-Me; 2.19, s, 1-Me; 2.09, d, $J_{Me,H3}$ 1.5 Hz, 4-Me. ^{13}C NMR ($CDCl_3$) δ 143.8, C4; 136.0, 134.2, 134.1, 134.0, C5, C6, C7, C10; 133.4, C8; 133.1, C9; 116.5, C3; 94.7, C1; 47.0, C2; 24.3, 23.6, 22.8, 22.6, methyl carbon atoms. The above assignments were confirmed by long range reverse detected ^{1}H - ^{13}C heteronuclear correlation spectra (HMBC).

5.2.2 Photonitration of 1,4,5,8-Tetramethylnaphthalene in Acetonitrile

Reactions in Acetonitrile at +20°C. - Reaction of 1,4,5,8-tetramethylnaphthalene-tetranitromethane at +20°C, as above, gave, after bleaching of the CT band, a product which was shown by ^{1}H NMR spectra to be a mixture of 4,5,8-trimethyl-1-nitromethylnaphthalene, (25) (17%) and 4,8-dimethyl-1,5-dinitromethylnaphthalene, (26) (53%), and unidentified material (30%); no trace of adducts (23) and (24) were detected.

Reactions in Acetonitrile at -20°C. - Reaction of 1,4,5,8-tetramethylnaphthalene-tetranitromethane at -20°C, as above, gave, after bleaching of the CT band, a product which was shown by ^{1}H NMR spectra to be a mixture of adduct (23) (7%), adduct (24) (2%), 4,5,8-trimethyl-1-nitromethylnaphthalene (25)(52%) and 4,8-dimethyl-1,5-dinitromethylnaphthalene (26) (11%), and unidentified material (28%).

5.2.3 Photonitration of 4,5,8-Trimethyl-1-nitromethylnaphthalene (25) with Tetranitromethane in Acetonitrile at +20°C.

Reaction of 4,5,8-trimethyl-1-nitromethylnaphthalene (25) (10 mg) and tetranitromethane (17 mg) in acetonitrile (1 ml) at +20°C, as above, gave after 2 h a product which was shown by ^{1}H NMR spectra to be a mixture (*c.* 1 : 1) of 4,5,8-trimethyl-1-nitromethylnaphthalene (25) and 4,8-dimethyl-1,5-dinitromethylnaphthalene (26), together with considerable amounts (*c.* 65%) of unidentified material, similar to that obtained in the photonitration of 1,4,5,8-tetramethylnaphthalene in acetonitrile at +20°C, above.

Stability of Adduct (23)*in Acetonitrile.* - The adduct (23) (5 mg) was dissolved in D_3-acetonitrile (0.7 ml) and the solution stored at +23°C for 48 h, during which time the ^{1}H NMR spectrum was monitored at appropriate intervals. The ^{1}H NMR spectrum of the solution remained unchanged during this period, indicating the stability of adduct (23) in acetonitrile.

5.3 EXPERIMENTAL RELATING TO CHAPTER 3

General Procedure for the Photonitration of 1,8-Dimethylnaphthalene with Tetranitromethane.

A solution of 1,8-dimethylnaphthalene (500 mg, equal to a 0.4 mol l^{-1} solution) and tetranitromethane (0.8 mol l^{-1}) in dichloromethane or acetonitrile (8 ml) was irradiated at +20°C or -20°C with filtered light (cut-off <435 nm). Aliquots were withdrawn from the reaction mixture at appropriate time intervals, the volatile material removed under reduced pressure at 0°C, and the product composition determined by ^{1}H NMR spectral analysis.

5.3.1 Photonitration of 1,8-Dimethylnaphthalene in Dichloromethane

Reaction of 1,8-dimethylnaphthalene-tetranitromethane in dichloromethane at +20°C, as above, gave, after bleaching of the CT band, a product which was shown by ^{1}H NMR spectra to be a mixture of unidentified aromatic compounds and adducts (total 73%). The adducts were partially separated by h.p.l.c. and gave in elution order:

1,8-Dimethyl-r-1-nitro-t-4-trinitromethyl-1,4-dihydronaphthalene (38), m.p. 119-121°C (X-ray crystal structure determined below), ν_{max} (KBr) 1601, 1560 cm^{-1}. ^{1}H NMR ($CDCl_3$) δ 2.13, s, 1-Me; 2.25, s, 8-Me; 5.51, br d, $J_{H4,H3}$ 4.3 Hz, H4; 6.33, dd, $J_{H2,H3}$ 10.2 Hz, $J_{H2,H4}$ 1.5 Hz, H2; 6.45, dd, $J_{H3,H2}$ 10.2 Hz, $J_{H3,H4}$ 4.4 Hz, H3; 7.13, dd, $J_{H5,H6}$ 6.3 Hz, $J_{H5,H7}$ 2.9 Hz, H5; 7.30-7.70, m, H6, H7. ^{13}C NMR ($CDCl_3$) δ 20.5, 8-Me; 26.3, 1-Me; 45.5, C4; 88.2, C1; 120.7, C3; 125.9, C2; 125.3, C4a; 125.9, C2; 129.9, C5; 133.7, C8a; 134.5, C6 or C7; 138.2, C8; 138.3, C7 or C6; **C**$(NO_2)_3$ resonance not observed. The above assignments were confirmed by long range reverse detected heteronuclear correlation spectra (HMBC).

1,8-Dimethyl-*r*-3-nitro-*t*-4-trinitromethyl-3,4-dihydronaphthalene (39), isolated only in admixture with adduct 33 above. ^{1}H NMR ($CDCl_3$) δ 2.30, d, $J_{Me,H2}$ 1.5 Hz, 1-Me; 2.50, s, 8-Me; 5.61, d, $J_{H4,H3}$ 2.9 Hz, H4; 5.64, br d, $J_{H3,H2}$ 7.3 Hz, H3; 5.80, dq, $J_{H2,H3}$ 7.3 Hz, $J_{H2,Me}$ 1.5 Hz, H2. The structure and stereochemistry of this adduct was confirmed by its thermal cyclization to give the nitro cycloadduct (42), below.

1,8-Dimethyl-*t*-4-nitro-*r*-3-trinitromethyl-3,4-dihydronaphthalene (40), m.p. 168-169°C (dec.) (insufficient for elemental analysis, parent ion not visible in mass

spectrum). ν_{max} (liquid film) 1601, 1565 cm^{-1}. ^1H NMR ($CDCl_3$) δ 2.30, d, $J_{Me,H2}$ 1.5 Hz, 1-Me; 2.52, s, 8-Me; 5.30, br d, $J_{H3,H2}$ 6.9 Hz, H3; 5.64, dq, $J_{H2,H3}$ 6.9 Hz, $J_{H2,Me}$ 1.5 Hz, H2; 5.77, br s, H4; 7.19, dd, $J_{H5,H6}$ 6.8 Hz, $J_{H5,H7}$ 2.4 Hz, H5; 7.30-7.34, m, H6, H7. N.O.e. experiments gave the following results: irradiation at δ 7.19 gave an enhancement at δ 5.77 (4.2%); Irradiation at δ 2.30 gave an enhancement at δ 5.64 (5.3%); irradiation at δ 5.77 gave an enhancement at δ 5.30 (1.7%). ^{13}C NMR ($CDCl_3$) δ 23.6, 8-Me; 24.3, 1-Me; 40.3, C3; 83.4, C4; 113.4, C2; 124.7, C8a; 125.9, C4a; 129.1, 130.9, C6, C7; 131.1, C8; 136.5, C5; 142.3, C1; **C**$(NO_2)_3$ resonance not observed. The above assignments were confirmed by long range reverse detected heteronuclear correlation spectra (HMBC).

1,8-Dimethyl-*r*-1-nitro-*c*-4-trinitromethyl-1,4-dihydronaphthalene (41), m.p. 119-121°C (dec.) (insufficient for elemental analysis, parent ion not visible in mass spectrum), ν_{max} (KBr) 1602, 1572, 1548 cm^{-1}. ^1H NMR ($CDCl_3$) δ 1.97, s, 1-Me; 2.28, s, 8-Me; 5.46, br d, $J_{H4,H3}$ 1.9 Hz, H4; 6.37, m, 2H, H2, H3; 7.09, dd, $J_{H5,H6}$ 7.3 Hz, $J_{H5,H7}$ 1.9 Hz, H5; 7.29-7.37, m, H6, H7. ^{13}C NMR ($CDCl_3$) δ 21.2, 8-Me; 28.1, 1-Me; 44.5, C4; 86.8, C1; 120.4, C3; 125.0, C4a; 125.6, C2; 129.6, C5; 132.8, C8a; 134.7, 136.7, C6 / C7; 138.9, C8; **C**$(NO_2)_3$ resonance not observed. The above assignments were confirmed by long range reverse detected heteronuclear correlation spectra (HMBC).

Nitro cycloadduct (42), m.p. 180°C (sublimed) (X-ray crystal structure determined below), ν_{max} (KBr) 1596, 1557 cm^{-1}. ^1H NMR ($CDCl_3$) δ 2.13, s, 1-Me; 2.51, s, 8-Me; 5.20, dd, $J_{H4,H3}$ 3.9 Hz, $J_{H4,H2}$ 2.9 Hz, H4; 5.46, $J_{H2,H4}$ 2.9 Hz, $J_{H2,H3}$ 2.0 Hz, H2; 5.66, dd, $J_{H3,H4}$ 3.9 Hz, $J_{H3,H2}$ 2.0 Hz, H3; 7.10-7.23, m, H5, H6, H7. N.O.e. experiment gave the following results: irradiation at δ 2.13 gave enhancements at δ 5.46 (9.0%) and δ 2.51 (5.3%). ^{13}C NMR ($CDCl_3$) δ 23.0, 8-Me; 26.3, 1-Me; 45.9, C4; 78.7, C1; 83.2, C2; 90.1, C3;

128.0, C4a; 135.9, 130.3, C6, C7; 134.3, C8a; 129.8, C5; 136.8, C8; **C**$(NO_2)_3$ resonance not observed. The above assignments were confirmed by long range reverse detected heteronuclear correlation spectra (HMBC).

Hydroxy cycloadduct (43), an oil (insufficient for elemental analysis; parent ion not visible in mass spectrum), ν_{max} (liquid film) 3544, 1590, 1558 cm^{-1}. ^1H NMR ($CDCl_3$) δ 2.04, s, 1-Me; 2.56, s, 8-Me; 4.65, dd, $J_{H2,H3}$ ~ 2 Hz, $J_{H2,H4}$ ~ 2 Hz, H2; 4.73, dd, $J_{H4,H2}$ ~ 2 Hz, $J_{H4,H3}$ ~ 4 Hz, H4; 4.86, dd, $J_{H3,H4}$ ~ 4 Hz, $J_{H3,H2}$ ~ 2 Hz, H3; 7.20-7.35, m, H5, H6, H7. N.O.e. experiments gave the following results: irradiation at δ 2.04 gave enhancements at δ 2.56 (2.9%) and δ 4.65 (6.6%); irradiation at δ 4.86 gave enhancements at δ 4.65 (1.5%) and δ 4.73 (2.5%). ^{13}C NMR ($CDCl_3$) δ 23.1, 8-Me; 26.8, 1-Me; 49.6, C4; 66.4, C3; 87.3, C2; 88.5, C1; 129.5, C5; 129.8, C4a; 130.9, C6; 134.8, C8a; 135.2, C7; 136.5, C8; **C**$(NO_2)_3$ resonance not observed. The above assignments were confirmed by long range reverse detected heteronuclear correlation spectra (HMBC).

5.3.2 Thermal Cycloaddition of 1,8-Dimethyl-r-3-nitro-t-4-trinitromethyl-3,4-dihydronaphthalene (39) in (D)-chloroform.

A solution of a mixture (10 mg, *c.* 1 : 1) of 1,8-dimethyl-*r*-3-nitro-*t*-4-trinitromethyl-3,4-dihydronaphthalene (39) and 1,8-dimethyl-*r*-1-nitro-*t*-4-trinitromethyl-1,4-dihydronaphthalene (38) in D-chloroform was stored at 22°C in the dark and the ^1H NMR spectrum monitored at appropriate time intervals. Under these conditions the 1-nitro-4-trinitromethyl adduct (38) was unchanged during the period of observation but the 3-nitro-4-trinitromethyl adduct (39) was slowly transformed (half-life ~ 12 h.) into the nitro cycloadduct. The material isolated by removal of the (D)-chloroform under reduced pressure was shown

(^{1}H NMR) to be a mixture (*c.* 1 : 1) of the 1-nitro-4-trinitromethyl adduct (38) and the nitro cycloadduct (42).

5.3.3 Photonitration of 1,4,5,8-Tetramethylnaphthalene in Acetonitrile

Reaction in Acetonitrile at -20°C and the Identification of 1,8-Dimethyl4-nitro-naphthalene (44).

Reaction of 1,8-dimethylnaphthalene-tetranitromethane at -20°C, as above, gave after 1 h a product which was shown by ^{1}H NMR spectra to be a mixture of unreacted 1,8-dimethylnaphthalene, adducts (38) - (41), 1,8-dimethyl-4-nitronaphthalene (44), and some unidentified aromatic compounds. A pure sample of 1,8-dimethyl-4-nitronaphthalene was isolated by chromatography on a silica gel Chromatotron plate to give:

1,8-Dimethyl-4-nitronaphthalene (44), m.p. 63-64°C (Lit.[19] 65-65.5°C), ν_{max} (KBr) 1514 cm^{-1}. ^{1}H NMR ($CDCl_3$) δ 2.92, Me; 2.95, Me; 7.31, d, $J_{H7,H6}$ 7.7 Hz, H7; 7.40, d, $J_{H5,H6}$ 6.8 Hz, H5; 7.51, dd, $J_{H6,H5}$ 6.8 Hz, $J_{H6,H7}$ 7.7 Hz, H7; 7.88, d, $J_{H2,H3}$ 8.8 Hz, H2; 8.22, $J_{H3,H2}$ 8.8 Hz, H3. ^{13}C NMR ($CDCl_3$) δ 26.4, 26.7, 121.6, 122.1, 127.5, 127.9, 128.0, 128.1, 131.0, 131.1, 136.2, 142.6.

The unidentified aromatic compounds could not be separated by chromatography.

5.3.4 Photonitration of 1,8-Dimethyl-4-nitronaphthalene (44) with Tetranitromethane in Dichloromethane at +20°C.

Reaction of 1,8-dimethyl-4-nitronaphthalene (44) (100 mg) and tetranitromethane (196 mg) in dichloromethane (4 ml) at +20°C, as above, gave after 1 h a product which was shown by ^{1}H NMR spectra to be a mixture of products, with considerable amounts (*c.* 65%) of unidentified material, similar to

that obtained in the photonitration of 1,8-dimethylnaphthalene in dichloromethane at +20°C, above.

5.4 EXPERIMENTAL RELATING TO CHAPTER 4

General Procedure for the Photonitration of 1-Methylnaphthalene with Tetranitromethane.

A solution of 1-methylnaphthalene (500 mg, equal to a 0.4 mol l^{-1} solution) and tetranitromethane (0.8 mol l^{-1}) in dichloromethane or acetonitrile (8 ml) was irradiated at +20°C with filtered light (cut-off <435 nm). Aliquots were withdrawn from the reaction mixture at appropriate time intervals, the volatile material removed under reduced pressure at 0°C, and the product composition determined by ^{1}H NMR spectral analysis.

5.4.1 Photonitration of 1-Methylnaphthalene in Dichloromethane

Reaction in Dichloromethane at +20°C *and the Identification of Products.*

Reaction of 1-methylnaphthalene-tetranitromethane in dichloromethane at +20°C, as above, gave, after bleaching of the CT band, a product which was shown by ^{1}H NMR spectra to be a mixture of adducts (total 69%) and a mixture of unidentified nitroaromatic compounds. The adducts were partially separated by h.p.l.c. and gave in elution order:

1-Methyl-r-3-nitro-t-4-trinitromethyl-3,4-dihydronaphthalene (61), m.p. 89-91°C (X-ray crystal structure determined below). Insufficient material for infrared spectrum. ^{1}H NMR ($CDCl_3$) δ 2.20, d, $J_{Me,H2}$ 1.0 Hz, Me; 5.63, d, $J_{H3,H2}$ 6.9 Hz, H3; 5.73, br s, H4; 5.85, dq, $J_{H2,H3}$ 6.9 Hz, $J_{H2,Me}$ 1.0 Hz, H2; 7.20, d,

$J_{H5,H6}$ 6.9 Hz, H5; 7.35-7.46, m, H6, H7, H8. ^{13}C NMR ($CDCl_3$) δ 19.2, Me; 43.8, C4; 88.6, C3; 113.0, C2; 120.7, C4a; 134.1, C8a; 125.1, 129.9, 130.3, 131.5, C5, C6, C7, C8; 141.9, C1; **C**$(NO_2)_3$ resonance not observed. The above assignments were confirmed by long range reverse detected heteronuclear correlation spectra (HMBC).

1-Methyl-*r*-1-nitro-*t*-4-trinitromethyl-1,4-dihydronaphthalene (62), an unstable oil. ^1H NMR ($CDCl_3$) δ 2.08, s, Me; 5.51, br d, $J_{H4,H3}$ 3.9 Hz, H4; 6.44, br d, $J_{H2,H3}$ 10.7 Hz, $J_{H2,H4}$ 1.0 Hz, H2; 6.51, dd, $J_{H3,H2}$ 10.7 Hz, $J_{H3,H4}$ 3.9 Hz, H3; 7.28, br d, $J_{H5,H6}$ 7.8 Hz, H5; 7.44-7.60, m, H6, H7, H8. ^{13}C NMR ($CDCl_3$) δ 28.0, Me; 44.3, C4; 86.9, C1; 121.3, C3; 127.1, C2; 124.3, 127.7, 130.5, 130.8, 135.1, 135.6, C4a, C5, C6, C7, C8, C8a; **C**$(NO_2)_3$ resonance not observed. The above assignments were confirmed by long range reverse detected heteronuclear correlation spectra (HMBC).

1-Methyl-r-*1-nitro*-c-*4-trinitromethyl-1,4-dihydronaphthalene* (63), m.p. 88-89°C (X-ray crystal structure determined below). $\nu_{(max)}$ (KBr) 1598, 1577, 1542 cm^{-1}. ^1H NMR ($CDCl_3$) δ 2.03, s, Me; 5.33, m, H4; 6.59, m, 2H, H2, H3; 7.19, br d, $J_{H5,H6}$ 7.8 Hz, H5; 7.40-7.60, m, H6, H7; 8.02, dd, $J_{H8,H7}$ 8.3 Hz, $J_{H8,H6}$ 1.5 Hz, H8. ^{13}C NMR ($CDCl_3$) δ 30.9, Me; 44.5, C4; 87.2, C1; 122.1, 127.5, 130.3, 130.5, 130.6, 130.7, 130.9, 136.0, C2, C3, C4a, C5, C6, C7, C8, C8a; **C**$(NO_2)_3$ resonance not observed. The above assignments were confirmed by long range reverse detected heteronuclear correlation spectra (HMBC).

8-Methyl-r-*1-nitro*-c-*4-trinitromethyl-1,4-dihydronaphthalene* (64), m.p. 129-131°C (X-ray crystal structure determined below). $\nu_{(max)}$ (KBr) 1595, 1552 cm^{-1}. ^1H NMR ($CDCl_3$) δ 2.36, s, Me; 5.39, m, H4; 6.04, dd, $J_{H1,H2}$ 5.4 Hz, $J_{H1,H4}$ 2.9 Hz, H1; 6.64, dd, $J_{H3,H2}$ 10.2 Hz, $J_{H3,H4}$ 4.4 Hz, H3; 6.88, dd, $J_{H2,H3}$ 10.2 Hz, $J_{H2,H1}$ 5.4 Hz, H2; 7.12, 7.44, both m, H5, H6, H7. N.O.e.

experiments gave the following results: irradiation at δ 5.39 gave enhancements at δ 6.64 (7.3%) and δ 7.12 (3.8%); irradiation at δ 6.04 gave enhancements at δ 2.36 (2.5%) and δ 6.88 (4.7%). ^{13}C NMR ($CDCl_3$) δ 19.5, Me; 45.1, C4; 79.2, C1; 125.8, C5; 126.3, C3; 127.4, C4a; 127.6, C8a; 130.4, C6; 130.9, C2; 132.8, C7; 141.1, C8; **C**$(NO_2)_3$ resonance not observed.

Nitro cycloadduct (65), m.p. 159-160°C (X-ray crystal structure determined below). $\nu_{(max)}$ (KBr) 1587, 1560 cm^{-1}. ^1H NMR ($CDCl_3$) δ 2.04, s, 1-Me; 5.26, dd, $J_{H4,H3}$ 4.0 Hz, $J_{H4,H2}$ 2.0 Hz, H4; 5.51, dd, $J_{H2,H4}$ 2.0 Hz, $J_{H2,H3}$ 2.0 Hz, H2; 5.72, dd, $J_{H3,H4}$ 4.0 Hz, $J_{H3,H2}$ 2.0 Hz, H3; 7.30-7.46, m, H5, H6, H7, H8. ^{13}C NMR ($CDCl_3$) δ 20.5, Me; 45.5, C4; 79.3, C1; 81.1, C2; 87.2, C3; 124.6, C8; 126.4, C4a; 130.6, 130.9, 131.2, C5, C6, C7; 136.4, C8a; **C**$(NO_2)_3$ resonance not observed. The above assignments were confirmed by long range reverse detected heteronuclear correlation spectra (HMBC).

r-1-Hydroxy-8-methyl-*c*-4-trinitromethyl-1,4-dihydronaphthalene (66), m.p. 86-87°C (insufficient for elemental analysis; parent ion not visible in mass spectrum). $\nu_{(max)}$ (KBr) 3447, 1619, 1594, 1570 cm^{-1}. ^1H NMR ($CDCl_3$) δ 2.53, s, Me; 5.13, m, H1; 5.25, m, H4; 6.39, dd, $J_{H3,H2}$ 10.2 Hz, $J_{H3,H4}$ 4.6 Hz, H3; 6.60, dd, $J_{H2,H3}$ 10.2 Hz, $J_{H2,H1}$ 5.2 Hz, H2; 7.00, br d, $J_{H5,H6}$ 7.3 Hz, H5; 7.23-7.33, m, H6, H7. N.O.e. experiments gave the following results: irradiation at δ 5.25 gave enhancements at δ 6.39 (3.0%) and δ 7.00 (2.5%); irradiation at δ 2.53 gave an enhancement at δ 5.13 (4.7%). ^{13}C NMR ($CDCl_3$) δ 19.1, Me; 45.2, C4; 62.5, C1; 121.9, C2; 125.6, C3; 126.4, C7, 129.1, C6; 132.5, C5; 136.2, C4a; 138.1, C8; 140.1, C8a; **C**$(NO_2)_3$ resonance not observed.

Hydroxy cycloadduct (67), m.p. 182-184°C (X-ray crystal structure determined below). $\nu_{(max)}$ (KBr) 3541, 1587 cm^{-1}. ^1H NMR ($CDCl_3$) δ 1.94, s, Me; 4.71,

dd, $J_{H2,H3}$ 2.4 Hz, $J_{H2,H4}$ 2.4 Hz, H2; 4.77, dd, $J_{H4,H2}$ 2.4 Hz, $J_{H4,H3}$ 3.9 Hz, H4; 4.96, br s, H3; 7.34-7.49, m, H5, H6, H7, H8. N.O.e. experiments gave the following results: irradiation at δ 1.94 gave enhancements at δ 4.71 (6.3%) and δ 7.36 (3.7%); irradiation at δ 7.34-7.49 gave enhancements at δ 1.94 (1.0%) and δ 4.77 (2.3%). ^{13}C NMR ($CDCl_3$) δ 20.9, Me; 49.0, C4; 66.9, C3; 85.0, C2; 85.8, C1; 124.3, C8; 128.7, C4a; 130.1, 130.2, C6, C7; 131.8, C5; 137.5, C8a; **C**$(NO_2)_3$ resonance not observed.

5.4.2 Thermal Cycloaddition of 4-Methyl-t-2-nitro-r-1-trinitromethyl-1,2-dihydro naphthalene (59)in (D)-chloroform.

A solution of the nitro trinitromethyl adduct (59) (1.5 mg) in D-chloroform was stored at 22°C in the dark and the ^1H NMR spectrum monitored at appropriate time intervals. The nitro trinitromethyl adduct (59) was slowly transformed (half-life 29 h) into the nitro cycloadduct (63) (see Fig. 7). The material isolated by removal of the (D)-chloroform under reduced pressure was identical with an authentic sample, above.

5.4.3 Photonitration of 1-Methylnaphthalene in Acetonitrile

Reaction of 1-Methyl\naphthalenei n Acetonitrile at -20 and +20°C.

Reaction of 1-methylnaphthalene-tetranitromethane Acetonitrile at -20 and +20°C as above, gave, after bleaching of the CT band, a product which was shown by ^1H NMR spectra to be a mixture of adducts (total up to 80%) and a mixture of unidentified nitroaromatic compounds.

APPENDIX I

PHOTONITRATION OF BENZENE

5.5 PHOTONITRATION OF BENZENE WITH TNM

We undertook a study of the photonitration of benzene to determine if even very unreactive monocyclic aromatics would form addition products derived from reaction within the triad of the benzene radical cation and the trinitromethanide ion followed by radical coupling with $^{\bullet}NO_2$.

General procedure for the photonitration of benzene with tetranitromethane.

A solution of benzene (0.8 mol dm^{-3}) and tetranitromethane (1.6 mol dm^{-3}) in dichloromethane or acetonitrile at +20°C was irradiated with filtered light (cut-off ≥ 435 nm). Aliquots were withdrawn at appropriate time intervals, the volatile material was removed under reduced pressure at ≤ 0°C and the product composition determined by NMR spectral analysis.

5.6 PHOTONITRATION OF BENZENE WITH TNM IN DICHLOROMETHANE

Reaction of benzene at +20°C, as above, for 48 h gave a product which was shown by ^1H NMR spectra to be a mixture of products which were characterised as summarised below and in Table 5.1.

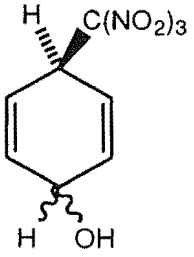

(74a) and 74(b)

The *cis*- and *trans*- 1-hydroxy-4-trinitromethylcyclohexa-2,5-dienes (74) could not be isolated but their structures were deduced from the analysis of NMR spectra of the crude product mixture in $CDCl_3$.[79,80] (See Experimental details at end of Appendix I.)

The following products were isolated from the product mixture by chromatography on a silica gel Chromatotron plate (Harrison & Harrison) using pentane and ether mixtures as the eluting solvents.

(i) Nitrobenzene (75), identical with an authentic sample.

(ii) 1,3-Dinitrobenzene (76), identical with an authentic sample.

(iii) 1,3-Dinitro-5-trinitromethylbenzene (77), ^{1}H NMR ($CDCl_3$) δ 9.42, dd, J' = 1.9 Hz, H2; 8.91, d, J 1.9 Hz, H4, H6.

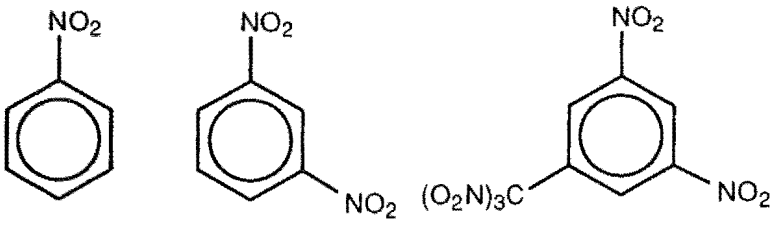

(75) (76) (77)

A sample of 1,3-dinitro-5-trinitromethylbenzene was heated under reflux for 16 h. with concentrated hydrochloric acid. The material isolated by means of ether was shown by ^{1}H NMR spectra to be 3,5-dinitrobenzoic acid (78) as illustrated in Scheme 5.1.

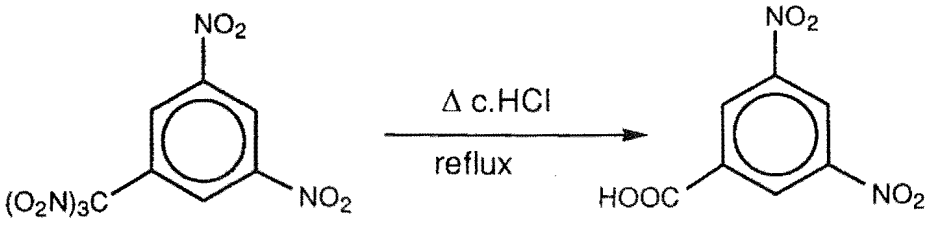

(77) (78)

SCHEME 5.1

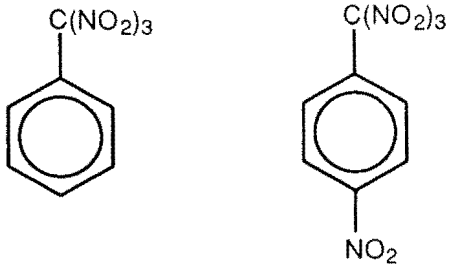

(79) (80)

(iv) A mixture of trinitromethylbenzene (79) and 4-trinitromethylnitrobenzene (80), ^{1}H NMR ($CDCl_3$) δ 7.62, d, *J* 3.4 Hz; 7.63, s; 7.57-7.66, m; 7.72-7.79, m; relative integrals for total regions δ 7.57-7.66 : 7.72-7.79, *c.* 4 : 1. A sample of this mixture was heated under reflux for 18 h with concentrated hydrochloric acid . The material isolated by means of ether was shown by ^{1}H NMR spectra (D_6-acetone) to be a mixture (*c.* 3 : 4) of benzoic acid (81) and 4-nitrobenzoic acid (82) as illustrated in Scheme 5.2.

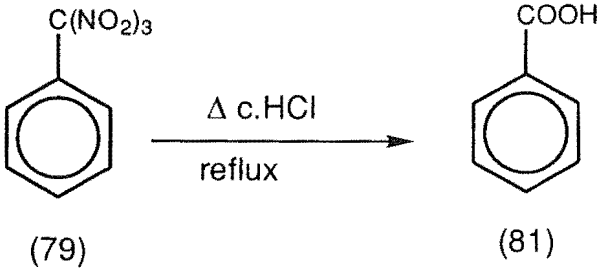

(79) (81)

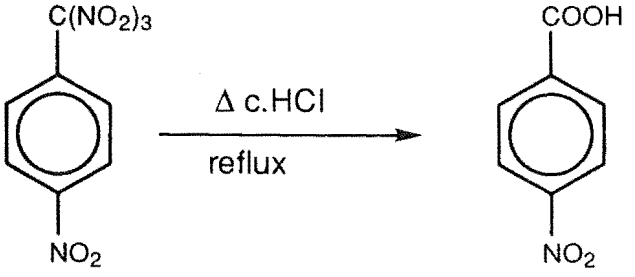

(80) (82)

SCHEME 5.2

H.p.l.c. separation of the product mixture on a Varian 5000 liquid chromatograph equipped with an Alltech cyanopropyl column and Varian UV-50 detector eluting with hexane-dichloromethane mixtures gave:

(v) 2,4-Dinitrophenol (83), identical with an authentic sample.

The following products were not isolated from the product mixture, but were identified from their ^1H NMR spectra and comparison with authentic samples:

(vi) 2,4,6-Trinitrophenol (84),

(vii) 2,6-Dinitrophenol (85),

(viii) 1,3,5-Trinitrobenzene (86).

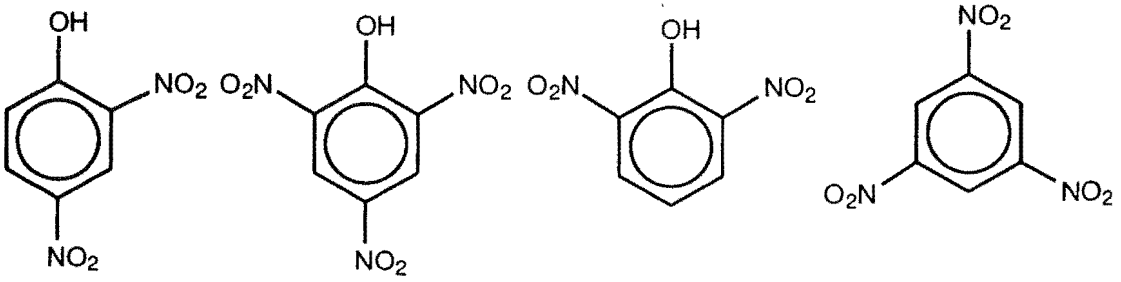

(83) (84) (85) (86)

The photolysis of benzene at +20°C and the formation of products was studied with time and an overview of the product yields is presented in Table 5.1.

Table 5.1. Overview of product yields from the photolysis of benzene (0.8 mol dm^{-3}) and tetranitromethane (1.6 mol dm^{-3}) in dichloromethane at +20°C.

	Absolute yield (%)		
Reaction period (h)	12	24	48
Adduct (74a)	1.2	2.6	6.5
Adduct (74b)	1.2	2.6	6.5
Nitrobenzene (75)	0.1	0.3	0.7
1,3-Dinitrobenzene (76)	0.2	0.4	1.2
1,3-Dinitro-5-trinitromethylbenzene (77)	0.1	0.1	0.4
Trinitromethylbenzene (79)	0.4	1.0	3.3
4-Trinitromethylnitrobenzene (80)	0.3	0.9	3.0
2,4-Dinitrophenol (83)	0.3	0.6	2.3
2,4,6-Trinitrophenol (84)	0	0	0.3
2,6-Dinitrophenol (85)	0.1	0.2	0.6
1,3,5-Trinitrobenzene (86)	0	0	0.1

The formation of these nitro and trinitromethyl aromatic products probably involves adduct decomposition through elimination of nitroform. Interesting nitration conditions must develop over the course of the photonitration reaction to obtain products such as 1,3,5-trinitrobenzene. Formation of the phenol products presumably arise from the hydroxy adducts after elimination of nitroform during the course of the reaction and /or workup.

5.7 PHOTONITRATION OF BENZENE WITH TNM IN ACETONITRILE

Reaction of benzene at +20°C in acetonitrile for 48 h under the same conditions as above gave a mixture of products similar to those obtained in

dichloromethane however one further product (87) was characterised from the acetonitrile reaction that was not observed in dichloromethane. The results are summarised in Table 5.2.

Table 5.2. Overview of product yields from the photolysis of benzene (0.8 mol dm^{-3}) and tetranitromethane (1.6 mol dm^{-3}) in acetonitrile at +20°C.

	Absolute yield (%)		
Reaction period (h)	12	24	48
Adduct (74a)	1.6	1.0	3.2
Adduct (74b)	0.8	0.5	1.6
Nitrobenzene (75)	0.3	0.5	7.0
1,3-Dinitrobenzene (76)	0.2	0.4	1.2
1,3-Dinitro-5-trinitromethylbenzene (77)	0.1	0.1	0.4
Trinitromethylbenzene (79)	1.7	3.8	10.9
4-Trinitromethylnitrobenzene (80)	0.4	0.8	2.4
2,4-Dinitrophenol (83)	0.8	1.1	5.3
2,4,6-Trinitrophenol (84)	0.2	0.15	1.1
2,6-Dinitrophenol (85)	0.25	0.4	0
1,3,5-Trinitrobenzene (86)	0	0	0.2
5-methyl-3-(4-nitrophenyl)-1,2,4-oxadiazole (87)	0.4	1.1	1.7

Reaction in acetonitrile at +20°C and isolation of 5-methyl-3-(4-nitrophenyl)-1,2,4-oxadiazole (87)

Reaction of benzene at +20°C, as above, for 48 h gave a product which was shown by NMR spectra to be a mixture of products as summarized in Table 5.2. Chromatography of this mixture of products on a silica gel Chromatotron plate and elution with pentane gave first a mixture (*c.* 5 : 1) of trinitromethylbenzene

(79) and 4-nitro-1-trinitromethylbenzene (80). The second material eluted was a small amount (yield *c.* 1.7%) of a compound the structure of which remains unknown.

Next was eluted *5-methyl-3-(4-nitrophenyl)-1,2,4-oxadiazole (87)*, m.p. 142-144° (X-ray crystal structure determined below), ν_{max} (KBr) 1612, 1584, C=N; 1539 cm^{-1}, NO_2. ^1H NMR ($CDCl_3$) δ 8.35, 8.27, ABq, *J* 9.3 Hz, 4H, phenyl-H; 2.70, s, Me. ^{13}C NMR ($CDCl_3$) δ 177.4, C5; 166.9, C3; 132.7, C4'; 129.9, C1'; 128.3, C3', C5'; 124.1, C2', C6'; 12.4, CH_3.

This compound is formally a 1,3-dipolar addition product of 4-nitrophenyl nitrile oxide (88) and acetonitrile. A perspective drawing is presented in Figure 5.4 and the corresponding coordinates are given in Table 5.11.

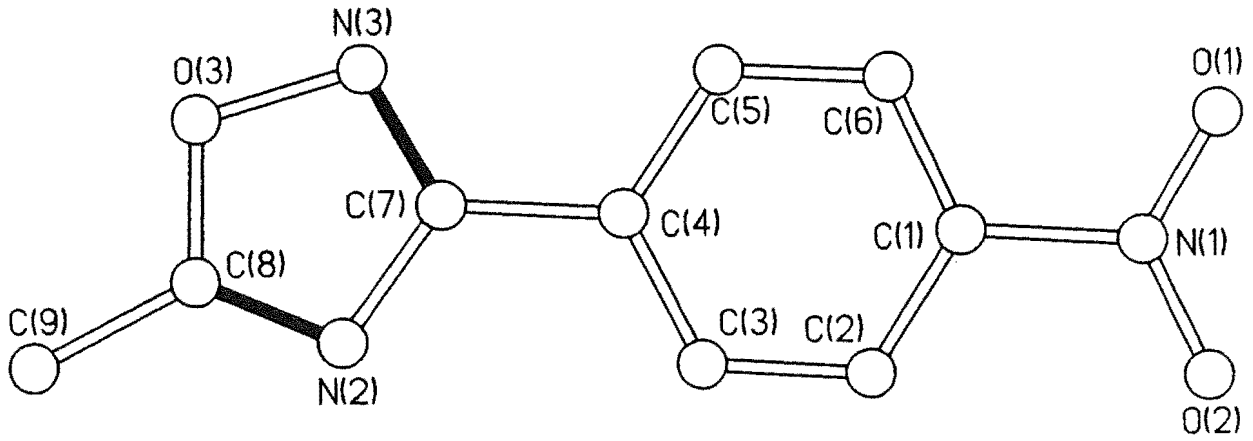

FIGURE 5.4 Perspective drawing of compound (87)

In the solid state the heterocyclic ring is essentially planar, and that plane is slightly displaced from coplanarity with the benzene ring [torsional angles: N(3)-C(7)-C(4)-C(5) 10.6(2)°, N(2)-C(7)-C(4)-C(3) 10.0(2)°], as is the plane of the nitro group [torsional angles: O(1)-N(1)-C(1)-C(6) -10.6(2)°, O(2)-N(1)-C(1)-C(2) -9.9(2)°]. The bond lengths in the heterocyclic ring are closely similar to those found[77] for the pyridyl derivative (88) (Figure. 5.5).

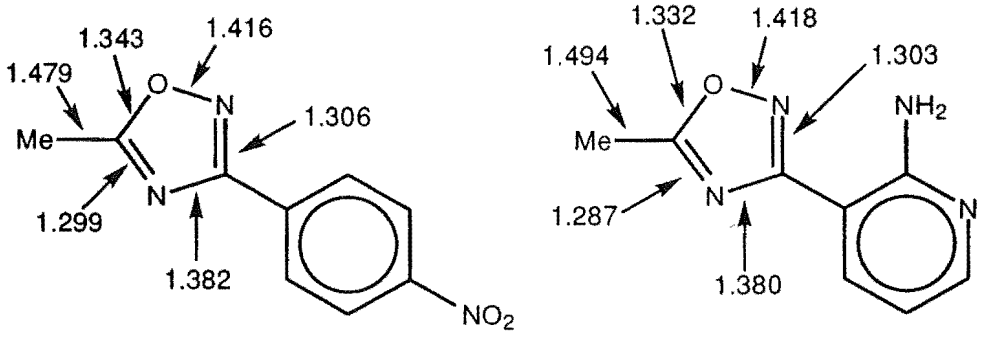

(87) (88)

FIGURE 5.5 Comparison of bond lengths for the similar compounds (87) and (88)

The spectroscopic data for compound (87) were in accord with the established structure.

Formation of the 1,3-dipolar addition product (87). The heterocyclic compound (87) is formally the product of 1,3-dipolar addition of 4-nitrophenyl nitrile oxide (88) and acetonitrile [c.f. ref. 78].

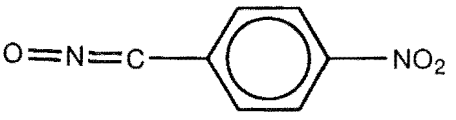

(88)

It seems likely that the nitrile oxide functionality is generated from a trinitromethyl group during the photolysis reaction, the nitrile oxide group then

reacting with the solvent, acetonitrile. As one of the products of the photolysis of the TNM/benzene charge-transfer complex is 4-trinitromethylnitrobenzene (80), this compound is the probable precursor of the proposed intermediate, 4-nitrophenyl nitrile oxide. However, as trinitromethylbenzene (79) is also present among the reaction products it is not possible to exclude a sequence of steps which include phenyl nitrile oxide formation, cycloaddition with acetonitrile, and subsequent nitration at C4 of the 5-methyl-3-phenyl-1,2,4-oxadiazole so formed.

5.8 X-RAY DISCUSSION RELATING TO THE SOLUTION OF STRUCTURE (87)

Obtaining the X-ray structure for product (87) required quite some effort. The product (87) was recrystallised from an ether/pentane mixture. The crystals obtained were thin colourless plates and were of appropriate quality for single crystal X-ray analysis. However, once the selected crystal was placed in the nitrogen air stream at -153°C on the diffractometer the crystal disintegrated. At such a low temperature there was a phase change within the crystal and the critical temperature for the phase change was found to be ≈ -140°C. The next attempt involved collection of the data at room temperature. This method gave good data and initial attempts at solving the data suggested that the structure (89) was as illustrated below and in Fig 5.6. This structure agreed with the NMR data that we had obtained. And we suggested that 1,4-dinitrobenzene had reacted either by a thermal or photochemical reaction with acetonitrile giving product (89) with a Mr of 209.

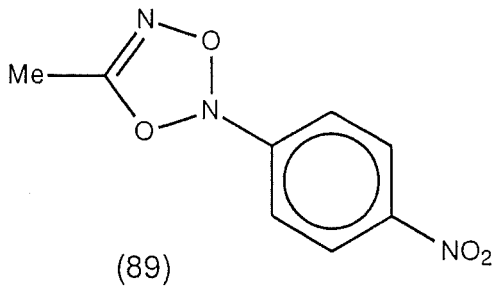

(89)

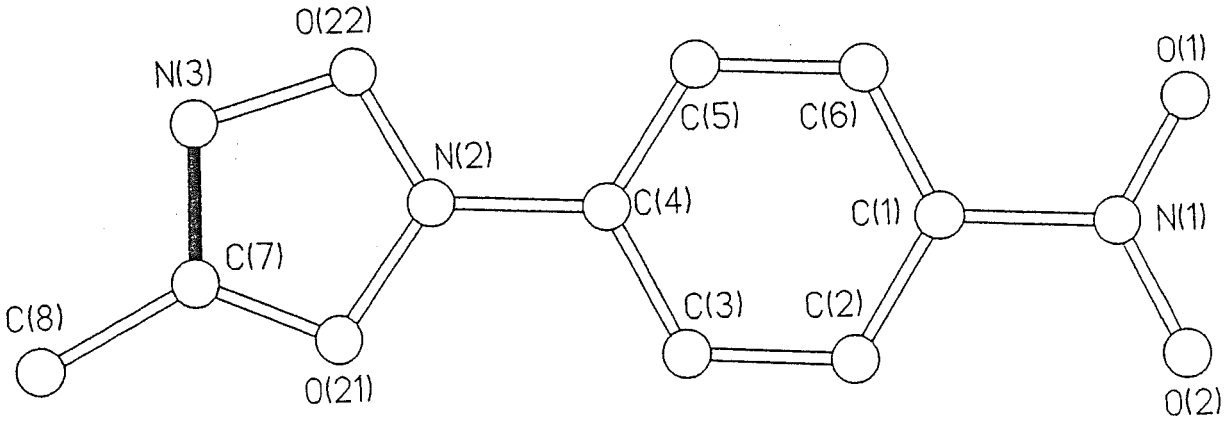

FIGURE 5.6

A perspective diagram of compound (89).

Although the data observed from the collection at room temperature was reasonable the refinement of the structure (89) illustrated in Figure 5.2 was not adequate and the R-factor related to that structure was at 8%. We thought that the room temperature collection was unsatisfactory and that recollection at a lower temperature would be more beneficial. Hence, the recollection of the data at -90°C was undertaken giving an improved cell refinement and 84% observed data. This meant that the data obtained was of excellent quality and was not going to be the limiting factor in the refinement. However, using the solution obtained above, followed by refinement with the excellent data there was no difference observed in the refinement with the R-factor still at ≈ 7%. Close inspection of the thermal ellipsoids and temperature factors indicated that some of the atoms in the heterocyclic ring were not refining satisfactorily. However it was not immediately obvious what was causing this. Mass spectrometry was then employed to obtain a parent ion for the product and this resulted in giving

an Mr of 205 as opposed to that of structure (89) being 207. It was at this stage realised that the heterocyclic ring was not as had originally been perceived and that upon closer inspection of thermal parameters and applying that the parent ion had a Mr of 205 did we obtain the structure (87) illustrated in Fig. 5.1. Subsequent refinement of the new structure (87) gave an excellent R-factor of 3.8%.

5.9 EXPERIMENTAL

General procedure for the photonitration of benzene with tetranitromethane.

A solution of benzene (0.8 mol dm^{-3}) and tetranitromethane (1.6 mol dm^{-3}) in dichloromethane or acetonitrile at +20°C was irradiated with filtered light (cut-off < 435 nm). Aliquots were withdrawn at appropriate time intervals, the volatile material was removed under reduced pressure at ≤ 0°C and the product composition determined by NMR spectral analysis (Tables 5.1 and 5.2).

Reaction in dichloromethane at +20°C and the identification of products. Reaction of benzene at +20°C, as above, for 48 h gave a product which was shown by ^{1}H NMR spectra to be a mixture of products as summarised in Table 5.1.

The *cis*- and *trans*- 1-hydroxy-4-trinitromethylcyclohexa-2,5-dienes (74) could not be isolated but their structures were deduced from the analysis of NMR spectra of the crude mixture in $CDCl_3$. Isomer (74a), ^{1}H NMR δ 6.59, ddd, $J_{3,2}$ 10.4 Hz, $J_{3,4}$ 3.9 Hz, $J_{3,1}$ 1.9 Hz, H3 (H5); 6.22, ddd, $J_{2,3}$ 10.4 Hz, $J_{2,1}$ 3.4 Hz, $J_{2,4}$ 1.6 Hz, H2 (H6); *c.* 5.48, m, H4; *c.* 4.64, m, H1. Isomer (74b), ^{1}H NMR δ 6.62, ddd, $J_{3,2}$ 10.4 Hz, $J_{3,4}$ 3.1 Hz, $J_{3,1}$ 2.1 Hz, H3 (H5); 6.24, ddd, $J_{2,3}$ 10.4 Hz, $J_{2,1}$ 3.5 Hz, $J_{2,4}$ 2.2 Hz, H2 (H6); *c.* 5.48, m, H4; *c.* 4.64, m, H1. By long

range reverse detected ^{1}H-^{13}C heteronuclear correlation spectra (HMBC) the ^{13}C NMR spectrum of adducts (74) was partially defined, ^{13}C NMR δ 41.21, C4 [(74a), (74b)]; 77.54, 77.62, C1 [(74a), (74b)]; 123.88, C3, C5 [(74a), (74b)]; 127.65, C2, C6 [(74a), (74b)].

The following products were isolated from the product mixture by chromatography on a silica gel Chromatotron plate (Harrison & Harrison) using pentane and ether mixtures as the eluting solvents.

(i) Nitrobenzene (75), identical with an authentic sample.

(ii) 1,3-Dinitrobenzene (76), identical with an authentic sample.

(iii) 1,3-Dinitro-5-trinitromethylbenzene (77), ^{1}H NMR ($CDCl_3$) δ 9.42, dd, J' = 1.9 Hz, H2; 8.91, d, J 1.9 Hz, H4, H6. A sample of 1,3-dinitro-5-trinitromethylbenzene (77) (4.3 mg) was heated under reflux for 16 h with concentrated hydrochloric acid (0.1 ml). The material (3.9 mg) isolated by means of ether was shown by ^{1}H NMR spectra to be 3,5-dinitrobenzoic acid (78).

(iv) A mixture of trinitromethylbenzene (79) and 4-trinitromethylnitrobenzene (80), ^{1}H NMR ($CDCl_3$) δ 7.62, d, J 3.4 Hz; 7.63, s; 7.57-7.66, m; 7.72-7.79, m; relative integrals for total regions δ 7.57-7.66 : 7.72-7.79, *c.* 4 : 1. A sample (43 mg) of this mixture was heated under reflux for 18 h with concentrated hydrochloric acid (1 ml). The material (38 mg) isolated by means of ether was shown by ^{1}H NMR spectra (D_6-acetone) to be a mixture (*c.* 3 : 4) of benzoic acid (81) and 4-nitrobenzoic acid (82).

H.p.l.c. separation of the product mixture on a Varian 5000 liquid chromatograph equipped with an Alltech cyanopropyl column and Varian UV-50 detector eluting with hexane-dichloromethane mixtures gave:

(v) 2,4-Dinitrophenol (83), identical with an authentic sample.

The following products were not isolated from the product mixture, but were identified from their ^1H NMR spectra and comparison with authentic samples:

(vi) 2,4,6-Trinitrophenol (84),

(vii) 2,6-Dinitrophenol (85),

(viii) 1,3,5-Trinitrobenzene (86).

Attempted photonitration of nitrobenzene (75) with tetranitromethane. A solution of nitrobenzene (0.5 mol dm^{-3}) and tetranitromethane (1.0 mol dm^{-3}) in dichloromethane or acetonitrile at +20°C was irradiated with filtered light (cut-off > 435 nm) for 48 h. The volatile material was removed under reduced pressure at ≤ 0°C and the product composition determined by NMR spectral analysis. In both solvents, only nitrobenzene (75) was recovered in good yield from the attempted reactions.

Attempted photonitration of 2,6-dinitrophenol (83) with tetranitromethane. A solution of 2,6-dinitrophenol (83) (20 mg) in acetonitrile (1 ml) and tetranitromethane (43 mg) was irradiated with filtered light (cut-off ≥ 435 nm) at +20°C for 48 h. The volatile material was removed under reduced pressure at ≤ 0°C and the product composition determined by NMR spectral analysis. Only 2,6-dinitrophenol (83) was recovered in good yield from the attempted reaction.

Attempted photonitration of a mixture (c. 3 : 4) of trinitromethylbenzene (79) and 4-trinitromethylnitrobenzene (80) with tetranitromethane. A solution of the mixture (3 : 4) (37 mg) of trinitromethylbenzene and 4-trinitromethylnitrobenzene in acetonitrile (1 ml) and tetranitromethane (59 mg) was irradiated with filtered light (cut-off ≥ 435 nm) at 20°C for 48 h. The volatile material was removed under reduced pressure at ≤ 0°C and the product composition determined by NMR spectral analysis. The product (35 mg) was a similar mixture of

trinitromethylbenzene (79) and 4-trinitromethylnitrobenzene (80) to that used for the attempted reaction.

Reaction in acetonitrile at +20°C and isolation of 5-methyl-3-(4-nitrophenyl)-1,2,4-oxadiazole (87)

Reaction of benzene at +20°C, as above, for 48 h gave a product which was shown by NMR spectra to be a mixture of products as summarized in Table 5.2. Chromatography of this mixture of products on a silica gel Chromatotron plate and elution with pentane gave first a mixture (*c.* 5 : 1) of trinitromethylbenzene and 4-nitro-1-trinitromethylbenzene. The second material eluted was a small amount (yield *c.* 1.7%) of a compound the structure of which remains unknown. Next was eluted *5-methyl-3-(4-nitrophenyl)-1,2,4-oxadiazole (87)*, m.p. 142-144° (X-ray crystal structure determined below), ν_{max} (KBr) 1612, 1584, C=N; 1539 cm^{-1}, NO_2. ^1H NMR ($CDCl_3$) δ 8.35, 8.27, ABq, *J* 9.3 Hz, 4H, phenyl-H; 2.70, s, Me. ^{13}C NMR ($CDCl_3$) δ 177.4, C5; 166.9, C3; 132.7, C4'; 129.9, C1'; 128.3, C3', C5'; 124.1, C2', C6'; 12.4, CH_3.

Further elution with pentane and pentane/ether gave only mixtures of what appeared to be products of decomposition of materials initially present.

APPENDIX II

5.10 CRYSTALLOGRAPHY

Crystal data, from a Siemens R3m/V four-circle diffractometer [molybdenum X-radiation, λ(Mo Kα) 0.71069 Å, from a crystal monochromator], are given below. In each case the space group was determined unambiguously as a result of the structure analysis reported below, but initially indicated by conditions limiting possible reflections. ω-Scans were used to collect reflection intensities out to a maximum Bragg angle θ, given below. The cell parameters were determined by least-squares refinements for which the setting angles of 20-25 accurately centred high-angle reflections were used.

Crystal Data

1,4,5,8-Tetramethyl-r-1-nitro-c-2-trinitromethyl-1,2-dihydronaphthalene (23). - $C_{15}H_{16}N_4O_8$, *M* 380.32, triclinic, space group $P\bar{1}$,*a* 6.4040(3), *b* 9.553(5), *c* 14.08(1) Å; α 83.74(5), β 86,12(5) ,γ 75.70(4)° *V* 829.1(8) Å^3, D_C 1.523 g cm^{-3}, Z 2, μ(Mo Kα) 1.26 cm^{-1}. The crystal was pale yellow and of approximate dimensions 0.64 by 0.38 by 0.22 mm. ω scan technique. Data were collected at 183 K out to a maximum Bragg angle θ 22.5°. Number of independent reflections measured 2149, 575 with $I > 2\sigma(I)$. Absorption corrections were not applied; g_1, 0,0465; g_2, 0.3897; $R_{(obs)}$-factor 0.037; $wR_{(all\ data)}$ 0.085.

1,8-Dimethyl-r-1-nitro-t-4-trinitromethyl-1,4-dihydronaphthalene 38 — $C_{13}H_{12}N_4O_8$, *M* 352.3, triclinic, space group *P* 1, *a* 8.932(2), *b* 9.147(2), *c* 9.815(2) Å, α 81.00(1), β 68.08(1), γ 89.61(1)°, *V* 733.6 Å^3, D_C 1.595 g cm^{-3}, *Z* 2, μ(Mo Kα) 1.35 cm^{-1}. The crystal was colourless and of approximate

dimensions 0.52 by 0.2 by 0.02 mm. Data were collected at 120 K out to a maximum Bragg angle θ 24.99°. The number of independent reflections measured 2499, 1692 with $I > 2\sigma(I)$; g_1 0.0666, g_2 0.4670; absorption corrections were not applied; $R_{(obs)}$-factor 0.053, $wR_{(all\ data)}$ 0.142.

Nitro cycloadduct 42— $C_{13}H_{12}N_4O_8$, M 352.3, monoclinic, space group $C\ 2/c$, a 15.980(3), b 6.864(1), c 25.912(5), β 105.98(3)°, V 2732.4 Å^3, D_c 1.713 g cm^{-3}, Z 8, μ(Mo Kα) 1.45 cm^{-1}. The crystal was colourless and of approximate dimensions 0.54 by 0.42 by 0.20 mm. Data were collected at 110 K out to a maximum Bragg angle θ 20.03°. The number of independent reflections measured 1295, 1080 with $I > 2\sigma(I)$; g_1 0.0407, g_2 2.2948; absorption corrections were not applied; $R_{(obs)}$-factor 0.029, $wR_{(all\ data)}$ 0.072.

1-Methyl-r-3-nitro-t-4-trinitromethyl-3,4-dihydronaphthalene (6 1) — $C_{12}H_{10}N_4O_8$, M 338.2, monoclinic, space group $P\ 2_1/c$, a 13.357(3), b 8.056(2), c 13.218(3) Å, β 103.75(3)°, V 1381.5(6) Å^3, D_c 1.626 g cm^{-3}, Z 4, μ(Mo Kα) 1.40 cm^{-1}. The crystal was colourless and of approximate dimensions 0.50 by 0.32 by 0.20 mm. Data were collected at 130 K out to a maximum Bragg angle θ 25.12°. The number of independent reflections measured 1945, 1344 with $I > 2\sigma(I)$; g_1 0.0651, g_2 1.4813; absorption corrections were not applied; $R_{(obs)}$-factor 0.059, $wR_{(all\ data)}$ 0.154.

1-Methyl-r-1-nitro-c-4-trinitromethyl-1,4-dihydronaphthalene (63) — $C_{12}H_{10}N_4O_8$, M 338.2, monoclinic, space group $P\ 2_1$, a 10.041(2), b 6.207(1), c 11.892(2) Å, β 103.47°, V 720.8(2) Å^3, D_c 1.558 g cm^{-3}, Z 2, μ(Mo Kα) 1.34 cm^{-1}. The crystal was colourless and of approximate dimensions 0.62 by 0.44 by 0.12 mm. Data were collected at 130 K out to a maximum Bragg angle θ 24.99°. The number of independent reflections measured 1359, 1003 with $I >$

$2\sigma(I)$; g_1 0.0686, g_2 0.0000; absorption corrections were not applied; $R_{(obs)}$-factor 0.056, $wR_{(all\ data)}$ 0.134.

8-Methyl-r-1-nitro-c-4-trinitromethyl-1,4-dihydronaphthalene (64)— $C_{12}H_{10}N_4O_8$, M 338.2, monoclinic, space group $P\ 2_1/n$, a 8.860(2), b 14.388(3), c 11.228(2) Å, β 104.02(3)°, V 1388.7(5) Å^3, D_c 1.618 g cm^{-3}, Z 4, μMo Kα) 1.39 cm^{-1}. The crystal was colourless and of approximate dimensions 0.53 by 0.22 by 0.16 mm. Data were collected at 130 K out to a maximum Bragg angle θ 25.07°. The number of independent reflections measured 2444, 1650 with $I > 2\sigma(I)$, g_1 0.0504, g_2 0.9874; absorption corrections were not applied; $R_{(obs)}$-factor 0.053, $wR_{(all\ data)}$ 0.129.

Nitro cycloadduct (65)— $C_{12}H_{10}N_4O_8$, M 338.2, orthorhombic, space group $P\ ca2_1$, a 12.291(2), b 8.840(3), c 12.551(3) Å, V 1363.7(6) Å^3, D_c 1.647 g cm^{-3}, Z 4, μ(Mo Kα) 1.42 cm^{-1}. The crystal was colourless and of approximate dimensions 0.68 by 0.61 by 0.25 mm. Data were collected at 130 K out to a maximum Bragg angle θ 27.49°. The number of independent reflections measured 1639, 1479 with $I > 2\sigma(I)$, g_1 0.0428, g_2 0.3175; absorption corrections were not applied; $R_{(obs)}$-factor 0.031, $wR_{(all\ data)}$ 0.077.

Hydroxy cycloadduct (67) — $C_{12}H_{11}N_3O_7$, M 309.2, monoclinic, space group $P\ 2_1/c$, a 10.782(2), b 6.802(1), c 16.920(3) Å, β 98.20(3)°, V 1228.2(4) Å^3, D_c 1.672 g cm^{-3}, Z 4, μ(Mo Kα) 1.40 cm^{-1}. The crystal was colourless and of approximate dimensions 0.62 by 0.33 by 0.14 mm. Data were collected at 130 K out to a maximum Bragg angle θ 27.5°. The number of independent reflections measured 2808, 1846 with $I > 2\sigma(I)$, g_1 0.0342, g_2 0.5278; absorption corrections were not applied; $R_{(obs)}$-factor 0.049, $wR_{(all\ data)}$ 0.100.

5-Methyl-3-(4-nitrophenyl)-1,2,4-oxadiazole **2**. - $C_9H_7N_3O_3$, *M* 205.18, triclinic, space group $P\bar{1}$, *a* 7.083(3), *b* 7.336(2), *c* 10.107(3) Å, α 76.47(1)°, β 72.38(3)°, γ 69.28(2)°, *V* 463.7(3) Å^3, D_c 1.469 g cm^{-3}, *Z* 2, μ(Mo Kα) 1.14 cm^{-1}. The crystal was colourless and of approximate dimensions 0.62 by 0.5 by 0.16 mm. Data were collected at 183 K. The number of independent reflections measured 1615, 1393 with $I > 2\sigma(I)$; absorption corrections were not applied; g_1 0.0522, g_2 0.0948, $R_{(obs)}$ 0.037, $wR_{(all\ data)}$ 0.098.

Structure Determination

Full matrix least-squares refinements (SHELXL-92)[81] were employed. This program is based on intensities and uses all data. The observed threshold $I > 2\sigma(I)$ was used only for calculating $R_{(obs)}$, shown here as a comparison for the refinements based on *F*. Reflection weights $1/[\sigma^2(F_o^2) + (0.325P)^2 + 1.9595P]$, where $P = [F_o^2 + 2F_c^2]/3$, were used.

All non-hydrogen atoms were assigned anisotropic thermal parameters. Methyl hydrogen atoms were included as rigid groups pivoting about their carbon atoms. Final Fourier syntheses show no significant residual electron density, and there were no abnormal discrepancies between observed and calculated structure factors.The structure was solved by direct methods and difference-Fourier syntheses. Full matrix least-squares refinements (SHELXL-92)[81] were employed. This program is based on intensities and uses all data. The observed threshold $I > 2\sigma(I)$ was used only for calculating $R_{(obs)}$, shown here as a comparison for the refinement based on *F*. Reflection weights $1/[\sigma^2(F_o^2) + (g_1P)^2 + g_2P]$, where $P = [F_o^2 + 2F_c^2]/3$, were used.

All non-hydrogen atoms were assigned anisotropic thermal parameters. Methyl hydrogen atoms were included as rigid groups pivoting about their carbon

atoms. Final Fourier syntheses show no significant residual electron density, and there were no abnormal discrepancies between observed and calculated structure factors.

Table 5.3. Fractional coordinates for atoms in 1,4,5,8-tetramethyl-*r*-1-nitro-*c*-2-trinitromethyl-1,2-dihydronaphthalene (23).

Atom	$10^4X/a$	$10^4Y/b$	$10^4Z/c$	10^3U
O(11)	3592(3)	-66(2)	8702(1)	38(1)
O(12)	593(3)	766(2)	7995(1)	33(1)
O(21)	-1346(3)	1419(2)	6262(1)	49(1)
O(22)	-1393(3)	3585(2)	6640(1)	44(1)
O(31)	2408(3)	237(2)	5238(1)	49(1)
O(32)	3946(3)	-228(2)	6604(1)	37(1)
O(41)	4057(4)	2885(2)	4957(1)	50(1)
O(42)	587(4)	3542(2)	4780(1)	57(2)
N(1)	2283(3)	913(2)	8280(1)	26(1)
N(2)	-501(3)	2399(3)	6393(1)	35(1)
N(3)	2837(3)	561(2)	6005(2)	31(1)
N(4)	2192(4)	2953(2)	5220(2)	38(2)
C(1)	2762(4)	2419(2)	8061(2)	21(1)
C(2)	3217(4)	2648(2)	6949(2)	22(1)
C(3)	3309(4)	4211(3)	6725(2)	26(1)
C(4)	2112(4)	5292(3)	7186(2)	23(1)
C(5)	507(4)	5006(2)	7947(2)	20(1)
C(6)	-1294(4)	6102(2)	8200(2)	23(1)
C(7)	-2578(4)	5783(3)	8990(2)	26(1)
C(8)	-2082(4)	4469(3)	9531(2)	25(1)
C(9)	-369(4)	3336(2)	9272(2)	21(1)
C(10)	870(3)	3591(2)	8437(2)	19(1)
C(11)	4818(4)	2395(3)	8547(2)	30(1)
C(12)	1920(4)	2160(3)	6216(2)	26(1)
C(13)	2615(4)	6768(3)	7008(2)	35(2)
C(14)	-2015(4)	7575(3)	7642(2)	32(1)
C(15)	13(4)	1944(3)	9933(2)	31(2)

Table 5.4. Fractional coordinates for atoms in 1,8-dimethyl-*r*-1-nitro-*t*-4-trinitromethyl-1,4-dihydronaphthalene (38)

The equivalent isotropic temperature factor in Tables 1 and 2 is defined as one-third of orthoganalized *U* tensor (Å^2)

Atom	$10^4X/a$	$10^4Y/b$	$10^4Z/c$	10^3U (Å^2)
O(11)	-2258(3)	5587(3)	9460(3)	33(1)
O(12)	-4014(4)	3836(3)	10887(3)	52(1)
O(21)	-3894(3)	1273(3)	8982(3)	43(1)
O(22)	-4169(3)	3517(3)	8024(3)	37(1)
O(31)	-1250(4)	2330(3)	10734(3)	42(1)
O(32)	-1040(3)	921(3)	9096(3)	34(1)
O(111)	5402(3)	2580(3)	5071(3)	36(1)
O(112)	4138(3)	4241(3)	4185(3)	27(1)
N(1)	-2836(4)	4330(3)	9798(3)	30(1)
N(2)	-3497(4)	2581(3)	8574(3)	28(1)
N(3)	-1418(4)	2035(3)	9637(3)	27(1)
N(11)	4167(3)	3167(3)	5068(3)	23(1)
C(1)	2526(4)	2543(3)	6296(3)	18(1)
C(2)	2133(4)	3724(4)	7260(3)	20(1)
C(3)	744(4)	4343(3)	7709(3)	18(1)
C(4)	-652(4)	3948(3)	7308(3)	16(1)
C(5)	-1218(4)	2962(3)	5312(3)	16(1)
C(6)	-829(4)	2228(3)	4113(3)	19(1)
C(7)	636(4)	1585(3)	3621(3)	21(1)
C(8)	1741(4)	1664(3)	4295(3)	18(1)
C(9)	-167(4)	3030(3)	6049(3)	13(1)
C(10)	1342(4)	2396(3)	5540(3)	15(1)
C(11)	2785(4)	1099(4)	7162(4)	30(1)
C(12)	-2047(4)	3218(3)	8753(3)	19(1)
C(13)	3339(4)	982(4)	3605(4)	25(1)

Table 5.5 Fractional coordinates for atoms in nitro cycloadduct (42)

Atom	$10^4X/a$	$10^4Y/b$	$10^4Z/c$	10^3U (Å^2)
O(31)	821(1)	-3377(3)	6128(1)	22(1)
O(32)	1954(1)	-4048(3)	5865(1)	21(1)
O(131)	4074(1)	1740(3)	6295(1)	23(1)
O(132)	3515(1)	4055(3)	6652(1)	29(1)
O(133)	4008(1)	-1799(3)	7159(1)	19(1)
O(134)	4188(1)	903(3)	7598(1)	24(1)
O(135)	2169(1)	280(3)	7271(1)	15(1)
O(136)	1879(1)	2747(3)	6705(1)	14(1)
N(3)	1590(2)	-3213(3)	6155(1)	15(1)
N(131)	3607(2)	2368(4)	6554(1)	17(1)
N(132)	3840(1)	-119(4)	7219(1)	16(1)
N(133)	2576(1)	1811(3)	7070(1)	14(1)
C(1)	1234(2)	1243(4)	6446(1)	13(1)
C(2)	1574(2)	-554(4)	6800(1)	13(1)
C(3)	2121(2)	-1913(4)	6580(1)	12(1)
C(4)	2695(2)	-624(4)	6341(1)	12(1)
C(5)	2314(2)	139(4)	5367(1)	15(1)
C(6)	1742(2)	835(4)	4609(1)	18(1)
C(7)	979(2)	1655(4)	4935(1)	17(1)
C(8)	738(2)	1818(4)	5410(1)	14(1)
C(9)	1319(2)	1102(4)	5874(1)	11(1)
C(10)	2106(2)	291(4)	5844(1)	12(1)
C(11)	388(2)	1882(4)	6538(1)	18(1)
C(12)	-114(2)	2807(4)	5372(1)	19(1)
C(13)	3119(2)	837(4)	6774(1)	14(1)

Table 5.6. Fractional coordinates for atoms in 1-methyl-*r*-3-nitro-*t*-4-trinitromethyl-3,4-dihydronaphthalene (59)

The equivalent isotropic temperature factor in Tables 3- is defined as one-third of orthoganalized *U* tensor (Å^2)

Atom	$10^4X/a$	$10^4Y/b$	$10^4Z/c$	10^3U (Å^2)
O(11)	6143(3)	4738(4)	7744(3)	46(1)
O(12)	7666(3)	5558(4)	7658(3)	41(1)
O(21)	7263(3)	167(4)	4893(3)	39(1)
O(22)	7603(3)	-962(4)	6442(3)	46(1)
O(31)	9907(3)	2674(4)	5818(3)	41(1)
O(32)	9062(3)	996(5)	4653(3)	46(1)
O(41)	9758(3)	-385(5)	7029(3)	54(1)
O(42)	9184(2)	1328(4)	8017(3)	33(1)
N(1)	6975(3)	4544(5)	7509(3)	28(1)
N(2)	7726(3)	74(5)	5803(3)	30(1)
N(3)	9210(3)	1716(5)	5471(3)	28(1)
N(4)	9200(3)	729(5)	7194(3)	30(1)
C(1)	5831(3)	2715(5)	5329(3)	24(1)
C(2)	6120(3)	2285(5)	6337(4)	26(1)
C(3)	7134(3)	2850(5)	7010(3)	21(1)
C(4)	7977(3)	3104(5)	6402(3)	19(1)
C(5)	8142(3)	5223(5)	5025(3)	24(1)
C(6)	7731(3)	6121(5)	4123(3)	28(1)
C(7)	6728(4)	5851(5)	3602(4)	29(1)
C(8)	6121(3)	4708(5)	3964(3)	24(1)
C(9)	6504(3)	3805(5)	4878(3)	18(1)
C(10)	7543(3)	4060(5)	5399(3)	18(1)
C(11)	4822(3)	2164(6)	4666(4)	31(1)
C(12)	8472(3)	1438(5)	6200(3)	20(1)

Table 5.7 Fractional coordinates for atoms in 1-methyl-*r*-1-nitro-*c*-4-trinitromethyl-1,4-dihydronaphthalene (61)

Atom	$10^4X/a$	$10^4Y/b$	$10^4Z/c$	10^3U (Å^2)
O(11)	444(6)	4156(9)	3677(4)	52(2)
O(12)	401(5)	4099(7)	1857(4)	36(1)
O(21)	2773(4)	-2470(7)	-414(4)	27(1)
O(22)	4603(4)	-486(7)	-229(4)	26(1)
O(31)	2679(4)	2633(7)	229(4)	29(1)
O(32)	3271(5)	2894(7)	2112(4)	28(1)
O(41)	5658(5)	862(8)	2434(4)	30(1)
O(42)	5393(5)	-2585(8)	2022(4)	28(1)
N(1)	417(5)	3210(8)	2772(5)	21(1)
N(2)	3629(5)	-1191(8)	100(4)	19(1)
N(3)	3131(5)	1947(8)	1195(5)	20(1)
N(4)	4983(5)	-686(9)	1997(4)	23(1)
C(1)	376(6)	677(9)	2780(5)	19(1)
C(2)	152(6)	-66(10)	1559(5)	20(2)
C(3)	1034(5)	-1175(9)	1123(5)	17(1)
C(4)	2461(6)	-1711(9)	1811(5)	15(1)
C(5)	3724(6)	-2364(11)	3880(5)	21(1)
C(6)	3946(7)	-2052(11)	5049(6)	26(2)
C(7)	3084(6)	-767(11)	5493(6)	28(2)
C(8)	1954(6)	152(10)	4745(5)	23(2)
C(9)	2638(6)	-1355(10)	3099(5)	17(1)
C(10)	1720(6)	-123(9)	3561(5)	14(1)
C(11)	-862(6)	98(12)	3250(6)	29(2)
C(12)	3514(6)	-431(9)	1308(5)	16(1)

Table 5.8 Fractional coordinates for atoms in 8-methyl-*r*-1-nitro-*c*-4-trinitromethyl-1,4-dihydronaphthalene (63)

Atom	$10^4X/a$	$10^4Y/b$	$10^4Z/c$	10^3U (Å^2)
O(11)	3903(3)	5797(2)	3965(2)	52(1)
O(12)	4269(3)	7280(2)	3776(2)	35(1)
O(21)	1373(3)	5700(2)	5032(3)	71(1)
O(22)	3234(3)	5488(2)	6680(2)	38(1)
O(31)	1426(2)	7587(2)	6064(2)	40(1)
O(32)	1608(3)	7878(2)	4215(2)	32(1)
O(41)	8321(4)	6950(2)	4099(2)	64(1)
O(42)	7124(3)	8236(2)	3737(2)	44(1)
N(1)	3852(3)	6607(2)	4270(2)	29(1)
N(2)	2589(3)	5906(2)	5759(3)	39(1)
N(3)	2006(3)	7490(2)	5195(2)	26(1)
N(4)	7665(3)	7607(2)	4409(2)	26(1)
C(1)	7075(3)	9325(2)	6093(2)	19(1)
C(2)	6121(4)	9998(2)	6418(3)	22(1)
C(3)	4776(4)	9759(2)	6764(3)	24(1)
C(4)	4336(3)	8836(2)	6762(3)	21(1)
C(5)	4756(3)	7129(2)	6469(3)	18(1)
C(6)	6079(4)	6455(2)	6513(3)	21(1)
C(7)	7360(3)	6687(2)	6175(3)	22(1)
C(8)	7661(3)	7846(2)	5781(3)	19(1)
C(9)	5222(3)	8143(2)	6385(2)	17(1)
C(10)	6605(3)	8391(2)	6055(2)	17(1)
C(11)	8592(4)	9619(2)	5823(3)	29(1)
C(12)	3354(3)	6802(2)	5444(3)	22(1)

Table 5.9 Fractional coordinates for atoms in nitro cycloadduct (64)

Atom	$10^4X/a$	$10^4Y/b$	$10^4Z/c$	10^3U (Å^2)
O(11)	4050(2)	-1457(2)	4467(2)	32(1)
O(12)	2342(2)	-1164(2)	4879(2)	32(1)
O(21)	2498(2)	-2933(2)	2640(2)	36(1)
O(22)	3831(2)	-1839(2)	1790(2)	27(1)
O(31)	5127(2)	2693(2)	1707(2)	33(1)
O(32)	3690(2)	4046(2)	1378(2)	39(1)
O(41)	1685(1)	444(2)	1935(2)	22(1)
O(42)	1500(1)	1206(2)	3617(2)	21(1)
N(1)	3116(2)	-1074(2)	4280(2)	20(1)
N(2)	3109(2)	-1879(2)	2451(2)	22(1)
N(3)	4146(2)	2862(3)	1625(2)	23(1)
N(4)	1765(2)	-85(2)	3007(2)	20(1)
C(1)	1936(2)	2573(2)	3064(2)	19(1)
C(2)	2238(2)	1901(3)	1946(2)	19(1)
C(3)	3441(2)	1498(3)	1840(2)	19(1)
C(4)	3789(2)	780(3)	2907(2)	17(1)
C(5)	4697(2)	2325(3)	4368(2)	22(1)
C(6)	4716(2)	3616(3)	5002(2)	25(1)
C(7)	3849(2)	4631(3)	4986(2)	26(1)
C(8)	2943(2)	4349(3)	4348(2)	22(1)
C(9)	2912(2)	3047(3)	3713(2)	18(1)
C(10)	3796(2)	2045(3)	3725(2)	18(1)
C(11)	1007(2)	3702(3)	2998(3)	26(1)
C(12)	2939(2)	-454(3)	3152(2)	17(1)

Table 5.10 Fractional coordinates for atoms in hydroxy cycloadduct (65)

Atom	$10^4X/a$	$10^4Y/b$	$10^4Z/c$	10^3U (Å^2)
O(11)	8558(2)	-3555(3)	4837(1)	27(1)
O(12)	8590(2)	-5943(2)	5692(1)	26(1)
O(21)	9329(1)	-2167(2)	7525(1)	18(1)
O(22)	8015(1)	-4602(2)	7144(1)	16(1)
O(3)	6915(1)	1421(2)	6796(1)	19(1)
O(31)	10160(2)	-46(2)	5876(1)	24(1)
O(32)	11031(2)	-2875(3)	6164(1)	29(1)
N(1)	8655(2)	-4227(3)	5511(1)	17(1)
N(2)	9122(2)	-3703(3)	6954(1)	16(1)
N(3)	10136(2)	-1767(3)	6062(1)	18(1)
C(1)	7184(2)	-3026(3)	7394(1)	16(1)
C(2)	8100(2)	-1253(3)	7509(1)	16(1)
C(3)	7976(2)	172(3)	6807(1)	15(1)
C(4)	7813(2)	-1131(3)	6054(1)	13(1)
C(5)	5697(2)	-2059(3)	5283(1)	17(1)
C(6)	4489(2)	-2798(3)	5272(2)	20(1)
C(7)	4121(2)	-3520(3)	5964(2)	21(1)
C(8)	4952(2)	-3547(3)	6675(1)	18(1)
C(9)	6527(2)	-2064(3)	5989(1)	14(1)
C(10)	6157(2)	-2837(3)	6683(1)	15(1)
C(11)	6778(2)	-3720(4)	8166(1)	21(1)
C(12)	8856(2)	-2673(3)	6169(1)	13(1)

Table 5.11 Fractional coordinates for atoms in 5-methyl-3-(4-nitrophenyl)-1,2,4-oxadiazole (2)

Atom	$10^4X/a$	$10^4Y/b$	$10^4Z/c$	10^3U (Å^2)
O(1)	-600(2)	11978(2)	8966(1)	54(1)
O(2)	475(2)	14326(2)	7571(1)	49(1)
O(3)	4751(2)	5570(2)	2235(1)	40(1)
N(1)	312(2)	12658(2)	7825(1)	37(1)
N(2)	4843(2)	8583(2)	2102(1)	37(1)
N(3)	3710(2)	6144(2)	3579(1)	39(1)
C(1)	1235(2)	11417(2)	6694(1)	30(1)
C(2)	1952(2)	12285(2)	5350(2)	31(1)
C(3)	2796(2)	11124(2)	4286(1)	30(1)
C(4)	2921(2)	9132(2)	4577(1)	28(1)
C(5)	2195(2)	8299(2)	5952(2)	32(1)
C(6)	1344(2)	9441(2)	7023(2)	33(1)
C(7)	3824(2)	7925(2)	3426(1)	30(1)
C(8)	5365(2)	7097(2)	1426(2)	38(1)
C(9)	6529(3)	6879(3)	-34(2)	56(1)

5.11 REFERENCES

1 Kosower, E. M., *Prog. Phys. Org. Chem.* **81**, 3, 1965.

2 Colter, A. K.; Dack, M. R., *J. Mol . Complexes,* **1**, 301, 1973.
Colter, A. K.; Dack, M. R., *J. Mol . Complexes,* **2**, 1, 1974.

3 Foster, R.,*"Organic Transfer Complexes"*, Academic Press: New York, 1969.

4 Andrews, L. J.; Keefer, R. Y., *"Molecular Complexes in Organic Chemistry"*; Holden-Day: San Francisco, 1964.

5 Mulliken, R.S., *J. Am. Chem. Soc.*, **74**, 811, 1952.

6 Masnovi, J. M.; Kochi, J. K., *J. Org. Chem.*, **50**, 5245, 1985.

7 Masnovi, J. M.; Seddon, E. A.; Kochi, J. K., *Can. J. Chem.*, **62**, 2552, 1984.

8 Mulliken, R.S.; Person, W. B., *"Molecular Complexes"*, A lecture and reprint volume, Wiley: New York, 1969.

9 Dewar, M.J.S.; Rogers, H., *J. Am. Chem. Soc.*, **83**, 4560, 1961.
Dewar, M.J.S.; Rogers, H., *J. Am. Chem. Soc.*, **84**, 395, 1962.

10 Goodman J. L.; Peters, K. S., *J. Am. Chem. Soc.*, **107**, 1441, 1985.

11 Mulliken, R.S., *J. Am. Chem. Soc.*, **72**, 600, 1950.

12 Benesi, H. A.; Hildebrand, J. H., *J. Am Chem. Soc.* **71**, 2703, 1949.

13 McConnell,H.; Ham, J.S.; Platt, J.R., *J. Chem. Phys.* **21**, 66, 1953.

14 Hastings, S. H.; Franklin; J. L., Schiller, J. C.; Matsen, F. A., *J. Am Chem. Soc.* **75**, 2900, 1953.

15 Briegleb, G.; Czekalla, J., *Z. Elektrochem*, **63**, 6, 1959.

16 Foster, R., *Nature*, **181**, 337, 1958 and **183**, 1253 1959.

17 Yada, H.; Tanaka, J.; Nagakura, S., *Bull. Chem. Soc. Japan*, **33**, 1660, 1960.

18 Chowdhury, M., *Trans. Faraday Soc.*, **57**, 1482, 1961.

19 Briegleb, G., *Angew. Chem. Int. Ed.*, **3**, 617, 1964.

20 Benesi, H. A.; Hildebrand, J. H., *J. Am. Chem. Soc.,* **71**, 2703, 1949.

21 Scott, R. L., *Proc. Int. Conf. on Co-ordination Compounds.,* Amsterdam 1955.

22 Foster, R.; Fyfe, C. A., *"Progress in Nuclear Magnetic Resonance Spectroscopy"*, Vol 4, Eds Emsley, J. W.; Feeney, J.; Sutcliffe, L. H.; Pergamon, Oxford, Ch 1, 1969.

23 Peover, M. E., *Trans. Faraday. Soc.,* **60**, 417, 1964.

24 Bolles, T. F.; Drago, R. S., *J. Am. Chem. Soc.*, **87**, 5015, 1965.
Bolles, T. F.; Drago, R. S., *J. Am. Chem. Soc.*, **88**, 3921, 1966.

25 Few, A. V.; Smith, J. W.G., *J. Chem. Soc.,* 2781, 1949.

26 Colter, A. K.; Wang, S. S., *J. Am. Chem. Soc.,* **85**, 114, 1963.

27 Hammond, P. R.; Burkhardt, L. A., *J. Phys. Chem.,* **74**, 639, 1970.

28 Newman, M. S.; LeBlanc, J. R.; Karnes, H. A.; Axelrod, G., *J. Am. Chem. Soc.*, **86**, 868, 1964.

29 Seltzer, S.; Lam, E.; Packer, L., *J. Am. Chem. Soc.,* **103**, 6470, 1982.

30 Masnovi, J. M.; Kochi, J. K.; Hillinski, E. F.; Rentzepis, P. M., *J. Am. Chem. Soc.*, **108**, 1126,1986.

31 Kochi, J. K., *Acc. Chem Res.*; **25**, 39 1992.

32 Hillinski, E. F.; Rentzepis, P. M., *Anal. Chem.,* **55**, 1121a,1983.

33 Rabani, J.; Mulac, W. A.; Matheson, M. S., *J. Phys. Chem.* **69**, 53, 1965.

34 Glover, P.J., *Tetrahedron*, **19**, 219, 1963.
Kamlet, M. J.; Glover, P. J., *J. Org. Chem.* ***27***, 537, 1962.

35 Young, R.P; Holt, A.; Walker, S., *Tetrahedron,* **20**, 2351, 1964.

36 Hammerich, O.; Parker, V. D., *"Electrooxidation in Organic Chemistry"*, Yoshida, K., Ed; Wiley: New York, pp. 64, 1984.

Parker, V. D., *Acc. Chem. Res.*, **17**, 243, 1984.

37 Brown, R. D., *J. Am. Chem. Soc.*, **1612**, 3129, 1951.

Brown, R. D., *J. Am. Chem. Soc.*, **691**, 3249, 1950.

38 O'Neal, H. E.; Benson, S. W., *"Free Radicals"*, Kochi, J. K., Ed.: Wiley-Interscience: New York, Vol II pp. 275, 1973.

39 Masnovi, J. M.; Levine, A; Kochi, J. K., *J. Am. Chem. Soc.*, **106**, 4356, 1985.

40 Daney, M.; Lapouyade, R.; Bouas-Laurent, H., *J.Org. Chem.*, **48**, 5055, 1983.

41 Kenner, J., *Nature*, **156**, 369, 1945.

42 Hughes, E. D.; Ingold, C. K., *J. Am. Chem. Soc.*, 1400, 1950.

43 Schofield, K., *"Aromatic Nitration"*, Cambridge University Press, Cambridge, London, p. 107, 1980.

44 Hughes, E. D.; Ingold, C. K., and co-workers, *Nature*, **156**, 688, 1945.

45 Perrin, C.L., *J. Am. Chem. Soc.*, **99**, 5516, 1977.

46 (a) Olah, G. A.; Narang, S. C.; Olah, J. A.; Lammertsma, K., *Proc. Natl. Acad. Sci. U.S.A.*, **79**, 4487, 1982.

(b) Olah, G. A., *Acc. Chem. Res.*, **4**, 240, 1971.

47 Barnett, J. W.; Moodie, R. B.; Schofield, K.; Weston, J. B., *J. Chem. Soc., Perkin Trans. 2.*, 648, 1975.

48 Kochi, J. K.; Sankararaman, S., *J. Chem. Soc, Perkin Trans. 2.*, 1,1992.

49 Ridd, J. H.; Sandall, P. B.; Trevellick, S. J., *Chem. Soc., Chem. Commun.*, 1195, 1988.

50 Ridd, J. H., *Chem. Soc. Rev.*, **20**, pp. 149, 1991; and references cited therein.

51 Eberson, L.; Radner, F., *Acc. Chem. Res.*, **20**, 53, 1987.

52 Eberson, L.; Jönsson, L.; Radner, F., *Acta. Chem. Scan. Ser. B.*, **32**, 749, 1978.

53 Eberson, L.; Radner, F., *Acta. Chem. Scan. Ser. B.*, **40**, 71, 1986.

54 Eberson, L.; Radner, F., *Acta. Chem. Scan. Ser. B.*, **34**, 739, 1980.

55 Eberson, L.; Hartshorn, M.P.; Radner, F., *J. Chem. Soc., Perkin. Trans. 2*, 1793, 1992.

56 Eberson, L.; Hartshorn, M.P.; Svensson, J. O., *J. Chem. Soc., Chem. Commun.*, In press.

57 Kim, K. E.; Bockman, M.; Kochi, J. K., *J. Chem. Soc., Perkin Trans. 2,* 1879, 1992.

58 Kim, K. E.; Bockman, M.; Kochi, J. K., *J. Am. Chem. Soc.*, **115**, 3091, 1992.

59 Eberson, L.; Hartshorn, M.P.; Radner, F.; Robinson, W. T., *J. Chem. Soc., Chem. Commun.*, 566, 1992.

60 Eberson, L.; Hartshorn, M.P.; Radner, F., *J. Chem. Soc., Perkin. Trans. 2*, 1799, 1992.

61 Fisher, A.; Wilkinson, A. L., *Can. J. Chem.*, **50**, 3988, 1972.

62 Terahara, A.; Ohya-Nishiguchi, H.; Hirota, N.; Oku, A., *J. Phys. Chem.* **90**,1564, 1986.

63 Howarth, O. W.; Fraenkel, G. K., *J. Chem. Phys.*, **52**,6258, 1970.

64 Eberson, L.; Calvert, J. L.; Hartshorn, M. P.; Robinson, W. T., *Acta. Chem. Scan. Ser. B.,* **47**, 1025, 1993.

65 Igliesas, E.; Garcia-Rio, L.; Leis. R.; Pena, M.E.; Williams, D. L. H., *J. Chem. Soc., Perkin. Trans. 2*, 1673, 1992.

66 Imashiro, F.; Takegoshi, K.; Saika, A.; Taira, Z.; Asahi, Y., *J. Am. Chem. Soc.*, **107**, 2341, 1985.

67 Eberson, L.; Radner, F., *J. Am. Chem. Soc.*, **113**, 5825, 1991.

68 (a) Maclagan, R. G. A. R., *Private communication.*

(b) Dewar, M. J. S.; Zoebisch, E. G.; Healy, E. A.; Stewart, J. J. P., *J. Am. Chem. Soc.,* **107**, 3902, 1985.

69 Butts, C. P.; Calvert, J. L.; Hartshorn, M. P.; Robinson., W. T., *Aust. J. Chem.,* In press.

70 Davies, A.; Warren, K. D., *J. Chem Soc. (B)* 873, 1969.

71 Husigen, R., *Angew. Chem.* **75**, 604, 1963.

72 Simonyan, L. A.; Gambaryan, N. P.; Petrovskii, P. V.; Knunyants, I. L., *Chem. Abstr.* **69**, 52077z, 1968.

73 Leitich, J., *J. Angew. Chem., Int. Ed. Engl.*, **15**, 372, 1976.

74 Balczewski, P.; Beddoes, R. L.; Joule, J. A., *J. Chem. Soc., Chem. Commun.,* 559, 1991.

75 Calvert, J. L.; Eberson, L.; Hartshorn, M. P.; Robinson, W. T., *Aust. J. Chem.*, In Press.

76 Calvert, J. L.; Eberson, L.; Hartshorn, M. P.; Robinson, W. T., *Aust. J. Chem.*, In Press.

77 Golic, L.; Leban, I.; Stanovnik, B.; Tisler, M., *Acta Cryst.*, 1979, **35B**, 2256.

78 "Comprehensive Heterocyclic Chemistry," vol. 6, Ed. K.T. Potts, Pergamon Press, 1984, pp. 389.

79 Eberson, L.; Hartshorn, M. P., *J. Chem. Soc., Chem. Commun.*, 1563, 1992.

80 Eberson, L.; Calvert, J. L.; Hartshorn, M. P.; Robinson, W. T., *Acta. Chem. Scan. Ser. B*, 3566, 1993.

81 Sheldrick, G. M., Unpublished data.

ACKNOWLEDGMENTS

I wish to express my sincere thanks to my supervisor Professor Michael Hartshorn and my associate supervisor Dr. Graeme Wright for their advice, enthusiastic encouragement and seemingly endless patience.

I also thank Dr. Ward Robinson and Mark Nieuwenhuyzen for their help throughout the course of several X-ray structures. The never ending help and expertise of the technical staff is also greatly appreciated.

The award of a Canterbury University Post-Graduate Scholarship is gratefully acknowledged.

Finally I would like to express much thanks to my family and friends. Their support and encouragement have helped to ensure the successful pursuit of an academic ambition.